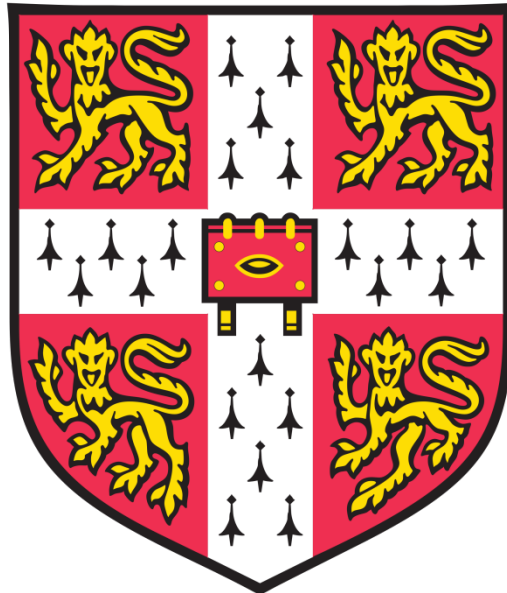


# **Vaccinia virus BTB-Kelch proteins**



**Ruiyao Zhang**

**Department of Pathology**

**Lucy Cavendish College**

**University of Cambridge**

**Supervisors: Professor Geoffrey L. Smith and Dr Mitchell A. Pallett**

**This thesis is submitted for the degree of Doctor of Philosophy**

**August 2020**

## **DECLARATION**

This thesis is the result of my own work and includes nothing which is the outcome of work done in collaboration except as declared in the Preface and specified in the text. It is not substantially the same as any that I have submitted, or, is being concurrently submitted for a degree or diploma or other qualification at the University of Cambridge or any other University or similar institution except as declared in the Preface and specified in the text. I further state that no substantial part of my thesis has already been submitted, or, is being concurrently submitted for any such degree, diploma or other qualification at the University of Cambridge or any other University or similar institution except as declared in the Preface and specified in the text. It does not exceed the 60,000 word limit set by the School of Biological Sciences.

## Vaccinia virus BTB-Kelch proteins - ABSTRACT

Ruiyao Zhang

Vaccinia virus (VACV) is a valuable tool to study host-virus interactions and encodes a plethora of immunomodulatory proteins, among which three, A55, C2 and F3, have a BTB/BACK-Kelch (BBK) structure and are the focus of this study.

Proteins containing BTB and Kelch domains function as adapters for the cullin 3 (Cul3)-based E3 ubiquitylation system. VACV BBKs are not essential for viral replication, but they all affect the lesion size induced by infection in an intradermal murine model. Viruses lacking any one of these BBK proteins also induce increased inflammatory cell infiltration into lesions. Deleting *A55R* or *C2L* also causes different plaque morphology and cytopathic effect in cultured cells. The mechanisms underpinning these observations were unknown, and hence were the objectives of this study. Besides, the interaction between Cul3 and VACV BBKs, the cellular substrates of A55, C2 and/or F3, and the outcome of targeting these substrates were also investigated.

The effect of VACV BBKs on innate immune signalling was studied, and NF- $\kappa$ B was selected as a starting point because the ectromelia virus (ECTV) orthologue of A55, ECTV EVM150, inhibits NF- $\kappa$ B signalling. Consistent with this, A55, C2 and F3 all inhibit NF- $\kappa$ B signalling pathway by diminishing p65 nuclear translocation. Specifically, A55 associates with importin KPNA2 and impairs the interaction between KPNA2 and p65, hence reducing p65 importation into the nucleus.

A55 interacts with Cul3 directly and with high affinity, although the ability to inhibit NF- $\kappa$ B is independent of binding Cul3. In contrast, C2 and F3 do not interact with Cul3. However, C2 associates with A55, and via A55, it forms a complex with Cul3. A working model was proposed in which A55, Cul3 and C2 form a complex, in which A55 binds Cul3 and C2 brings in substrates, leading to the ubiquitylation of substrates followed by protein degradation or modification.

To examine this working model and to identify novel viral BBKs substrates, an unbiased tandem mass tag (TMT) mass spectrometry was carried out. Three cellular proteins, Fer, Scrib and RASA2, are degraded during infection by wild type VACV,

but not by mutant VACVs lacking either C2 or A55. Thus, A55 and C2 function collaboratively. A55 and C2 degrade Scrib, and an interaction between A55 and Cul3 is required for this. Using Scrib knockout (KO) cell lines, it was found that Scrib restricts VACV spread. It was also found that VACV upregulates TGF- $\beta$  signalling and Scrib influences the pathway.

Besides its adaptor protein role in the A55/Cul3 complex, C2 also associates with a small GTPase named Cdc42. Cdc42 is stable during VACV infection, meaning that C2 does not degrade Cdc42 via A55/Cul3. However, Cdc42 is activated by VACV, and this activation is promoted by C2.

Overall, this study shows VACV expresses the family of BBK proteins to modulate intracellular signalling and hijack host Cul3-ubiquitin system to target cellular proteins.

## ACKNOWLEDGEMENTS

Firstly I would like to thank my supervisor Professor Geoffrey L. Smith, without whom none of this would have happened. I will always be grateful that he helped me out of a very difficult situation and gave me such an interesting project to work on in the most amazing team one can hope for. He has always been generous with his precious time to guide me through my study or to discuss the projects with his scientific insights.

I cannot image myself having achieved so much in this book either, without my kindest and smartest daily supervisor Dr. Mitchell A. Pallett, who is basically a brother to me. He has been very patient teaching me all the essential skills and helping me build the foundation for my career. Even though no longer working in the same group, he still helped me generously and thoroughly with my thesis for the past months.

Smith lab is my family here in the UK. Thank you Dr. Yongxu Lu, Dr. Alice Torres, Dr Jonas Dutra-Albarnaz, Dr. Chen Gao, Dr. Iliana Georgana and Dr. David Carpentier who have provided lots of scientific advices that helped build up this work. I would also like to thank Dr. Sebastian Boehm, Dr. Ka Fai Leung, Dr. Dong Li, Dr. Arwen Altenburg, Rachel Seear, Stephanie Macilwee, and my PhD buddies Dr. William Gao, Dr. Simon Scutts, Callum Talbot-Cooper, John Shannon, Qi Zhong, Ana Gali, Delphine Depierreux, for their support, the diversity of the multi-national environment, and countless events, parties, movie nights, lab trips that have made the past four years a fun and unforgettable journey.

Lastly I would like to acknowledge my family, especially my parents and my partner Matthijs, for their love and support as well as all the happy memories along the way.

# Table of Contents

1	Introduction .....	8
1.1	Vaccinia virus.....	8
1.1.1	VACV genome .....	9
1.1.2	VACV life cycle .....	10
1.1.3	Current studies of VACV .....	12
1.2	VACV-host interplay.....	14
1.2.1	Immune response.....	14
1.2.2	Other cellular signalling pathways .....	24
1.2.3	VACV-induced cell motility.....	26
1.2.4	Apoptosis.....	27
1.2.5	VACV and the cellular ubiquitin system .....	28
1.3	BTB-Kelch proteins .....	31
1.3.1	Kelch proteins .....	31
1.3.2	BTB proteins .....	32
1.3.3	Functions of Kelch and BTB proteins .....	33
1.4	VACV BTB-Kelch proteins .....	37
1.5	Project aims .....	39
2	Material and Methods .....	40
2.1	Bioinformatic analysis .....	40
2.2	Cell culture .....	40
2.2.1	Maintenance of cells .....	40
2.2.2	Transfection of cells .....	41
2.2.3	Construction of inducible cell lines.....	44
2.3	Vaccinia virus work .....	44
2.3.1	Amplification and titration of VACV.....	44
2.3.2	Infection of cells.....	46
2.3.3	Recombinant VACV construction.....	46
2.4	Molecular biology work .....	50
2.4.1	Polymerase chain reaction (PCR).....	50
2.4.2	Real-time qPCR (RT-qPCR).....	51
2.4.3	Agarose gel electrophoresis and DNA purification.....	55
2.4.4	Restriction enzyme digestion.....	55

2.4.5	DNA ligation .....	55
2.4.6	Bacterial transformation .....	56
2.4.7	Bacterial colony screening by PCR .....	56
2.4.8	Preparation of plasmid DNA .....	57
2.4.9	Sequencing .....	57
2.4.10	Site-directed mutagenesis .....	57
2.5	Protein analysis .....	58
2.5.1	Cell lysates preparation.....	58
2.5.2	Polyacrylamide gel electrophoresis (PAGE) and immunoblotting.....	59
2.5.3	Immunoprecipitation (IP) .....	62
2.5.4	Immunofluorescence (IF) .....	63
2.5.5	Enzyme-linked immunosorbent assay (ELISA) .....	64
2.6	Luciferase reporter gene assays.....	64
2.7	Statistical analysis.....	64
3	Results 1 – A55, C2 and F3 are inhibitors of NF- $\kappa$ B signalling pathway .....	66
3.1	A55, C2 and F3 are conserved in the OPXV genus .....	69
3.2	A55, C2 and F3 inhibit activation of the NF- $\kappa$ B signalling pathway .....	70
3.3	A55, C2 and F3 inhibit NF- $\kappa$ B downstream of p65.....	75
3.4	A55, C2 or F3 does not prevent I $\kappa$ B $\alpha$ degradation.....	78
3.5	A55, C2 and F3 diminish p65 nuclear translocation .....	79
3.6	Over-expressed C2 does not co-precipitate with cullin-3 or Flag-KPNA2 .....	82
4	Results 2 – C2 Co-IPs Cul3 when A55 is present.....	85
4.1	The problem of detecting C2 by immunoblotting .....	85
4.2	C2 co-immunoprecipitates Cul3 during infection .....	88
4.3	Cul3-C2 association is A55 dependent.....	90
5	Results 3 – VACV proteins A55 and C2 collaborate to target cellular proteins for degradation .....	98
5.1	Cellular targets of A55 and/or C2.....	99
5.1.1	Fer .....	99
5.1.2	RASA2 .....	100
5.1.3	FRMD6.....	101
5.1.4	Scrib .....	101
5.2	A55 and C2 collaborate to degrade Scrib.....	103
5.3	A55 and C2 are sufficient to degrade Scrib.....	106

5.4	Degradation of Scrib requires the interaction between A55 and Cul3.....	108
6	Results 4 – Role of Scrib in VACV infection and the mechanisms in antiviral signalling	115
6.1	Construction of Scrib knockout cell lines using CRISPR-Cas9 .....	115
6.2	Characterisation of VACV infection in Scrib KO cells .....	121
6.3	Loss of Scrib upregulates Smad signalling .....	125
6.3.1	VACV activates TGF- $\beta$ signalling.....	126
6.3.2	Loss of Scrib enhances TGF- $\beta$ stimulated Smad signalling .....	128
7	Results 5 – C2 is a potential Cdc42 activator .....	137
7.1	C2 associates with Cdc42.....	137
7.2	C2 is a potential Cdc42 activator .....	139
7.3	Loss of Cdc42 does not affect Scrib degradation by VACV .....	141
8	Discussion .....	144
8.1	A55, C2 and F3 are inhibitors of NF- $\kappa$ B pathway .....	145
8.2	C2 associates with Cul3 when A55 is present.....	149
8.3	A55 and C2 collaborate to target cellular proteins for degradation.....	151
8.4	Scrib in VACV infection .....	155
8.5	C2 is a potential Cdc42 activator .....	158
8.6	Summary .....	160
9	Bibliography .....	161

# 1 Introduction

## 1.1 Vaccinia virus

*Vaccinia virus* (VACV), the live vaccine used to eradicate smallpox (Fenner et al., 1998), is a member of the genus *Orthopoxvirus* (OPXV) of the family *Poxviridae*: a family of large double-stranded DNA viruses that replicate in the host cytoplasm (Fenner et al., 1988; Moss, 2013). There are two sub-families of *Poxviridae*: *Entomopoxvirinae* that infect insects and *Chordopoxvirinae* that infect vertebrates. The *Chordopoxvirinae* is subdivided into eight genera: *Avipoxvirus*, *Leporipoxvirus*, *Molluscipoxvirus*, *Suipoxvirus*, *Yatapoxvirus*, *Capripoxvirus*, *Parapoxvirus* and *Orthopoxvirus* (OPXV). The most intensively studied of these is the OPXV genus, including VACV, camelpox virus, cowpox virus, ectromelia virus, monkeypox virus and variola virus. Although VACV has been studied intensively, its origin and natural host remain unknown (Baxby, 1981). After smallpox was eradicated, VACV has continued to be studied because of its potential for development of new live vaccines and its use as a research tool. Genetically engineered VACV strains are being tested as vaccines for many diseases including infectious diseases such as HIV, malaria, Ebola and tuberculosis (TB), as well as tumours such as melanoma and other adenocarcinomas (Walsh and Dolin, 2011). As a research tool, recombinant VACVs are used to synthesise proteins and analyse structure-function relationships, and to study the innate immune system (Moss, 1991). Since the concept of reusing VACV as a vaccine for infectious diseases and tumours is attractive, improving the safety and potency of VACV as a vaccine has been an important area of research.

### 1.1.1 VACV genome

The VACV genome is a linear dsDNA molecule about 190 kb in length and encodes about 200 genes (Goebel et al., 1991). At each end there are inverted terminal repeat (ITRs), and the DNA strands are connected by hairpin loops to form a continuous polynucleotide chain (Geshelin and Berns, 1974). The ITRs contain sets of short, tandemly repeated sequences (Wittek and Moss, 1980). The VACV genome is A+T rich (67%), with little noncoding DNA and mRNAs are not spliced (Smith, 2008). The genome is generally divided into three regions: the central region, and the left and right terminal regions. The central region is about 100 kb and encodes proteins that are highly conserved between VACV strains and other OPXVs, most of which are essential for virus replication such as virion entry, DNA replication and gene expression regulation (Upton et al., 2003). The terminal regions encode proteins that are more variable between VACV strains and other OPXVs. These proteins are mostly nonessential for viral replication and are involved in virus host range, virulence and interactions with the host immune system (Gubser et al., 2004). VACV genes are named based on the nomenclature established for VACV strain Copenhagen (Goebel et al., 1991). The genome is divided into HindIII restriction fragments, lettered alphabetically according to size with A being the largest, and within each fragment the genes are numbered from left to right and given R (rightward) or L (leftward) to indicate the direction of transcription. The only exception to this is the HindIII C fragment in which genes are numbered from right to left. Thus, the A55R gene is the 55<sup>th</sup> gene within the HindIII A fragment and is transcribed rightward. More recently with other VACV strains, genes are numbered continuously from left to right across the whole genome (Moss, 2013). Note that genes within the ITRs are diploid.

### 1.1.2 VACV life cycle

Infected cells produce two morphologically different forms of infectious VACV particles, named the intracellular mature virus (IMV) also called mature virus (MV) and extracellular enveloped virus (EEV) also called extracellular virus (EV) (Roberts and Smith, 2008). IMV is brick-shaped with dimensions 250 nm x 250 nm x 350 nm, and contains the virus core and is surrounded by a single lipid membrane. The majority of IMVs are released upon cell lysis. However, some IMV are enveloped at sites away from the viral factory by 2 additional membranes to form a triple enveloped virion called intracellular enveloped virus (IEV) or wrapped virus (WV) (Roberts and Smith, 2008). This virion is transported to the cell surface on microtubules where the outer membrane fuses with the plasma membrane so externalising a double enveloped virus. If this virion remains attached to the cell surface it is called cell associated enveloped virus (CEV) whereas if it is released it is called EEV. Some authors refer to all extracellular virions as EV and do not distinguish between EEV and CEV.

As mentioned before, most IMVs are released by cell lysis, whilst some IMVs are transported and wrapped by a double membrane derived from early endosomes (Tooze et al., 1993) and the trans-Golgi network (Schmelz et al., 1994), leading to the production of intracellular enveloped virus (IEV) (Moss, 2006). IEVs are IMVs with two more membranes (three in total) and are transported to the cell surface on microtubules. The outer membrane of IEV fuses with the plasma membrane. These enveloped virion particles with two layers of membrane are either cell-associated enveloped virus (CEV) if retained on the cell surface (Blasco and Moss, 1992) or EEV if released from cell surface (Sanderson et al., 1998a). CEVs induce the formation of actin tails which drive viruses into neighbouring cells. In addition to cell-

to-cell spreading driven by actin tails, VACV can also be disseminated by IMV release after cell lysis, long-range dissemination of EEV and increased cell motility induced by VACV (Roberts and Smith, 2008; Sanderson et al., 1998b). VACV infection induces dramatic changes in cell function, metabolism and morphology. These phenotypes are collectively termed the cytopathic effect (CPE) (Sanderson and Smith, 1998), which includes the induction of early cell rounding, damage to the host genome and RNA, inhibition of host protein synthesis, increase in cell migration resulting from cytoskeletal remodelling and eventually, death of the infected cells (Bablanian, 1968; Sanderson et al., 1998b; Tsung et al., 1996).

IMV enters cells via direct fusion with the plasma membrane (Carter et al., 2005) or endocytosis (Townsend et al., 2006). EEV takes two steps to get rid of both membranes and to expose virion core into cells: first shedding the external membrane outside of cells and then fusion as an IMV with the plasma membrane (Law et al., 2006). Alternatively, EEV can be taken up by endocytosis then the same steps take place within an intracellular vesicle. After entry, the infecting viral core is transported on microtubules deeper into the cytoplasm (Carter et al., 2003). Unlike most other DNA viruses, poxviruses replicate and express their genomes within the cytoplasm instead of in the nucleus of the infected cells (De Silva et al., 2007). The viral core is partially uncoated, which allows the early mRNA transcription by the virus-associated DNA-dependent RNA polymerase. The early mRNAs further uncoat the core and lead to DNA replication. The perinuclear region of the infected cell where cores accumulate is called the viral factory, where immature virions (IVs) are assembled and processed to form IMV (reviewed in (Condit et al., 2006)).

### **1.1.3 Current studies of VACV**

After its use for the eradication of smallpox, VACV has continued to be studied as a tool to further explore biology and to develop therapeutics to battle infectious and cancerous diseases in the modern world.

#### **1.1.3.1 Oncolytics**

VACV has desirable characteristics to be an oncolytic virus for clinical application, for example, 1) it is highly cytolytic for a wide range of tumour cell types; 2) it does not integrate its genome into the host genome; 3) proven success in safely treating patients with advanced cancer (Minev et al., 2019). Several phase I clinical studies have demonstrated the safety and anticancer effect on patients who received oncolytic VACV with attenuated virulence (Lauer et al., 2018; Mell et al., 2017; Minev et al., 2019).

#### **1.1.3.2 Model for virus-host interactions**

VACV is a good model to study virus-host interactions. VACV IMV was shown to use micropinocytosis and apoptotic mimicry to enter host cells (Mercer and Helenius, 2008). IMV causes the formation of blebs in the plasma membrane, and the IMV membrane is enriched in phosphatidylserine (PS) (Ichihashi and Oie, 1983). During apoptosis, PS is exposed on the external leaflet of the plasma membrane (Leventis and Grinstein, 2010). By mimicking apoptosis, VACV tricks cells to uptake its very big viral particle without triggering immune detection. Now about 20 clinically relevant viruses have been shown to employ this apoptotic mimicry entry pathway, such as hepatitis A virus, dengue virus and Ebola virus (Amara and Mercer, 2015). VACV is a safer virus to work with than Ebola, and its research shed light on the potential target for the treatment of Ebola infection.

### 1.1.3.3 Vaccines

The COVID-19 pandemic, a global outbreak of the novel severe acute respiratory syndrome coronavirus 2 (SARS-CoV-2) which started in late 2019, and the acute respiratory disease caused by the virus, COVID-19 (coronavirus disease) ((WHO), 2020), has caused >21 million infections and more than 0.75 m deaths (August 2020) (Dong et al., 2020). More than 10 clinical trials of anti-viral drugs such as remdesivir and other treatment options such as neutralising antibodies and even the use of convalescent serum are undergoing (Amanat and Krammer, 2020), however vaccine development is still pursued as the ultimate solution.

VACV has several useful features as an expression system, including: 1) the high capacity for foreign DNA of at least 25 kb (Smith et al., 1983), 2) easy methods to construct recombinant viruses, 3) ability to infect a wide option of cell types, 4) cytoplasmic replication and not integrating its genome into the host genome and 5) relatively high expression levels (Moss, 1996). Those advantages, plus the proven success of eradicating smallpox, have brought VACV once again into the spotlight during the pandemic. Recombinant VACV strains expressing foreign genes were already shown to have potential application as vaccines as they could induce both antibody and T-cell responses to the foreign antigen (Bennink et al., 1984). The highly attenuated strain modified vaccinia virus Ankara (MVA) has little or no replication in most mammalian cells, hence could be used as an expression vector with a high degree of safety, even for immune-deficient animals (Stickl et al., 1974). MVA has already been used to research and develop vaccines against AIDS, TB and malaria (Sebastian and Gilbert, 2016; Volz and Sutter, 2017). MVA expressing full-length MERS (Middle East respiratory syndrome) -CoV spike (S) glycoprotein can induce specific CD8<sup>+</sup> T cells and virus-neutralising antibodies in mice (Volz et al.,

2015), and to induce a safe immunisation against MERS-CoV in a phase 1 clinical trial (Koch et al., 2020). Although it is unlikely that MERS-CoV vaccines would induce strong cross-neutralising antibodies against SARS-CoV-2 due to the phylogenetic distance between the two viruses, the initial success in MERS-CoV can be applied to SARS-CoV-2. In fact about four MVA-based and one horsepox vaccine (another VACV strain) candidates are being investigated among all studies utilising either novel or conventional vaccine technology according to a WHO report (WHO, 2020).

In addition to therapeutic values, VACV also serves as a system to study cellular biology, as many viral proteins are homologues of cellular proteins, such as VACV B1 (Bidgood, 2019). B1 is highly conserved among poxviruses although it is missing from molluscum contagiosum virus, and is essential for viral replication (Rempel et al., 1990). As a protein kinase, B1 was found to share ~40% identity with a group of cellular serine/threonine kinases, leading to the discovery of VACV-related kinases (VRKs) (Nezu et al., 1997), probably due to the viral evolution to mimic VRK activity. VRKs play important roles in regulating DNA replication, cell cycle progression and cell proliferation. VRKs are also involved in several cancers including liver, lung and breast cancer (Huang et al., 2016; Kim et al., 2015; Salzano et al., 2014), thus have been treated as potential drug targets to battle cancer. VACV B1 studies are still ongoing to better understand the VRK family (Olson et al., 2017).

## **1.2 VACV-host interplay**

### **1.2.1 Immune response**

Hosts deploy innate and adaptive immune responses against virus infection and in turn viruses have evolved countermeasures. The study of viral evasion strategies

aids understanding of the how the innate immune system works. The initiation of the immune response to an invading pathogen such as a virus requires the host to sense the organism and/or cellular metabolic changes and damage caused by infection. This initial response to infection is primarily performed by germline-encoded pattern recognition receptors (PRRs) triggered by pathogen-associated molecular patterns (PAMPs) (reviewed by (Janeway and Medzhitov, 2002)). A variety of PRRs are expressed by the innate immune system and are located on the cell surface, in intracellular compartments (cytoplasm or nucleus) or secreted into the bloodstream and tissue fluids (Medzhitov and Janeway Jr, 1997). Four major sub-families of PRRs have been identified, including the Toll-like receptors (TLRs), the nucleotide-binding oligomerisation domain (NOD)-leucine-rich repeats (LRR)-containing receptors (NLR), the retinoic acid-inducible gene 1 (RIG-1) -like receptors (RLR; also known as RIG-1-like helicases—RLH), and the C-type lectin receptors (CLRs) (Walsh et al., 2013). PRRs then activate immune signalling pathways and lead to the activation of transcription factors to promote expression of pro-inflammatory molecules such as cytokines, chemokines and type I interferons (IFNs). These may restrict virus replication and activate immune cells (macrophages, neutrophils, dendritic cells (DCs) and natural killer (NK) cells), among which NK cells serve as the major innate immune effector cells. PRRs also inhibit viral spreading by inducing apoptosis in infected cells (Williams, 1999). After release from cells, cytokines, chemokines and IFNs engage with their receptors on the cell surface, inducing inflammation that amplifies the immune response and recruits other immune cells to the infection sites (reviewed by (Medzhitov, 2007)). During these processes, IFNs induce signalling via the JAK-STAT pathway leading to the transcription of a diverse range of genes called IFN-stimulated genes (ISGs), which

restrict viral infection by multiple mechanisms (Randall and Goodbourn, 2008). Innate immunity restrains virus replication and/or spreading, and promotes the elimination of the infection until the antigen-specific long-lasting adaptive immune responses are developed (Bonilla and Oettgen, 2010).

PRR-mediated signalling activates antigen-presenting cells (APCs) such as DCs and macrophages to upregulate the expression of MHC class II molecules, co-stimulatory molecules (such as CD80 and CD86) and pro-inflammatory cytokines (type I IFNs, tumour necrosis factor (TNF), interleukin (IL)-1, IL-6 and IL-12) (Takeuchi and Akira, 2010). Activated professional APCs migrate to draining lymph nodes where they prime naïve virus-specific CD4<sup>+</sup> T cells to differentiate into antiviral effectors. CD4<sup>+</sup> T cells promote antibody production by B cells and enhance effector CD8<sup>+</sup> T cell responses and memory during certain viral infection infections such as VACV (reviewed by (Swain et al., 2012)). The co-stimulatory ligands expressed by CD4<sup>+</sup> T cells such as CD40 ligand (CD40L) contribute to B cell activation and antibody production. The interaction between CD40L and CD40 (expressed on B cells) is crucial for humoral responses against some viruses such as HSV (Edelmann and Wilson, 2001).

During infection, some of the viral proteins will be degraded into peptide fragments, which will be presented on MHC class I molecules to be recognised by CD8<sup>+</sup> T cells. Viral antigens from virions or infected cells may also be picked up and processed by professional APCs to present viral peptides on MHC class I and class II molecules. CD4<sup>+</sup> T cells recognise MHC class II-peptide complexes on APCs and activate APCs by the interaction of CD40 and CD40L (on DCs). Activated APCs such as DCs can upregulate the expression of maturation markers CD80/CD86, which interact with CD28 on naïve CD8<sup>+</sup> T cells. Both the CD28 signalling and the recognition of

the MHC class I-peptide complex by the T cell receptor (TCR) on CD8<sup>+</sup> T cells leads to the activation of the CD8<sup>+</sup> T cells, which then release cytotoxic granules, induce apoptosis in virus-infected cells and produce cytokines such as TNF- $\alpha$  and IFN- $\gamma$ . After the primary infection, some activated T cells will develop into memory T cells and can rapidly mature into effector cells should a secondary infection happen (reviewed by (Sietske et al., 2014)).

During innate immune responses, several signalling pathways including the NF- $\kappa$ B, IRF3 and MAPK signalling pathways are important in stimulating the synthesis of IFNs, cytokines and chemokines in response to PAMP recognition. Extensive studies have shown that VACV encodes a plethora of proteins to regulate those signalling pathways.

#### **1.2.1.1 The NF- $\kappa$ B (nuclear factor kappa light-chain enhancer of activated B cells) signalling pathway**

NF- $\kappa$ B represents a family of inducible transcription factors that play an important role in almost all mammalian cells, controlling DNA transcription, cytokine production, cell survival and other important cell events, especially in regulating the immune response to infection (Oeckinghaus and Ghosh, 2009). The NF- $\kappa$ B family is composed of five structurally related members, including NF- $\kappa$ B1 (p50), NF- $\kappa$ B2 (p52), RelA (p65), RelB and c-Rel. These NF- $\kappa$ B members bind to a specific DNA element ( $\kappa$ B enhancer) as hetero- or homo- dimers to mediate transcription of target genes (Sun et al., 2013).

NF- $\kappa$ B is activated by two signalling pathways – the canonical and noncanonical pathway. The activation of the canonical NF- $\kappa$ B pathway is a common event especially in response to PRRs activation expressed by innate immune cells

including macrophages, DCs and neutrophils, leading to the transcriptional induction of pro-inflammatory cytokines (e.g. IL-1, IL-2, IL-6, IL-18, TNF- $\alpha$ ) and chemokines (IL-8, CXCL10). The canonical NF- $\kappa$ B pathway also regulates the activation and differentiation of T cells of adaptive immune response, for which the noncanonical NF- $\kappa$ B pathway is nonessential (reviewed by (Liu et al., 2017)).

The canonical NF- $\kappa$ B pathway begins from the activation of cell surface receptors of pro-inflammatory cytokines and PAMPs, such as TNF receptors (TNFRs), PRRs, TLRs and T/B cell receptor (Zhang and Sun, 2015). Different PRR pathways converge at the transforming growth factor- $\beta$ -activated kinase 1 (TAK1) (Sato et al., 2005), with 2-3 regulatory subunits TAB1/2/3. TAB2 binds poly-ubiquitin chains and is required for TAK1 activation. TAK1 then activates the I $\kappa$ B kinase (IKK) complex (Karin and Delhase, 2000). IKK is composed of two catalytic subunits, IKK $\alpha$  and IKK $\beta$ , and a regulatory subunit NF- $\kappa$ B essential modulator (NEMO) (also known as IKK $\gamma$ ) (Israël, 2010). Once activated, IKK phosphorylates I $\kappa$ B $\alpha$ , triggering the ubiquitin-dependent proteasomal degradation of I $\kappa$ B $\alpha$ , which then releases canonical NF- $\kappa$ B members, predominantly the p65/p50 heterodimer, into the nucleus (Hayden and Ghosh, 2008). Here it binds to the  $\kappa$ B enhancer and stimulates gene expression through the transcriptional activation domain (TAD) of p65 (Ghosh and Karin, 2002) (Figure 1.1). The posttranslational modifications (phosphorylation, acetylation and methylation) of p65 play a key role in regulating the transcriptional activity of NF- $\kappa$ B. Especially, the reversible acetylation of p65 by enzymes such as p300/CBP regulates diverse functions of NF- $\kappa$ B, including DNA binding activity, transcriptional activity and association ability with I $\kappa$ B $\alpha$ , thus playing important roles in the NF- $\kappa$ B-mediated inflammatory response (reviewed by (Huang et al., 2010)). In addition, the nuclear translocation of p65/p50 is regulated by nucleocytoplasmic transport

mediators. For example, karyopherin alpha 2 (KPNA2) interacts with the nuclear localisation signal of p65, and transports the p65/p50 dimer into the nucleus in TNF- $\alpha$ -treated A549 cells (Liang et al., 2013a).

Unlike the canonical pathway, the noncanonical NF- $\kappa$ B pathway responds selectively to a specific group of stimuli, such as the ligand of the TNFR family member CD40, and it does not involve I $\kappa$ B $\alpha$  degradation. The central signalling molecule NF- $\kappa$ B-inducing kinase (NIK) activates IKK $\alpha$ , and the latter phosphorylates the NF- $\kappa$ B2 (p52) precursor protein p100, leading to p100 ubiquitylation and processing to generate mature p52. The noncanonical NF- $\kappa$ B complex p52/RelB then translocates into the nucleus. The noncanonical NF- $\kappa$ B is involved in the regulation of certain functions of the adaptive immune system as a supplementary signalling in collaboration with canonical NF- $\kappa$ B pathway (reviewed by (Liu et al., 2017)).

Besides PAMPs and pro-inflammatory factors, a group of proteins called the TNFR-associated factors (TRAFs) activate both canonical and noncanonical NF- $\kappa$ B pathways (Zhang et al., 2011). The TRAF family has 6 typical members (TRAF1-6) and an atypical member (TRAF7). Except TRAF1, all TRAF members contain a RING domain (really interesting new gene) (Ha et al., 2009) which mediates protein ubiquitylation of the E3 ubiquitin ligases (Deshaies and Joazeiro, 2009). TRAF6 has a crucial role in mediating signalling from TNFRs as well as other immune receptors such as the IL-1 receptor, TGF- $\beta$  receptor and antigen receptors. TRAF6 conjugates ubiquitin chains onto itself as well as TAB2/3 (Kanayama et al., 2004), NEMO (Liu and Chen, 2011), and TAK1/IKK (Lamothe et al., 2007). TRAF2 functions in TNFR1 and TNFR2 signalling. TRAF2 binds to the cytoplasmic domain of TNFR2 and recruits E3 ubiquitin ligases cIAP1 and cIAP2. Upon activation, cIAPs conjugate K63-linked ubiquitin chains to receptor-interacting protein kinase 1 (RIP1), which

recruits and activates TAK1 and recruits linear ubiquitin ligase complex (LUBAC). LUBAC further conjugates linear ubiquitin chains to NEMO. The activation of both TAK1 and NEMO leads to the downstream activation of NF- $\kappa$ B. In TNFR1 signalling, instead of binding to TNFR1 receptor, TRAF2, along with TRAF5, forms a complex with TNFR1, TNF receptor-associated death domain (TRADD), RIP1 and cIAPs (reviewed by (Shi and Sun, 2018)).

So far 16 VACV proteins (13 published; unpublished: C2 and F3 in this thesis; C16 (Scutts, 2017)) have been shown to inhibit NF- $\kappa$ B signalling pathway. These proteins are expressed early during infection, and interfere with the NF- $\kappa$ B signalling at different stages of the pathway. For example from up- to downstream, VACV B15 (Alcami and Smith, 1992), cytokine response modifier C (CrmC, protein A53) and E (CrmE) (Alcami et al., 1999) act as soluble IL-1 $\beta$  or TNF receptors to compete with the interaction between IL-1 $\beta$ /TNF and the respective host receptors. A52 and K7 interact with TRAF6 (Harte et al., 2003; Schröder et al., 2008b). VACV B14 binds IKK $\beta$  and prevents IKK $\beta$  phosphorylation and activation (Chen et al., 2008; Tang et al., 2018). A49 binds the E3 ligase  $\beta$ -TrCP and prevents the ubiquitylation and degradation of I $\kappa$ B $\alpha$  (Mansur et al., 2013). A55 associates with KPNA2 to impair p65 translocating to the nucleus (Pallett et al., 2019). K1 acts at one of the most downstream events of NF- $\kappa$ B activation because it inhibits CBP/p300-mediated NF- $\kappa$ B activation and prevents p65 acetylation (Bravo Cruz and Shisler, 2016). N1 has also been reported to inhibit NF- $\kappa$ B activation (DiPerna et al., 2004), however it is disputed whether N1 inhibits the pathway by binding to IKK complex (Chen et al., 2008) and the mechanism by which N1 inhibits the pathway remains unclear. A full list of published VACV NF- $\kappa$ B inhibitors (Smith et al., 2013) except A55 (Pallett et al., 2019) and C16 are summarised in (Scutts, 2017).

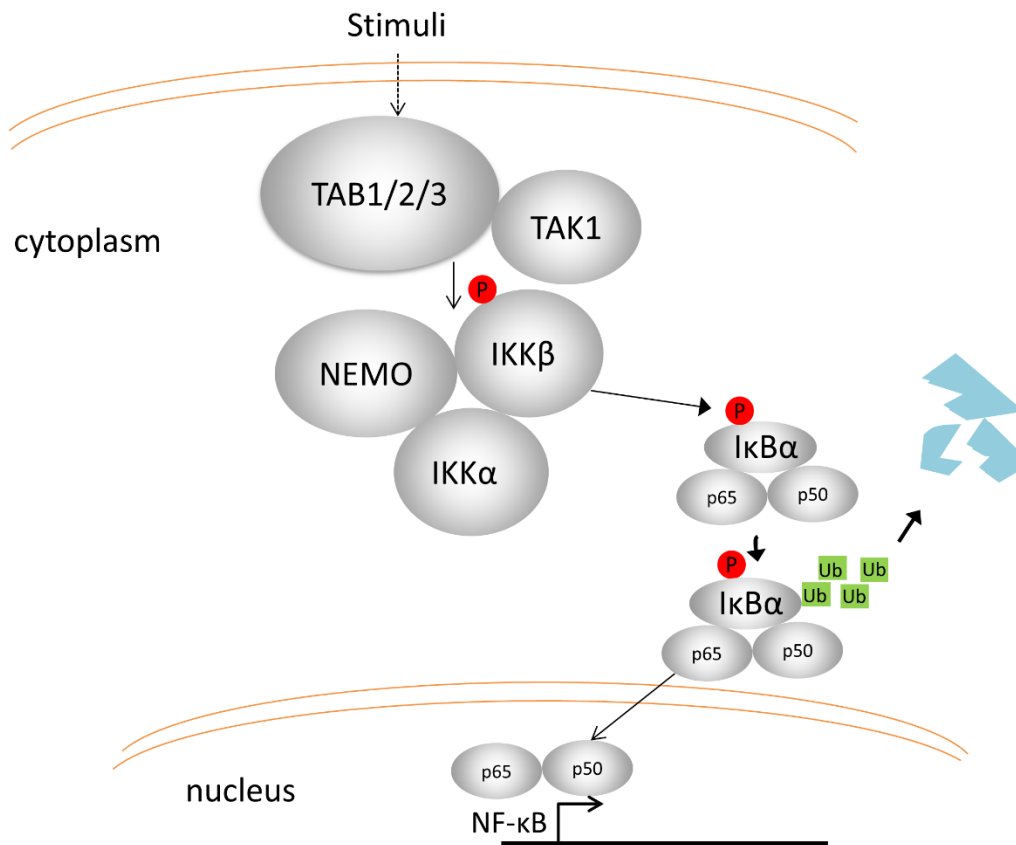


**Figure 1.1. Simplified canonical NFκB signalling pathway.** Upon external or internal stimulation the TAK/TAB complex is activated, which phosphorylates IKKα or IKKβ. The activated IKK complex further phosphorylates IκBα, leading to its ubiquitylation and degradation, freeing NF-κB subunits to translocate into the nucleus, and to induce transcription from NF-κB responsive genes that encode cytokines, chemokines and IFNs.

### 1.2.1.2 The IRF3 (interferon (IFN) regulatory factor 3) signalling pathway

Antiviral signalling is also regulated by IRF3 signalling pathway. IRF3 is essential for innate immune response and type I IFN production. Viral RNA, cytosolic DNA and the bacterial cell wall component lipopolysaccharide (LPS) activate downstream signalling through PRR-adaptor protein pairs, including RIG-I-MAVS, cGAS-STING and TLR3/4-TRIF. MAVS, STING and TRIF activate IKKξ and TBK1 through adaptor proteins, which then recruit and phosphorylate IRF3. Phosphorylated IRF3 dimerises and enters the nucleus to induce transcription of IFNα, cytokines and chemokines (reviewed by (Liu et al., 2015)). For example, upon recognition of viral RNA, the

CARD domain of RIG-I is exposed and binds to the E3 ubiquitin ligase TRIM25, which then conjugates K63 polyubiquitin chains (Gack et al., 2007). The K63 ubiquitin chains promote the interaction between RIG-I and MAVS, and the latter recruits E3 ligases TRAF2, TRAF5 and TRAF6 to synthesise more polyubiquitin chains that recruit NEMO to the MAVS complex, leading to the recruitment and activation of IKK and TBK1 (Liu et al., 2013).

IRF3 is essential for the innate immune response, making it a target of viral infection. For example, VACV C6 inhibits IRF3 activation downstream of TBK1 and IKK $\xi$ , by associating with the TBK1 complex scaffold proteins TRAF family member-associated NF- $\kappa$ B activator (TANK), NAK-associated protein 1 (NAP1) and similar to NAP1 TBK1 adaptor (SINTBAD) (Unterholzner et al., 2011b). K7 binds to DDX3, an adaptor for TBK1 and IKK $\xi$ , or directly interacts with the IFN- $\beta$  promoter to inhibit IRF3 signalling (Mulhern and Bowie, 2010; Schröder et al., 2008a; Soulat et al., 2008). N2 inhibits IRF3 activation in the nucleus by an unknown mechanism (Ferguson et al., 2013).

#### **1.2.1.3 The MAPK (mitogen-activated protein kinase) signalling pathway**

MAPKs are serine/threonine kinases regulated by a cascade phosphorylation system, in which a series of three protein kinases, MAPKKK (MAPK kinase kinase), MAPKK (MAPK kinase) and MAPK are phosphorylated and activated sequentially. MAPKs are grouped into three main families in mammals, including ERKs (extracellular signal regulated kinases), JNKs (Jun amino-terminal kinases) and p38 isoforms (reviewed by (Morrison, 2012)). The ERK pathway is mainly activated by growth factors and hormones whilst the JNK and p38 pathways are activated by environmental stress and pro-inflammatory cytokines. Once activated MAPKs translocate into the nucleus and phosphorylate a large number of substrates

(Cargnello and Roux, 2011). Among the substrates, MAPK increases and regulates the abundance and trans-activating capacities of DNA-binding proteins: Jun family, Fos family and ATF family. The basic region-leucine zipper (bZIP) proteins of these three protein families as well as of the Maf family, form homo- or hetero- dimers transcription factor named activating protein 1 (AP-1). AP-1 binds and controls the transcription of several genes containing AP-1 sites also known as TPA-responsive elements (TREs) (Angel and Karin, 1991) with critical functions in a wide variety of cellular processes, including inflammation, proliferation, differentiation and apoptosis (Gazon et al., 2018).

MAPK signalling is upregulated during VACV infection to support viral replication and spread (de Magalhães et al., 2001). VACV-induced growth factor (VGF), a secreted virulence factor, shares structural homology with epidermal growth factor (EGF) and competes with EGF for binding to EGF receptor (EGFR) (Twardzik et al., 1985), leading to the activation of EGFR-Ras-MEK-ERK and the enhancement of cell survival (Postigo et al., 2009). VACV A52, B14 and K7 also contribute to AP-1 activation during VACV infection by unclear mechanisms (Torres et al., 2016).

VACV has evolved many strategies to counteract the host response that restricts virus replication and spread (Smith et al., 2013) and additional VACV proteins that inhibit innate immune signalling pathways probably remain to be identified. A better understanding of these immunomodulators will provide potential to create more immunogenic VACV strains. In addition to modulating the host immune response, VACV deploys other strategies such as targeting cell motility and apoptosis signalling in order to benefit viral replication and/or spreading.

### 1.2.2 Other cellular signalling pathways

Poxviruses in general, and VACV in particular, are known to cause a cytopathic effect (CPE) in infected cells, which includes the induction of early cell rounding, increase in cell migration resulting from cytoskeletal remodelling and eventually, death of the infected cells (Bablanian, 1968; Sanderson et al., 1998b; Tsung et al., 1996). VACV promotes cell motility (Sanderson et al., 1998b), and the viral factors such as F11L (Valderrama et al., 2006; Zwilling et al., 2010) and VGF (Beerli et al., 2019) promote infected cell motility and it was suggested that this enhanced the spread of viral infection. Given that epithelial cells, particularly at the skin, are the primary sites of infection for many poxviruses, and due to the shared characteristics of VACV-infected cells, such as the induction of migratory and invasive properties in infected cells, VACV CPE has been linked to EMT (epithelial to mesenchymal transition) as a potential mechanism of viral spread within the host (McKenzie, 2016). EMT is an integral process in development, wound healing and cancer progression (Kalluri and Weinberg, 2009; Thiery et al., 2009). In this process, epithelial cells lose their polarity and associations with neighbouring cells and become invasive and motile, subsequently separating from the epithelium to take on mesenchymal characteristics (Lamouille et al., 2014). Because VACV CPE is reminiscent of EMT processes such as cell migration, elongation and detachment, it has been proposed that VACV repurposes EMT signalling pathways to force a mesenchymal transition to enhance viral spread (Gowripalan, 2018).

There are three major EMT signalling pathways, namely TGF- $\beta$ , Wnt and Notch signalling (Lamouille et al., 2014). VACV upregulates TGF- $\beta$  during infection (Beerli et al., 2019; Gowripalan et al., 2019), and ectopic VACV protein A49 upregulates Wnt signalling (Maluquer de Motes and Smith, 2017).

TGF- $\beta$  signalling is initiated by extracellular TGF- $\beta$  superfamily members (TGF- $\beta$ , BMPs (bone morphogenetic protein), activins, GDFs) binding to their heterodimeric transmembrane receptor complexes. Binding of a constitutively active kinase, the type II TGF- $\beta$  receptor, leads to the phosphorylation of the type I receptor, which in turn phosphorylates Smad family proteins (Javelaud and Mauviel, 2004). Receptor-activated Smads (R-Smads) are ligand-specific: Smad1, Smad5 and Smad8 are phosphorylated by BMP receptors whilst Smad2 and Smad3 are activated by TGF- $\beta$  and activating receptors. The R-Smads form heteromeric complexes with the common mediator for all Smad pathways, Smad4, and then translocate to the nucleus. In the nucleus, this signalling complex initiates transcription of Smad target genes with the assistance of DNA binding partners (DBPs). More than 500 genes have been identified as Smad targets (Massagué et al., 2005). In certain conditions, a subclass of Smads, known as the inhibitory Smads, Smad7 and Smad6, are able to impede signalling by inhibiting R-Smads phosphorylation (Figure 1.2). Loss of components of cell adhesion and polarity promotes EMT, and TGF- $\beta$  is involved in promoting EMT during both development and disease (Thiery et al., 2009). The link between TGF- $\beta$  and cell polarity proteins has been studied. For example, an essential factor for cell polarity named Scrib has been shown to downregulate TGF- $\beta$  signalling (Yamben et al., 2013).

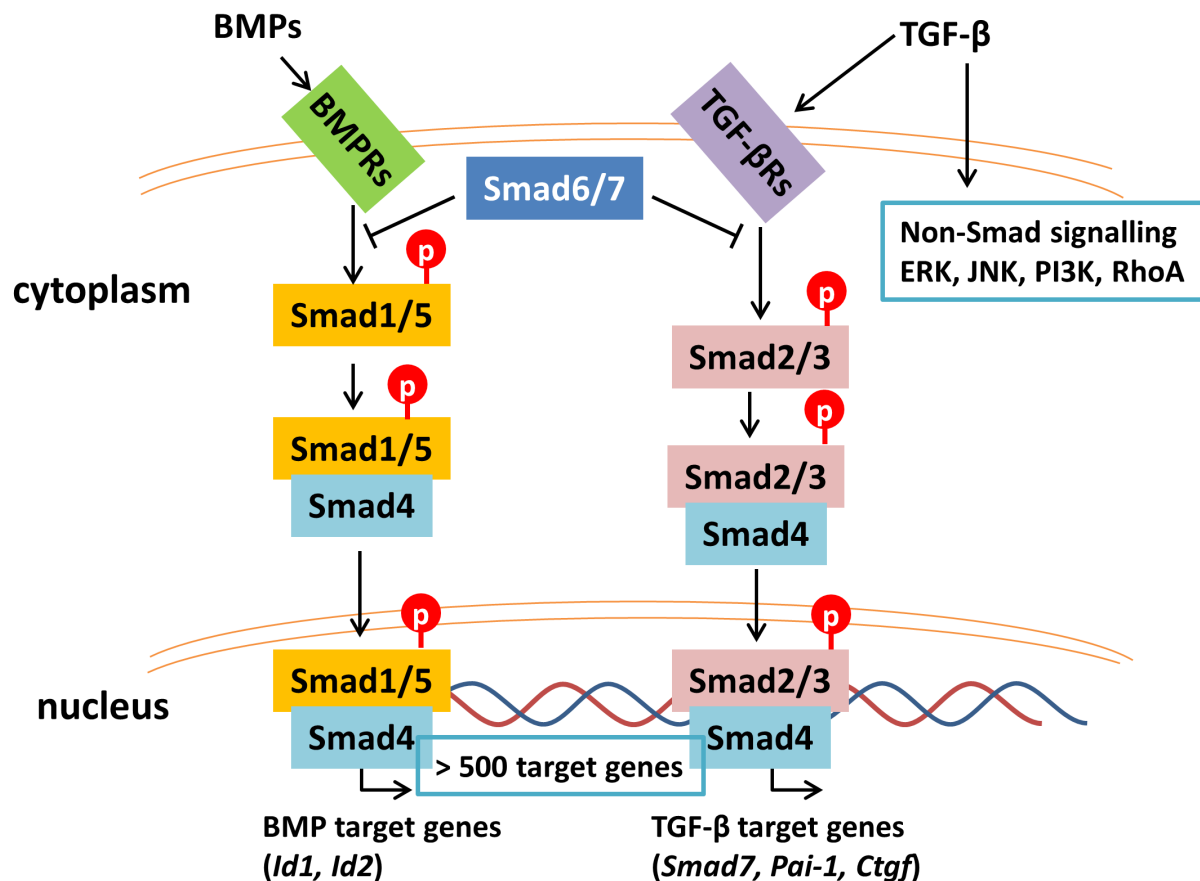


**Figure 1.2. The TGF- $\beta$  signalling pathway.** Signalling is initiated by extracellular TGF- $\beta$  superfamily members binding to their heterodimeric transmembrane receptor complexes at the cell surface. Binding of a constitutively active kinase, the type II TGF- $\beta$  receptor, leads to the phosphorylation of the type I receptor, which then phosphorylates Smad family proteins. The R-Smads form heteromeric complexes with Smad4, the common mediator for all Smad pathways, and then translocate to the nucleus. In the nucleus this signalling complex initiates transcription of Smad target genes with the assistance of DBPs. A subclass of Smads, known as the inhibitory Smads, Smad7 and Smad6, are able to impede signalling by inhibiting R-Smads phosphorylation in certain conditions. Diagram is adapted from (Mauviel et al., 2012).

### 1.2.3 VACV-induced cell motility

VACV induces two forms of cell motility: cell migration and formation of cellular projections, controlled by the expression of early and late genes respectively (Sanderson et al., 1998b). Both the cell motility changes are key events in VACV-induced CPE, which resembles wound healing and tumour metastasis

(Lauffenburger and Horwitz, 1996). The Rho GTPase family, Rac1/Cdc42 and RhoA have been well demonstrated to control cell motility by regulating actin dynamics for leading edge extension and rear edge retraction (Ridley, 2015).

VACV F11 is required for VACV-induced cell motility by inhibiting RhoA signalling. F11 binds RhoA and blocks RhoA interaction with its downstream effectors Rho-associated kinase (ROCK) and mDia (Valderrama et al., 2006). F11 promotes migration of infected cells. Loss of F11 or its ability to interact with RhoA also significantly reduces actin tails and cell-to-cell viral spread, and maintains cell-to-cell contacts. A virus lacking F11 showed reduced viral spreading to lungs and spleen in intranasal mouse models of infection (Cordeiro et al., 2009). However F11 alone is not sufficient for VACV-induced cell migration, and other factors seem to be required (Zwilling et al., 2010). Another example is VGF, the VACV homolog of EGF. Viruses lacking VGF produce plaques with reduced size and decreased cell migration. The activation of EGFR/MEK/FAK signalling is critical for cell motility and cell-to-cell virus spread. VGF mimics EGF to activate this pathway and hijacks cell movement to spread infection (Beerli et al., 2019).

#### **1.2.4 Apoptosis**

In host defence, three mechanisms are used to molecularly control cell death, i.e. apoptosis, necroptosis and pyroptosis, and eliminate infected cells (Amarante-Mendes et al., 2018). Apoptosis is a genetically encoded programme leading to cell death and production of immunosuppressive cytokines (Griffith and Ferguson, 2011). Apoptosis typically goes through two signalling cascades, the intrinsic and extrinsic pathways, and both lead to the activation of the executioner caspases, caspase 3 and caspase 7. In the extrinsic pathway, ligands such as FAS or TNF are recognised by a death receptor, leading to the recruitment of FAS-associated death domain

protein (FADD). FADD binds, dimerises and activates caspase 8, which directly activates caspase 3 and caspase 7. The intrinsic pathway is initiated by apoptotic stimuli such as DNA damage or ER stress. B-cell lymphoma 2 (Bcl-2) homology 3 (BH3)-only proteins are then activated, leading to the activation of Bcl-2-associated X protein (BAX) and Bcl-2 antagonist or killer (BAK). BAX and BAK cause the crucial event of mitochondrial outer membrane permeabilisation (MOMP). Proteins such as cytochrome c are released from the mitochondrial intermembrane space (IMS). Cytochrome c then binds apoptotic protease-activating factor 1 (APAF1), causing oligomerisation and the apoptosome structure, which recruits and activates caspase 9. Caspase 9 cleaves and activates caspase 3 and caspase 7, leading to apoptosis (reviewed by (Tait and Green, 2010)). Alternatively, apoptosis also encompasses caspase-independent cell death (CICD) (Tait and Green, 2008).

Viruses have evolved molecular strategies to subvert host cell apoptotic defences (Kvansakul, 2017). VACV encodes several proteins to inhibit apoptosis signalling at different stages (Veyer et al., 2017), including B13 (Dobbelstein and Shenk, 1996; Kettle et al., 1997), E3 (Kibler et al., 1997), F1 (Wasilenko et al., 2003), N1 (Cooray et al., 2007), Golgi anti-apoptotic protein (GAAP, present in some VACV strains) (Gubser et al., 2007) and M1 (Ryerson et al., 2017). For example, the most potent apoptosis inhibitor from VACV, B13 (Veyer et al., 2014), protects FAS or TNF-induced apoptosis and targets caspase 8 (Dobbelstein and Shenk, 1996) and caspase 3 (Veyer et al., 2014).

### **1.2.5 VACV and the cellular ubiquitin system**

Ubiquitin is a 76 amino acid protein that is important for protein degradation and post-translational modification (Pickart and Fushman, 2004). Proteins are modified by mono-ubiquitin or poly-ubiquitin in 3 steps: first, ubiquitin activation by ubiquitin

activating enzyme (E1); second, ubiquitin transfer to a ubiquitin-conjugating enzyme (E2); third, ubiquitin transfer to the target protein by a ubiquitin ligase (E3) (Barry et al., 2010; Komander and Rape, 2012).

E3s are the most heterogeneous class of enzymes in the ubiquitylation pathway and RING E3s are the most abundant type of ubiquitin ligases. RING E3s are characterised by the presence of a zinc-binding domain named RING (Really Interesting New Gene), which is responsible for binding the ubiquitin-charged E2 and stimulating ubiquitin transfer. Some RING E3s are composed of multiple subunits, such as the cullin-RING ligases (CRLs) (reviewed by (Morreale and Walden, 2016)). Cullins are a family of hydrophobic scaffold proteins which bind a RING protein at its N terminus and an adaptor protein and a substrate receptor (responsible for substrate specificity) at its C terminus (Morreale and Walden, 2016). The human genome contains eight cullin genes, including Cul1, Cul2, Cul3, Cul4A, Cul4B, Cul5, Cul7 and Cul9 (Bosu and Kipreos, 2008).

The ubiquitin-proteasome system is involved in regulating many important host pathways including antigen presentation, cell cycle progression, signal transduction and DNA repair (Weissman, 2001), and therefore has become an attractive target by viruses. Ubiquitin constitutes at least 3% of the total protein in VACV virions (Chung et al., 2006). In fact, a functional ubiquitin-proteasome is necessary for the replication cycle of poxviruses, and inhibition of the ubiquitin-proteasome system by proteasome inhibitors such as MG132 interferes with the formation of virus factories, prevents VACV DNA replication, prolongs early gene expression, and inhibits the expression of intermediate and late genes (Teale et al., 2009). Specifically, MG132 mediates its adverse effect 2-4 h after infection, the time of the onset of viral DNA synthesis (Satheshkumar et al., 2009).

Poxviruses deploy various strategies to target and subvert host ubiquitin systems (reviewed by (Barry et al., 2010)). For example, poxviruses encode Ankyrin-F-box-like proteins and BTB-Kelch proteins to interact with cellular Cul1 and Cul3, respectively. Ectromelia virus (ECTV) encodes 4 Ankyrin-F-box proteins EVM002, EVM005, EVM154 and EVM165. These proteins contribute to the inhibition of NF- $\kappa$ B activation by preventing I $\kappa$ B $\alpha$  degradation potentially via targeting SCF (Skp1, Cul1, F-box) ubiquitin ligase, as I $\kappa$ B $\alpha$  is recruited to the SCF and degraded by the F-box domain containing protein  $\beta$ TrCP (Burles et al., 2014). VACV A49 binds the E3 ligase  $\beta$ -TrCP and prevents the ubiquitylation and degradation of I $\kappa$ B $\alpha$  (Mansur et al., 2013). In addition, poxviruses encode their own RING-domain-containing ubiquitin ligase as well (Shchelkunov, 2010; Zhang et al., 2009).

Poxvirus proteins can also be modified by host ubiquitin. For example VACV N1 is covalently ubiquitylated both during viral infection and following ectopic expression (Maluquer de Motes et al., 2014). A global LC-MS/MS-based ubiquitinome analysis identified 137 conserved ubiquitylation sites in 54 viral proteins among five CPXV (cowpox virus) strains and revealed extensive ubiquitylation of structural core proteins (Grossegesse et al., 2018).

Among the proteins encoded by VACV to exploit the ubiquitin-proteasome system, three proteins have a BTB-Kelch structure including A55, C2 and F3. Proteins containing BTB and Kelch domains function as adapters for the Cul3-based ubiquitylation system. In theory, a BTB-Kelch protein interacts with Cul3 via its BTB domain and substrates via its Kelch domain, leading to the ubiquitylation, modification or degradation of substrates.

### 1.3 BTB-Kelch proteins

The BTB and Kelch domains have distinct structures and binding partners, and they are brought together in the BTB-Kelch proteins. Therefore, the BTB and Kelch domains are described separately before discussing proteins containing both domains.

#### 1.3.1 Kelch proteins

Kelch proteins (Kelch-like proteins) are a superfamily of proteins that contain multiple Kelch motifs. Kelch proteins are arranged in five subgroups based on their molecular architecture and one of those is the subgroup of BTB-Kelch proteins that contain an N-terminal BTB/POZ domain (for Broad-Complex, Tramtrack and Bric-a-brac; also known as a Poxvirus and Zinc-finger domain) and four to six Kelch motifs located within the C-terminal region (Adams et al., 2000).

The name Kelch derives from a mutation in *Drosophila* egg chambers that causes the malformation of the egg shell, and, in some most extreme cases, the anterior of the egg shell is open, forming a cup shape. Therefore, the mutated gene was named Kelch, German for goblet (Schupbach and Wieschaus, 1991; Xue and Cooley, 1993). First identified in 1993 as a repeated element in the sequence of the *Drosophila* Kelch ORF1 protein, the Kelch motif is ancient and has been widely dispersed during evolution (Bork and Doolittle, 1994; Xue and Cooley, 1993). The Kelch motif is a segment of 44–56 amino acids with low overall sequence identity between individual Kelch motifs, but all Kelch motifs contain eight key conserved residues, including four hydrophobic residues followed by a double glycine element, separated from two characteristically-spaced aromatic residues tyrosine and tryptophan (Adams et al., 2000) (Figure 3.2).

The crystal structure of the Kelch motif in fungal galactose oxidase was solved and showed how the set of seven Kelch motifs collectively form a  $\beta$ -propeller (Ito et al., 1994). Each Kelch motif represents one  $\beta$ -sheet blade, and several (4-7) of these repeats can associate to form a beta-propeller (Figure 1.3A).

So far five subgroups of the Kelch superfamily have been defined according to the position of the Kelch  $\beta$ -propeller and the presence of other protein domains within the primary sequences, as summarised by Adams and colleagues (Adams et al., 2000). The five groups are termed: N-dimer C-propeller proteins, C-propeller proteins, N-propeller C-dimer proteins, N-propeller proteins, and propeller proteins. Among these five subgroups of the Kelch proteins, the N-dimer C-propeller proteins contain an N-terminal BTB/POZ domain and four to six Kelch motifs located within the C-terminal region (Adams et al., 2000), which will be the focus of this review.

### **1.3.2 BTB proteins**

The BTB/POZ domain is found at the N terminus of zinc-finger transcription factors, and in some actin-associated proteins bearing the Kelch motif (Ahmad et al., 1998). This domain was found in proteins encoded by *Drosophila* genes Broad-Complex, Tramtrack and Bric-a-brac, thus it was named a BTB domain (Zollman et al., 1994) or POZ domain because it is also found in several poxvirus zinc finger proteins (Bardwell and Treisman, 1994). When contained in a subgroup of Kelch proteins, the N-terminal BTB domain, which seems also conserved in evolution, makes additional protein-protein contacts to Kelch proteins (Adams et al., 2000). The BTB/POZ domain of *Drosophila* Kelch plus a 147-residue intervening region (IVR) mediate Kelch dimerisation, which is essential for the normal function of Kelch proteins (Xue and Cooley, 1993).

The core structure of the BTB domain consists of five  $\alpha$ -helices with A1/2 and A4/5 forming  $\alpha$ -helical hairpins, and three  $\beta$ -strands (B1/B2/B3) forming a  $\beta$ -sheet. The B1/B2/A1/A2/B3 region is connected to the A4/A5 region by helix A3 and a variable linker region (Ahmad et al., 1998; Chaharbakhshi and Jemc, 2016b; Li et al., 1999) (Figure 1.3B).

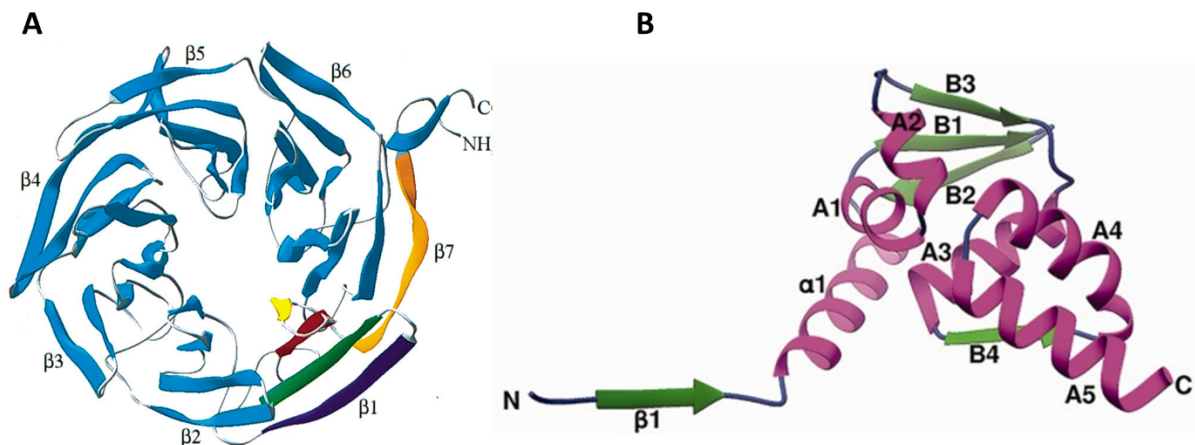


**Figure 1.3. Crystal structure of BTB and Kelch domain.** (A) En-face view of Kelch domain of galactose oxidase from *Hypomyces rosellus*, taken from review by (Adams et al., 2000). (B) Ribbon diagram of BTB domain taken from review by (Chaharbakhshi and Jemc, 2016a)

### 1.3.3 Functions of Kelch and BTB proteins

Kelch proteins display considerably structural diversity thus it is not surprising that they participate in many biological events. By interacting with different binding partners, Kelch proteins are involved in actin association, cell morphology, cytoskeleton organisation and gene expression (Adams et al., 2000).

#### 1.3.3.1 Actin association

Originally, the Kelch protein was shown to localise to ring canals, an actin-rich intercellular bridge connecting the developing oocyte and nurse cells in *Drosophila* females (Xue and Cooley, 1993). Since then several Kelch proteins have been shown to interact with actins (Adams et al., 2000). For example, human Kelch protein Mayven, predominantly expressed in the brain, was demonstrated to

associate with actin, and this association was enhanced during KCl-mediated depolarisation of primary hippocampal neurons, suggesting its role in the dynamics of cytoskeletal processes in neurons (Soltysik-Espanola et al., 1999).

### **1.3.3.2 Cell morphology and cytoskeleton organisation**

Other than directly binding to or co-localising with actins, some Kelch proteins affect the organisation of the cytoskeleton, plasma membrane or organelle structure indirectly (Adams et al., 2000). *Saccharomyces cerevisiae* protein Kel1p, a Kelch protein containing six Kelch repeats, exhibited a function in cell fusion and morphology change in yeast, which is driven by actin organisation, yet no obvious evidence shows Kel1p interacts directly with actin or the microtubule cytoskeleton (Philips and Herskowitz, 1998).

### **1.3.3.3 Gene expression**

Several mammalian Kelch proteins play a role in gene expression. An often mentioned example is Keap1, a human Kelch protein that inhibits the transcriptional activity of Nrf2 (NF-E2 related factor 2) by binding to its evolutionarily conserved amino-terminal regulatory domain and thereby retaining Nrf2 in the cytoplasm. When the electrophilic agent diethylmaleate (DEM) was added, Nrf2 was released from Keap1 and translocated to nucleus. This resulted in the induction of expression of phase II detoxifying enzymes and antioxidative stress genes in response to electrophiles and reactive oxygen species, suggesting the role of Keap1 and Nrf2 as cellular sensors for oxidative stress (Itoh et al., 1999).

### **1.3.3.4 Immune modulation**

A family of Kelch-like proteins, KLHL, are involved in several cellular and molecular processes such as inflammatory responses, oxidative stress responses, cytokinesis,

embryonic development and lymphogenesis (Mei et al., 2016). The protein mentioned before, Keap1 (also known as KLHL19), interacts with IKK $\beta$ , thereby promoting IKK $\beta$  degradation and so inhibits the phosphorylation of IKK $\beta$  in response to extracellular stimuli (Kim et al., 2010; Lee et al., 2009). Another example, KLHL21, also negatively regulates IKK $\beta$ , hence inhibiting NF- $\kappa$ B signalling. In this paper (Mei et al., 2016), KLHL21 inhibits the activation of IKK $\beta$  and the degradation of I $\kappa$ B $\alpha$ , probably by interacting with the kinase domain of IKK $\beta$  via its Kelch domains. Interestingly, this inhibitory function of KLHL21 is independent of its E3 ubiquitin ligase activity (Mei et al., 2016).

The BTB/POZ domain facilitates protein homo- and heterodimerisation, as well as oligomerisation (Bardwell and Treisman, 1994; Bonchuk et al., 2011). BTB proteins have been identified in poxviruses and many eukaryotes, and have diverse functions, ranging from transcriptional regulation and chromatin remodelling to protein degradation and cytoskeletal regulation.

#### **1.3.3.5 BTB-Kelch proteins interact with Cullin 3**

The available data suggest that various BTB-Kelch proteins interact with cullin 3 (Cul3) rather than with the other cullins, and therefore can function as substrate-specific adaptors for the Cul3ubiquitin–ligase complex and regulate modification and/or degradation of various proteins (Pintard et al., 2004b).

The SCF (Skp1–Cul1–F-box) and ECS (ElonginC–Cul2–SOCS box) complexes are very well-characterised cullin-based ligases (Pintard et al., 2004b). The BTB domain fold shows structural similarity with Skp1 and ElonginC, which led to the hypothesis that BTB proteins might interact directly with cullins (Schulman et al., 2000). This prediction was confirmed and several BTB domains have been shown to only

interact with Cul3 and not with other cullins (Pintard et al., 2004b). For example, human BTB-Kelch proteins KLHL13 and KLHL9 were shown to bind to Cul3 *in vitro*, but not to human Cul1, Cul2, Cul4A or Cul5, indicating their selective interaction (Furukawa et al., 2003).

Apart from mimiviruses, poxviruses are the only viruses that encode BTB-Kelch proteins (Shchelkunov, 2010). As summarised by (Shchelkunov, 2010) in Table 1.1, various orthopoxviral BTB-Kelch proteins have been shown to associate with Cul3 (Shchelkunov, 2010). For example, ECTV (strain Moscow) proteins EVM150 and EVM167 are involved in formation of active Cul3-containing ubiquitin ligases (Wilton et al., 2008b). Two other proteins, EVM18 and EVM27, also associate with Cul3 (Zhang et al., 2009). It is worth mentioning that these BTB-Kelch proteins are not obligatory subunits of Cul3-containing E3 ligases but can be components of protein complexes that determine modifications of cell morphology, modulation of the cytoskeleton and elongation of pseudopodia (Adams et al., 2000; Gray et al., 2009).

VAR-IND		VAR-GAR		ECT-MOS		CPV-GRI		VAC-WR		VAC-MVA	
ORF	Size, aa	ORF	Size, aa	ORF	Size, aa	ORF	Size, aa	ORF	Size, aa	ORF	Size, aa
–	–	–	–	–	–	<i>D11L</i>	521	–	–	–	–
<i>D13L</i>	201	<i>B19L</i>	154	<b>018</b>	512	<b>C18L</b>	512	<i>C2L</i>	512	–	–
<i>D13.5L</i>	79	<i>B20L</i>	65	–	–						
<i>C7L</i>	179	<i>E3L</i>	179	<b>027</b>	482	<b>G3L</b>	485	<i>F3L</i>	480	<i>31L</i>	476
<i>J7R</i>	71	<i>K7R</i>	71	<b>150</b>	563	<b>A57R</b>	564	<b>A55R</b>	564	–	–
<i>J8R</i>	172	<i>K8R</i>	70								
–	–	–	–	–	–	<i>B9R</i>	501	–	–	<i>178R</i>	158
<i>B22R</i>	70	<i>D11R</i>	70	–	–	<b>B19R</b>	557	–	–	–	–
<i>B23R</i>	83	<i>D12R</i>	127	–	–						
<i>B24R</i>	88	<i>D13R</i>	88	–	–						

**Table 1.1. Orthopoxviral BTB-Kelch proteins.** ORFs that are full length are shown in italics whereas gene fragments are not. The ORFs for the proteins with experimentally confirmed interaction with the cellular Cul3-containing CRL complex are indicated by bold letters in red. Table is modified from (Shchelkunov, 2010).

#### 1.4 VACV BTB-Kelch proteins

VACV strain Western Reserve (WR) contains three genes, *A55R*, *C2L* and *F3L* that encode BTB-Kelch proteins A55, C2 and F3 respectively (Figure 3.1). In addition to the features described above these proteins also contain a BACK domain, which is a highly conserved sequence of ~130 residues between the BTB and Kelch domains, and may structurally interact with the BTB domain (Stogios and Privé, 2004). VACV WR also encodes a BTB-only protein, C5 (Barry et al., 2010).

VACV BBK (BTB/Back-Kelch) proteins are expressed early during infection (Yang et al., 2010b). They are intracellular proteins with protein sizes of 64 kDa (A55) (Beard et al., 2006), 56 kDa (C2) (Pires de Miranda et al., 2003) and 56 kDa (F3) which might be cleaved into 27 and 25 kDa fragments (Froggatt et al., 2007). None of these three BBK proteins are essential for viral replication. VACV strains lacking *A55R*, *C2L* or *F3L* show unaltered growth rates *in vivo*. Deleting *A55R* or *C2L* cause different plaque morphology and cytopathic effect, and reduce Ca<sup>2+</sup>-independent cell-extracellular matrix adhesion (Beard et al., 2006; Pires de Miranda et al., 2003). Deleting *F3L* does not obviously affect plaque morphology compared to A55 or C2 (Froggatt et al., 2007). VACV lacking *C2L* also affects VACV-induced cellular projections but not actin tail formation or cell motility (Pires de Miranda et al., 2003). In an intradermal murine model, viruses lacking BBKs show altered virulence. Viruses lacking A55 or C2 result in larger lesion size (Beard et al., 2006; Pires de Miranda et al., 2003), whilst virus lacking F3 gives smaller lesion size (Froggatt et al., 2007). Lesions infected by vΔC2 show an increase in the total number of immune

cells infiltrated, including neutrophils, CD8<sup>+</sup> T cells, macrophages and DCs. vΔA55 also increase CD8<sup>+</sup> T cells and macrophage numbers in lesions (Pallett et al., 2019). In contrast, vΔF3 increases the number of NK cells and TCR γδ cells (Froggatt et al., 2007). All three BBKs do not contribute to virus virulence in the intranasal mouse model of infection.

*A55R*, *C2L* and *F3L* are conserved in several members of the orthopoxvirus (OPXV) genus (> 90 % amino acid identity) (Table 3.2) therefore functions of their orthologues in other OPXVs may provide helpful insights to study VACV BBKs. The ECTV orthologue of A55, ECTV EVM150, inhibits NF-κB signalling (Wang et al., 2014) and associates with Cul3 (Wilton et al., 2008a). Ectopically expressed ECTV EVM018 (the orthologue of VACV C2) or EVM027 (the orthologue of VACV F3) did not coimmunoprecipitate Cul3 (Wilton et al., 2008a), however it was reported that both EVM018 and EVM027 associate with Cul3 during infection (Couturier, 2009a). Deletion of individual genes encoding EVM018 or EVM027 radically decreases the ECTV virulence for white mice, while the damage of EVM150 gene has no effect on the virulence (Kochneva et al., 2009a). Deletion of four CPXV BTB-Kelch genes led to a decrease in the cytopathic effect on cell culture and statistically significant reduction in formation of the virus-induced cytoplasmic pseudopodia (Kochneva et al., 2005; Kochneva et al., 2009b).

Recently A55 was shown to inhibit NF-κB activation by competitively associating with importin protein KPNA2 and so blocking p65 translocation into the nucleus (part of the data was obtained by the author of this thesis hence are included later in the result chapters) (Pallett et al., 2019). Since A55 is a BTB protein, the interaction between A55 and Cul3 was investigated and confirmed. A55 binds Cul3 directly with a higher affinity than cellular BTB proteins. A55-BTB/Back (A55-B) domain and Cul3

N-terminal (Cul3-N) domain form a 2:2 complex. A55 residue Ile-48 is important for the affinity of A55-B for Cul3-N, and this residue is absent in C2 and F3 (Gao et al., 2019).

In summary, BTB-Kelch proteins are well-conserved and widely spread proteins during evolution. To date, of the 3 VACV BTB-Kelch proteins, only A55 has been shown to interact with Cul3 and the substrates of C2 or F3 have not been identified. A better understanding of the features and biological roles of these proteins would help to draw a more complete picture of the interaction between viruses and the host, and would provide more insights into cellular biology and immunology.

## **1.5 Project aims**

This thesis was to investigate the functions of VACV BBK proteins C2, A55 and F3.

Specific aims were to:

- Investigate whether A55, C2 and F3 regulate the innate immune response, and if so which signalling pathways are affected and how;
- study how A55 and C2 induce morphological changes of VACV-infected cells;
- examine if these BTB-Kelch proteins interact with cullin 3 and study the functional consequences of such interaction;
- exploit data from a quantitative temporal viromic study to investigate how A55 and C2 contribute to the degradation of specific cellular proteins and what is the consequence of this degradation;
- examine whether these VACV BTB-Kelch proteins interact with each other.

## **2 Material and Methods**

### **2.1 Bioinformatic analysis**

Protein sequence alignments were performed using Clustal Omega program to view their characteristics alongside each other (Sievers et al., 2011). The Basic Local Alignment Search Tool (BLAST) was used to find regions of local similarity between sequences and species. Information resource of genes and expression was obtained from NCBI Gene.

### **2.2 Cell culture**

#### **2.2.1 Maintenance of cells**

HEK-293T (human embryonic kidney epithelial cell line), HeLa (human cervical cancer cell line), BSC-1 (African green monkey fibroblast cell line), CV-1 (African green monkey fibroblast cells), HFF (human foreskin fibroblasts), Hap (human male chronic myelogenous leukaemia cell line), RK-13 (rabbit kidney epithelial cell line) cells were cultured in Dulbecco's modified Eagle medium (DMEM) (Invitrogen) supplemented with 50 µg/ml penicillin/streptomycin (P/S) (PAA laboratories), 1% non-essential amino acids (NEAA, Gibco) and filtered 10% (v/v) foetal bovine serum (FBS) (Pan Biotech). Cells were cultured in an incubator at 37 °C with 5% CO<sub>2</sub>. The Hap Cdc42 knockout cell line was a kind gift by Dr. Anthony Davidson from the Koronakis group.

When performing experiments requiring optimal cell attachment such as infection, transfection or immunofluorescence (IF) with semi-adherent HEK-293T cells, plates/dishes were coated with poly-D-Lysine (Sigma) at 0.01 mg/ml for at least 1 h and washed with 1x PBS for 3 times before seeding the cells.

## 2.2.2 Transfection of cells

All transfections were performed using *Trans-IT* LT1 reagent (Mirus) unless otherwise stated. Cells were seeded 24 h prior to transfection into 10 cm dishes (Falcon), 6-well plates (Nunc™ Thermo Scientific) or 96-well plates (Nunc™ Thermo Scientific), and were transfected when cells reached 70-80% confluence. Transfection mixtures were prepared by gently mixing DNA at desired mass with Opti-MEM (Gibco) (50 µl for 1 µg DNA) and with LT1 (2 µl for 1 µg DNA). Mixtures were incubated at room temperature for 20 min and then topped with DMEM containing 2% (v/v) FBS and supplements before added to the cells. Plasmids used in this study are listed in Table 2.1.

<b>Construct</b>	<b>Insert</b>	<b>Vector</b>	<b>Ref. /source</b>
nTAP-A55 *	TAP- codon optimised (co) A55	pcDNA4/TO	Smith lab
nV5-A55	V5- co A55	pcDNA3	Smith lab
nTAP-I48E	TAP- co A55 with I48E mutation	pcDNA4/TO	Constructed by R.Y. Zhang (Smith lab)
nTAP-C2	TAP- co C2	pcDNA4/TO	Smith lab
nV5-C2	V5- co C2	pcDNA3	Smith lab
nV5-GFP	V5-GFP	pcDNA3	Smith lab
nTAP-F3	TAP- co F3	pcDNA4/TO	Smith lab
nTAP-C2-BTB	TAP- co C2 BTB domain	pcDNA4/TO	Smith lab
nTAP-C2-Kelch	TAP- co C2 Kelch domain	pcDNA4/TO	Smith lab
cTAP-B14	Co B14-TAP	pcDNA4/TO	Smith lab
Flag-KLHL12	Flag-Kelch like protein 12	pcDNA3	Smith lab
Flag-TRAF6	Flag-TRAF6	M5P	Smith lab
Flag-TRAF2	Flag-TRAF2	M5P	Smith lab
TAK1	HA-TAK1	pcDNA3	Smith lab
TAB1	HA-TAB1	pcDNA3	Smith lab

pLuc-NF-κB	NF-κB promoter fused to a firefly luciferase gene		A gift from R. Hofmeister (University of Regensburg)
pRL-SV40P	Renilla SV40 promoter (no enhancer) reporter gene	pRL-TK	A gift from Ron Prywes (Addgene plasmid # 27163)
pCMV-PACK	Packaging plasmid for lentivirus production with HIV Gag, Pol, Rev and Tat under the CMV promoter; Amp-R		Smith lab
pCMV-ENV	VSV-G pseudotyped envelop protein under the CMV promoter for lentivirus production; Amp-R		Smith lab
pLDT-TetR	Tetracycline promoter repressor	pLKO puro	Smith lab
pLDT-nTAP-A55	TAP- co A55	pLKO puro	Constructed by R.Y. Zhang (smith lab)
pLDT-nTAP-C2	TAP- co C2	pLKO puro	Same as above
pLDT-nTAP-C2-BTB	TAP- co C2-BTB	pLKO puro	Same as above
pLDT-nTAP-C2-Kelch	TAP- co C2-Kelch	pLKO puro	Same as above
pLDT-nTAP-B14	TAP-co B14	pLKO puro	Same as above
pLDT-nTAP-C6	TAP- co C6	pLKO puro	Same as above
pCW57-nTAP-A55	TAP- co A55	pCW57-GFP-P2A-MCS	Smith lab
pCW57-nTAP-C2	TAP- co C2	pCW57-GFP-P2A-MCS	Smith lab
pEE-I48E	WT A55 containing I48E mutation to	pUC13-Ecogpt-EGFP	Constructed by R.Y. Zhang (Smith lab)

	construct recombinant VACV-I48E		
Myc-Scrib	Myc-Scrib	pCMV-Tag3B	A gift from Professor Andrew P. Rice (Liu et al., 2010)
pCMV-Tag3B	EV control for Myc-Scrib	pCMV-Tag3B	Stratagene
GFP-myc	GFP-myc	pCMV/myc/nuc	A gift from Trevor Archer lab (NIH) (Chen and Archer, 2005)
Myc-Cdc42	Myc-Cdc42	pRK5	Smith lab
Myc-Cdc42 <sup>Q61L</sup>	Myc- dominant positive Cdc42	pRK5	A gift from Gad Frankel, Imperial College London (Bulgin et al., 2009)
Myc-Cdc42 <sup>T17N</sup>	Myc- dominant negative Cdc42	pRK5	Same as above
Myc-hASC	Myc-hASC	pcDNA3	Smith lab
pSpCas9(BB)-2A-Puro (PX459) V2.0	Cas9 from S. pyogenes with 2A-Puro and cloning backbone for sgRNA	PX459	A gift from Feng Zhang (Addgene plasmid # 62988)
CAGA <sub>12</sub> -Luc	CAGA box sequence	pGL3 luciferase reporter	A gift from Caroline Hill (Francis Crick Institute UK) (Dennler et al., 1998b)
BRE-Luc	BMP response element	pGL3 luciferase reporter	Same as above

**Table 2.1. Plasmids used in this study.** \*TAP, short for tandem affinity purification, contains two strep tags and one flag tag.

### **2.2.3 Construction of inducible cell lines**

The pLKO-based lentivirus vector plasmids or pCW57 plasmids were co-transfected with envelope (pCMV-ENV) and the packaging (pCMV-PACK) plasmids into HEK-293T cells for lentivirus production. The medium was collected and filtered 24 and 48 h after transfection, and added onto fresh monolayers of HEK-293T TetR (pLDT TetR transduced HEK-293T) cells, which act under a tet-on controlled mechanism. Two days later, cells were selected with puromycin at 2 µg/ml (Invivogen) and the expression of target proteins were induced by doxycycline at 2 µg/ml. Transduction and expression were confirmed by immunoblotting of cell lysates.

## **2.3 Vaccinia virus work**

### **2.3.1 Amplification and titration of VACV**

To amplify viruses, RK-13 cells were seed in a T175 flask. When cells were confluent they were infected cells with viruses at 0.1 p.f.u./cell for 48-72 h. Cells were scraped from the flask and collected by centrifugation (500 x *g*, 10 min, 4°C). The supernatant was removed and the pellet was re-suspended in 1 ml MEM. Cells were then frozen-thawed 3 times to release viruses.

Virus titres were determined by plaque assay on monolayers of BSC-1 cells. Sonicated and vortexed viruses were diluted in 2 % DMEM to make 10<sup>-6</sup> to 10<sup>-8</sup> dilutions and 400 µl of each dilution was incubated with cells for 90 min with regular rocking of the plate. The virus-containing medium was aspirated and each well was overlaid with 2.5 ml of semi-solid MEM/CMC (carboxy methyl cellulose) at 1:1. The plates were incubated at 37 °C for 2-3 days. The overlay was aspirated and cells were washed with Dulbecco's phosphate buffered saline (PBS, Sigma-Aldrich) for 3-4 times. Cells were stained with 2 ml/well crystal violet solution (5 % (v/v) crystal

violet (Sigma-Aldrich), 25 % (v/v) ethanol) for 1 h at room temperature. Cells were then washed with water and the number of plaques was counted.

Plaque size analysis was performed after staining the monolayers of cells. The plaque areas were measured on a Zeiss Axiovert 200 M microscope using Axiovision 4.6 software.

<b>Virus name</b>	<b>Description</b>
vC2	Wild type VACV WR, parental virus used to construct vΔC2
vΔC2	VACV strain WR lacking the C2 ORF, made by M. Miranda (Pires de Miranda et al., 2003)
vA55	Wild type VACV WR, parental virus used to construct vΔA55
vΔA55	VACV strain WR lacking the A55 ORF, made by P. Beard (Beard et al., 2006). Also the parental virus used to construct vI48E
vΔF3	VACV strain WR lacking the F3 ORF, made by G. Froggatt (Froggatt et al., 2007)
vΔAC	VACV strain WR lacking A55 and C2 ORFs, made by P. Beard
vΔACF	VACV strain WR lacking A55, C2 and F3 ORFs, made by P. Beard
vI48E	VACV strain WR containing a point mutation I48E in the A55 ORF, made by Rui-Yao Zhang

**Table 2.2. Viruses used in this study.**

### **2.3.2 Infection of cells**

Cells were seeded in plates or dishes depending on the assays used. When cells reached desired confluence a spare plate or a well in a dish was used to count the cell number using the Countess automated cell counter (Invitrogen). Virus working stocks were thawed at 37 °C and sonicated for 20 second at 120 w to release and separate virus particles. The viruses were diluted in infection medium and added onto the cells in the minimum volume to be covered. The primary infection was incubated for 90 min with gentle rocking every 15 min, then the medium was aspirated and fresh infection medium was added and were further incubated at 37 °C until the desired time point.

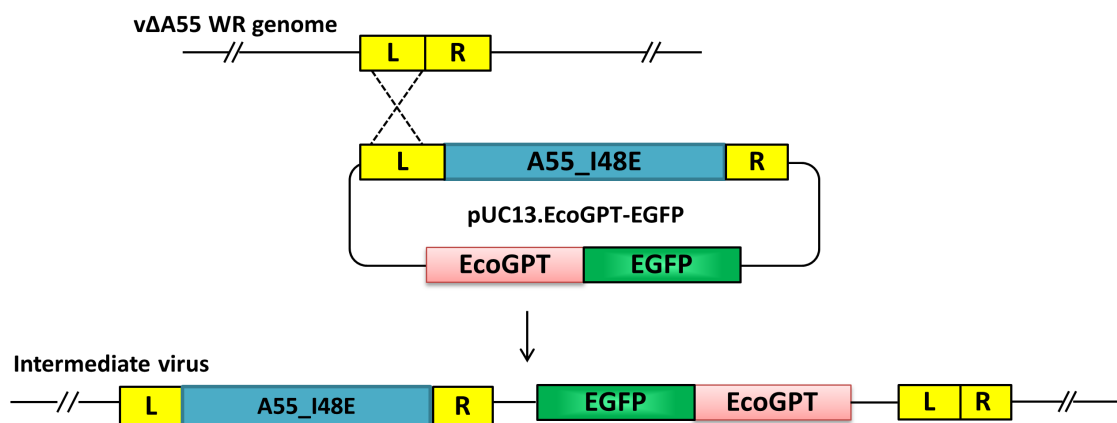
### **2.3.3 Recombinant VACV construction**

Recombinant viruses were generated using the transient-dominant selection (TDS) method as described in (Falkner and Moss, 1988). These viruses could be selected by growth in the presence of mycophenolic acid (MPA), xanthine (X) and hypoxanthine (HX). MPA is an inhibitor of purine metabolism, which blocks the replication of WT VACV in normal cell lines but can be overcome by expression of EcoGPT, in the presence of X and HPX. A single cross-over event results in the integration of the full length plasmid into the genome. The presence of EGFP allowed plaques formed by these intermediate viruses to be visualised and selected with ease. Due to the instability of the resulting intermediate virus, a second recombination event, between repeated right or left flanking sequences, occurred when the drug selection was removed, resolving the virus and excising the inserted plasmid yielding either the parental virus or the mutant virus. This instability is consistent with the known high frequency of intramolecular recombination in VACV-infected cells. TDS works well in VACV because of high rates of recombination and a

large DNA capacity such that genomes incorporating the entire plasmid may be packaged. It could work with other viruses that have these same properties.

In this study a VACV strain named vI48E containing a point mutation I48E in the A55R gene was constructed by inserting A55\_I48E into vΔA55 using TDS (Figure 2.1). A pUC13-EcoGPT-EGFP plasmid containing A55\_I48E (pEE\_I48E) was constructed. This plasmid contains A55R with I48E mutation and its left (L) and right (R) flanking regions as well as the guanylphosphoribosyl transferase-gene from *E. coli* (EcoGPT) fused to the gene for enhanced green fluorescent protein (EGFP), driven by a VACV promoter.

**1<sup>st</sup> recombination event:**



**2<sup>nd</sup> recombination event:**

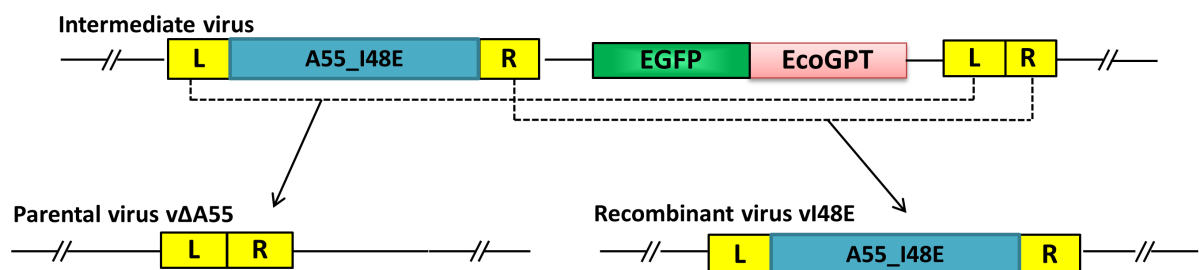


**Figure 2.1. Construction of vI48E mutant virus by transient dominant selection.** The first recombination event occurs in the infected and transfected cells between regions of homology in the virus genome and the plasmid. An unstable intermediate virus is generated with the mutated A55R gene (A55\_I48E) with its left and right flanking regions alongside EcoGPT and EGFP selection sites. Due to its unstable

nature of the intermediate virus a second recombination happens after removing the selection pressure is removed, resulting in either the parental virus with the incorporated plasmid removed or a mutant virus with the selection cassette and duplicated flanking regions removed.

### **2.3.3.1 Infection/transfection**

CV-1 cells were prepared in T25 flasks and infected with vΔA55 at 0.1 p.f.u/cells when 70% confluent. Cells were incubated with virus-containing medium at 37 °C for 90 min and rocked every 15 min. The medium was then aspirated and infected cells were washed twice in serum- and antibiotic-free DMEM, before transfected with 10 µg pEE\_I48E plasmid using LT1 reagent for 48 h.

### **2.3.3.2 Harvesting intermediate viruses**

The majority of cells should be green if the infection/transfection has been successful. CV-1 cells were scraped in their medium and pelleted by centrifugation at 500 g for 10 min. Supernatant was removed and cells were resuspended in 500 µl DMEM with 2.5% FBS, P/S and selection drugs (MPA 25 µg/ml, X 250 µg/ml and HX 250 µg/ml). The virus containing medium was frozen and thawed three times (80 °C then 37 °C), and sonicated for 20 seconds. Viruses were then diluted and added to wells of a 6-well plate of confluent BSC-1 cells, which were pre-treated with selection drugs overnight in advance. Infection was incubated for 90 min with occasional rocking before the medium was aspirated. Cells were then overlaid with 2 ml 2-Hydroxyethylagarose (low gelling temperature) /MEM mix (sterile 2% agarose and 50% 2x MEM) containing selection drugs. Agarose was allowed to set at room temperature for 15 min before cells were incubated at 37 °C for 2 d.

After infection, green plaques were picked and transferred into 500 µl medium containing selection drugs. Virus-containing medium was frozen and thawed 3 times and sonicated for 20 seconds. Viruses were then diluted in medium containing

selection drugs at 1:2, 1:20 and 1:200, and added to 6-well plates of confluent BSC-1 cells pre-treated with selection drugs overnight. Infection was incubated, aspirated, overlaid with agarose/MEM mix containing selection drugs and incubated as described before. This plaque purification step of the intermediate viruses was performed three times.

### 2.3.3.3 Screening plaques by PCR

HeLa cells were seeded in a 96-well plate and infected for 48 h with 100  $\mu$ l medium containing intermediate viruses after three times of plaque purification. Additional wells of HeLa cells were infected with WT VACV and  $v\Delta A55$  as controls. After infection, the virus-containing medium was aspirated and cells were lysed in 50  $\mu$ l proteinase K buffer (PK, Sigma), and incubated at 56 °C for 15 min followed by 85 °C for 10 min in a thermocycler (Applied Biosystems). The lysates were then used in a PCR to amplify *A55R* (primers vI48E LF and vI48E RF). Each PCR was carried out in a total volume of 30  $\mu$ l and contained 5  $\mu$ l lysates, 6  $\mu$ l 5x GoTaq Flexi buffer (Promega), 0.32  $\mu$ l dNTPs (25 mM), 1.2  $\mu$ l MgCl<sub>2</sub> (25 mM), forward and reverse primers (2  $\mu$ l each) and 0.25  $\mu$ l GoTaq polymerase (Promega) using a thermocycler (Table 2.3). PCR products were analysed by agarose gel electrophoresis.

Cycles	Temperature (°C)	Time
1	95	3 min
30	95	30 sec
	60	30 sec
	72	3 min
1	72	5 min
1	4	$\infty$

**Table 2.3. Cycling conditions of PCR to amplify A55R from VACV infected cell lysates.**

#### **2.3.3.4 Resolution**

An intermediate virus containing A55R was selected for resolution to obtain the desired mutant virus. This virus went through 3 rounds of plaque purification in the absence of selection drugs. Non-green plaques were picked and screened by PCR as above and sequenced to confirm the presence of I48E mutation. The positive plaque was also screened by PCR to rule out intermediate virus contamination, using a pair of EcoGPT primers. Master, sub-master and working stocks of vI48E were made and titrated as described before, aliquoted and stored at -80 °C.

## **2.4 Molecular biology work**

### **2.4.1 Polymerase chain reaction (PCR)**

DNA of interest was amplified by PCR using suitable templates such as plasmids, cell genome or VACV genome. PCR was performed using Platinum® *Taq* DNA polymerase High Fidelity. The reactions were set up using the recommended protocol (Table 2.4) and performed using a Veriti 96-well thermal cycler (Applied Biosystems) (Table 2.5). Primers used in this study are detailed in Table 2.7.

<b>Component</b>	<b>Final concentration</b>
Molecular biology grade water	Up to 50 µl reaction
10x High Fidelity PCR Buffer	1x
50 mM MgSO <sub>4</sub>	2.0 mM
10 mM dNTP Mix	0.2 mM
10 µM forward primer	0.2 µM
10 µM reverse primer	0.2 µM

Template DNA	< 500 ng
Platinum® <i>Taq</i> DNA Polymerase High Fidelity (5 U/μL)	1 U/rxn

**Table 2.4. PCR mixture setup.**

Step		Temperature (°C)	Time
Initial denaturation		94	2 min
30 PCR cycles	Denature	94	15 sec
	Anneal	~55 (depending on primer T <sub>m</sub> )	30 sec
	Extend	68	1 min/kb
Hold		4	∞

**Table 2.5. PCR cycling conditions with Platinum® *Taq* DNA Polymerase High Fidelity.**

#### 2.4.2 Real-time qPCR (RT-qPCR)

Cells were washed in ice-cold PBS, and mRNA was isolated with an RNeasy minikit according to the manufacturer's instructions (Qiagen). Samples were treated with RQ1 DNase-I (Promega) at 37°C for 30 min, followed by 15 min at 72°C. Reverse transcription-PCR was carried out according to the manufacturer's instructions (Promega) with the following adaptations. RNasin (Promega) was added to the reaction buffer at 2 to 4 U/μl. cDNAs of interested genes and control genes were amplified with primer pairs by RT-qPCR using the 7300 real-time PCR system (Applied Biosystems) under standard cycle conditions. A RT-qPCR mixture was 10 μl, including 5 μl FAST SYBR Green Mix (2x), 4.8 μl cDNA and 0.2 μl primer pair mix (10 pmol/μl each primer, final of 200 nM). Cycle steps are shown in Table 2.6. Changes in gene expression levels were analysed relative to the control levels (see

figure legends for individual experiments), with glyceraldehyde-3-phosphate dehydrogenase (GAPDH) or HPRT as a standard, using the  $\Delta\Delta C_T$  method.

<b>Cycles</b>	<b>Temperature (°C)</b>	<b>Time</b>
1	50	2 min
1	95	10 min
40	95	15 sec
	60	30 sec
	72	30 sec
1	72	10 min
1	4	$\infty$

**Table 2.6. RT-qPCR cycles.**

name	sequence	description	restriction enzymes	TM initial
<b>RYZ6</b>	<b>CTAGCTAGC</b> ATGTGGTCTCATCCTCAGTTTG	nTAP Fwd	NheI	60.3
<b>RYZ7</b>	<b>GCGGTCGAC</b> TCACTGCAGGAAGTCTTCTC	coC2L Rv	Sall	61.3
<b>RYZ10</b>	<b>GCGGTCGAC</b> TTA GGTCACGGGCTTGGTGC	coC2L BTB Rv	Sall	59.6
<b>RYZ8</b>	<b>GCGGTCGAC</b> TTACTTGCCGTCCCAGATGTTC	coF3L Rv	Sall	62.1
<b>RYZ9</b>	<b>GCGGTCGAC</b> TCAGCTTCCGATGAAGCTTTC	coA55 Rv	Sall	59.4
<b>A55 Fw</b>	GAC <b>GCGGCCGCG</b> AACAAACAGCAGCGAGC	nTAP coA55 FL Fwd	NotI	50
<b>A55 Rv</b>	GAC <b>TCTAGA</b> TCA GCTTCCGATGAAGC	nTAP coA55 FL Rv	XbaI	52
<b>co I48E Fw</b>	GCGAGTACTTCAGCGAGCTGTTCAGCAACAAC	Overlap primer for QuickChange mutagenesis; coA55 with I48E mutation		
<b>co I48E Rv</b>	GTTGTTGCTGAACAGCTCGCTGAAGTACTCGC			
<b>A55 I48E non-codon ol rv</b>	gataaaattattggaaaacagCTCggaaaaatattcggaggctcc	overlap including mutation in the middle reverse		75.3
<b>A55 I48E non-codon ol fw</b>	gagcctccgaatattttccGAGctgtttccaataattttatcg	overlap including mutation in the middle reverse		75.3
<b>vI48E LF</b>	CCATTTCTCCATGCAAACATC	A55 Left Flank Fwd		61.1
<b>vI48E RF</b>	TTGGGCTCCTTATACCAAGCAC	A55/Kelch/BTB right Flank Rev		62.1
<b>IL-8 Fw</b>	AGAAACCACCGGAAGGAACCATCT			
<b>IL-8 Rv</b>	AGAGCTGCAGAAATCAGGAAGGCT			
<b>GAPDH Fw</b>	ACC CAG AAG ACT GTG GAT GG			
<b>GAPDH Rv</b>	TTC TAG ACG GCA GGT CAG GT			
<b>sgRNA1 Fw</b>	<b>CACCG</b> CTGGAGATCGCGGACTTCAG	Scrib Exon 3		
<b>sgRNA1 Rv</b>	<b>AAAC</b> CTGAAGTCCGCGATCTCCAG <b>C</b>	Scrib Exon 3		
<b>sgRNA2 Fw</b>	<b>CACCG</b> CCTGAATGATGTGTCTCTGC	Scrib Exon 4		
<b>sgRNA2 Rv</b>	<b>AAAC</b> GCAGAGACACATCATTGAGG <b>C</b>	Scrib Exon 4		
<b>Rice Fw</b>	CACCGCAGACAAACCCTTGAACCA	guide RNA control from Yongxu		
<b>Rice Rv</b>	AAACTGGTTCAAGGGTTTGTCTGC			

<b>Ex3 seq1 Fw</b>	CCATGGCATCTGTCCACTGT	To amplify part of Exon 3 to sequence sgRNA1	
<b>Ex3 seq1 Rv</b>	TGGATGGGAGGAAGCAGAGG		
<b>Ex3 seq2 Fw</b>	CTGAGCGACAACGAGATCCA	To amplify a larger part of Exon 3 to sequence sgRNA1	59.83
<b>Ex3 seq2 Rv</b>	CATCATTGAGGGCCAGGTGA		59.74
<b>Ex4 seq1 Fw</b>	TCGGTAGGGGCTATGGGTC	To amplify a part of Exon 4 to sequence sgRNA2	
<b>Ex4 seq1 Rv</b>	AGGAAGGAAAGCAGTGGCAG		
<b>Ex4 seq2 Fw</b>	CTGCAAGGCTCTGGAGATCG	To amplify a larger part of Exon 4 to sequence sgRNA2	
<b>Ex4 seq2 Rv</b>	TTGGCGAGGCTGAAAGAGAG		

**Table 2.7. Oligonucleotide primers used in this study.** Primers are all listed 5' to 3'.

### **2.4.3 Agarose gel electrophoresis and DNA purification**

DNA samples were analysed by agarose gel electrophoresis where samples were separated by size. Agarose gel was prepared by dissolving 1% (w/v) agarose (Invitrogen) in TAE buffer (40 mM Tris, 1 mM ethylenediaminetetraacetic acid (EDTA) and 20 mM acetic acid) supplemented with 10,000 SYBR® Safe (Thermo Scientific). Once set, DNA samples were carefully loaded and the gel was run at 100 v for 30 min to 1 h, and DNA was visualised by ultraviolet (UV) illumination using Gel Doc XR+ imaging system (Bio-Rad) and Image Lab 5.2 software. When necessary DNA bands of correct size were excised from agarose gels using a clean scalpel and DNA was purified with the QIAquick Gel Extraction Kit (Qiagen) according to the manufacturer's protocol. DNA or RNA concentration was quantified with a NanoDrop 2000 spectrophotometre (Thermo Scientific). The purity of DNA was verified by ensuring an optical density A<sub>260</sub>/A<sub>280</sub> ratio between 1.8 and 2.0.

### **2.4.4 Restriction enzyme digestion**

Plasmids and insert DNA were cleaved at specific restriction sites using restriction enzymes (New England BioLabs) at 37 °C for 1 h. Each digestion mixture consists of 1-1.5 µg DNA, appropriate digestion buffer, 1 µl restriction enzymes and H<sub>2</sub>O, of a total volume of 20 µl. Digested products were purified by agarose gel electrophoresis and gel extraction (section 2.4.3), or by the QIAquick PCR Purification Kit (Qiagen) performed according to the manufacturer's instructions.

### **2.4.5 DNA ligation**

DNA ligation was performed using T4 DNA Ligase kit (New England BioLabs). The vector to insert molar ratio was 1:3, and the mixture was 20 µl in total containing T4 DNA ligase buffer, vector DNA, insert DNA and T4 DNA ligase. The mixture was

prepared on ice and incubated at 37 °C for 1 h before transformed into competent cells.

#### 2.4.6 Bacterial transformation

Bacterial transformation was performed in sterile conditions (near a Bunsen light). Competent cells were thawed on ice (10 µl for purified plasmid, 50 µl for ligation product), mixed with DNA (1 µl for purified plasmid, 5-10 µl for ligation product) and incubated on ice for 30 min. Cells were then subjected to heat shock at 42 °C for 30 s, and left on ice to recover for 2 min before topped up with 500 µl pre-warmed broth. The mixture was then incubated at 37 °C for 1 h and centrifuged at 500 g for 1 min, and 450 µl supernatant was discarded. Cells were resuspended in the remaining buffer, and spread onto a Lysogeny broth (LB) agar plate (LB medium with 15 g/l agar, sterile) supplemented with appropriate selection drug. The plates were incubated at 37 °C overnight.

#### 2.4.7 Bacterial colony screening by PCR

GoTaq Polymerase was used for bacterial colony PCRs. The reaction mixture and cycle program were set up as detailed in Table 2.8 and Table 2.9. In the mixture, instead of lysates, bacterial cells were picked up from marked colonies with a tip and mixed well in ddH<sub>2</sub>O in each PCR tube first before PCR mixture was added into each tube. PCR products were analysed by agarose gel electrophoresis (2.4.3).

Reagent	Vol. (µl)
GoTaq Flexi Buffer	5
dNTP	1
MgCl	2
Primers	0.5 each
GoTaq Polymerase	0.25
ddH <sub>2</sub> O	10.75

**Table 2.8. PCR mixture for bacterial colony screening.**

Cycles	Tmp (°C)	Time
--------	----------	------

Stage 1 X1	94	5 min
Stage 2 X30	94	15 sec
	55	30 sec
	72	2.30 min
Stage 3 X1	72	10 min
	4	∞

**Table 2.9. PCR cycle program for bacterial colony screening.**

#### **2.4.8 Preparation of plasmid DNA**

Bacterial clones, for which the sequence of the plasmid DNA had been validated, were amplified overnight at 37 °C in a 250 ml (Maxi) or 100 ml (Midi) culture supplemented with appropriate selection antibiotics. High concentration stocks of the correct plasmid were obtained using the HiSpeed® Plasmid Maxi/Midi kit (Qiagen) according to the manufacturer's manual.

#### **2.4.9 Sequencing**

All generated expression plasmids and PCR product from cell/viral genome were sent for sequencing to Source BioScience for verification.

#### **2.4.10 Site-directed mutagenesis**

To introduce the I48E mutation into codon optimised pcDNA4-nTAP-A55 and pEE-WT\_A55, site-directed mutagenesis using the QuikChange® Site-Directed Mutagenesis Kit (Agilent Technologies) was performed. To do this, PCR primers were designed that included the I48E mutation in the middle with ~10-15 bases of correct sequence on both sides. Besides, according to the primer design guidelines of the kit, primers were designed between 25 and 45 bases in length with a melting temperature of  $\geq 78$  °C (Table 2.7). The reactions were set up as shown in Table 2.10, and the cycling parameters are shown in Table 2.11. After PCR the amplification were checked by agarose gel electrophoresis and 1  $\mu$ l of *Dpn* I restriction enzyme (10 U/ $\mu$ l) was added to each amplification reaction. The reaction

mixture was then gently and thoroughly mixed by pipetting up and down, spun down for 1 min and immediately incubated at 37 °C for 1 h to digest the parental supercoiled dsDNA before transformed in bacterial cells. Resultant bacterial clones were analysed by DNA sequencing to identify those containing the plasmid with I48E mutation.

Reagent	Vol. / amount
10x reaction buffer	5 µl
dsDNA template	10 ng
Fw primer	125 ng
Rv primer	125 ng
dNTP mix	1 µl
QuikSolution	3 µl
ddH <sub>2</sub> O	To a final volume of 50 µl
<i>PfuTurbo</i> DNA polymerase (2.5 U/µl)	1 µl

**Table 2.10. QuikChange mutagenesis reaction mixture.**

Cycles	Tmp (°C)	Time
Stage 1 X1	95	1 min
Stage 2 X18	95	50 sec
	60	50 sec
	68	1 min/kb of plasmid length
Stage 3 X1	68	7 min
	4	∞

**Table 2.11. Cycling parameters for the QuikChange mutagenesis.**

## 2.5 Protein analysis

### 2.5.1 Cell lysates preparation

Cells were lysed in appropriate lysis buffers shown in Table 2.12 and collected as whole cell lysates. A portion of the whole cell lysates were taken and centrifuged at

14,000 g for 20 min (30 min for RIPA buffer) at 4 °C. The supernatant was collected as cleared lysates. For infected cells, cells were lysed and kept on ice for 40 min, and then the whole cell lysates and cleared lysates were collected as stated before. One x Laemmli buffer or 2 x Laemmli buffer (for immunoprecipitation) was added to each sample, then samples were stored at -20 °C. Lysis buffers and Laemmli buffer used in this study are shown in Table 2.12.

Name	Recipe	Source
Normal IP buffer	150 mM NaCl 20 mM Tris-HCl, pH 7.4 10 mM CaCl <sub>2</sub> 0.1 % Triton-X100 10 % Glycerol	Smith lab
HEPES-based mild IP buffer	150 mM NaCl 0.5 % NP-40 10 mM HEPES pH 7.4	
RIPA	150 mM NaCl 50 mM Tris HCl, pH 8.0 1 % NP-40 0.5 % sodium deoxycholate 0.1 % SDS	
Laemmli buffer (4 x)	Tris 0.5 M pH 6.8, 250 mM, 5 ml Glycerol, 40%, 4 ml SDS, 6 %, 600 mg Bromophenol blue 1 %, 200 µl β-mercaptoethanol, 800 µl	
Passive Lysis Buffer	N/A	Promega

**Table 2.12. Lysis buffers and Laemmli buffer used in this study.**

### 2.5.2 Polyacrylamide gel electrophoresis (PAGE) and immunoblotting

Samples were thawed at room temperature, heated at 100 °C, 60 °C or without being heated at all, and then loaded on a 12 % or 8 % polyacrylamide gel for

separation at 80-130 v for 120 min in 1 x Tris-glycine-SDS (TGS) buffer. After electrophoresis, proteins were transferred to a PVDF membrane (GE healthcare) at 23 v for 1 h in the transfer buffer (Tris-glycine (TG)). The membrane was blocked in 1 x phosphate buffer saline (PBS) (Hutchison/MRC Research Centre)/0.1 % Tween (PBST; Sigma-Aldrich) with 5 % (w/v) semi-skimmed milk (Marvel) for 30-60 min before incubating with antibodies (primary antibody: overnight, 4 °C; secondary antibody: 1 h, room temperature). Membranes were washed 3 times in TBST after incubation with antibody. Immunoblotting was visualised by Odyssey infrared imager (LI-COR Bioscience). Antibodies used for immunoblotting are shown in Table 2.13. Recipes for buffers used are shown in Table 2.14.

<b>Primary antibody</b>	<b>Source</b>	<b>Dilution</b>
Mouse anti-FLAG	Sigma-Aldrich (F1804)	1:1000
Rabbit anti-FLAG	Sigma-Aldrich (F7425)	1:5000
Rabbit anti-actin	Sigma-Aldrich (A2066)	1:1000
Mouse anti- $\alpha$ -tubulin	Merck Millipore (05-829)	1:5000
Mouse anti- $\alpha$ -tubulin	Santa Cruz	1:2500
Rabbit anti-C16	(Fahy et al., 2008)	1:1000
Mouse anti-D8	MAB 1.1 (Parkinson and Smith, 1994)	1:1000
Rabbit anti-C6	Eurogentech (Unterholzner et al., 2011a)	1:700
Rabbit anti-I $\kappa$ B $\alpha$	Cell Signalling Technology (9242L)	1:1000
Rabbit anti-IKK $\beta$	Cell Signalling Technology	1:1000
Rabbit anti-IKK $\alpha$	Cell Signalling Technology	1:1000

Rabbit anti-NEMO	BD Biosciences	1:1000
Rabbit anti- $\beta$ -TrCP	Cell Signalling Technology	1:1000
Mouse anti-p65	Santa Cruz sc8008	1:500
Mouse anti-RelB	Cell Signalling Technology	1:1000
Rabbit anti-p50/p105	Abcam 32360	1:1000
Rabbit anti-FRMD6	Cell Signalling Technology (D8X3R)	1:1000
Rabbit anti-Phospho-YAP (Ser397)	Cell Signalling Technology (D1E7Y)	1:1000
Rabbit anti-Phospho-YAP (Ser127)	Cell Signalling Technology (D9W2I)	1:1000
Mouse anti-Scrib (C-6)	Santa Cruz sc-55543	1:1000
Mouse anti-Scrib (D-2)	Santa Cruz sc-374139	1:1000
Mouse anti-YAP (G-6)	Santa Cruz sc-376830	1:1000
Mouse anti-GST (B-14)	Santa Cruz sc-138	1:1000
Rabbit anti-Cdc42	Cell Signalling Technology (2462)	1:1000
Rabbit anti-Cullin3	Abcam ab75851	1:1000
Mouse anti-KPNA1	Santa Cruz sc-101292	1:1000
Rabbit anti-KPNA2	Abcam ab70160	1:2000
Mouse anti-Smad2/3	Santa Cruz sc-133098	1:1000
Rabbit anti-Phospho-Smad2 (Ser465/467)	Cell Signalling Technology (3108)	1:1000
Rabbit anti-Phospho-Smad3 (Ser423/425)	Abcam ab52903	1:1000

Secondary antibody	Source	Dilution
IRDye 800 CW Goat anti-rabbit	LI-COR Biosciences	1:10000
IRDye 680 RD Goat anti-rabbit	LI-COR Biosciences	1:10000
IRDye 800 CW Goat anti-mouse	LI-COR Biosciences	1:10000
IRDye 680 RD Goat anti-mouse	LI-COR Biosciences	1:10000
IRDye 800 CW Donkey anti-goat	LI-COR Biosciences	1:10000
Donkey anti-mouse 488	ThermoFisher Scientific/A21202	1:1000
Anti-555 phalloidin	ThermoFisher Scientific/A34055	1:200

**Table 2.13. Antibodies used in this study.**

Name	Recipe	Source
10 x TGS (1 L)	121.14 g/mol Tris-HCl 112.60 g Glycine	Smith lab
10 x TG (1 L)	121.14 g/mol Tris-HCl 112.60 g Glycine 10 g SDS	

**Table 2.14. Buffers used for immunoblotting.**

### 2.5.3 Immunoprecipitation (IP)

Cleared lysates were prepared as described in 2.5.1 and 10% volume of the cleared lysates was transferred to a screw cap tube supplemented with 4x protein sample loading buffer (Laemmli buffer) as the INPUT sample stored at -20 °C. The remaining cleared lysates were incubated with IP beads at 4 °C overnight on a rotator. To prepare the IP beads, Protein G Sepharose® Fast Flow beads (GE Healthcare), commercial anti-FLAG M2 agarose beads (Sigma-Aldrich) or GST-PBD beads (a kind gift from Dr Anthony Davidson, University of Cambridge) were washed

once in H<sub>2</sub>O and twice in IP buffer prior to addition to lysates. When using G sepharose beads, beads were washed and incubated with appropriate antibody (1:200 dilution) at 4 °C overnight on a rotator before IP experiments. Beads were washed three times by repeatedly centrifuging at 4000 x *g* for 1 min at 4 °C (Eppendorf 5424R) and resuspending in 1 ml IP buffer. Finally all supernatant was removed and 30 µl 4x protein sample buffer was added to the beads. Samples were stored at -20 °C and analysed by immunoblotting.

#### **2.5.4 Immunofluorescence (IF)**

Cells were seeded on coverslips in 6-well plates and transfected as described before. Cells were washed 3 times in ice-cold PBS and incubated in 4 % PFA (paraformaldehyde, Sigma-Aldrich) for 45 min at room temperature. Then the PFA was removed and cells were washed again and used for staining, or stored in PBS at 4°C. Cells were quenched in 50 mM NH<sub>4</sub>Cl for 10 min, washed quickly with PBS once and then permeabilised with 0.2 % Triton X-100/PBS for 5 min. Then coverslips were washed in PBS 3 times and blocked in 5 % FBS/PBS (Blocking buffer) for 30 min at room temperature. Primary antibodies were diluted in blocking buffer and coverslips were incubated in the dark for 30-60 min. Coverslips were then washed 3 times with blocking buffer and incubated with secondary antibodies diluted in blocking buffer (5% donkey serum was added when using a donkey secondary antibody). After incubation with antibodies and washing 2 times in blocking buffer, 1 time in PBS, and 1 time in ddH<sub>2</sub>O, coverslips were mounted on SuperFrost slides (VWR) with Mowiol + DAPI and dried in the dark and stored in the dark at 4 °C. Images were taken using a Zeiss confocal microscope.

### **2.5.5 Enzyme-linked immunosorbent assay (ELISA)**

HEK-293Ts were starved for 3 h in DMEM without supplements before being stimulated for 18 h with 20 ng/ml TNF- $\alpha$ . IL-8 levels in cell supernatants were measured using an IL-8 DuoSet ELISA kit (R&D Systems) in accordance with the manufacturer's protocol and a FLUOstar Omega plate reader (BMG Labtech). Experiments were carried out in triplicate and measured with technical repeats.

### **2.6 Luciferase reporter gene assays**

Cells were seeded in 96-well plates and transfected when they had reached 70-80% confluence. All conditions were transfected with equal amounts of total plasmid DNA by supplementation with EV. After stimulation or infection, cells were lysed in passive lysis buffer (Promega) and frozen overnight to get better lysis. Then 15  $\mu$ l cell lysates were used for luminescence measurements with 50  $\mu$ l firefly luciferase substrate (Smith lab, 20 mM Tricine, 0.1 mM EDTA, 2.67 mM MgSO<sub>4</sub>·7H<sub>2</sub>O, 33.3 mM DTT, 530  $\mu$ M ATP, 5 mM NaOH, 270  $\mu$ M acetyl coenzyme A, 132  $\mu$ g/ml Luciferin, and 0.26 mM (MgCO<sub>3</sub>)<sub>4</sub>Mg(OH)<sub>2</sub>·5H<sub>2</sub>O) or 2  $\mu$ g/ml renilla luciferase substrate (Prolume Ltd.) using a FLUOstar luminometer (BMG Labtech). The firefly luciferase activity was normalised to the renilla luciferase activity first, then the data were normalised to non-stimulated either EV group or the same plasmid group, or mock groups to calculate fold inductions.

### **2.7 Statistical analysis**

All experiments were carried out in triplicate or quadruplicate and are representative or an average of at least three independent experiments unless otherwise stated. Data are the means  $\pm$  standard deviations (SD). All assays were analysed by unpaired *t* test with GraphPad Prism, version 6, software.

## **RESULTS**

### **3 Results 1 – A55, C2 and F3 are inhibitors of NF- $\kappa$ B signalling pathway**

Vaccinia virus (VACV) strain Western Reserve (WR) contains three genes, *A55R*, *C2L* and *F3L* that encode BTB-Kelch proteins called A55, C2 and F3, respectively. The ORFs encoding these BTB-Kelch proteins are located near the ends of the VACV genome, which contain many non-essential proteins such as host range proteins and immunomodulators (Figure 3.1). Although the sequences of the 3 VACV BTB-Kelch proteins are rather distantly related to cellular BTB-Kelch proteins and to each other, and the degree of identity is similar across different domains (Table 3.1), the sequence alignment of VACV WR A55, C2, F3 and a cellular BTB-Kelch protein Keap1 shows key conserved residues of BTB-Kelch proteins (Figure 3.2). All three VACV WR BTB-Kelch proteins contain a BTB domain, a BACK domain (a highly conserved sequence of ~130 residues between the BTB and Kelch domains, and that may interact with the BTB domain), and a Kelch domain. The Kelch domain is formed by 6 Kelch motifs characterised by eight key conserved residues, including four hydrophobic residues followed by a double glycine element, separated from two characteristically-spaced aromatic residues tyrosine and tryptophan (Adams et al., 2000; Stogios and Privé, 2004). Thus, VACV-WR A55, C2 and F3 are all BTB/Back-Kelch proteins.

## The vaccinia virus BTB/BACK-Kelch family

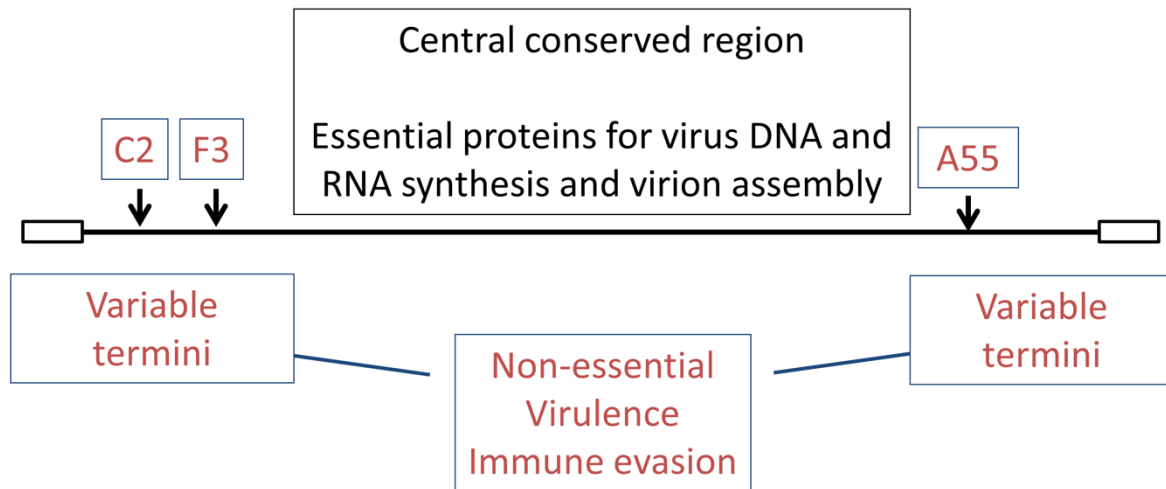


**Figure 3.1. VACV WR encodes three BTB/Back-Kelch proteins.** The ORFs encoding these BTB-Kelch proteins are located near the ends of the VACV genome, which contain many non-essential proteins such as host range proteins and immunomodulators.

	Keap1	KLHL12	F3	C2
A55	17	16	21	20
C2	16	15	17	
F3	14	17		
KLHL12	32			
Total identity of 5 proteins: 4%				

**Table 3.1. Percentage of amino acid identity between VACV WR and cellular BBK proteins.** Protein sequences of VACV WR BBK proteins A55, C2, F3 and two cellular BBK protein KLHL12 and Keap1 were aligned using the Clustal Omega.

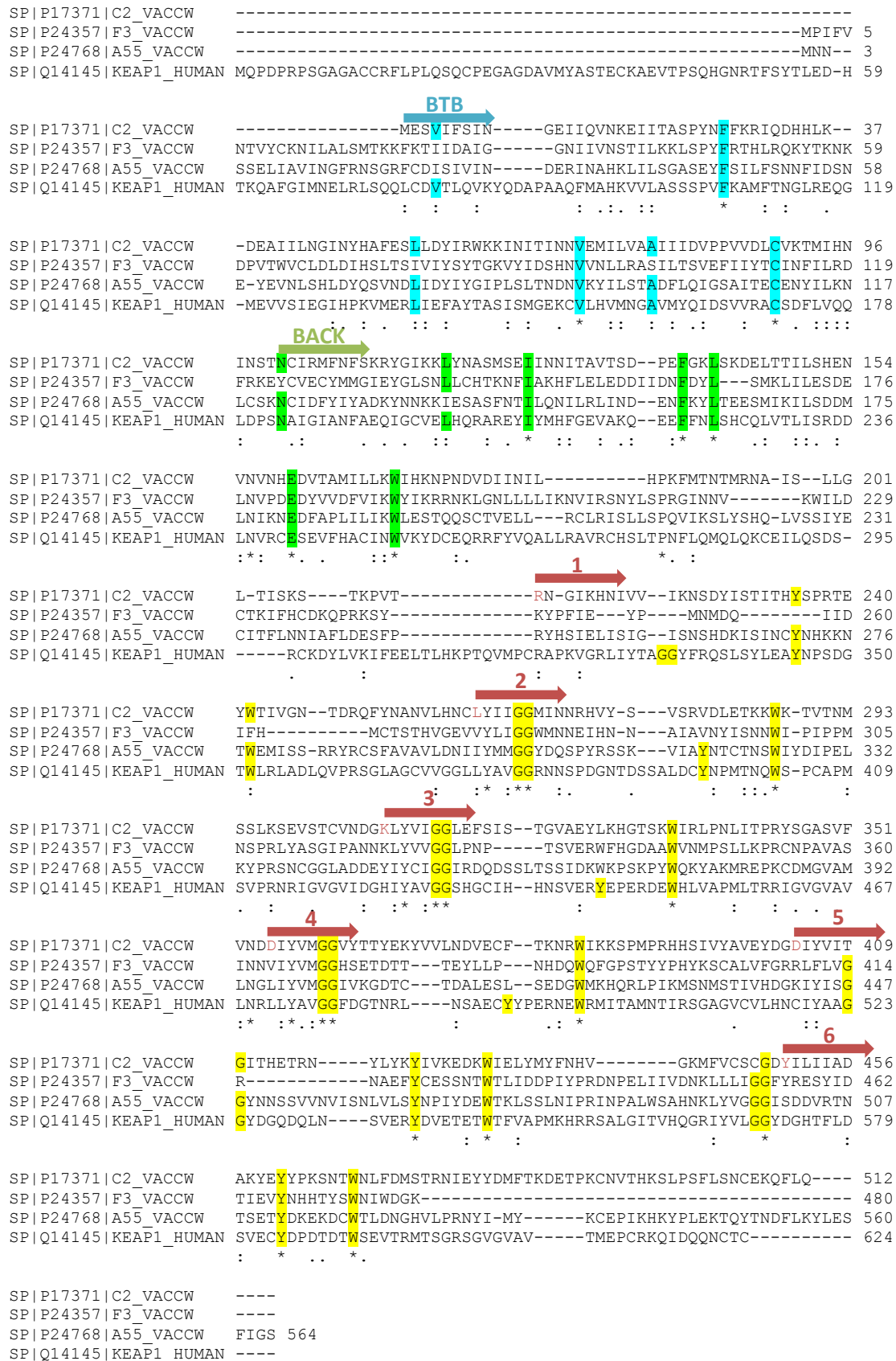


**Figure 3.2. CLUSTAL O (1.2.4) multiple sequence alignment.** Protein sequences of VACV WR (shown as VACCW) C2, F3, A55 and a well-characterised human BTB-Kelch protein Keap1 were aligned using the Clustal Omega. Key residues identified

by (Chaharbakhshi and Jemc, 2016a) for the BTB, BACK domain and Kelch motifs are shaded in turquoise, green and yellow respectively. The typical Kelch motifs are indicated by red arrows numbered from 1 to 6. All three BTB-Kelch proteins of VACV WR contain a BTB domain, a BACK domain, and a Kelch domain formed by 6 Kelch motifs, thus they can be called BTB/Back-Kelch proteins.

### 3.1 A55, C2 and F3 are conserved in the OPXV genus

VACV WR genes A55R, C2L and F3L are conserved in several members of the orthopoxvirus (OPXV) genus. Where present each protein shares more than 90% amino acid identity between different OPXVs. ORFs are broken in variola virus and in the orthologues of A55 and C2 in monkeypox – ZAI (Table 3.2) (Shchelkunov et al., 2002). For some of these broken ORFs, although parts of the BTB or Kelch domain might remain, unless the ORF is located at the 5' end of the mRNA it cannot be translated. It is also unclear whether different truncated proteins would be stable due to possible abnormal folding.

<b>Virus</b>	<b>Gene name &amp; orthologue % aa identity to VACV-WR A55</b>	<b>Gene name &amp; orthologue % aa identity to VACV-WR C2</b>	<b>Gene name &amp; orthologue % aa identity to VACV-WR F3</b>
VACV-WR	A55R; <b>100</b>	C2L; <b>100</b>	F3L; <b>100</b>
Variola virus-IND	J7R-J8R; ORF broken: no BTB domain, only 3 Kelch motifs remain	D13L-D13.5L; ORF broken: both BTB and Kelch domains broken	C7L; ORF broken: broken BTB domain, no Kelch domain
Camelpox-CMS	CMP172R; <b>94</b>	CMP24L; <b>97</b>	CMP38L; <b>96</b>
Cowpox-Brighton	CPXV193; <b>95</b>	CPXV035; <b>98</b>	CPXV050; <b>95</b>

Red			
Cowpox-GRI-90	A57R; <b>99</b>	C18L; <b>99</b>	G3L; <b>96</b>
Ectromelia- Moscow	EVM150; <b>93</b>	EVM018; <b>97</b>	EVM027; <b>95</b>
Monkeypox-ZAI	B1R; ORF broken: no BTB domain, only 1 Kelch motif remains	D16L-D19L; ORF broken, remaining: half BTB domain, half BACK domain, and 2 Kelch motifs	C9L; <b>97</b>

**Table 3.2. VACV WR BTB/Kelch proteins are conserved in some other OPXVs.** Amino acid sequences of A55, C2 and F3, and their orthologues from different OPXVs, were aligned using Clustal Omega. A55, C2 and F3 are conserved in several OPXVs with high sequence conservation (> 90% amino acid identity).

### 3.2 A55, C2 and F3 inhibit activation of the NF- $\kappa$ B signalling pathway

All three VACV BTB/BACK-Kelch (BBK) proteins A55, C2 and F3 were shown to alter the recruitment of immune cells in a mouse intradermal model by unknown mechanisms (Beard et al., 2006; Froggatt et al., 2007; Pires de Miranda et al., 2003), and the ectromelia virus (ECTV) orthologue of A55 (ECTV EVM150) was reported to target NF- $\kappa$ B (Wang et al., 2014). Hence, the effect of A55, C2 and F3 on innate immune signalling pathways (NF- $\kappa$ B, IRF-3, JAK-STAT and AP-1) was investigated. To determine whether A55, C2 and F3 regulate the activation of NF- $\kappa$ B signalling pathway, HEK-293Ts were co-transfected with plasmids expressing TAP-tagged A55, C2 or F3, along with plasmids expressing NF- $\kappa$ B-Luc (firefly luciferase under the control of the NF- $\kappa$ B promoter) and SV40-Renilla (Renilla luciferase under control of

the constitutive SV40 promoter (no enhancer) reporter gene for normalization of luciferase experiments) (Chen and Prywes, 1999). Empty vector (EV) and a cellular BBK protein KLHL12 tagged in the same way were included as negative controls, and VACV protein B14 was included as a well characterised inhibitor of NF- $\kappa$ B signalling (Chen et al., 2008). Cells were untreated or stimulated by addition of IL-1 $\beta$  (Figure 3.3A) or TNF $\alpha$  (Figure 3.3B) or transfection with plasmids expressing TRAF2 (Figure 3.3C) or TRAF6 (Figure 3.3D) and the luciferase activity was measured in cell lysates. Relative luminescence levels were calculated by normalizing firefly luminescence to *Renilla* luminescence and are represented as relative to levels of the nonstimulated EV condition. A55, C2 and F3 inhibited the NF- $\kappa$ B signalling pathway in response to both IL-1 $\beta$  and TNF $\alpha$  (Figure 3.3A, B), indicating that each protein either inhibits both pathways separately before they converge, or that each protein inhibits at a position at or downstream of the position at which these 2 pathways converge. Each VACV protein also inhibited pathway activation induced by TRAF2 or TRAF6 over-expression (Figure 3.3C, D). For A55, these results are consistent with the prior observation that the closely related orthologue of A55, ECTV EVM150, inhibits NF- $\kappa$ B pathway activation (Wang et al., 2014).

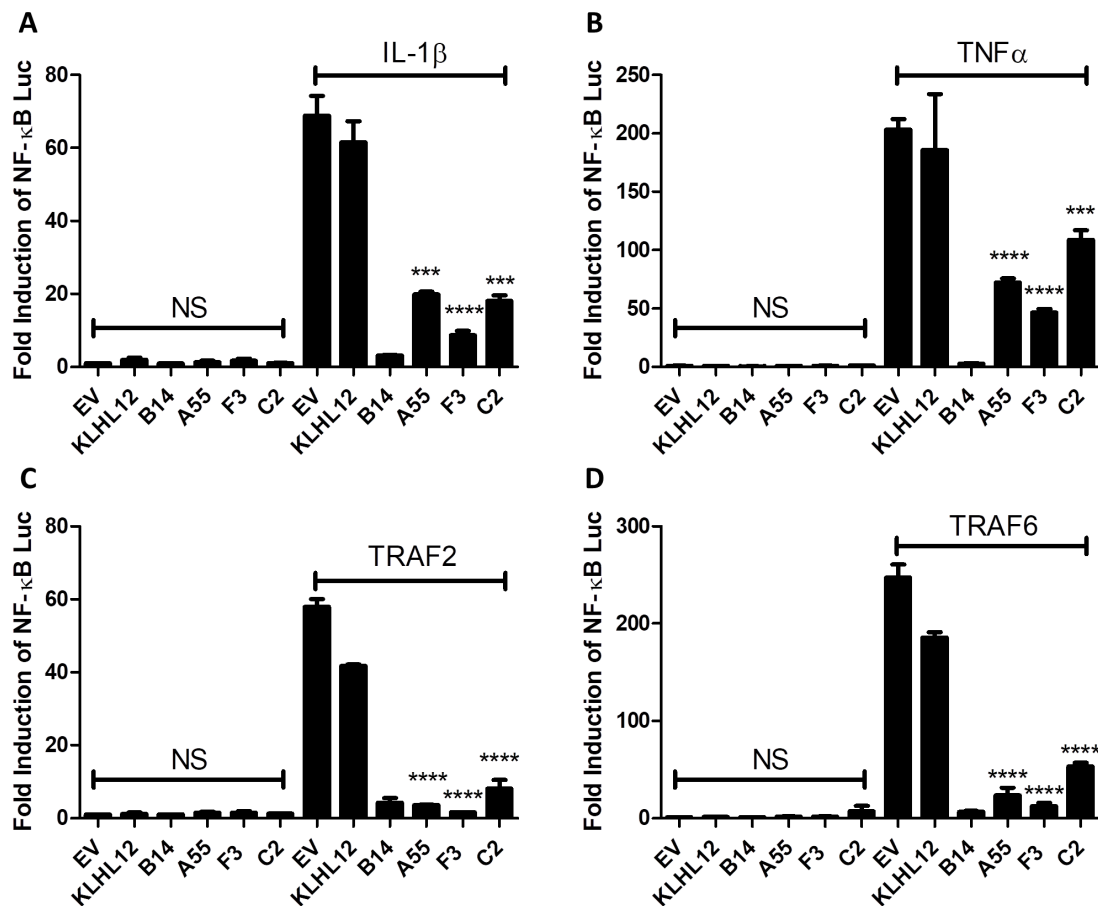


**Figure 3.3. A55, C2 and F3 inhibit activation of the NF- $\kappa$ B signalling pathway.** HEK-293Ts were transfected with the NF- $\kappa$ B reporter, SV40-renilla luciferase and plasmids for expression of proteins indicated. Cells were untreated or stimulated with IL-1 $\beta$  or TNF $\alpha$  at 20 ng/ml (A-B) or TRAF2 at 40 ng (C) or TRAF6 at 10 ng (D) for 6 h and luciferase activity was measured in cell lysates. Data shown (mean  $\pm$  SD) are representative of 3 experiments carried out in quadruplicate and were analysed by an unpaired Student's t-test (\*\* P<0.01, \*\*\* P<0.001, \*\*\*\* P<0.0001) in comparison to stimulated EV control.

To validate the inhibitory effect of A55, C2 and F3, alternative assays such as RT-qPCR and ELISA ought to be carried out to measure the expression of an endogenous NF- $\kappa$ B-responsive gene at the transcriptional and protein level. Transient transfection could be used for reporter gene assays as plasmids formed a complex before being delivered to cells and the reporter signal comes from cells expressing target genes such as TAP-C2. However for assays like RT-qPCR and ELISA, signals are measured from the cell population and inefficient transfection would lead to misleading conclusions. Thus, stable cell lines inducibly expressing

BBK proteins or other control proteins such as B14, were constructed using lentivirus transduction system. A HEK-293T and a HeLa cell line transduced with the tetracycline repressor (TetR) were available in the lab. These cell lines were transduced with lentivirus vectors to generate cell lines inducibly expressing A55, C2, C2-B, C2-K, F3, B14 and C6, all N-terminally TAP-tagged. Cells were also transduced with an empty vector as a control. Transduced cells were selected with puromycin. Data shown are representative immunoblots of target proteins with tubulin as the loading control from the whole cell lysates of HEK-293T cell lines (Figure 3.4).

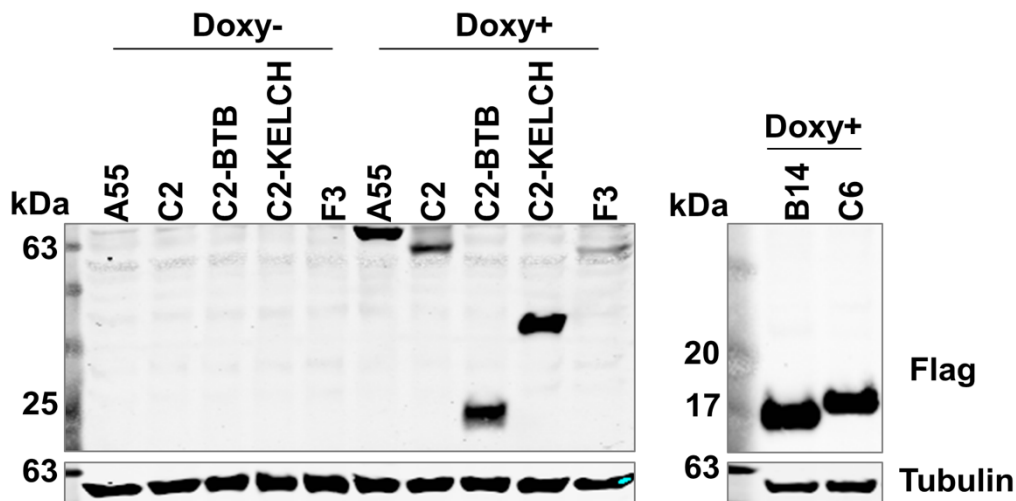


**Figure 3.4. Inducible HEK-293T cell lines.** Inducible cell lines were constructed as described. After puromycin selection, cells were induced by doxycycline at 2  $\mu\text{g/ml}$  for 24 h. Whole cell lysates were harvested by lysing cells in 0.5 % NP-40/PBS and analysed by SDS-PAGE followed by immunoblotting with specific rabbit anti-Flag antibody. Molecular masses (in kDa) are indicated on the left.

HEK-293T cell lines were then used for RTqPCR and ELISA. Cells were stimulated with  $\text{TNF}\alpha$ , and the levels of *IL-8* mRNA and secreted IL-8 were measured. C6 is an inhibitor of IRF3 (Unterholzner et al., 2011b) and JAK-STAT signalling downstream of type I IFN (Stuart et al., 2016). As expected, B14 inhibited strongly. A55, C2 and F3 each inhibited the transcription of *IL-8* and the secretion of IL-8 (Figure 3.5).

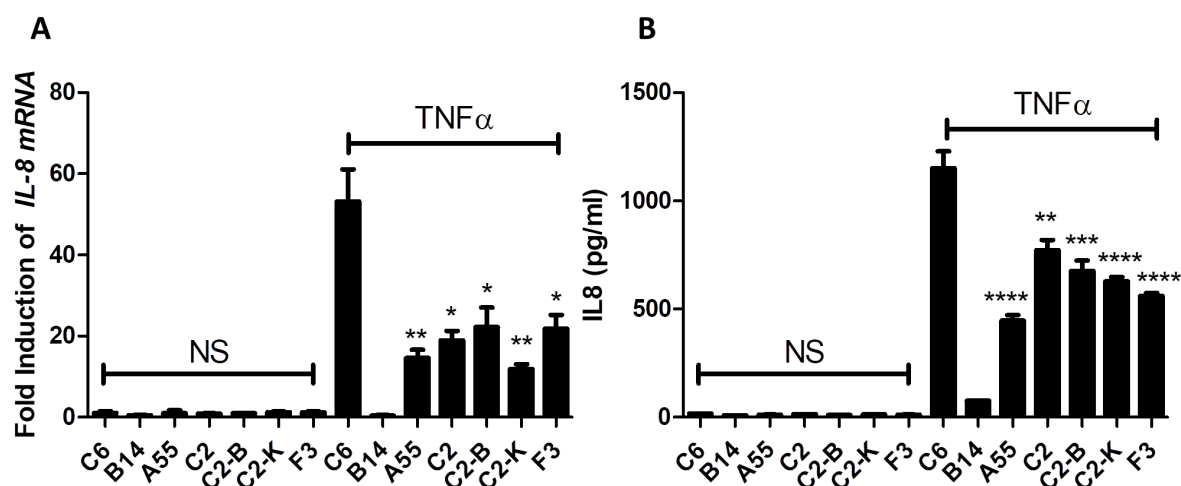


**Figure 3.5. A55, C2 and F3 inhibit activation of the NF- $\kappa$ B signalling pathway at transcriptional and protein levels.** (A) HEK-293Ts cells were induced with 2  $\mu$ g/ml doxycycline to express C6, B14, A55, C2, C2-B, C2-K or F3 for 24 h and left unstimulated or stimulated with 20 ng/ml TNF for 1.5 h. *IL-8* transcription levels were analysed by RT-qPCR relative to GAPDH, as the house keeping gene. (B) ELISA. Cells were starved for 3 h in DMEM and left unstimulated or stimulated with TNF for 18 h. Levels of secreted IL-8 in the cell culture medium were assayed by ELISA. Data shown (mean  $\pm$  SD) are representative of 3 experiments carried out in quadruplicate and were analysed by an unpaired Student's t-test (\*\* P<0.01, \*\*\* P<0.001, \*\*\*\* P<0.0001) in comparison to C6 control.

To determine which domain of the VACV BTB-Kelch proteins mediates the NF- $\kappa$ B inhibitory activity, HEK-293Ts were co-transfected with plasmids expressing TAP-tagged full length C2/F3 or the N-terminal BTB-BACK domains (C2/F3-B) or the C-terminal Kelch domains (C2/F3-K), along with plasmids expressing NF- $\kappa$ B-Luc or SV40-Renilla. EV and KLHL12 were included as negative controls, and B14 as the positive control. Cells were untreated or stimulated by addition of IL-1 $\beta$  and the luciferase activity was measured in cell lysates. Immunoblotting for the Flag tag showed that these proteins were expressed at similar levels (Figure 3.6C-D). Interestingly, both the BTB-BACK and Kelch domains of C2 showed independent inhibitory activity, although this inhibition was stronger for C2-K (Figure 3.6A). These observations were consistent with the RT-qPCR and ELISA data (Figure 3.5). In

contrast, for F3 it is the Kelch domain that inhibits the pathway but not the BTB domain (Figure 3.6B). This is similar to published data of A55, which also showed A55-Kelch but not A55-BTB inhibits the NF- $\kappa$ B signalling pathway (Pallett et al., 2019).

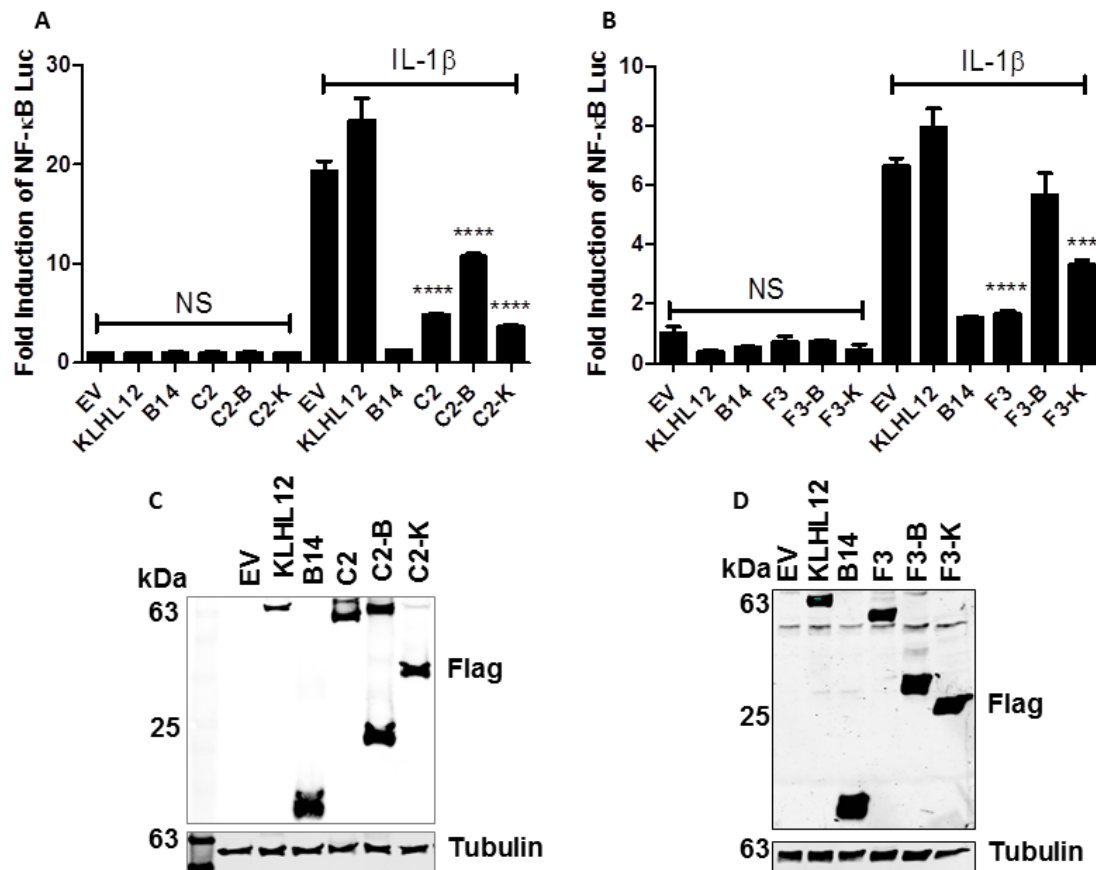


**Figure 3.6. BTB and Kelch domains of C2 and F3 show different inhibition of NF- $\kappa$ B.** (A, B) HEK-293Ts were transfected with the NF- $\kappa$ B reporter, SV40-renilla luciferase and plasmids for expression of the TAP-tagged proteins indicated. Cells were untreated or stimulated with IL-1 $\beta$  at 20 ng/ml for 6 h and luciferase activity was measured in cell lysates. Data shown (mean  $\pm$  SD) are representative of 3 experiments carried out in quadruplicate and were analysed by an unpaired Student's t-test (\*\* P<0.01, \*\*\* P<0.001, \*\*\*\* P<0.0001) in comparison to stimulated EV (A-B). (C, D) Immunoblotting. Protein expression of cells treated in (A, B); molecular masses (in kDa) are indicated on the left.

### 3.3 A55, C2 and F3 inhibit NF- $\kappa$ B downstream of p65

To determine at what stage A55, C2 and F3 inhibit the NF- $\kappa$ B pathway, the pathway was activated by overexpression of TAK1/TAB1, IKK $\beta$  or p65. A55 was shown to

inhibit the TAK1/TAB1 or IKK $\beta$ -induced activation of NF- $\kappa$ B signalling (Pallett et al., 2019). Only data from experiments performed by the author of this thesis will be shown here. Like B14, C2 and F3 were able to inhibit the pathway when it was activated by overexpression of TAK1/TAB1 or IKK $\beta$  (Figure 3.7A, B). However, unlike B14, A55, C2 and F3 also inhibited the p65-induced signalling in a dose-dependent manner (Figure 3.7A-C). In contrast, the host BBK protein KLHL12 did not inhibit NF- $\kappa$ B activation under any condition. Immunoblotting showed reasonably consistent expression of the different proteins and equivalent loading was shown by blotting for  $\alpha$ -tubulin (lower panels) (Figure 3.7D-F). These data suggest A55, C2 and F3 interfere with NF- $\kappa$ B activation at or downstream of p65. Notably a reduced level of TAK1 and TAB1 was observed when cells were overexpressing B14 or C2 (Figure 3.7D) as well as reduction in p65 expression in cells overexpressing F3 (Figure 3.7F).

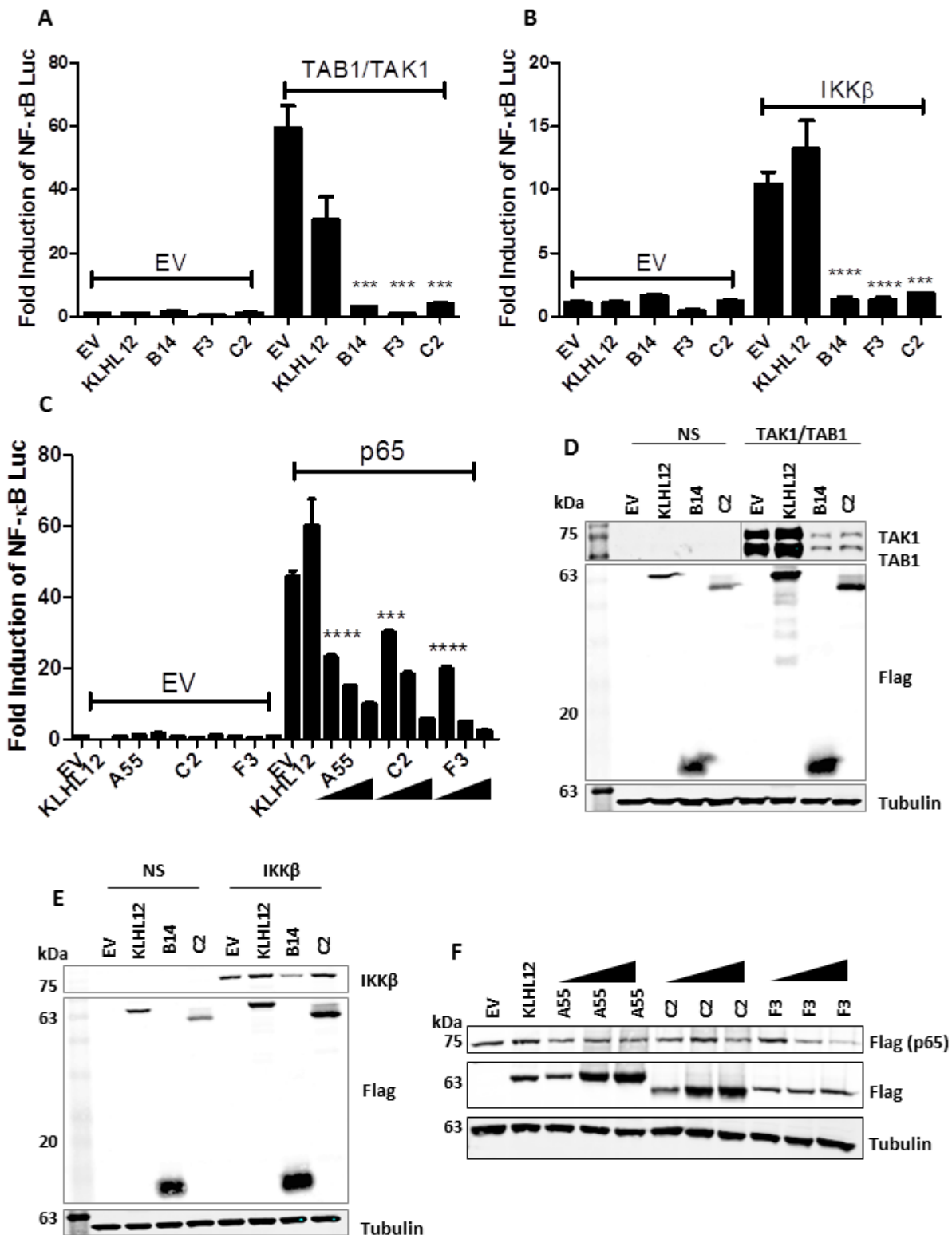


**Figure 3.7. A55, C2 and F3 inhibit NF-κB at or downstream of p65.** (A-C) HEK-293Ts were transfected with the NF-κB reporter, SV40-renilla luciferase and plasmids for expression of the TAP-tagged proteins indicated. Cells were untreated or stimulated by co-transfecting TAK1/TAB1, IKKβ or p65. Cells were lysed 24 h after transfection and the luminescence was measured. Data shown (mean ± SD) are representative of 3 experiments carried out in quadruplicate. Statistical

analysis was performed by unpaired Student's t-test (\*\* P<0.01, \*\*\* P<0.001, \*\*\*\* P<0.0001) in comparison to stimulated EV control. (D-F) Immunoblotting. Protein expression of cells treated in (A, B, C) except F3 in D and E; molecular masses (in kDa) are indicated on the left.

### **3.4 A55, C2 or F3 does not prevent I $\kappa$ B $\alpha$ degradation**

Upon activation of the NF- $\kappa$ B signalling pathway, the inhibitor of  $\kappa$ B (I $\kappa$ B $\alpha$ ) is phosphorylated by activated IKK $\beta$ , leading to its ubiquitylation and degradation by the proteasome. This causes release of the NF- $\kappa$ B subunits p50 and p65, their translocation into the nucleus and induction of transcription of NF- $\kappa$ B-responsive genes. Preliminary data from reporter gene assay indicated that A55, C2 and F3 inhibited NF- $\kappa$ B activation at or downstream of p65. To obtain independent evidence for the stage in the pathway at which these proteins mediate their inhibition, the activation of the pathway was examined by monitoring the level and phosphorylation of I $\kappa$ B $\alpha$ . Transduced HEK-293T cell lines inducibly expressing B14/A55/C2/F3, as well as EV as a negative control, were induced to express the viral protein by addition of doxycycline (where indicated) and then either left untreated or stimulated with TNF- $\alpha$  for 30 min. The level of expression of I $\kappa$ B $\alpha$  was examined by immunoblotting. Upon stimulation, I $\kappa$ B $\alpha$  was degraded in the EV group compared to the untreated EV cells, whereas it was stabilised by B14 that binds to IKK $\beta$  and inhibits I $\kappa$ B $\alpha$  phosphorylation (Chen et al., 2008). In comparison, A55, C2 or F3 did not stabilise I $\kappa$ B $\alpha$  (Figure 3.8A). The levels of I $\kappa$ B $\alpha$  relative to an internal control p50 were quantified by densitometry from multiple experiments and no significant difference in I $\kappa$ B $\alpha$  levels in the presence of A55, C2 or F3 compared to EV was found (Figure 3.8B).

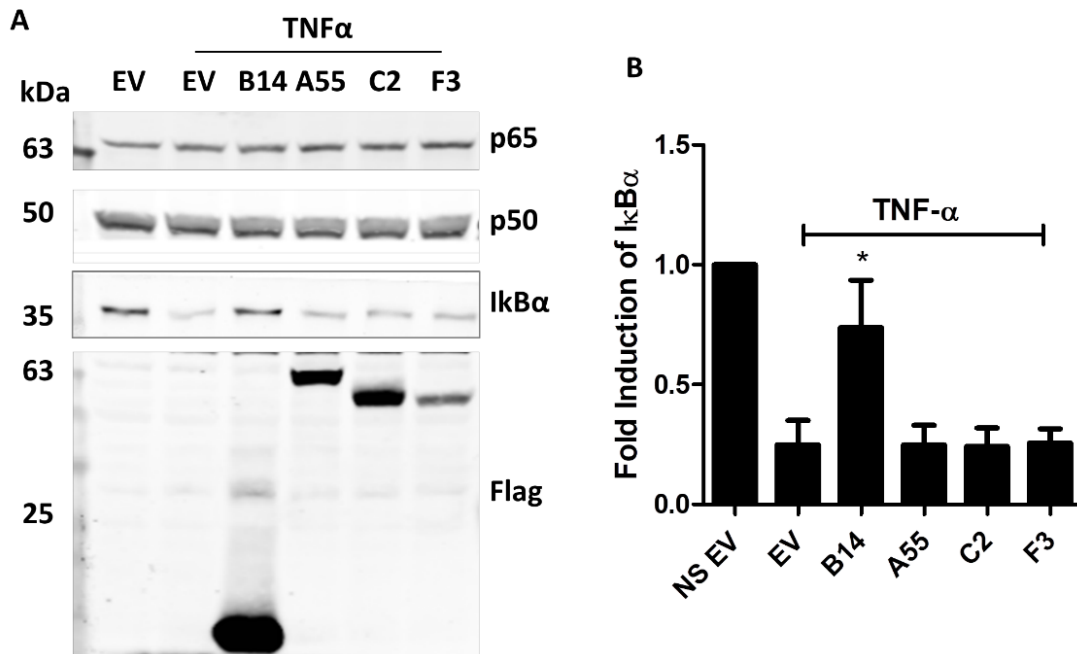


**Figure 3.8. A55, C2 or F3 do not prevent IkB $\alpha$  degradation.** (A) Immunoblot for IkB $\alpha$  levels following TNF- $\alpha$  stimulation of EV, B14 A55, C2 or F3 HEK cell lines induced with 2  $\mu$ g/ml doxycycline for 24 h. The protein expression levels were determined using anti-Flag. Molecular masses (in kDa) are indicated on the left. (B) Levels of IkB $\alpha$  relative to p50 as quantified by densitometry. Data shown (mean  $\pm$  SD) are the average of 3 independent experiments and were analysed by an unpaired Student's t-test (\*\* P<0.01, \*\*\* P<0.001, \*\*\*\* P<0.0001) in comparison to stimulated EV control.

### 3.5 A55, C2 and F3 diminish p65 nuclear translocation

Next the ability of A55, C2 or F3 to prevent p65 translocation into the nucleus was examined by immunofluorescence. HeLa cells were transfected with plasmids encoding TAP-tagged B14, F3, A55, C2, C2-B, C2-K or empty vector (EV). To achieve a clean p65 exclusion from the nucleus without stimulation, transfected cells were starved for 3 h in serum-free medium before being stimulated with TNF- $\alpha$  for 30 min followed by fixation and immunofluorescence. In the EV group, p65 was mainly cytoplasmic when untreated and nuclear after TNF- $\alpha$  stimulation. In contrast, p65 remained in the cytoplasm following stimulation in the presence of B14 as expected. Interestingly, those cells expressing A55, F3, C2, C2-B and C2-K showed a partially inhibitory effect on the p65 nuclear translocation, compared to EV and non-

transfected cells (Figure 3.9A). Cells expressing Flag-tagged proteins were quantified from three independent experiments, with or without nuclear p65. The results are shown as a percentage of Flag-positive cells with nuclear p65 (Figure 3.9B). This showed that with EV, the proportion of cells with nuclear p65 increased from 15% to 90% following TNF- $\alpha$  stimulation. B14 inhibited p65 translocation into the nucleus, with only 10% cells having p65 in the nucleus. For A55, C2, C2-B or C2-K positive cells about 40%-50% showed nuclear p65 after TNF- $\alpha$  stimulation, about 20% for F3, indicating partial inhibition on the p65 translocation (Figure 3.9B). Collectively, these data indicate that A55, C2 and F3 inhibit the NF- $\kappa$ B signalling pathway downstream of I $\kappa$ B $\alpha$  degradation and at or upstream of p65 translocation. Note that cells expressing C2 and C2-B showed an unusual morphology change that cells were rounded up. This is likely linked to the association between C2 and Cdc42 via its BTB domain, which will be illustrated later. Due to the morphology change, the data collection was challenging which makes the data less certain, and one should be more cautious about interpreting p65 translocation.

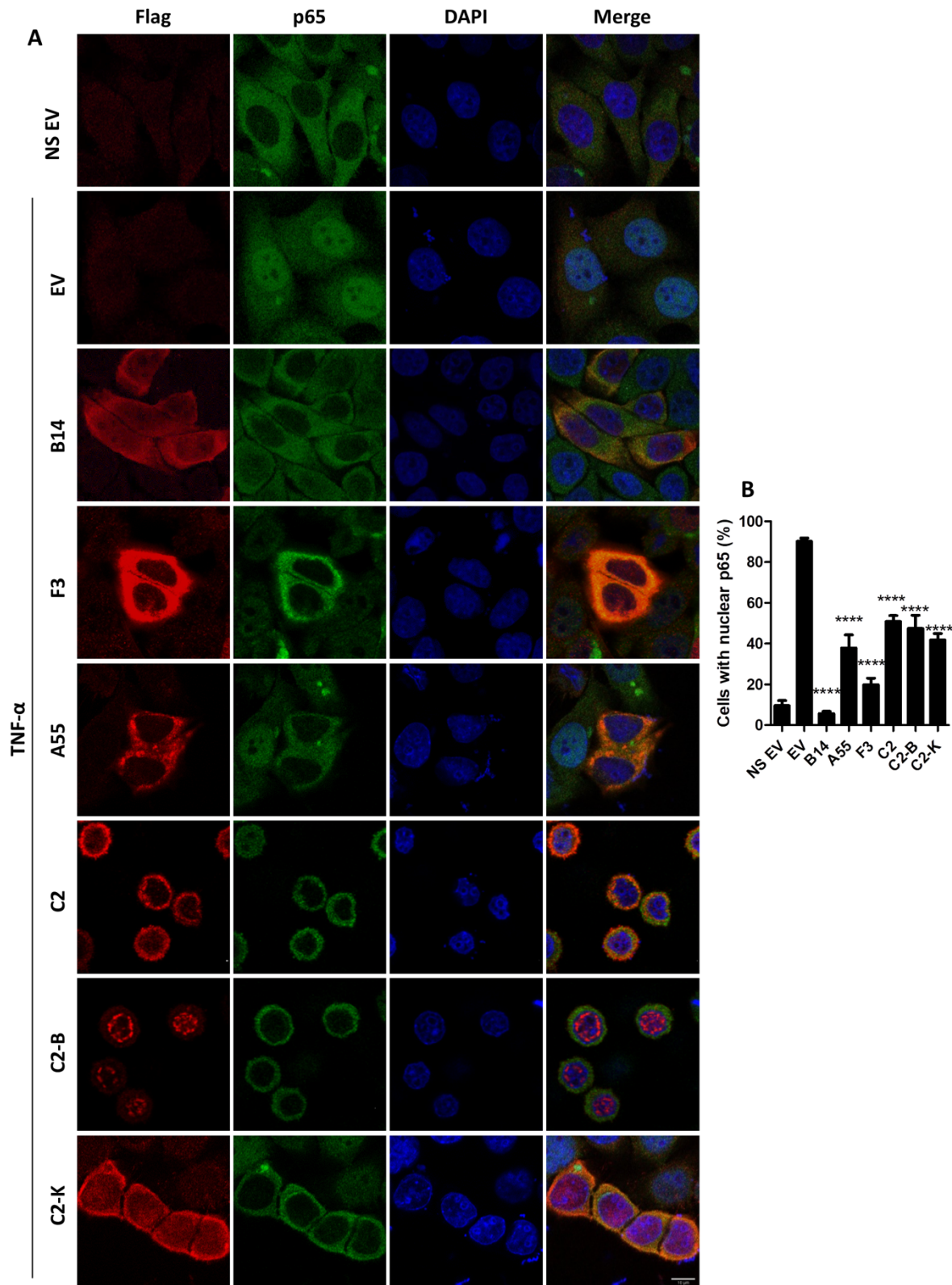


**Figure 3.9. A55, C2 and F3 diminish p65 nuclear translocation.** (A) Representative immunofluorescent staining of p65 localisation in HeLa cells transfected with plasmids encoding Flag-tagged, B14, F3, A55, C2, C2-B, C2-K or empty vector (EV) and left untreated or stimulated with 20 ng/ml TNF- $\alpha$  for 30 min. Cells were stained with DAPI (blue), anti-Flag (red) and anti-p65 (green). Scale bar: 10  $\mu$ m. (B) Average number of cells with nuclear p65. Data shown (mean  $\pm$  SD) are

representative of 3 experiments, each carried out in triplicate and 100 cells counted per conditions. Data were analysed by an unpaired Student's t-test (\*\*\*\* P<0.0001) in comparison to stimulated EV control.

### **3.6 Over-expressed C2 does not co-precipitate with cullin-3 or Flag-**

#### **KPNA2**

BTB-Kelch proteins have been implicated as substrate-specific adaptors for protein ubiquitylation in Cul3-based E3 ubiquitin-ligase complexes. In BTB-Kelch proteins, the BTB domain is proposed to interact with the Cul3 component of the complex, whereas the Kelch domain is presumed to act as the substrate-recognition module, leading to the degradation or modification of the substrate (Pintard et al., 2004a). Therefore, it was investigated if C2 interacts with Cul3. HEK-293Ts were transfected with pcDNA4 A55 or C2 for 18 h followed by Flag-tagged immunoprecipitation (IP) of cleared lysates. Co-immunoprecipitation of Cul3 was probed with an endogenous anti-Cul3 antibody. Similar amounts of A55 and C2 were pulled down, but whereas Cul3 was co-IPed by A55, consistent with published data (Gao et al., 2019; Pallett et al., 2019), C2 did not co-IP Cul3 (Figure 3.10A). Notably data shown in reporter gene assays (Figure 3.6A) indicated that both full length C2 and also the BTB and Kelch domains separately, inhibited the NF- $\kappa$ B signalling pathway. This observation, and the failure of C2 to co-IP with Cul3, indicates that C2 likely inhibits the NF- $\kappa$ B signalling pathway via a Cul3-independent mechanism.

The inhibitory effect of A55, C2 and F3 on NF- $\kappa$ B signalling pathway has been narrowed down to downstream of I $\kappa$ B $\alpha$  degradation and at or upstream of p65 translocation. It would be interesting to know how exactly these VACV BBK proteins block p65 nuclear translocation. The activation of the IKK complex causes phosphorylation of I $\kappa$ B $\alpha$ , leading to the polyubiquitylation of I $\kappa$ B $\alpha$ , which is then rapidly degraded by the proteasome (Henkel et al., 1993; Karin and Ben-Neriah,

2000). This results in the release of p50 and p65, exposing the nuclear localisation signals (NLSs) of these NF- $\kappa$ B dimers. With the help of importin  $\alpha/\beta$  heterodimers, in which importin  $\alpha$  binds to NLS, and importin  $\beta$  docks the importin-cargo complex, the dimers of p50 and p65 are translocated into the nucleus where they activate NF- $\kappa$ B responsive genes (Fagerlund et al., 2005; Görlich. and Kutay., 1999; Macara, 2001). Importin  $\alpha$ -1 (also known as KPNA2), was shown to be most important for p65 import (Liang et al., 2013b). KPNA2 is co-immunoprecipitated by A55, with or without the context of infection, and ectopic A55 reduces the level of KPNA2 co-immunoprecipitated by HA-p65 (Pallett et al., 2019). Therefore, the possible interaction between C2 and KPNA2 was examined in this study as well.

HEK-293Ts were transfected with pcDNA4 TAP-A55, -C2 or another VACV protein - N1, for 18 h followed by Flag-tagged IP of cleared lysates. Co-IP of KPNA2 was probed with an endogenous anti-KPNA2 antibody. Consistent with published data, KPNA2 was co-IPed by TAP-A55, but this was not observed with TAP-C2 despite the amount of A55 and C2 pulled down being similar (Figure 3.10B) (Pallett et al., 2019). A little bit of KPNA2 was co-IPed by the negative control TAP-N1, probably due to the stickiness and/or higher level of N1 expression.

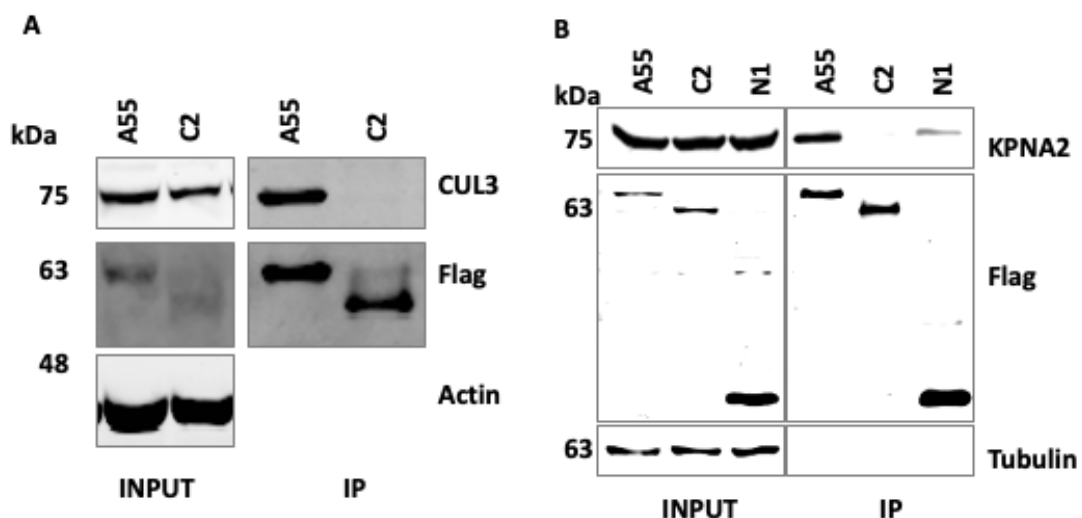


**Figure 3.10. Overexpressed C2 does not co-precipitate with cullin-3 or KPNA2.** HEK-293Ts were transfected with pcDNA4/TO-nTAP-A55, pcDNA4/TO-nTAP-C2 or pcDNA4/TO-nTAP-N1 for 18 h. Cells were lysed in (A) NP40 buffer or (B) RIPA buffer, followed by Flag-tagged immunoprecipitation (IP) of cleared lysates. Co-immunoprecipitation of cullin-3 (A) or KPNA2 (B) was probed with an endogenous anti-CUL3 or anti-KPNA2 antibody. Molecular masses (in kDa) are indicated on the left. Data shown are representative of at least 3 experiments.

## **4 Results 2 – C2 Co-IPs Cul3 when A55 is present**

As a BTB-Kelch protein, C2 is predicted to interact with Cul3, however Cul3 was not co-IPed by ectopic C2 (Figure 3.10A). Another VACV BTB-Kelch protein A55 has been shown to interact directly with Cul3 (Gao et al., 2019). In addition ECTV EVM018 (the orthologue of VACV C2) or EVM027 (the orthologue of VACV F3) expressed as EGFP fusion proteins did not co-IP Flag-Cul3 (Wilton et al., 2008a). However, Flag-EVM018 was reported to co-IP with endogenous Cul3 during VACV-Cop infection, and a weak interaction between EVM027 and Cul3, was also noted (Couturier, 2009b). This chapter focuses on the investigation of the putative interaction between VACV C2 and Cul3.

### **4.1 The problem of detecting C2 by immunoblotting**

Several studies reported a difficulty in detecting C2 protein expression, especially in the cleared cell lysates (Couturier, 2009b; Pires de Miranda et al., 2003). A few possible reasons that might cause this were explored. *C2L* or *A55R* cloned in the pcDNA4/TO vector were transfected into HEK-293Ts and cells were lysed in several commonly used lysis buffers in the lab, namely normal lysis buffer (Tris based buffer containing Triton-X100), HEPES-based lysis buffer (HEPES based buffer containing NP-40) and 0.5% NP-40/PBS, to test if the method of lysis (different compartments, protein solubility, etc.) could improve detection. Whole cell lysates from passive lysis buffer (commercial; Promega E1941) were obtained as a positive control as it worked fine for the immunoblottings (whole cell lysates) for the reporter gene assays carried out in the beginning of the study. Cleared lysates were also obtained after centrifugation at 14,000 rcf for 20 min. Then samples were then boiled and analysed by SDS-PAGE followed by immunoblotting with the indicated antibodies. As shown in Figure 4.1A, the level of protein in the cleared lysates dropped greatly compared

to the level of protein in the whole cell lysates for all buffers, which suggested either the stability of C2 was disrupted, or C2 associated with the insoluble fraction. To address this, a harsher buffer (RIPA containing SDS, sodium deoxycholate and NP-40) was used but the levels of protein were not improved (data not shown).

The same problem remained even when C2 or F3 proteins were enriched by pulling down with specific anti-Flag M2 affinity gel from cleared lysates of cells engineered to inducibly express these proteins or the BTB or Kelch domains of C2 (Figure 4.1B). HEK-C2, HEK-C2-B, HEK-C2-K and HEK-F3 cell lines were induced or not with doxycycline for 24 h before lysed in passive lysis buffer, followed by Flag-tagged IP of cleared lysates. Proteins pulled down were analysed by immunoblotting. The parental cell line HEK tetR was included as a negative control. Interestingly, it seemed proteins were stuck in the stacking gel and quite possibly the Kelch domain is responsible for this effect (red arrow).

Different approaches were tried to solve this problem, which was evident whether the samples were prepared from transfected or infected cells. When it came to the different heat treatments during sample preparation, interesting differences emerged (Figure 4.1C). HeLa cells were infected with a recombinant VACV expressing Flag-tagged C2 (vC2-Flag) (Pires de Miranda et al., 2003), harvested after overnight infection and lysed in 0.5% NP-40/PBS. Both whole cell lysates and cleared lysates were collected. Samples were heated at 100°C or 60°C or not heated. The detection of C2 protein increased as the temperature dropped in comparison to the loading control. Consistent with previous experiments, samples that were boiled had the majority of C2 stuck in the stacking gel. Thus, protein samples for all immunoblotting in this thesis were not heated unless otherwise stated.



Methods). Whole cell lysates lysed in passive lysis buffer were obtained as a positive control and cleared lysates were obtained by centrifugation. Then samples were boiled and analysed by SDS-PAGE followed by immunoblotting with the indicated antibodies. (B) Enriched proteins by incubating with anti-Flag M2 affinity gel from cell lines inducibly-expressing Flad-tagged C2, the BTB or Kelch domains of C2, or F3. Where indicated cells were induced with doxycycline for 24 h and lysed in passive lysis buffer. Blue band of 25 kDa is the Ig light chain. (C) Different temperatures and sample density during sample preparation. HeLa cells were infected at 5 p.f.u. / cell with vC2-Flag, harvested after 16 h and lysed in 0.5 % NP-40/PBS. Samples were heated at 100°C or 60°C for 5 min or not heated (w/o) and then analysed by SDS-PAGE and immunoblotting. Data shown are representative of at least 3 experiments.

## **4.2 C2 co-immunoprecipitates Cul3 during infection**

To test the possible interaction between C2 and Cul3 during infection, HeLa cell lines engineered to express TAP-tagged A55 or C2 inducibly after doxycycline addition were mock-treated or infected with WT VACV at 10 p.f.u./cell for 14 h, before lysing the cells in 0.5% NP-40/PBS. Cell lines were chosen for this assay instead of infecting wild type cells with vC2-Flag because a positive control vA55-Flag was not available. Cell lysates were cleared by centrifugation at 14,000 rcf for 15 min, followed by Flag-tagged IP of cleared lysates. Co-IP of Cul3 was probed with an endogenous anti-Cul3 antibody. A small proportion of cleared lysates were kept with loading buffer as the input. Flag-A55 co-IPed Cul3 in mock-infected and infected cells, whilst Flag-C2 could not co-IP Cul3 from mock-infected cells, but interestingly, Cul3 was co-IPed with C2 during VACV infection (Figure 4.2A). This result is consistent with the observations made with the ECTV orthologues of C2 and A55 (Couturier, 2009b). Although the infection control D8 was not perfect, it does not weaken the conclusion as even with less infection context, Flag-C2 was still able to pull down Cul3. The same result was obtained when HeLa cell lines inducibly expressing C2 or A55 were infected with viruses lacking A55 or C2, to avoid competition between tagged and untagged viral protein. EV was included as the IP

beads control, and B14 as a viral protein control. This showed that endogenous Cul3 was co-IPed by Flag-A55 and Flag-C2 but only during infection, and not by EV or Flag-B14 (Figure 4.2B). A double-band signal was picked up by the Cul3 antibody in the C2 IP group, and the upper band might be neddylated Cul3. Conjugation of NEDD8 (neural precursor cell expressed developmentally down-regulated protein 8) to the C terminus of Cul3 is required for the E3 ubiquitin ligase activity, and the Cul3 antibody used in this study was designed to recognise the C terminus of Cul3 (Merlet et al., 2009). Although Figure 4.2 suggest that Cul3 seems activated when C2 was over expressed, this pattern was not observed repeatedly. Moreover, the double band of Cul3 could also be seen in conditions when A55 was over expressed (Figure 4.3).

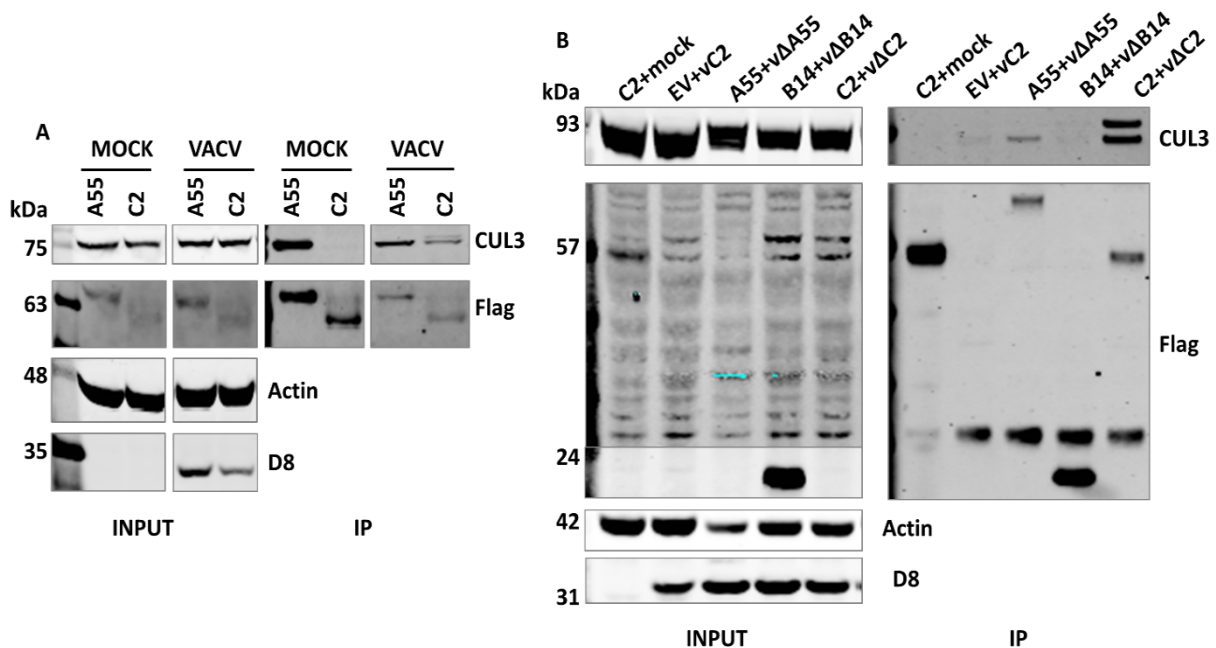


**Figure 4.2. C2 coimmunoprecipitates Cul3 during VACV infection.** HeLa cell lines were induced with 2  $\mu$ g/ml doxycycline to express TAP-EV/A55/C2/B14 for 24 h. Cells were then mock treated or infected with WT VACV (A) or viruses lacking A55 or B14 or C2 (B) at 10 p.f.u./cell for 14 h. Cells were lysed in 0.5% NP40/PBS buffer followed by Flag-tagged IP of cleared lysates. Samples were analysed by SDS-PAGE and immunoblotting with the indicated antibodies. Some of (B) was under exposed to better detect B14. Molecular masses (in kDa) are indicated on the left. Data shown are representative of at least 3 experiments.

### 4.3 Cul3-C2 association is A55 dependent

The fact that C2 could not co-IP Cul3 by itself, but could within the context of infection, lead to the hypothesis that C2 interacts with Cul3 via one or more other VACV proteins. Since A55 was shown to interact with Cul3 directly, and BTB domains can form homodimers and heteromers (Stogios et al., 2005), it was logical to test if C2 interacts with Cul3 via A55. HeLa cell lines were induced with doxycycline for 16 h to express TAP-A55/C2, then mock-treated or infected by viruses lacking A55 or C2, or lacking both A55 and C2, or lacking all three BTB-Kelch proteins i.e. A55, C2 and F3. After infection, cells were lysed in 0.5% NP40/PBS buffer followed by Flag-tagged IP of cleared lysates. Co-immunoprecipitation of Cul3 was probed with an endogenous anti-Cul3 antibody. Flag-A55 pulled down Cul3 when infected by v $\Delta$ A55. C2 could not co-IP Cul3 under mock condition, but Cul3 came down with Flag-C2 when cells were infected by v $\Delta$ C2. However, when Flag-C2 cells were infected by the virus lacking A55 and C2 (v $\Delta$ A55 $\Delta$ C2) or A55, C2 and F3 (v $\Delta$ A55 $\Delta$ C2 $\Delta$ F3), Cul3 was no longer co-IPed. No difference was observed in the triple deletion virus (v $\Delta$ A55 $\Delta$ C2 $\Delta$ F3) group compared to the double deletion virus (Figure 4.3). This result suggests C2 needs A55 to associate with Cul3.

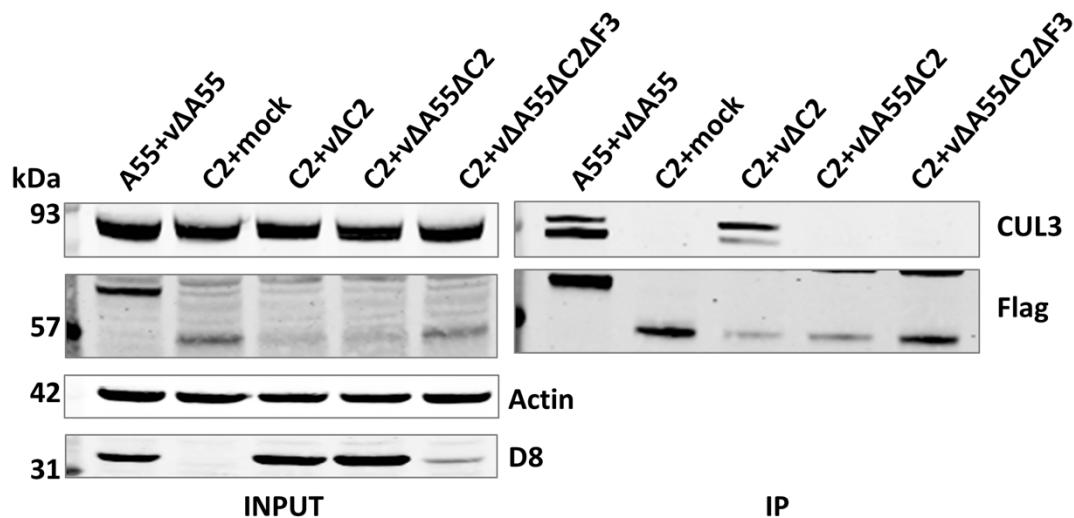


**Figure 4.3. C2 requires A55 to co-IP Cul3.** HeLa cell lines were induced to express TAP- A55/C2 by addition of 2  $\mu$ g/ml doxycycline for 24 h. Cells were then mock-treated or infected by viruses lacking A55 or C2, or lacking both A55 and C2, or lacking all three BTB-Kelch proteins i.e. A55, C2 and F3, at 10 p.f.u./cell for 9 h. Cells were lysed in 0.5% NP40/PBS buffer followed by Flag-tagged IP of cleared lysates. Samples were analysed by SDS-PAGE and immunoblotting with the indicated antibodies. Co-immunoprecipitation of Cul3 was probed with an endogenous anti-Cul3 antibody. Molecular masses (in kDa) are indicated on the left. Data shown are representative of at least 3 experiments.

Next it was examined if A55 alone is sufficient for C2 to interact with Cul3, and if C2 and A55 interact with each other (Figure 4.4). HeLa cell lines were induced with doxycycline to express TAP-C2 or B14 and then transfected with V5-tagged C6 (Unterholzner et al., 2011b) or A55, or EV control. Sixteen hours later cells were mock treated or infected by viruses lacking C2, or lacking both A55 and C2, or lacking all three BTB-Kelch proteins i.e. A55, C2 and F3. After infection, cells were lysed in RIPA buffer followed by Flag-tagged IP of cleared lysates. Note that the level of C2 expression from the cell lines was reduced by virus infection due to virus induced host shut-off. Co-immunoprecipitation of Cul3 and V5 was probed with an endogenous anti-Cul3 antibody or V5 antibody. Cul3 was co-IPed by C2 when C2-expressing cells were infected by  $v\Delta$ C2, or when HeLa-C2 cells were transfected

with V5-A55 and infected by either double deletion or triple deletion viruses. Interestingly, Flag-C2 co-IPed Cul3 outside the context of infection, when V5-A55 was co-expressed. Co-expression of two other VACV proteins C6 or B14 did not enable C2 to pull down Cul3, and V5-A55 was co-IPed by Flag-C2 with or without the context of infection. A very small amount of V5-C6 was also detected with Flag-C2, probably due to too much protein expressed.

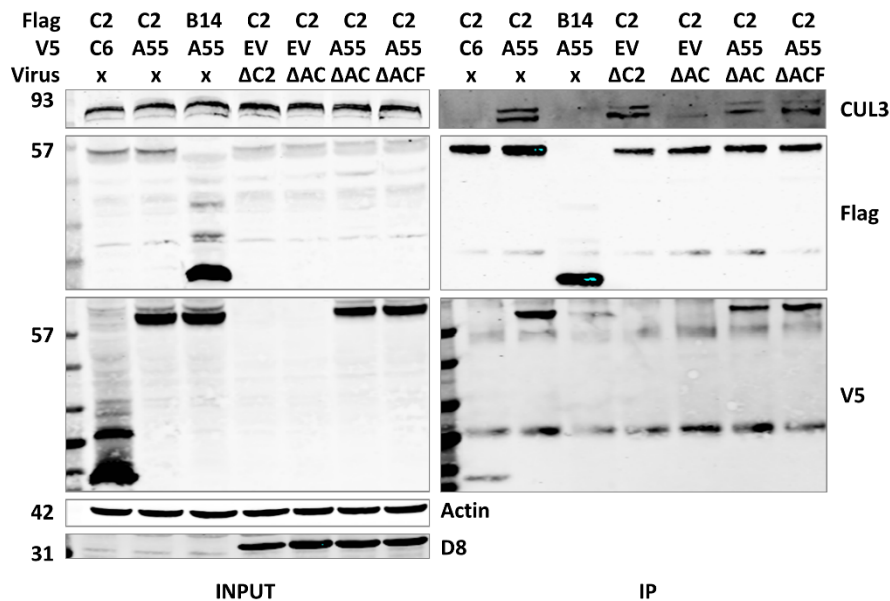


**Figure 4.4. A55 alone is sufficient for C2 to co-IP Cul3 and C2 might interact with A55.** HeLa cell lines were induced to express TAP- C2/B14 by addition of 2 µg/ml doxycycline for 24 h (Flag, top line), and then were transfected with V5-tagged C6 or A55 as indicated or EV control (V5, 2<sup>nd</sup> line). After 24 h cells were mock-treated or infected by viruses lacking C2, or lacking both A55 and C2, or lacking all three BTB-Kelch proteins i.e. A55, C2 and F3, at 5 p.f.u./cell for 12 h. Cells were lysed in RIPA buffer followed by Flag IP of cleared lysates. Samples were analysed by SDS-PAGE and immunoblotting with the indicated antibodies. Molecular masses (in kDa) are indicated on the left. Data shown are representative of at least 3 experiments.

To investigate if these proteins interacted at endogenous levels and to determine which domains were required for the interaction, HEK-293Ts were transfected with TAP-tagged C2 or F3, or the BTB or Kelch domain of each protein. Twenty-four hours post transfection, cells were either mock treated or infected by viruses lacking

C2 or F3. Cells were lysed in RIPA buffer followed by Flag IP of cleared lysates. Co-immunoprecipitation of Cul3 and A55 was probed with an endogenous anti-Cul3 or anti-A55 antibody (Figure 4.5A) (Beard et al., 2006). Consistently, in the absence of A55, Flag-C2 did not co-IP Cul3. During infection, Cul3 was pulled down by Flag-C2, and endogenous A55 produced by VACV was pulled down by Flag-C2 as well. This association was via the BTB domain of C2 but not Kelch domain, suggesting C2 associates with A55 via the BTB domain of C2, either directly or indirectly. No interaction was observed between F3 and Cul3, or between the two truncation parts of F3 and Cul3 during infection. This could mean that F3 does not interact with Cul3, or the interaction is extremely weak, or the expression level of F3 in this experiment is too low to reveal the interaction.

Next it was tested which domain of A55 might be interacting with C2. HEK-293Ts were co-transfected with TAP-tagged A55 or A55 BTB or Kelch domain, or VACV N1 as a negative control, and V5-tagged C2 or a GFP control. Twenty-four hours post transfection cells were lysed in RIPA buffer followed by V5-tagged IP of cleared lysates. Co-immunoprecipitation of TAP-tagged proteins was probed with Flag antibody (Figure 4.5B). Full length Flag-A55 and -A55-BTB was co-IPed by full length V5-C2, whilst A55-Kelch or the negative control VACV protein N1 was not pulled down. This suggests A55-BTB associates with C2. Taken together, these data suggest that A55 and C2 associate with each other via the BTB domain of both proteins to form heterodimers.

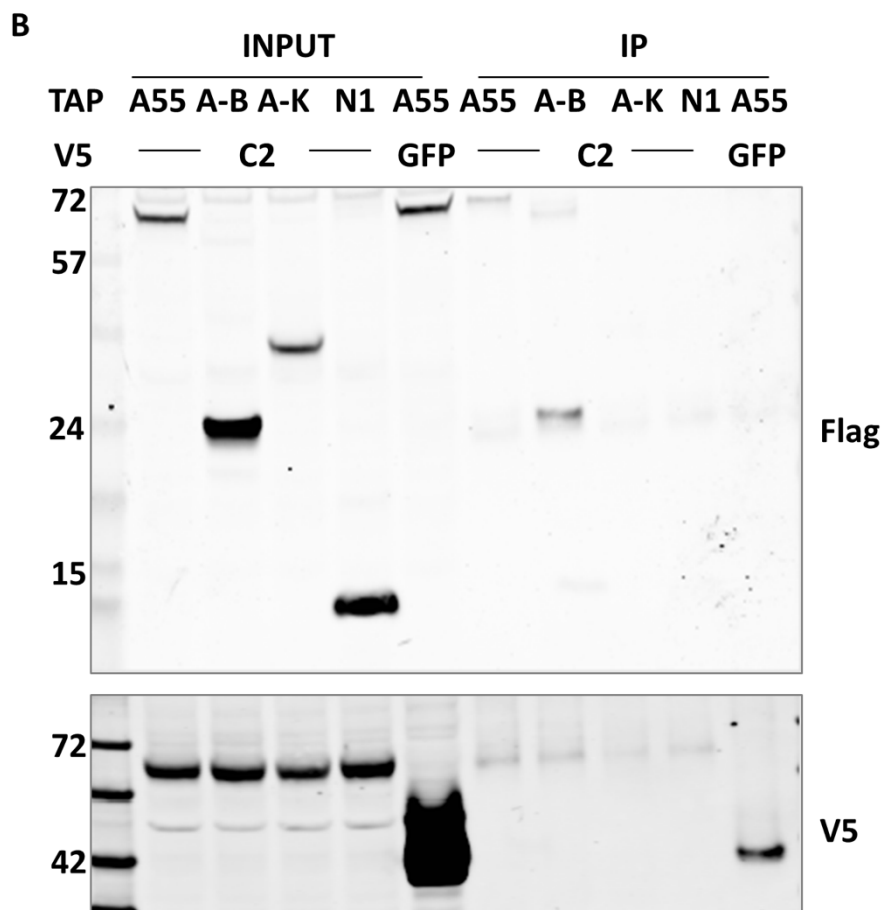
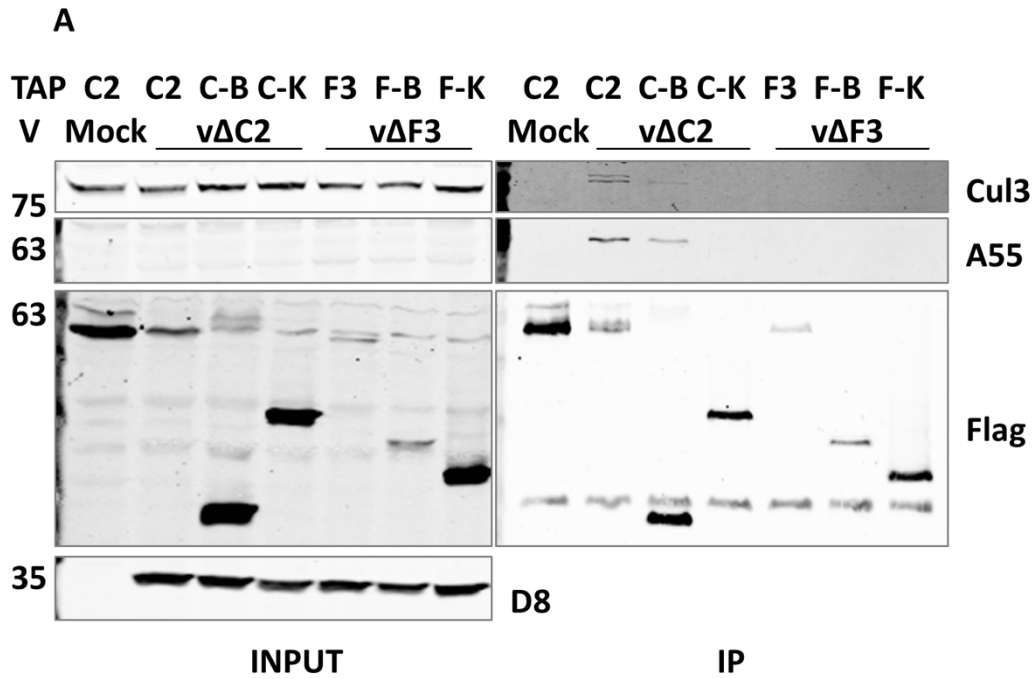


**Figure 4.5. A55 and C2 interact via each other's BTB domain.** (A) HEK-293Ts were transfected with TAP-C2/C2-BTB/C2-Kelch/F3/F3-BTB/F3-Kelch. 24 h later cells were mock treated or infected by viruses lacking C2 or F3 at 5 p.f.u./cell for 12 h. Cells were lysed in RIPA buffer followed by Flag IP of cleared lysates. In all panels

samples were analysed by SDS-PAGE and immunoblotting with the indicated antibodies (right) and molecular masses (in kDa) are indicated on the left. (B) HEK-293Ts were co-transfected with TAP-A55/A55-BTB/A55-Kelch/N1 and V5-C2/GFP for 24 h. Cells were then lysed in RIPA buffer followed by V5 IP of cleared lysates. Data shown are representative of at least 3 experiments.

Of note, in Figure 4.5B, an upper band in the A55-BTB group was observed to be co-IPed by V5-C2 too, and it is suspected to be the dimerised BTB domain of A55 based on the protein size. A55 was shown to interact with Cul3 directly, and the structure was shown as a 2:2 heterotetramer complex of A55-BTB homodimer and Cul3 N-terminal domain (Gao et al., 2019). Since C2 associates with Cul3 via A55, it was investigated if C2 out-competes the dimerisation of A55 to hijack Cul3 from A55. HEK-293Ts were transfected with V5-tagged C2 or EV along with TAP tagged A55-BTB. Cells were lysed in RIPA buffer 24 h after transfection and cleared lysates were analysed by immunoblotting. The expression level of A55-BTB both lower and upper band (red arrow) was not convincingly affected by C2, and the amount of C2 did not make an obvious difference either (Figure 4.6). It could be that C2 does not affect the dimerisation of A55-BTB, or the upper band is not the dimerised A55-BTB. Besides, A55-BTB was shown to have a very high affinity constant for Cul3, so if C2 did out-compete A55 to hijack Cul3 via the same interaction surface, C2 would have to have at least an equally high affinity to be an effective competitor. Or, C2 binds to A55 via a different interaction surface from Cul3 and the 3 proteins form a complex to work together. An alternative hypothesis might be the relative abundances of these 3 proteins enables formation of different complexes when one of the partners is low abundance.

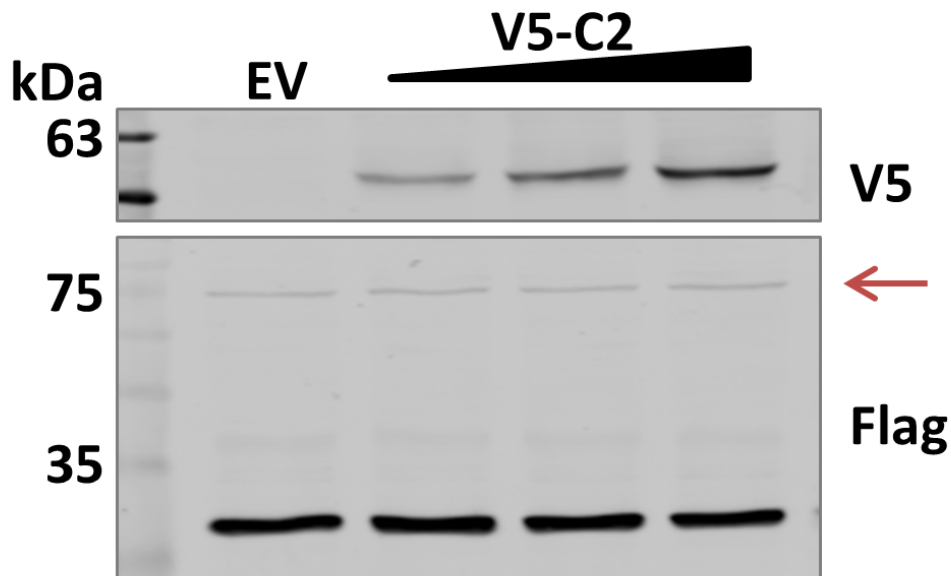


**Figure 4.6. C2 does not out-compete A55 dimerisation.** HEK-293Ts were co-transfected with V5-C2/EV control and TAP-A55-BTB for 24 h. Cells were then lysed in RIPA buffer and cleared lysates were analysed by SDS-PAGE and immunoblotting with the indicated antibody (right). Red arrow points the upper band. Molecular masses (in kDa) are indicated on the left. Data shown are representative of at least 3 experiments.

Collectively, these data suggest the working model shown in Figure 4.7. In this complex, A55 and C2 interact with each other directly or indirectly. A55 brings in Cul3 via direct interaction between A55-BTB and Cul3, whilst C2 brings in substrates, potentially via its Kelch domain, leading to the ubiquitylation of substrates followed by protein degradation or modification. For simplicity the model does not show A55 / Cul3 as the tetramer but only heterodimer. As no substrates of viral BBKs have been identified, an unbiased TMT-Mass spec was carried out to test the hypothesis of this working model as well as to identify novel viral BBKs substrates.

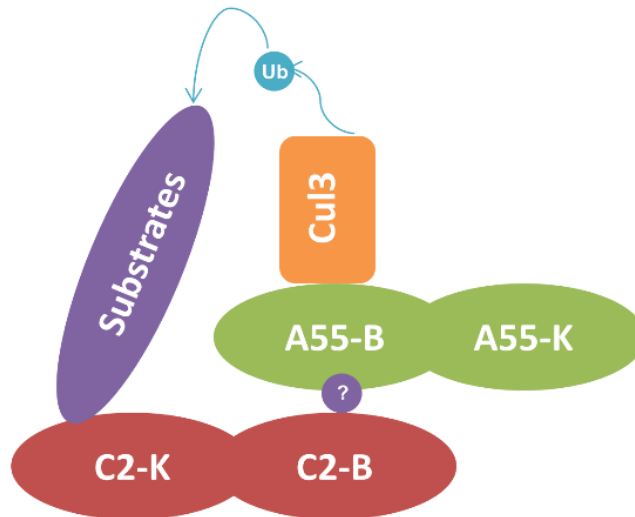


**Figure 4.7. A55 C2 working model.** A55 and C2 interact with each other directly or indirectly. A55 brings in Cul3 via direct interaction between A55-BTB and Cul3, whilst C2 brings in substrates, potentially via its Kelch domain, leading to the ubiquitylation of substrates followed by protein degradation or modification.

## **5 Results 3 – VACV proteins A55 and C2 collaborate to target cellular proteins for degradation**

The model presented in Figure 4.7 predicts that VACV needs both A55 and C2 to target cellular proteins for ubiquitylation and/or degradation to benefit some aspect of the virus life cycle. To test this model, HFFFs were infected by WT VACV or viruses lacking individual viral genes, and an unbiased quantitative temporal viromic analysis of VACV infection was performed by others (Soday et al., 2019). This approach would determine if cellular proteins degraded following infection by WT VACV were “rescued” when specific VACV genes were missing. From these experiments, several cellular proteins targeted by A55 and/or C2 were identified to be differentially regulated (unpublished) (Figure 5.1). For example, proteins Fer, Scrib, RASA2 and FRMD6 were downregulated by WT VACV more than 50% compared to mock (Figure 5.1A). The multiple lines represent 3 independent experiments. Losing C2 or A55 rescued the protein level of Fer, Scrib and RASA2 with the other mutant viruses showing very consistent flat lines, suggesting both A55 and C2 but no other VACV proteins are needed for VACV to downregulate these proteins. Notably the downregulation of these proteins were also observed in the presence of AraC (cytosine arabinoside) (Figure 5.1A), indicating that early genes were responsible and intermediate or late gene expression was not needed, which is consistent with the expression kinetics of A55 and C2 as early genes (Yang et al., 2010b). This study identifies cellular proteins specifically targeted by A55 and/or C2, as there are cellular proteins targeted by other VACV proteins but not affected by A55 or C2, such as HDAC5 degraded by VACV protein C6 (Soday et al., 2019). Interestingly, the protein level of FRMD6 was rescued by loss of A55 but not C2 (Figure 5.1B). This unbiased viromic result suggests that A55 and C2 indeed collaborate to target

cellular proteins in some cases such as Fer, Scrib or RASA2, however A55 can also downregulate cellular proteins like FRMD6 independent of C2.

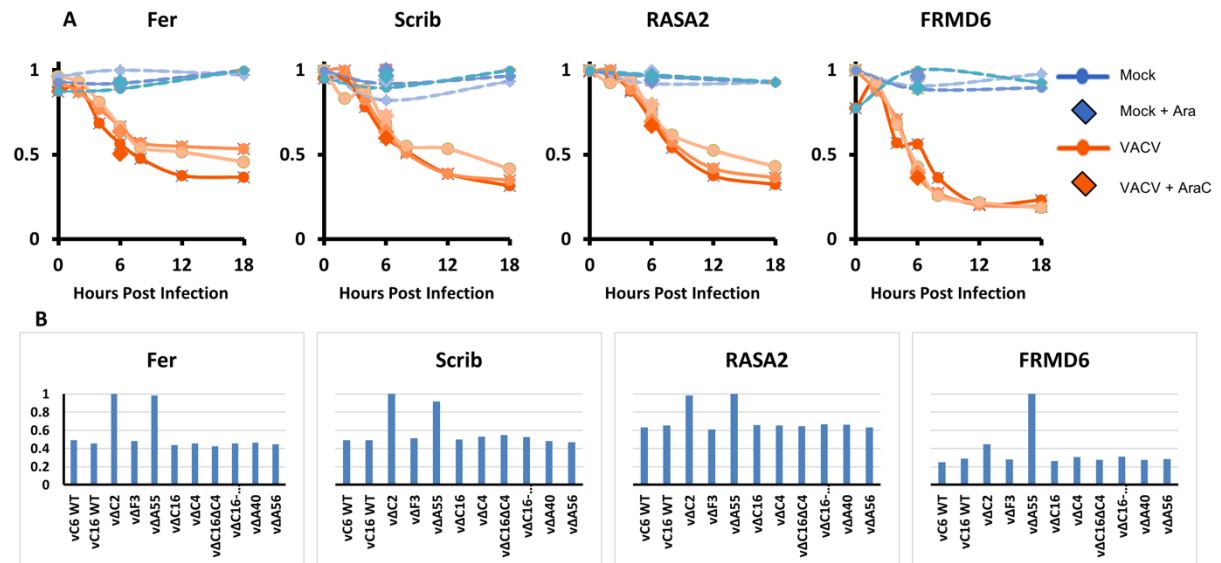


**Figure 5.1. Cellular proteins targeted for degradation by A55 and/or C2.** This work was done by others (Soday et al., 2019). (A). Telomerase reverse transcriptase (TERT)-immortalised primary human foetal foreskin fibroblasts (HFFF-TERTs) were mock-infected or infected at 5 p.f.u./cell in triplicate with WT VACV strain WR for the indicated times or one mock and one infected sample for 6 h in the presence of 40 µg/ml of cytosine arabinoside (AraC). For triplicate samples data are represented as mean ± SEM. (B) Single cultures of HFFF-TERTs were infected with mutant VACVs (derived from WT VACV WR) lacking the individual viral genes indicated at 5 p.f.u./cell for 12 h. All samples were then processed for analysis of the abundance of virus peptides by mass spectrometry as described by Soday et al., 2019.

## 5.1 Cellular targets of A55 and/or C2

### 5.1.1 Fer

Tyrosine-protein kinase FES-related (Fer) protein was identified in 1988 and is a cytoplasmic tyrosine kinase that belongs to a small family of non-transmembrane receptor tyrosine kinases. The only other member of the family is FES (Feline sarcoma). Fer and FES kinases consist of a unique amino-terminal FCH (FES/FER/Cdc-42-interacting protein homology) domain, three coiled-coil motifs that promote oligomerisation, a central Src homology 2 (SH2) domain for protein

interactions, and a kinase domain in the C-terminal region (Hao et al., 1989; Letwin et al., 1989; Siveen et al., 2018). Fer is expressed ubiquitously and acts downstream of cell surface receptors for growth factors such as platelet-derived growth factor (PDGF), and plays a role in the regulation of cell adhesion, cell migration and cytoskeleton regulation (Greer, 2002; Rosato et al., 1998; Yoneyama et al., 2012). Fer can inhibit Wnt/ $\beta$ -catenin signalling but activate EGF-dependent NF- $\kappa$ B signalling (Chen et al., 2014; Guo and Stark, 2011). Fer promotes the progress and/or metastasis of multiple malignancies such as pancreatic cancer, breast cancer and lung adenocarcinoma (Ahn et al., 2013; Ivanova et al., 2013; Liu et al., 2014). Fer was also shown to enhance the innate immune response in a murine model of pneumonia, by promoting the recruitment of inflammatory monocytes and activating STAT signalling (Dolgachev et al., 2018).

### **5.1.2 RASA2**

Ras GTPase-activating protein 2 or Ras p21 protein activator 2 (RASA2), also known as GAP1<sup>m</sup> (as a mammalian counterpart of the *Drosophila* Gap1), is a member of the GAP1 family of GTPase-activating proteins (Maekawa et al., 1994). Ras, as a small GTPase, cycles between an active GTP-bound and inactive GDP-bound form. This cycle is controlled by guanine nucleotide exchange factors (GEFs), which stimulate the exchange of GDP for GTP, and by GTPase-activating proteins (GAPs), which terminate the active state by stimulating GTP hydrolysis (Trahey and McCormick, 1987). Among the GAPs, the GAP1 subfamily consists of RASA3, RASA2 (or GAP1<sup>m</sup>), RASA4 (or CAPRI) and RASAL (or RASAL1) (Allen et al., 1998; Cullen et al., 1995; Lockyer et al., 2001; Maekawa et al., 1994). RASA2 controls cellular proliferation and differentiation by suppressing Ras function. Since Ras is over-activated in some cancers, RASA2 is seen as a tumour-suppressive

gene. In fact, a study showed RASA2 expression was lost in more than 30% of human melanomas and was associated with reduced patient survival. Loss-of-function mutations of RASA2 were also found in 5% of melanomas, leading to overactive Ras, melanoma cell growth and migration (Arafah et al., 2015).

### **5.1.3 FRMD6**

FERM domain-containing protein 6 (FRMD6), also known as Willin (after William Dick, founder of the Royal (Dick) School Veterinary College, University of Edinburgh, Scotland, UK) was firstly identified in 2005. The level of FRMD6 in human tissue was found to be low and FRMD6 was shown to bind phospholipids (Gunn-Moore et al., 2005). FRMD6 belongs to the 4.1 superfamily, with other members including ezrin, radixin, moesin (ERM), merlin, talin and protein-tyrosine phosphatases. The 4.1 superfamily proteins are involved in maintaining submembrane cytoskeleton, and have a conserved region called the FERM (4.1 ERM) domain near the N terminus (Bretscher et al., 2002). Not much is known about the functional role of FRMD6 in mammalian cells, but ectopic expression of FRMD6 could activate Hippo signalling pathway, by increasing the phosphorylation of Hippo signalling pathway components MST1/2, LATS1 and YAP (Angus et al., 2012).

### **5.1.4 Scrib**

Protein scribble homologue (Scrib) was originally identified in *Drosophila* and is highly conserved between *Homo sapiens* and *Drosophila*. Scrib is a member of the LAP (for “LRR and PDZ”) family of adaptor proteins that are involved in polarity and proliferation of epithelial cells. LAP proteins feature a combination of 16 leucine-rich repeats (LRR) at the N terminus and either four (LAP4), one (LAP1) or no (LAP0) copies of the PDZ domain at the C terminus. PDZ is short for “PSD95/DLG/ZO-1”,

the three proteins where this domain was first identified. Scrib is a LAP4 protein (Bilder and Perrimon, 2000; Santoni et al., 2002).

Scrib localises at the base of adherence junctions (Bryant, 1997; Dow et al., 2003). So far Scrib has been associated with roles in cell-cell adhesion, maintaining cell polarity, pro-apoptotic signalling, and suppressing tumour progression (Humbert et al., 2003). For example, Scrib was downregulated and mis-localised by mammary tumours (Zhan et al., 2008). Disruption of cell-cell adhesion and cell polarity can lead to the loss of epithelial identity through a process called epithelial to mesenchymal transition (EMT), a crucial process in tumour progression providing tumour cells with the ability to escape from the primary tumour, to migrate to distant regions and to invade tissues (Moreno-Bueno et al., 2008). Scrib has also been reported to be targetted by viral factors such as high-risk human papillomavirus (HPV) E6, with which Scrib interacts directly via its PDZ domain, leading to Scrib degradation (Nakagawa and Huibregtse, 2000). As a scaffold protein, Scrib binds to other proteins as well. BetaPIX ( $\beta$ PIX), a GEF for Rac/Cdc42, directly binds to the Scrib PDZ domains, bridging PAK, a Rac/Cdc42 effector, to Scrib, enabling Scrib to regulate the activity of PAK. Overexpression of Scrib also inhibits  $\beta$ PIX and Cdc42 recruitment to the leading edge of cells (Audebert et al., 2004; Nola et al., 2008; Osmani et al., 2006). Cdc42 functions at the cell membrane to stabilise the Arp2/3 complex to promote actin polymerisation (Watson et al., 2017). Scrib has been shown to regulate MAPK-ERK signalling (Elsum et al., 2013), Hippo signalling (Cordenonsi et al., 2011) and cell-cycle progression from G1 to S phase (Nagasaka et al., 2006). Loss of Scrib has also been shown to upregulate TGF- $\beta$  / Smad signalling in mice (Yamben et al., 2013).

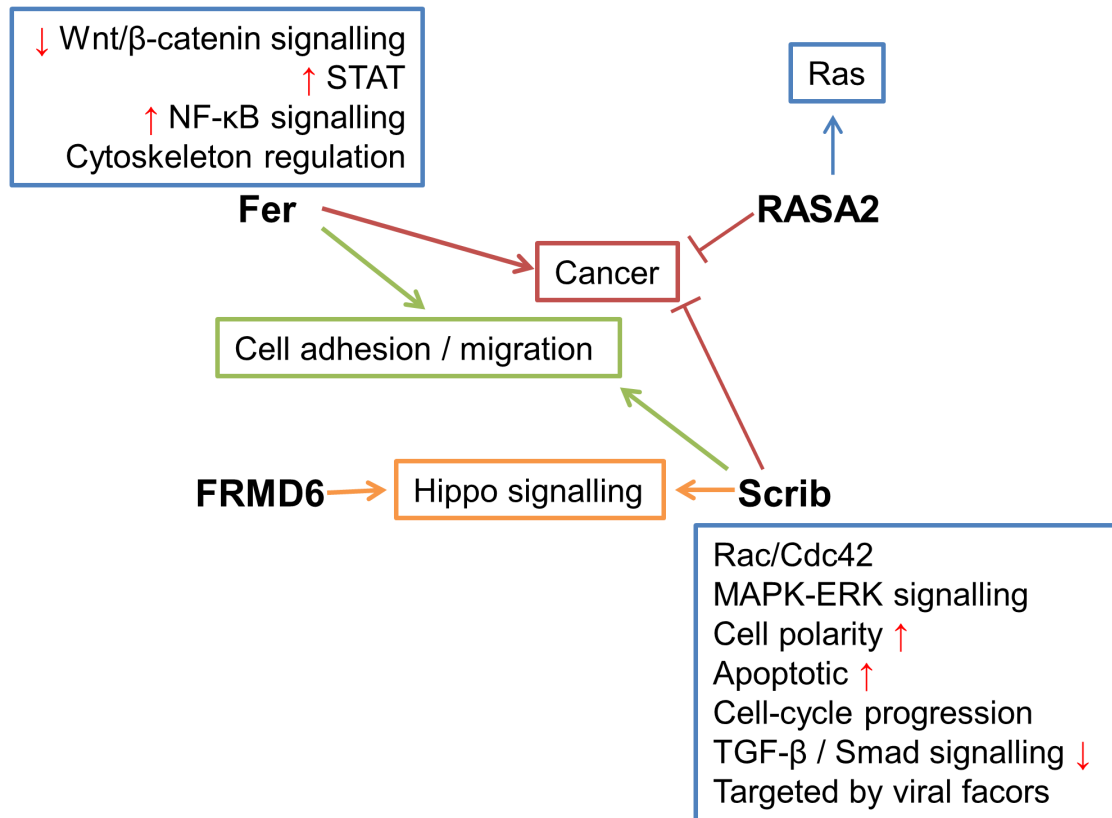


**Figure 5.2. Summary of A55 and/or C2 cellular targets.**

## **5.2 A55 and C2 collaborate to degrade Scrib**

To validate the viromic data, as well as to screen cell lines and test antibodies for the expression and detection of target proteins, a few commonly used human cell lines in the lab such as HEK-293T, HeLa and HFF were infected with VACV or mutant strains lacking A55 or C2, and all three proteins, Fer, RASA2 and Scrib, targeted by both A55 and C2 were tested by immunoblotting. Due to either low protein expression levels or lack of a sensitive / specific antibody, it was difficult to detect endogenous Fer or RASA2, but this was not the case for Scrib. Scrib has been shown to regulate the activity of Cdc42, a potential binding partner of C2 (more details in chapter 7), providing a link to C2, hence work on Scrib was prioritised and is the focus of this chapter. As the main interest of this thesis is the collaborative

function of A55 and C2, and FRMD6 seems to be the target of A55 solely according to the viromic data, FRMD6 was not the primary focus but is included in some assays as an additional testing target or a control.

HEK-293Ts were mock-treated or infected by WT VACV (vC2, the parental viruses used to construct vΔC2) at 10 p.f.u./cell. A proteasome inhibitor MG132, which reduces the degradation of ubiquitin-conjugated proteins in mammalian cells, was added 3 h p.i. to allow virus attachment and early gene expression including *A55R* and *C2L* (Lee and Goldberg, 1998; Satheshkumar et al., 2009; Yang et al., 2010a). Cells were then lysed in 1% NP-40/PBS at the indicated time p.i.. Cleared lysates were analysed by immunoblotting. Endogenous Scrib was detected with a specific antibody. Scrib is a rather big protein of 210 kDa, therefore 8% polyacrylamide gels were used to optimise Scrib detection by immunoblotting. Tubulin was probed as the protein loading control as its level is not altered during VACV infection. VACV protein C16 was probed as the infection control (Figure 5.3). After infection with WT VACV the levels of Scrib decreased, consistent with the viromic data, however adding MG132 prevented this, suggesting that this downregulation is due to proteasome dependent degradation.

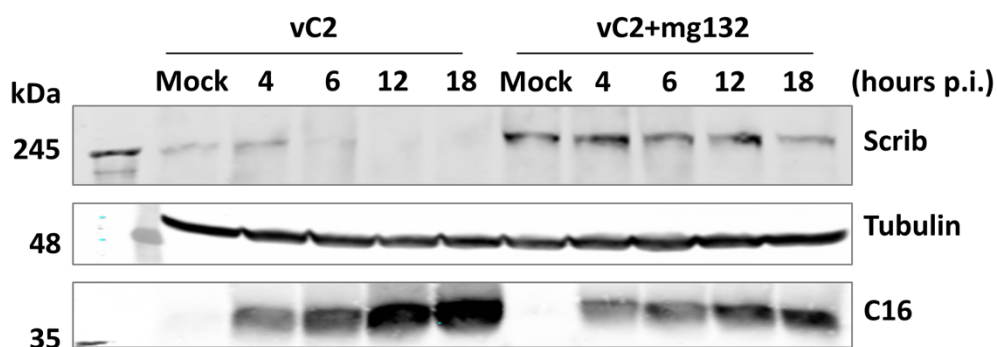


**Figure 5.3. Validation of Scrib degradation by VACV.** HEK-293Ts were mock treated or infected by WT VACV at 10 p.f.u./cell for the times shown. Where indicated MG132 (10  $\mu$ M) was added 3 h p.i. Cells were lysed in 1% NP-40/PBS and cleared lysates were analysed by immunoblotting (8% polyacrylamide for Scrib, 12%

polyacrylamide for tubulin and C16). Molecular masses (in kDa) are indicated on the left. Data shown are representative of at least 3 experiments.

Next, to validate if Scrib is targeted by A55 and C2 collaboratively, HEK-293Ts were mock-treated or infected at 10 p.f.u./cell with VACV, or viruses lacking A55 or C2. Cells were then lysed in 1% NP-40/PBS when indicated and cleared lysates were analysed by immunoblotting. As above, Scrib was degraded by WT VACV compared to mock control, but infection with strains lacking either C2 or A55 did not induce Scrib degradation (Figure 5.4A). This is consistent with the viromic data (Figure 5.1). Infection with a virus lacking both C2 and A55 ( $v\Delta AC$ ) resulted in similar levels of Scrib to infection with viruses lacking either A55 or C2 (Figure 5.4B). This showed that both C2 and A55 are needed for Scrib degradation and loss of either has the same outcome as loss of both. To validate the viromic data for FRMD6, and to provide further evidence that A55 and/or C2 target cellular proteins by more than one mechanism, HeLa cells were mock treated or infected by WT VACV, or viruses lacking C2 or A55 or both A55 and C2. Cells were lysed in a harsher buffer RIPA to better detect FRMD6, and cleared lysates were analysed by immunoblotting. Actin was detected as the loading control and D8 as the infection control (Figure 5.4C). Little FRMD6 was detected in the mock infected cells, which could be a technical issue or low protein expression in the particular cell line (HeLa), and is inconsistent with the viromic data in Figure 5.1 (HFFF cells). No FRMD6 was detected after WT VACV or  $v\Delta C2$  infection, however FRMD6 was observed after infection by  $v\Delta A55$  and  $v\Delta AC$ . This result suggests that FRMD6 is targeted by A55 but not C2. The viromic data (Figure 5.1) do not indicate that FRMD6 is upregulated after infection.

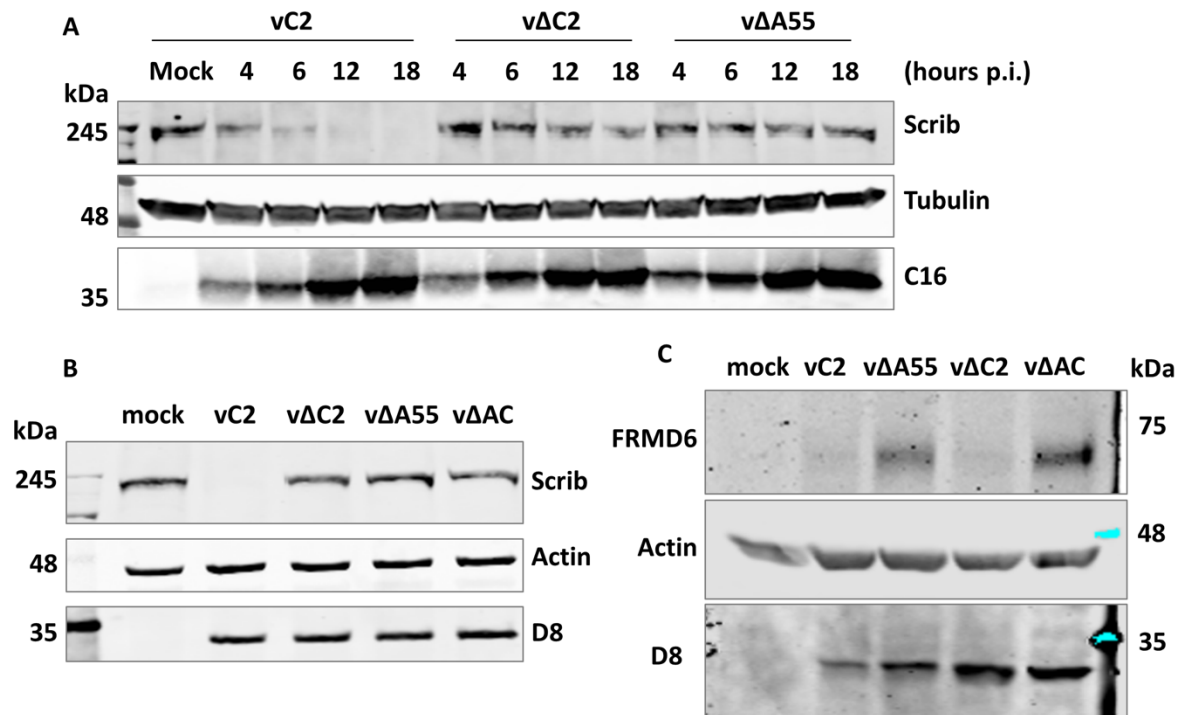


**Figure 5.4. Validation of protein rescue by loss of A55 and/or C2.** (A) HEK-293Ts were mock treated or infected by WT VACV, or viruses lacking C2 or A55 at 10 p.f.u./cell. Cells were lysed in 1% NP-40/PBS at indicated h p.i. Cleared lysates were analysed by immunoblotting (8% polyacrylamide for Scrib and 12% polyacrylamide for alpha-tubulin and C16). (B) HEK-293Ts were mock treated or infected by WT VACV, or viruses lacking C2 or A55 or both A55 and C2 at 5 p.f.u./cell. Cells were lysed in 1% NP-40/PBS 18 h p.i.. Cleared lysates were analysed by immunoblotting (8% polyacrylamide for Scrib, 12% polyacrylamide for actin and D8). (C) HeLa cells were mock treated or infected by WT VACV, or viruses lacking C2 or A55 or both A55 and C2 at 5 p.f.u./cell. Cells were lysed in RIPA buffer 14 h p.i. Cleared lysates were analysed by immunoblotting (12% polyacrylamide). Molecular masses (in kDa) are indicated on the left (A and B) or the right (C). Data shown are representative of at least 3 experiments.

### 5.3 A55 and C2 are sufficient to degrade Scrib

A55 and C2 are both needed for VACV to induce degradation of Scrib, but it is not known if A55 and C2 are sufficient to degrade Scrib without the help of other VACV proteins. To examine this, HEK-293T cell lines that inducibly express A55 or C2 were produced (Methods) and initially the stability of Scrib in these cells was examined after infection by VACVs lacking A55, C2 or both proteins (Figure 5.5A), and if the protein level of A55 or C2 in these cell lines, aided by the context of infection, is enough to degrade Scrib, i.e. if these cell lines are a good tool to study

the degradation of Scrib. HEK-293T cell lines were induced with doxycycline to express TAP-A55 / C2 or left untreated and 24 h later cells were mock treated or infected by viruses lacking A55 or C2 (to avoid competition between tagged A55 and C2, made by the cell lines, and untagged A55 or C2, made by virus infection) for 14 h. Cleared lysates were collected and analysed by immunoblotting (Figure 5.5A). The protein level of Scrib was abundant in mock-infected, induced HEK-A55 or HEK-C2 cell lines, once again suggesting A55 or C2 alone is not enough to degrade Scrib. Viruses lacking A55 or C2 could not degrade Scrib in non-induced HEK-293T cell lines, but Scrib was degraded in cells that were induced to express A55 or C2, and then infected by viruses expressing either C2 or A55. Note that the level of tagged-A55 or C2 made by the cell line is much reduced 14 h p.i. compared to mock infected cells because of virus induced host shutoff. These results suggest that: 1) these inducible HEK-293T cell lines are a good tool to study Scrib degradation, and 2) mechanistically the degradation of Scrib requires both A55 and C2, although whether other viral factors are also required cannot be ruled out at this stage.

Next a HEK-293T cell line inducibly expressing both A55 and C2 (named HEK-AC) was constructed to determine if A55 and C2 are sufficient to degrade Scrib. HEK-293T cell lines were induced to express TAP-A55, C2, or A55 and C2 (AC). Twenty-four h later cells were lysed and cleared lysates were analysed by immunoblotting (Figure 5.5B). Scrib was not detected in the cell line expressing both A55 and C2, but was clearly visible in cell lines expressing only A55 (HEK-A55) or C2 (HEK-C2). Tubulin showed relatively equal protein loadings. This result indicates that A55 and C2 are sufficient to degrade Scrib, and other factors induced by or expressed by VACV are not needed.

Altogether, these data show that: 1) Scrib is degraded by VACV in a proteasome-dependent manner; 2) the degradation of Scrib requires both A55 and C2; 3) A55 and/or C2 can target cellular proteins together or independently; and 4) A55 and C2 are sufficient to degrade Scrib in the absence of other viral factors.

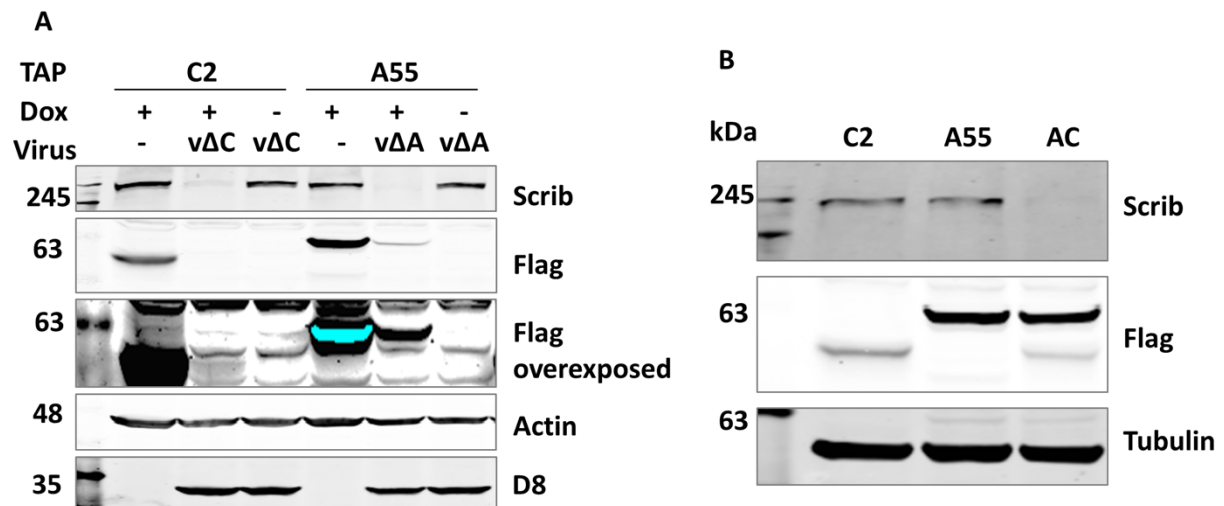


**Figure 5.5. A55 and C2 are sufficient to degrade Scrib.** (A) HEK-293T cell lines were induced where indicated (+) with 2  $\mu$ g/ml doxycycline to express TAP- A55/C2 for 24 h. Cells were mock treated or infected by viruses lacking A55 or C2 at 5 p.f.u./cell for 14 h. Cells were lysed in 1% NP40/PBS buffer and cleared lysates were collected and analysed by immunoblotting. (B) HEK-293T cell lines were induced with 2  $\mu$ g/ml doxycycline to express TAP-A55, C2, or A55 and C2 for 24 h. Then cells were lysed in 1% NP40/PBS buffer and cleared lysates were collected and analysed by immunoblotting. Molecular masses (in kDa) are indicated on the left. Data shown are representative of at least 3 experiments.

#### 5.4 Degradation of Scrib requires the interaction between A55 and Cul3

Previously, purified recombinant A55 and Cul3 was used to demonstrate that the interaction of these proteins was direct and the crystal structure of these proteins was determined (Gao et al., 2019). Structure based mutagenesis and isothermal titration calorimetry (ITC) demonstrated that substitution of isoleucine 48 for glutamic acid (I48E) reduced the binding of A55 to Cul3 greatly (>100 fold) in vitro (Gao et al., 2019). Isoleucine 48 was conserved in A55 orthologues from other poxviruses, but not in the VACV proteins C2 or F3 (Gao et al., 2019). This suggests that A55-I48 might be highly important for A55 binding to Cul3 in vivo. Further, the fact that C2 or

F3 lack I48 is consistent with the observation that they do not interact with Cul3 on their own, as shown before (Chapter 4).

To investigate if A55 and C2 targeting of cellular proteins requires an interaction between A55 and Cul3, a TAP-tagged I48E A55 cloned into pcDNA4/TO was constructed and checked by DNA sequencing (Figure 5.6B). To test the dependence on I48E for A55 interaction with Cul3, HEK-293Ts were transfected with a low (0.5  $\mu$ g) and a high (3  $\mu$ g) dose of TAP-A55 or TAP-A55-I48E for 18 h. Cells were then lysed in 1% NP-40/PBS followed by Flag-tagged IP of cleared lysates. Co-immunoprecipitation of Cul3 was probed with an endogenous anti-Cul3 antibody. Endogenous Cul3 was co-IPed by both low and high levels of wild type A55. With similar protein levels to wild type A55 in the input, In contrast, Cul3 was not co-IPed by A55-I48E despite respectable levels of expression compared to WT A55 (Figure 5.6A). Hence it is validated that I48E mutation of A55 very greatly reduces the interaction between A55 and Cul3 inside cells, making it a good tool for further study.

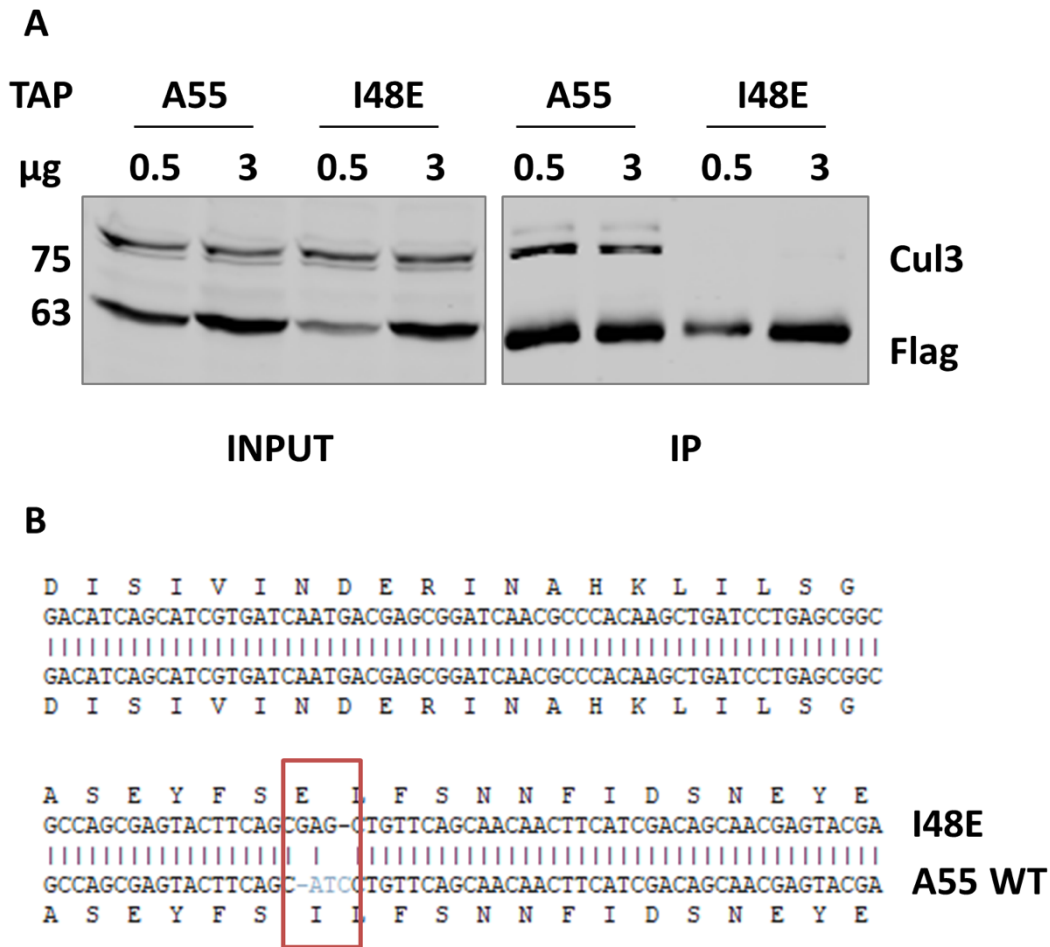


**Figure 5.6. A55 I48E mutation abolishes A55 & Cul3 interaction.** (A) Plasmids expressing TAP-tagged A55 or a mutant A55 (I48E) containing a point mutation at the 48th amino acid where a non-charged isoleucine changed to negatively charged glutamate (both hydrophobic) were transfected into HEK-293T cells for 18 at the indicated doses. Cells were lysed in 1% NP-40/PBS followed by Flag-tagged IP of cleared lysates and immunoblotting. Co-immunoprecipitation of Cul3 was probed with an endogenous anti-Cul3 antibody. Molecular masses (in kDa) are indicated on the left. Data shown are representative of at least 3 experiments. (B) Sequence alignment of I48E and wild type A55 showing point mutation.

Next, to investigate if A55 and/or C2 targeting of cellular proteins requires the interaction between A55 and Cul3, a mutant VACV containing A55\_I48E mutation (vI48E) was constructed and characterised by inserting A55R containing I48E mutation into vΔA55 using TDS as described in Materials and Methods. The virus was checked by PCR of A55 locus and DNA sequencing (Figure 5.7).

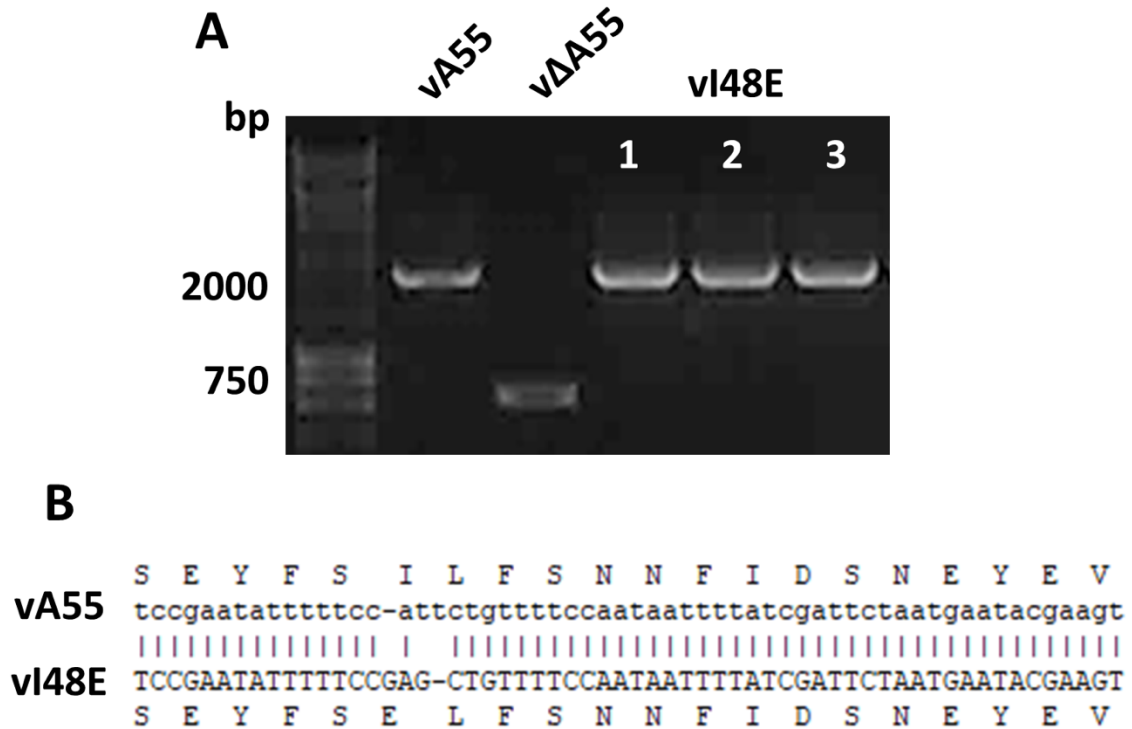


**Figure 5.7. vI48E checking.** (A) PCR product of A55 locus from vA55 (WT VACV), vΔA55 and vI48E (3 clones). (B) Sequence alignment of vA55 and vI48E shows I48E mutation and the rest of A55 intact in vI48E.

HEK-293Ts were mocked treated or infected with WT VACV (vA55, the parental virus used to construct vΔA55), vI48E or vΔA55 for 16 h. Cells were then lysed in RIPA buffer and cleared lysates were analysed by immunoblotting with antibodies to Scrib and FRMD6 (Figure 5.8). Protein levels of Scrib and FRMD6 were detectable in the mock-infected cells but not after infection with WT VACV (vA55). In contrast, in cells infected by vΔA55 or vI48E Scrib and FRMD6 were present at levels similar to uninfected cells. This shows that a mutant VACV with impaired interaction between A55 and Cul3 can no longer induce degradation of certain cellular proteins, such as Scrib and FRMD6. Thus the degradation of Scrib and FRMD6 requires the interaction between A55 and Cul3. Although the I48E expression during infection has not been examined in this experiment, the protein showed a stable expression level when overexpressed in mammalian cells.

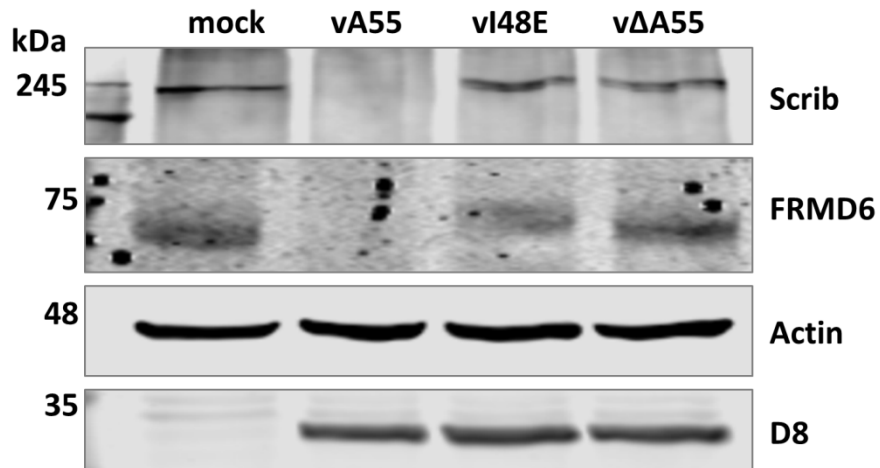


**Figure 5.8. Scrib degradation by VACV requires the interaction between A55 and Cul3.** A VACV strain containing the A55 I48E mutation (vI48E) was constructed as described in Methods. HEK-293Ts were mock treated or infected with wild type VACV (vA55), vI48E or vΔA55 at 5 p.f.u./cell for 16 h. Cells were then lysed in RIPA buffer and cleared lysates were analysed by SDS-PAGE and immunoblotting with the indicated antibodies. Molecular masses (in kDa) are indicated on the left. Data shown are representative of 2 independent experiments.

It was hypothesised that in the case of A55 and C2 targeting cellular proteins collaboratively, whilst A55 interacts with Cul3, C2 might interact with substrates to be brought to the complex for ubiquitylation. To examine if C2 acts as the substrate receptor for Scrib, HEK-293Ts were co-transfected with TAP-tagged VACV BBK proteins C2, A55 and F3 plus C6 as an unrelated control, and Myc-tagged Scrib or EV. Flag-tagged proteins were IPed and co-IP of Myc-Scrib was probed with Myc antibody. A harsh buffer RIPA was chosen for this assay because Myc-Scrib was found to be sticky in other experiments. Myc-Scrib was enriched in the Flag-C2 condition in comparison to A55, F3 and C6, even though the protein levels of enriched A55 or C6 were higher than C2 (Figure 5.9). This result suggests that C2 brings Scrib to a complex containing A55 and Cul3 for it to be degraded.

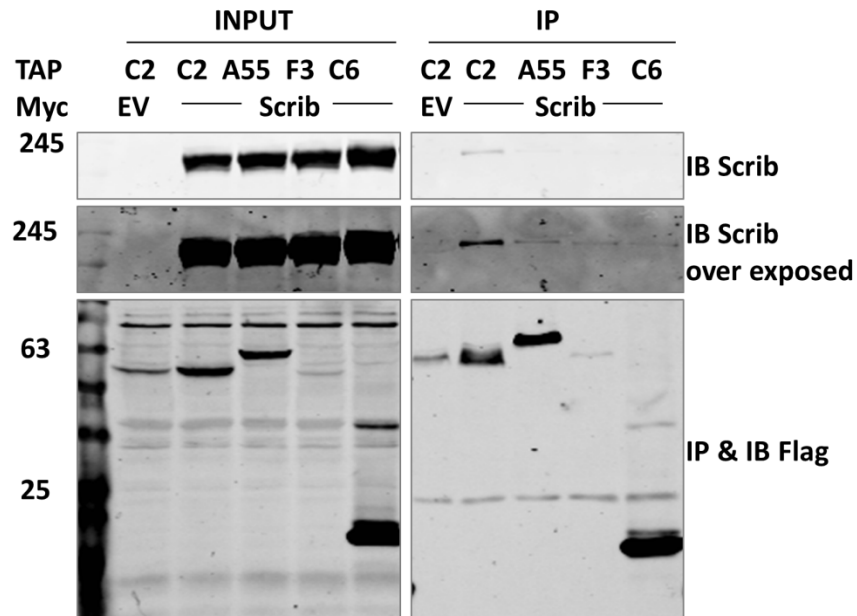


**Figure 5.9. C2 associates with Myc-Scrib.** HEK-293Ts were co-transfected with TAP-C2, A55, F3 or C6 and Myc-Scrib or EV for 18h. Cells were lysed in RIPA buffer followed by Flag-tagged IP of cleared lysates. Samples were analysed by SDS-PAGE and immunoblotting with indicated antibodies. Molecular masses (in kDa) are indicated on the left. Data shown are representative of 3 experiments.

Based upon the data obtained a model for the degradation of Scrib was proposed as illustrated (Figure 5.10). A55 and C2 associate with each other, although it is unknown if this is a direct or indirect interaction. A55 also interacts with Cul3 directly via its BTB domain and with high affinity (Gao et al., 2019). C2 associates with Scrib, leading to its ubiquitylation and degradation.

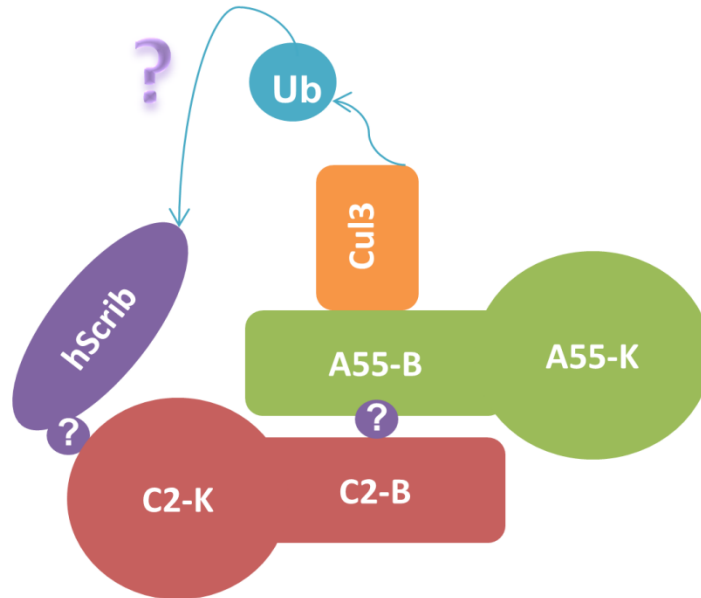


**Figure 5.10. Working model for how A55 and C2 induce degradation of Scrib in a Cul3- and proteasome-dependent way.** A55 and C2 interact with each other directly or indirectly. A55 brings in Cul3 via direct interaction between A55-BTB and Cul3, whilst C2 brings in Scrib as the substrate, potentially via its Kelch domain (not confirmed), leading to the ubiquitylation of Scrib followed by protein degradation. Note that the structure of the A55-BTB/Cul3 complex showed a 2:2 heterotetrameric complex rather than the 1:1 heterodimer illustrated for simplicity.

## **6 Results 4 – Role of Scrib in VACV infection and the mechanisms in antiviral signalling**

### **6.1 Construction of Scrib knockout cell lines using CRISPR-Cas9**

To further investigate the role of Scrib during VACV infection, *SCRIB*<sup>-/-</sup> cell lines were generated using CRISPR-Cas9 genome editing (Ran et al., 2013).

Clustered regularly interspaces short palindromic repeats (CRISPR)-Cas9 (CRISPR associated) is a microbial adaptive immune system that uses RNA-guided nucleases to cleave foreign genetic elements (Garneau et al., 2010). Cas9 is a nuclease that is guided by small RNAs via Watson-Crick base pairing with target DNA and belongs to the Type II CRISPR system (Gasiunas et al., 2012). In this system, Cas9 targets genomic DNA guided by a sgRNA (single guide RNA) containing a 20-nt guide sequence. The guide sequence pairs with the DNA target, usually a specific gene of interest, and is immediately followed by the proto-spacer adjacent motif (PAM) sequence which is essential for Cas9 binding to the targeting sequence. Each Cas9 orthologue has a unique PAM sequence. In this study, the CRISPR-Cas system derived from *Streptococcus pyogenes* is used, and the target DNA must immediately precede a 5'-NGG-3' PAM (Jinek et al., 2012). Cas9 then mediates a double-stranded break (DSB) 3 bp upstream of PAM. Upon cleavage by Cas9, the target locus initiates two major DNA repair pathways, either via non-homologous end joining (NHEJ) or homology-directed repair (HDR). Without a repair template, DSBs are re-ligated through the error-prone NHEJ. This process leaves scars that may be random insertion/deletion (indel) mutations. Gene knockouts can be introduced by NHEJ because indels occurring within a coding exon can lead to frameshift mutations

(when indel bp numbers are not divisible by three) or by the creation of premature stop codons (Perez et al., 2008).

Human *SCRIB* is located on chromosome 8 (8q24.3, NCBI GeneID: 23513). There are 3 described isoforms, and the canonical isoform is a protein of 1630 amino acids that is encoded by 37 exons. Of the 3 isoforms, although isoform 2 lacks exon 1 and part of exon 2, and isoform 3 has an insertion at the end of the protein, all three isoforms have complete exon 3 and exon 4 (Figure 6.1). Two gRNAs were designed as shown in Fig. 6B to minimise the chances of false phenotypes due to off-target effects. These target exon 3 and exon 4 and were designed using the tool online (MIT, <http://crispr.mit.edu/>) (Ran et al., 2013). The tool gives a ranking score based on the likelihood of off-target effects, so the top-scored sequences were chosen (Figure 6.2B). The gRNA sequences were then designed for primers to anneal and ligated into the pSPCas9-2A-Puro (px459) plasmid (Ran et al., 2013). px459 encodes a sgRNA scaffold for insertion of the gRNA, and a human codon-optimised Cas9 nuclease fused with 2A – puromycin (puro) resistance marker for cell selection after transfection. The 2A stop-go sequence linking Cas9 with the puro resistance gene means that both are expressed from one ORF, so the amount of Cas9 produced should correlate with puro resistance (Sharma et al., 2012).

SP|Q14160|SCRIB\_HUMAN MLKCIPLWRCNRHVESVDKRCSLQAVPEEIIYRYSRSLEELLLDANQLRELPKPFFRLIN 60  
 SP|Q14160-2|SCRIB\_HUMAN -----  
 SP|Q14160-3|SCRIB\_HUMAN MLKCIPLWRCNRHVESVDKRCSLQAVPEEIIYRYSRSLEELLLDANQLRELPKPFFRLIN 60

SP|Q14160|SCRIB\_HUMAN LRLKGLSDNEIQRLPPEVANFMQLVELDVSRLDIPETIPESIKFCKALEIADFSGNPLSRL 120  
 SP|Q14160-2|SCRIB\_HUMAN -----MQLVELDVSRLDIPETIPESIKFCKALEIADFSGNPLSRL 39  
 SP|Q14160-3|SCRIB\_HUMAN LRLKGLSDNEIQRLPPEVANFMQLVELDVSRLDIPETIPESIKFCKALEIADFSGNPLSRL 120  
 \*\*\*\*\*

SP|Q14160|SCRIB\_HUMAN PDGFTQLRSLAHLALNDVSLQALPGDVGNLNLANLVLTLELRENLLKSLPASLSFLVKLEQLD 180  
 SP|Q14160-2|SCRIB\_HUMAN PDGFTQLRSLAHLALNDVSLQALPGDVGNLNLANLVLTLELRENLLKSLPASLSFLVKLEQLD 99  
 SP|Q14160-3|SCRIB\_HUMAN PDGFTQLRSLAHLALNDVSLQALPGDVGNLNLANLVLTLELRENLLKSLPASLSFLVKLEQLD 180  
 \*\*\*\*\*

SP|Q14160|SCRIB\_HUMAN LGGNDLEVLPTDLGALPNLRELWLDRNQLSALPPELGNLRLRVCLDVSENRLLEELPAELG 240  
 SP|Q14160-2|SCRIB\_HUMAN LGGNDLEVLPTDLGALPNLRELWLDRNQLSALPPELGNLRLRVCLDVSENRLLEELPAELG 159  
 SP|Q14160-3|SCRIB\_HUMAN LGGNDLEVLPTDLGALPNLRELWLDRNQLSALPPELGNLRLRVCLDVSENRLLEELPAELG 240  
 \*\*\*\*\*

SP|Q14160|SCRIB\_HUMAN GLVLLTDLLLSQNLRLRRLPDGIGQLKQLSILKVDQNRLCEVTEAIGDCENLSELILTENL 300  
 SP|Q14160-2|SCRIB\_HUMAN GLVLLTDLLLSQNLRLRRLPDGIGQLKQLSILKVDQNRLCEVTEAIGDCENLSELILTENL 219  
 SP|Q14160-3|SCRIB\_HUMAN GLVLLTDLLLSQNLRLRRLPDGIGQLKQLSILKVDQNRLCEVTEAIGDCENLSELILTENL 300  
 \*\*\*\*\*

SP|Q14160|SCRIB\_HUMAN LMALPRSLGKLTKLTNLNVDNRHLEALPPEIGGCVALSVLSLRDNRLAVLPPPELAHTTEL 360  
 SP|Q14160-2|SCRIB\_HUMAN LMALPRSLGKLTKLTNLNVDNRHLEALPPEIGGCVALSVLSLRDNRLAVLPPPELAHTTEL 279  
 SP|Q14160-3|SCRIB\_HUMAN LMALPRSLGKLTKLTNLNVDNRHLEALPPEIGGCVALSVLSLRDNRLAVLPPPELAHTTEL 360  
 \*\*\*\*\*

SP|Q14160|SCRIB\_HUMAN HVLDVAGNRLQSLPFALHNLKALWLAENQAQPMLRFQTEDDARTGEKVLTCYLLPQQP 420  
 SP|Q14160-2|SCRIB\_HUMAN HVLDVAGNRLQSLPFALHNLKALWLAENQAQPMLRFQTEDDARTGEKVLTCYLLPQQP 339  
 SP|Q14160-3|SCRIB\_HUMAN HVLDVAGNRLQSLPFALHNLKALWLAENQAQPMLRFQTEDDARTGEKVLTCYLLPQQP 420  
 \*\*\*\*\*

SP|Q14160|SCRIB\_HUMAN PPSLEDAGQQGSLSETWSDAPPSRVSVIQFLEAPIGDEDAEEAAAEKRLQRRATPHPSE 480  
 SP|Q14160-2|SCRIB\_HUMAN PPSLEDAGQQGSLSETWSDAPPSRVSVIQFLEAPIGDEDAEEAAAEKRLQRRATPHPSE 399  
 SP|Q14160-3|SCRIB\_HUMAN PPSLEDAGQQGSLSETWSDAPPSRVSVIQFLEAPIGDEDAEEAAAEKRLQRRATPHPSE 480  
 \*\*\*\*\*

SP|Q14160|SCRIB\_HUMAN LKVMKRSIEGRRSEACPCQPDGSGSPLFAEEKRLSAESGLSEDSRPSASTVSEAEPEGFS 540  
 SP|Q14160-2|SCRIB\_HUMAN LKVMKRSIEGRRSEACPCQPDGSGSPLFAEEKRLSAESGLSEDSRPSASTVSEAEPEGFS 459  
 SP|Q14160-3|SCRIB\_HUMAN LKVMKRSIEGRRSEACPCQPDGSGSPLFAEEKRLSAESGLSEDSRPSASTVSEAEPEGFS 540  
 \*\*\*\*\*

SP|Q14160|SCRIB\_HUMAN AEAQGSQQEATTAGGEEDAEEEDYQEPTVHFAEDALLPGDDREIEEGQPEAPWTLPGGRQ 600  
 SP|Q14160-2|SCRIB\_HUMAN AEAQGSQQEATTAGGEEDAEEEDYQEPTVHFAEDALLPGDDREIEEGQPEAPWTLPGGRQ 519  
 SP|Q14160-3|SCRIB\_HUMAN AEAQGSQQEATTAGGEEDAEEEDYQEPTVHFAEDALLPGDDREIEEGQPEAPWTLPGGRQ 600  
 \*\*\*\*\*

SP|Q14160|SCRIB\_HUMAN RLIRKDTPHYKHKFKISKLPQPEAVVALLQGMQPDGEGPVPAGGWHNGPHAPWAPRAQKE 660  
 SP|Q14160-2|SCRIB\_HUMAN RLIRKDTPHYKHKFKISKLPQPEAVVALLQGMQPDGEGPVPAGGWHNGPHAPWAPRAQKE 579  
 SP|Q14160-3|SCRIB\_HUMAN RLIRKDTPHYKHKFKISKLPQPEAVVALLQGMQPDGEGPVPAGGWHNGPHAPWAPRAQKE 660  
 \*\*\*\*\*

SP|Q14160|SCRIB\_HUMAN EEEEEEGSPQEEVEVEEENRAEEEEASTEEDKEGAVVSAPSVKGVSTFDQANNLLIEPA 720  
 SP|Q14160-2|SCRIB\_HUMAN EEEEEEGSPQEEVEVEEENRAEEEEASTEEDKEGAVVSAPSVKGVSTFDQANNLLIEPA 639  
 SP|Q14160-3|SCRIB\_HUMAN EEEEEEGSPQEEVEVEEENRAEEEEASTEEDKEGAVVSAPSVKGVSTFDQANNLLIEPA 720  
 \*\*\*\*\*

SP|Q14160|SCRIB\_HUMAN RIEEELTLTILRQTGGLGISIAGGKGSTPYKGDDEGIFISRVSEEGPAARAGVVRVGDKL 780  
 SP|Q14160-2|SCRIB\_HUMAN RIEEELTLTILRQTGGLGISIAGGKGSTPYKGDDEGIFISRVSEEGPAARAGVVRVGDKL 699  
 SP|Q14160-3|SCRIB\_HUMAN RIEEELTLTILRQTGGLGISIAGGKGSTPYKGDDEGIFISRVSEEGPAARAGVVRVGDKL 780  
 \*\*\*\*\*

SP|Q14160|SCRIB\_HUMAN LEVNGVALQGAEHHEAVEALRGAGTAVQMRVWRERMVEPENAVTITPLRPEDDYSRPRER 840  
 SP|Q14160-2|SCRIB\_HUMAN LEVNGVALQGAEHHEAVEALRGAGTAVQMRVWRERMVEPENAVTITPLRPEDDYSRPRER 759  
 SP|Q14160-3|SCRIB\_HUMAN LEVNGVALQGAEHHEAVEALRGAGTAVQMRVWRERMVEPENAVTITPLRPEDDYSRPRER 840  
 \*\*\*\*\*

SP|Q14160|SCRIB\_HUMAN GGGLRLPLLPPESPGPLRQRHVACLARSERGLGFSIAGGKGSTPYRAGDAGIFVSRIAEG 900  
 SP|Q14160-2|SCRIB\_HUMAN GGGLRLPLLPPESPGPLRQRHVACLARSERGLGFSIAGGKGSTPYRAGDAGIFVSRIAEG 819  
 SP|Q14160-3|SCRIB\_HUMAN GGGLRLPLLPPESPGPLRQRHVACLARSERGLGFSIAGGKGSTPYRAGDAGIFVSRIAEG 900  
 \*\*\*\*\*

SP|Q14160|SCRIB\_HUMAN GAAHRAGTLQVGDRLVLSINGVDVTEARHDHAVSLTAAASPTIALLLEREAGGPLPSPFLP 960  
 SP|Q14160-2|SCRIB\_HUMAN GAAHRAGTLQVGDRLVLSINGVDVTEARHDHAVSLTAAASPTIALLLEREAGGPLPSPFLP 879

```

SP|Q14160-3|SCRIB_HUMAN  GAAHRAGTLQVGDRVLSINGVDVTEARHDAVSLTAAASPTIALLLEREAGGPLPPSPLP 960
*****

SP|Q14160|SCRIB_HUMAN    HSSPPTAAVATTSITTATPGVPGLPSLAPSLAAALEGPYPVEEIRLPRAGGPLGLSIVG 1020
SP|Q14160-2|SCRIB_HUMAN  HSSPPTAAVATTSITTATPGVPGLPSLAPSLAAALEGPYPVEEIRLPRAGGPLGLSIVG 939
SP|Q14160-3|SCRIB_HUMAN  HSSPPTAAVATTSITTATPGVPGLPSLAPSLAAALEGPYPVEEIRLPRAGGPLGLSIVG 1020
*****

SP|Q14160|SCRIB_HUMAN    GSDHSSHPFGVQEPGVFISKVLPRLGLAARSLRVGDRILAVNGQDVRDATHQEAVSALLR 1080
SP|Q14160-2|SCRIB_HUMAN  GSDHSSHPFGVQEPGVFISKVLPRLGLAARSLRVGDRILAVNGQDVRDATHQEAVSALLR 999
SP|Q14160-3|SCRIB_HUMAN  GSDHSSHPFGVQEPGVFISKVLPRLGLAARSLRVGDRILAVNGQDVRDATHQEAVSALLR 1080
*****

SP|Q14160|SCRIB_HUMAN    PCLELSLLVRRDPAPPGLRELICIQKAPGERLGISIRGGARGHAGNPRDPTDEGIFISKVS 1140
SP|Q14160-2|SCRIB_HUMAN  PCLELSLLVRRDPAPPGLRELICIQKAPGERLGISIRGGARGHAGNPRDPTDEGIFISKVS 1059
SP|Q14160-3|SCRIB_HUMAN  PCLELSLLVRRDPAPPGLRELICIQKAPGERLGISIRGGARGHAGNPRDPTDEGIFISKVS 1140
*****

SP|Q14160|SCRIB_HUMAN    PTGAAGRDGRLRVGLRLLLEVNQSSLGLTHGEAVQLLRVSGDTLTLVLCVCDGFEASTDAAL 1200
SP|Q14160-2|SCRIB_HUMAN  PTGAAGRDGRLRVGLRLLLEVNQSSLGLTHGEAVQLLRVSGDTLTLVLCVCDGFEASTDAAL 1119
SP|Q14160-3|SCRIB_HUMAN  PTGAAGRDGRLRVGLRLLLEVNQSSLGLTHGEAVQLLRVSGDTLTLVLCVCDGFEASTDAAL 1200
*****

SP|Q14160|SCRIB_HUMAN    EVSPGVIANPFAAGIGHRNSLESISSIDRELSPEGPGKEKELPGQTLHWGPEATEAARG 1260
SP|Q14160-2|SCRIB_HUMAN  EVSPGVIANPFAAGIGHRNSLESISSIDRELSPEGPGKEKELPGQTLHWGPEATEAARG 1179
SP|Q14160-3|SCRIB_HUMAN  EVSPGVIANPFAAGIGHRNSLESISSIDRELSPEGPGKEKELPGQTLHWGPEATEAARG 1260
*****

SP|Q14160|SCRIB_HUMAN    LQPLKLDYRALAAVPSAGSVQRVPSGAAGGKMAESPCSPSGQQPPSPDEL PANVKQA 1320
SP|Q14160-2|SCRIB_HUMAN  LQPLKLDYRALAAVPSAGSVQRVPSGAAGGKMAESPCSPSGQQPPSPDEL PANVKQA 1239
SP|Q14160-3|SCRIB_HUMAN  LQPLKLDYRALAAVPSAGSVQRVPSGAAGGKMAESPCSPSGQQPPSPDEL PANVKQA 1320
*****

SP|Q14160|SCRIB_HUMAN    YRAFAAVPTSHPPEDAPAQPPTPGPAASPEQLSFRERQKYFELEVRVPQAE GPPKRVSLV 1380
SP|Q14160-2|SCRIB_HUMAN  YRAFAAVPTSHPPEDAPAQPPTPGPAASPEQLSFRERQKYFELEVRVPQAE GPPKRVSLV 1299
SP|Q14160-3|SCRIB_HUMAN  YRAFAAVPTSHPPEDAPAQPPTPGPAASPEQLSFRERQKYFELEVRVPQAE GPPKRVSLV 1380
*****

SP|Q14160|SCRIB_HUMAN    GADDLRKMQEEEARLQKQRAQMLREAAEAGAEARLALDGETLGE EEQEDEQPPWASPS 1440
SP|Q14160-2|SCRIB_HUMAN  GADDLRKMQEEEARLQKQRAQMLREAAEAGAEARLALDGETLGE EEQEDEQPPWASPS 1359
SP|Q14160-3|SCRIB_HUMAN  GADDLRKMQEEEARLQKQRAQMLREAAEAGAEARLALDGETLGE EEQEDEQPPWASPS 1440
*****

SP|Q14160|SCRIB_HUMAN    TSRQSPASPPPLGGGAPVRTAKAERRHQERLRVQSPEPPAPERALS PAELRALEAEKRAL 1500
SP|Q14160-2|SCRIB_HUMAN  TSRQSPASPPPLGGGAPVRTAKAERRHQERLRVQSPEPPAPERALS PAELRALEAEKRAL 1419
SP|Q14160-3|SCRIB_HUMAN  TSRQSPASPPPLGGGAPVRTAKAERRHQERLRVQSPEPPAPERALS PAELRALEAEKRAL 1500
*****

SP|Q14160|SCRIB_HUMAN    WRAARMKSLEQDALRAQMVLRSRQEGRGTGTRGFLERLAEAPSAPT PTPVEDLGPQTST 1560
SP|Q14160-2|SCRIB_HUMAN  WRAARMKSLEQDALRAQMVLRSRQEGRGTGTRGFLERLAEAPSAPT PTPVEDLGPQTST 1479
SP|Q14160-3|SCRIB_HUMAN  WRAARMKSLEQDALRAQMVLRSRQEGRGTGTRGFLERLAEAPSAPT PTPVEDLGPQTST 1560
*****

SP|Q14160|SCRIB_HUMAN    SPGRL-----SPDFAEELRSLESPSPGPGQEEDGEVALVL 1595
SP|Q14160-2|SCRIB_HUMAN  SPGRL-----SPDFAEELRSLESPSPGPGQEEDGEVALVL 1514
SP|Q14160-3|SCRIB_HUMAN  SPGRLPLSGKKFDYRAFAALPSSRPVYDIQSPDFAEELRSLESPSPGPGQEEDGEVALVL 1620
*****

SP|Q14160|SCRIB_HUMAN    LGRPSPGAVGPEDVALCSSRRPVRRPGRRGLGPVPS 1630
SP|Q14160-2|SCRIB_HUMAN  LGRPSPGAVGPEDVALCSSRRPVRRPGRRGLGPVPS 1549
SP|Q14160-3|SCRIB_HUMAN  LGRPSPGAVGPEDVALCSSRRPVRRPGRRGLGPVPS 1655
*****

```

**Figure 6.1. CLUSTAL O(1.2.4) multiple sequence alignment of 3 described isoforms of Scrib produced by alternative splicing.** Human *SCRIB* locates on chromosome 8 (8q24.3). There are 3 described isoforms of Scrib, and the canonical one is translated from an mRNA that has 37 exons and encodes a protein of 1630 amino acids. Highlightened sequences are translated from *SCRIB* exon 1 (yellow), exon 2 (green), exon 3 (purple) and exon 4 (turquoise). All isoforms contain complete exon 3 and exon 4.



line, a PCR-amplified DNA fragment containing exon 3 or exon 4 was purified and cloned into TOPO TA vector (Invitrogen) and then transformed into competent *E. coli* cells. From each bacterial transformation at least 10 clones were sequenced. Mammalian cell lines are diploid but HEK-293T cells are known to be a heterogeneous population and could be diploid or triploid, meaning there should be 2-3 copies of chromosome 8 and thus 2-3 copies of *SCRIB*. KO\_11 showed 3 sequences and KO\_28 cell lines showed 2 sequences, both containing frameshift mutations. Importantly, there was an absence of the wild type allele (Figure 6.3B). Together, these data suggest KO\_11 and KO\_28 are *SCRIB*<sup>-/-</sup> cells ready for further characterisation studies.



**Figure 6.3. CRISPR-Cas9 mediated genome editing of Scrib in HEK-293T cells.** HEK-293Ts were transfected with px459 plasmids containing gRNA1, gRNA2, or a scrambled sequence then selected by puromycin. Survived cells went through single cell selection by serial dilution. More than 15 individual cell clones of each gRNA were amplified. (A) Individual cell clones after single cell selection were amplified and analysed by SDS-PAGE and immunoblotting. Clone KO\_11 (exon 3 targeted) and KO\_28 (exon 4 targeted) plus a few other clones were chosen for genomic

sequencing. (B) Genomic DNA from potential knockout clones was sequenced at the gRNA target sites. For each cell line at least 10 clones were sequenced. Both alleles of KO\_11 (exon 3) and KO\_28 (exon 4) contained frameshift mutations and an absence of the wild type allele.

## **6.2 Characterisation of VACV infection in Scrib KO cells**

Scrib is degraded by high risk human papilloma virus (HPV) (Nakagawa and Huibregtse, 2000), influenza A virus (Liu et al., 2010) and hepatitis C virus (HCV) (Awad et al., 2013) thus it may be a viral restriction factor (Thomas and Banks, 2018). To determine whether and how Scrib affects VACV replication or spread, Scrib KO cell lines were infected at high or low multiplicity of infection (MOI) and the yield of virus and size of virus plaque was determined. As HEK-293Ts are semi-adherent cells and to ensure they stayed on the surface of tissue culture plates, 6-well plates were coated with poly-D-lysine (0.01 mg/ml) for 2 h and then washed with PBS 3 times. The parental HEK-293Ts used to construct Scrib KO cells (WT), KO\_11 and KO\_28 were seeded at the same cell number in triplicate for each experiment (low and high MOI). Each cell type also had an additional well seeded for cell counting. Cell counting showed a similar number of WT and KO cells in each well before infection, and given that these different cell lines reached confluency with similar kinetics, this suggested no obvious effect of Scrib KO on HEK-293T cell proliferation. Similarly, morphological examination of the KO cell lines showed no obvious difference compared to WT cells.

Once cells had grown to form a monolayer, cells were infected with VACV at 0.01 p.f.u./cell for 48 h or at 5 p.f.u./cell for 24 h. After infection, cells and the supernatant were frozen and thawed 3 times before titration of infectious virus by plaque assay on BSC-1 cells. To investigate a role of Scrib in viral replication and to rule out spread as a contributing factor, cells were infected at 5 p.f.u./cell (MOI = 5) to ensure

every cell was infected. On the contrary, infecting cells at 0.01 p.f.u./cell (MOI = 0.01), ensured very few cells (about 1 in 100) would be infected, so any phenotypic difference could be either caused by changes in virus replication or spread from cell to cell. Both KO cell lines showed an increased virus yield after infection at low MOI compared to the parental HEK-293Ts (WT): this was about a 7-fold increase for KO\_11 and a 10-fold increase for KO\_28 (Figure 6.4A). In contrast, after high MOI there were marginal or insignificant differences (Figure 6.4B). At low MOI in KO\_11 cell line, the virus titres showed a significant difference, whilst in KO\_28 cell line, although the average virus titres were greater than both WT and KO\_11, the variation among the replicates caused these data not to reach statistical significance (Figure 6.4A). A repeat experiment showed that the virus titres in KO\_28 at low MOI was significantly higher than WT whilst no difference between KO\_11 and WT (Figure 6.4C). Together, these data suggest that virus titres in Scrib KO cell lines are higher than WT when cells are infected at low MOI.

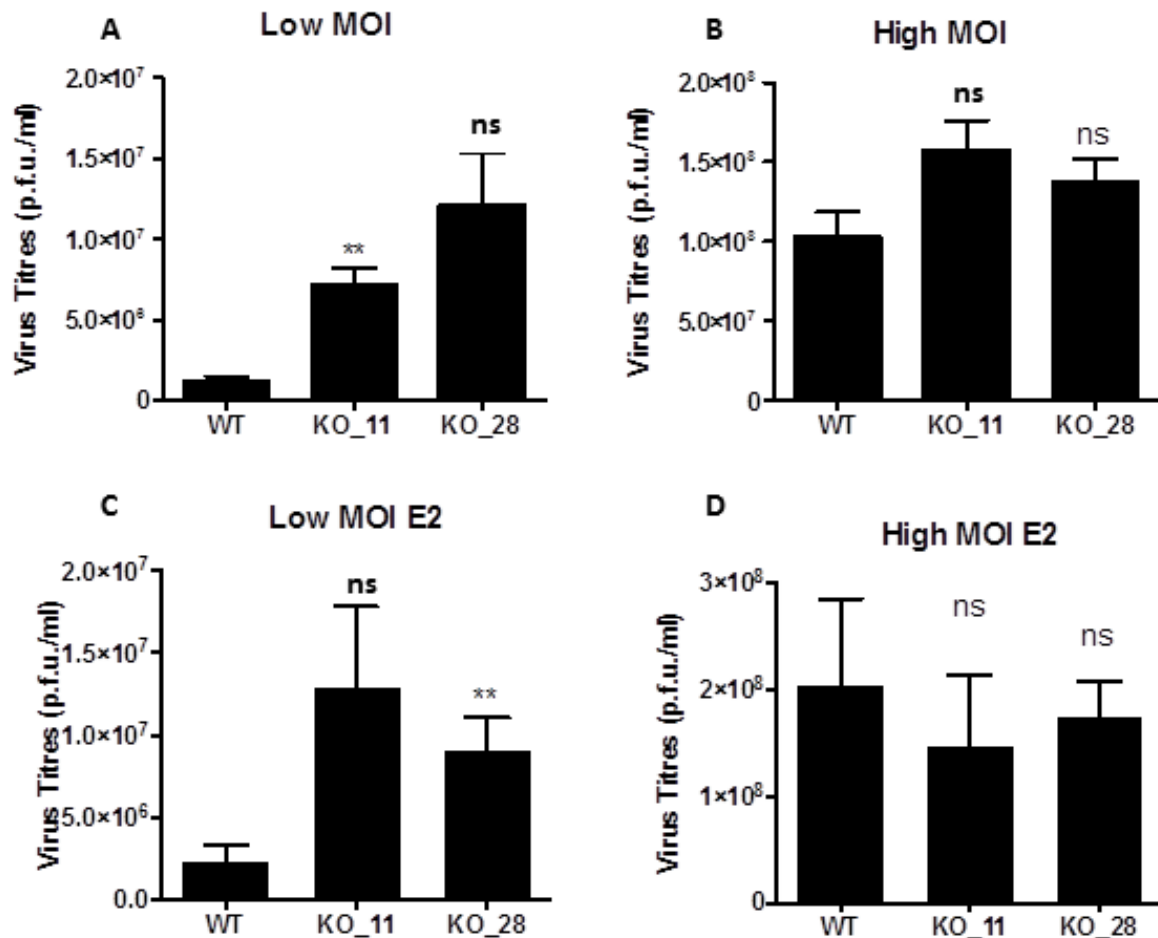


**Figure 6.4. VACV titration on Scrib KO cells lines.** Six-well plates were coated with poly-D-lysine (0.01 mg/ml) for 2 h then washed with PBS 3 times. WT (parental) HEK-293T cells and Scrib KO cells KO\_11 and KO\_28 were seeded at the same cell number in triplicate for each experiment (low and high MOI). Once cells reached a confluent monolayer, cells were counted and infected with VACV at 0.01 p.f.u./cell for 48 h or at 5 p.f.u./cell for 24 h. After infection, cells and the supernatant were frozen and thawed 3 times before infectious virus was titrated by plaque assay on BSC-1 cells. Data shown are 2 experiments. Statistical analysis was performed by unpaired Student's t-test (\*\* P<0.01) in comparison to WT control.

To investigate further the effect of Scrib on VACV spread, the size of virus plaques was measured. Monolayers of WT, KO\_11 and KO\_28 cell lines were infected with a VACV strain in which GFP is fused to the late virus capsid protein A5 (vA5-EGFP (Carter et al., 2003)) so as to give only about 20 plaques in each well of a 6-well plate. After initial inoculation for 90 min, the inoculum was removed and replaced with semi-solid overlay (1.5% carboxymethyl cellulose (CMC), in MEM / 2% FBS) to allow viral spreading through cell-to-cell spread but not through the release of virus

into the medium. The images of plaques were taken and plaque sizes were measured 48 h p.i. Compared to WT, the average plaque area on both KO cell lines was larger (Figure 6.5A & C). The numbers of plaque formed were also counted (Figure 6.5B). A small difference was observed between WT and KO\_28, but KO\_11 was not different to WT. Given that the 2 KO cell lines did not give a consistent phenotype regarding plaque number it was not possible to conclude that Scrib is affecting the number of plaques formed. However, the difference in plaque size was clear and combined with the data in Figure 6.4, it suggests that loss of Scrib benefits VACV spread: in other words Scrib is restricting VACV spread by an unknown mechanism.

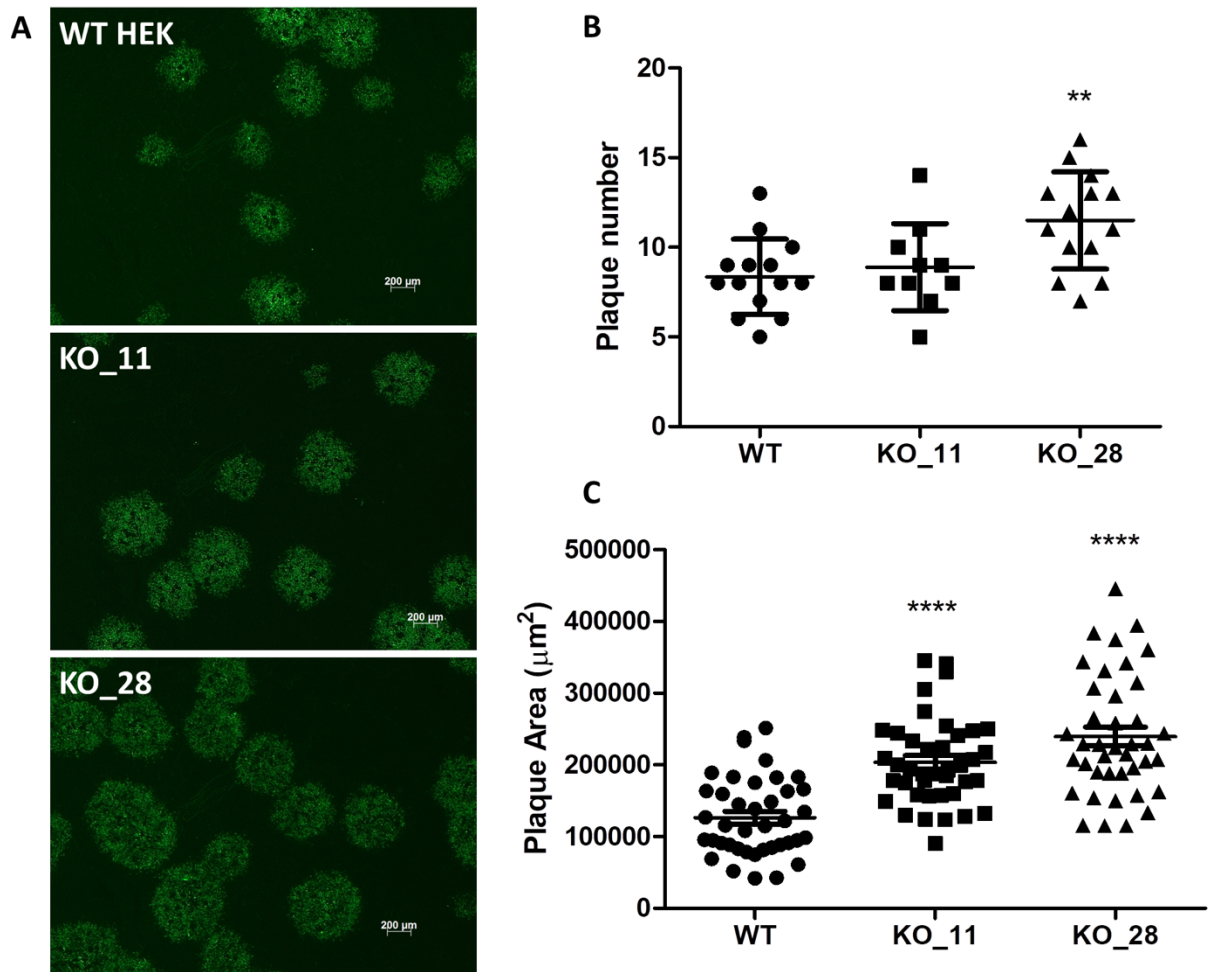


**Figure 6.5. VACV plaque assays on Scrib KO cell lines.** (A) Six-well plates were coated with poly-D-lysine (0.01 mg/ml) for 2 h then washed with PBS for 3 times. The parental HEK-293Ts used to construct Scrib KO cells (WT), KO\_11 and KO\_28 were seeded in duplicate. Once cells reached a confluent monolayer, cells were infected with vA5L-EGFP (Carter et al., 2003) at 20 p.f.u./well for 48 h. (B) The average number of plaques formed on each cell line were counted ( $n > 10$  per condition). (C) The plaque area of 40 plaques (20 from each monolayer) were measured. Data shown are representative of 2 experiments. Statistical analysis was performed by unpaired Student's t-test (\*\*  $P < 0.01$ , \*\*\*\*  $P < 0.0001$ ) in comparison to WT control.

### 6.3 Loss of Scrib upregulates Smad signalling

VACV CPE has been linked to EMT process, and VACV has been shown to upregulate an EMT signalling pathway, TGF- $\beta$  signalling pathway (more details see Section 1.2.2). Interestingly, Scrib is required to maintain epithelial polarity which is a key identity for epithelial cells in comparison to mesenchymal cells. In the mouse, Scrib prevents EMT and loss of *Scrib* activates TGF- $\beta$  signalling (Yamben et al.,

2013). Based upon this, it was investigated if loss of Scrib enhanced TGF- $\beta$  signalling, which could be the mechanism for Scrib restricting VACV spread.

### **6.3.1 VACV activates TGF- $\beta$ signalling**

In order to confirm that VACV infection activates TGF- $\beta$  signalling (Gowripalan et al., 2020; McKenzie, 2016), CAGA reporter gene assays were carried out in HaCaT cells (Figure 6.6). HaCaT is a human keratinocyte cell line that is highly responsive to TGF- $\beta$  (Wang et al., 2016), and VACV has been shown to cause HaCaT cells profound morphological changes such as loss of cell-to-cell adhesion (Gowripalan et al., 2019). The CAGA<sub>12</sub>-Luc (CAGA) plasmid was derived from the promoter of the Smad3/4-responsive genes (a kind gift from Professor Caroline Hill, Crick Institute, London, first described in (Dennler et al., 1998a)), therefore the CAGA-Luc reporter activity shows the activation of Smad3/4. HaCaT cells were transfected with the CAGA-Luc reporter plasmid and Renilla control and then infected with VACV for different times (Figure 6.6A). At 4 h p.i. there was not much difference between infected and mock-infected cells, but thereafter the activation increased sharply in the VACV-infected cells. To avoid false positive results caused by contamination with TGF- $\beta$  in the unpurified viral stock, HaCaT were transfected with CAGA-Luc and Renilla reporters for 18 h, before infection with VACV that had been purified by sucrose density gradient centrifugation for 14 h. Treatment of human TGF- $\beta$  was included as a positive control for signal activation (Figure 6.6B). Upon stimulation, TGF- $\beta$  treated cells showed an ~80 fold activation of the signalling pathway compared to mock. Cells infected by VACV and sucrose-purified VACV both showed an increase in the activation of CAGA reporter compared to mock, and an even higher activation effect than TGF- $\beta$ . Immunoblotting for C16 and tubulin of cells treated in Figure 6.6B was carried out to show the loading and infection level. A

slightly stronger signal of C16 was shown in the purified-sucrose VACV lane, which could explain the higher activation of purified VACV than VACV. Together, these results show VACV activates Smad signalling without needing TGF- $\beta$  stimulation, and VACV can activate the pathway at a higher level than TGF- $\beta$ , under certain conditions, for example, when infecting cells at 5 p.f.u./cell for 14 h (Figure 6.6B).

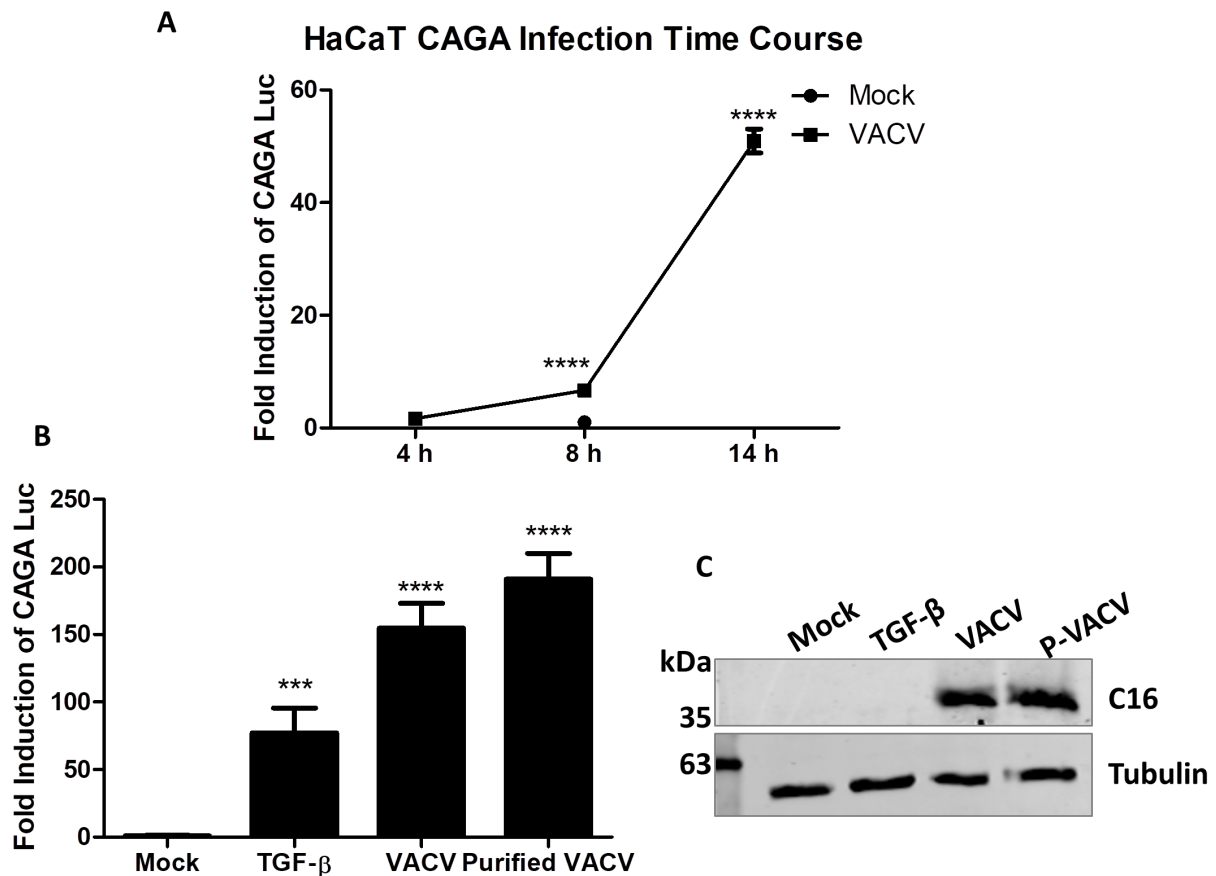


**Figure 6.6. VACV WR activates TGF- $\beta$  signalling.** (A) HaCaT cells were transfected with the CAGA reporter and SV40-renilla luciferase for 18 h before being mock treated or infected with WT VACV at 5 p.f.u./cell for indicated time. (B) HaCaT cells were transfected with the CAGA reporter and SV40-renilla luciferase for 18 h before being mock treated, stimulated by TGF- $\beta$  at 2.5 ng/ml, or infected by WT VACV or sucrose purified VACV at 5 p.f.u./cell for 14 h. Luciferase activity was measured in cell lysates. Data shown (mean  $\pm$  SD) are representative of 3 experiments carried out in quadruplicate and were analysed by an unpaired Student's t-test (\*\* $P < 0.001$ , \*\*\*\*  $P < 0.0001$ ) in comparison to mock control. (C) Immunoblotting for C16 and tubulin of whole cell lysates treated in (B).

### 6.3.2 Loss of *Scrib* enhances TGF- $\beta$ stimulated Smad signalling

It was shown that loss of *Scrib* caused Smad3 and Smad4 accumulation in the nucleus in mouse models (Yamben et al., 2013). The nuclear translocation of Smad3/4 after phosphorylation leads to the transcription of Smad-responsive genes (Figure 1.2). To further investigate the role of *Scrib* on TGF- $\beta$ /Smad signalling, WT HEK-293Ts (WT, the parental cells for *Scrib* KO cell lines) and *Scrib* KO cells were transfected with CAGA-Luc and Renilla-Luc for 18 h before stimulation with TGF- $\beta$  for 14 h or left un-treated (Figure 6.7A). No significant difference was observed between un-treated WT and KO cells. However, upon stimulation, WT showed a ~40 fold activation of Smad signalling compared to un-treated WT, whilst stimulated *Scrib* KO showed a ~100 fold activation compared to un-treated KO, 2.5 times higher than that of WT. Immunoblotting of the cell lysates confirmed the loss of *Scrib* (Figure 6.7B). This suggests loss of *Scrib* enhances the activation of TGF- $\beta$ /Smad signalling following stimulation. As a control, loss of *Scrib* did not make a difference in the activation of NF- $\kappa$ B or IRF3 signalling (Figure 6.8).

To confirm that the enhanced activation of Smad was caused by loss of *Scrib* but not by off-target effects, a complementing reporter gene assay was carried out (Figure 6.7C). WT, KO11 and KO28 cells were transfected with EV, or plasmids encoding Myc-*Scrib* or Myc-GFP, along with CAGA-Luc and Renilla-Luc, and then were stimulated with TGF- $\beta$  or left untreated. Consistently, *Scrib* KO cells showed a higher activation of CAGA reporter compared to WT, and the levels were similar between EV and Myc-GFP groups for each cell line. However, when complementing with Myc-*Scrib*, both KO cell lines showed a decreased activation after TGF- $\beta$  treatment compared to EV or GFP controls, and the activation returned to levels seen with stimulated WT-EV controls. Immunoblotting showed the Myc-*Scrib*/-GFP protein

levels in the cell lysates (Figure 6.7D). This result shows that complementing Scrib reverts the enhancement of TGF- $\beta$ /Smad signalling caused by Scrib KO, hence ruling out off-target effects.

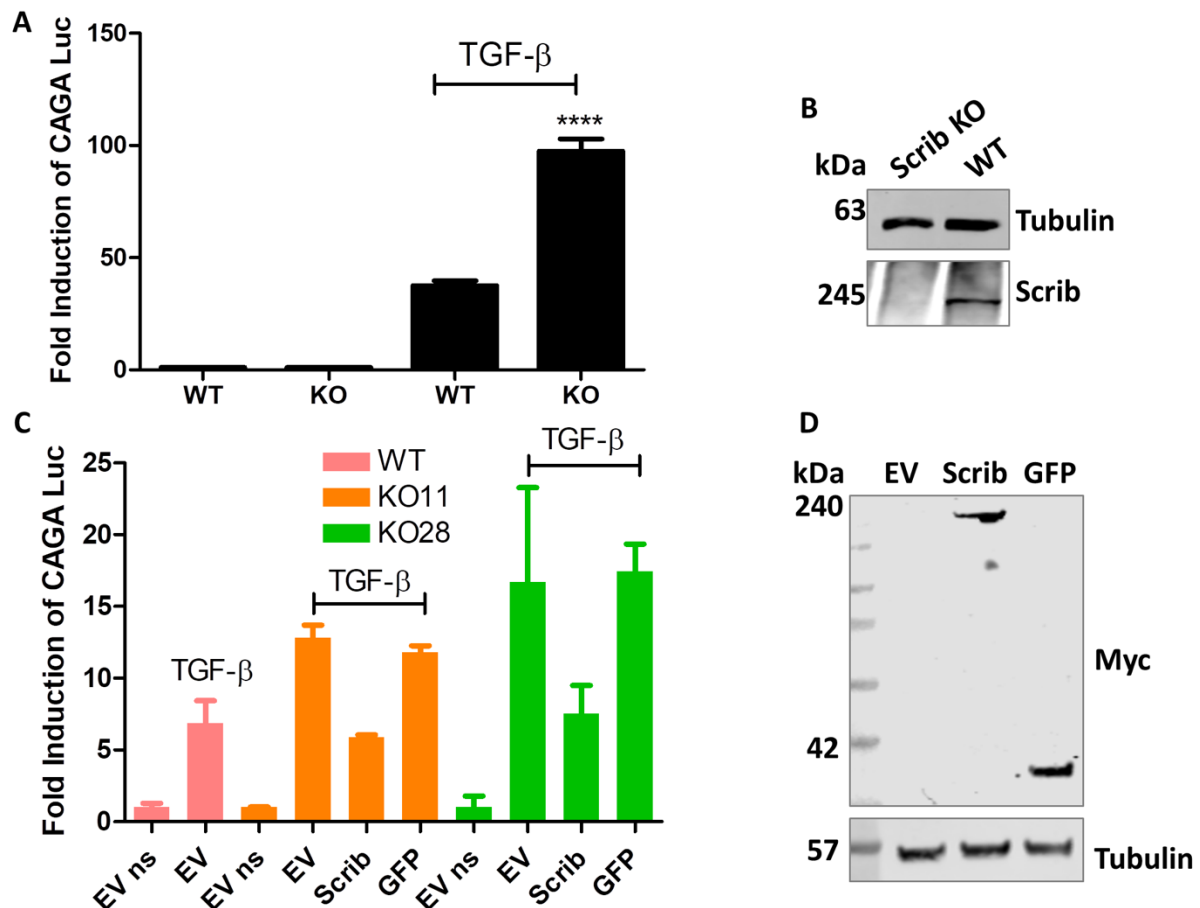


**Figure 6.7. Loss of Scrib leads to an enhancement of TGF- $\beta$ -stimulated Smad signalling.** (A) WT HEK-293Ts (the parental cells of Scrib KO) and Scrib KO cells were transfected with CAGA-Luc and renilla-Luc for 18 h. Cells were then un-treated or stimulated with TGF- $\beta$  for 14 h. Luciferase activity was measured from cell lysates. Data shown (mean  $\pm$  SD) are representative of 3 experiments of 2 Scrib KO cell lines (KO\_11 and KO\_28) carried out in quadruplicate and were analysed by an unpaired Student's t-test (\*\* P<0.01, \*\*\* P<0.001, \*\*\*\* P<0.0001) in comparison to unstimulated controls. (B) Immunoblotting of Scrib and tubulin present in cell lysates from (A). (C) WT HEK-293Ts, KO\_11 and KO\_28 were transfected with EV, Myc-Scrib or Myc-GFP, along with CAGA-Luc and renilla-Luc for 18 h, before being stimulated with TGF- $\beta$  for 14 h or un-treated (ns). Luciferase activity was measured from cell lysates. Data shown (mean  $\pm$  SD) are representative of 2 experiments carried out in quadruplicate and were analysed by an unpaired Student's t-test (\*\* P<0.01, \*\*\* P<0.001, \*\*\*\* P<0.0001) in comparison to unstimulated EV controls. (D) Immunoblotting of Myc and tubulin of cell lysates from stimulated KO28 conditions in (C).

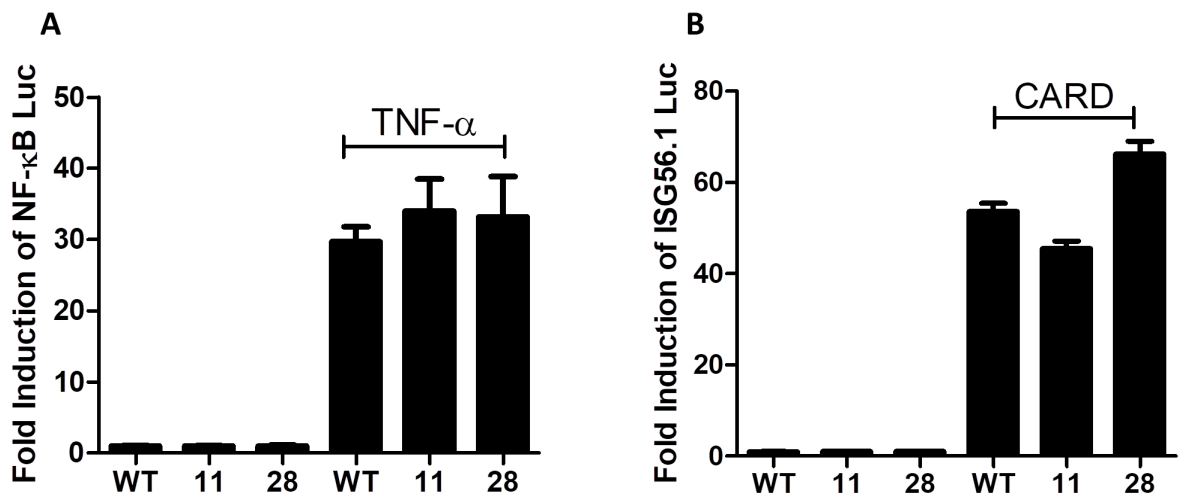


**Figure 6.8. Loss of Scrib does not affect NF-κB or IRF3 signalling.** (A) WT and Scrib KO cells (2 KO clones: 11 and 28) were transfected with the NF-κB-luc reporter and SV40-Renilla luciferase. Cells were untreated or stimulated with TNF $\alpha$  at 20 ng/ml for 6 h and luciferase activity was measured in cell lysates. (B) WT and Scrib KO cells were transfected with ISG56.1-luc reporter and SV40-Renilla luciferase. Cells were untreated or stimulated by transfecting with 5 ng Flag-RIG-I-CARD for 24 h and luciferase activity was measured in cell lysates. Data shown (mean  $\pm$  SD) are representative of 3 experiments carried out in quadruplicate and were analysed by an unpaired Student's t-test (\*\* P<0.01, \*\*\* P<0.001, \*\*\*\* P<0.0001) in comparison to unstimulated control.

While the luciferase reporter gene assays suggest Scrib KO enhances Smad signalling, they are not direct evidence of activation of Smad proteins. To investigate this, WT and Scrib KO cells were seeded, starved for 18 h by incubation in DMEM and then stimulated with 2 doses of TGF- $\beta$  or left untreated. Phosphorylation of Smad2 and Smad3 were examined by immunoblotting (Figure 6.9). Stimulation of TGF- $\beta$  led to the phosphorylation of both Smad2 and Smad3 in WT HEK-293Ts in a dose-dependent manner. Scrib KO cells displayed a higher degree of Smad2 phosphorylation compared to WT, but not Smad3. Additionally, this result shows Scrib KO enhances Smad signalling by increasing Smad2 phosphorylation following stimulation.

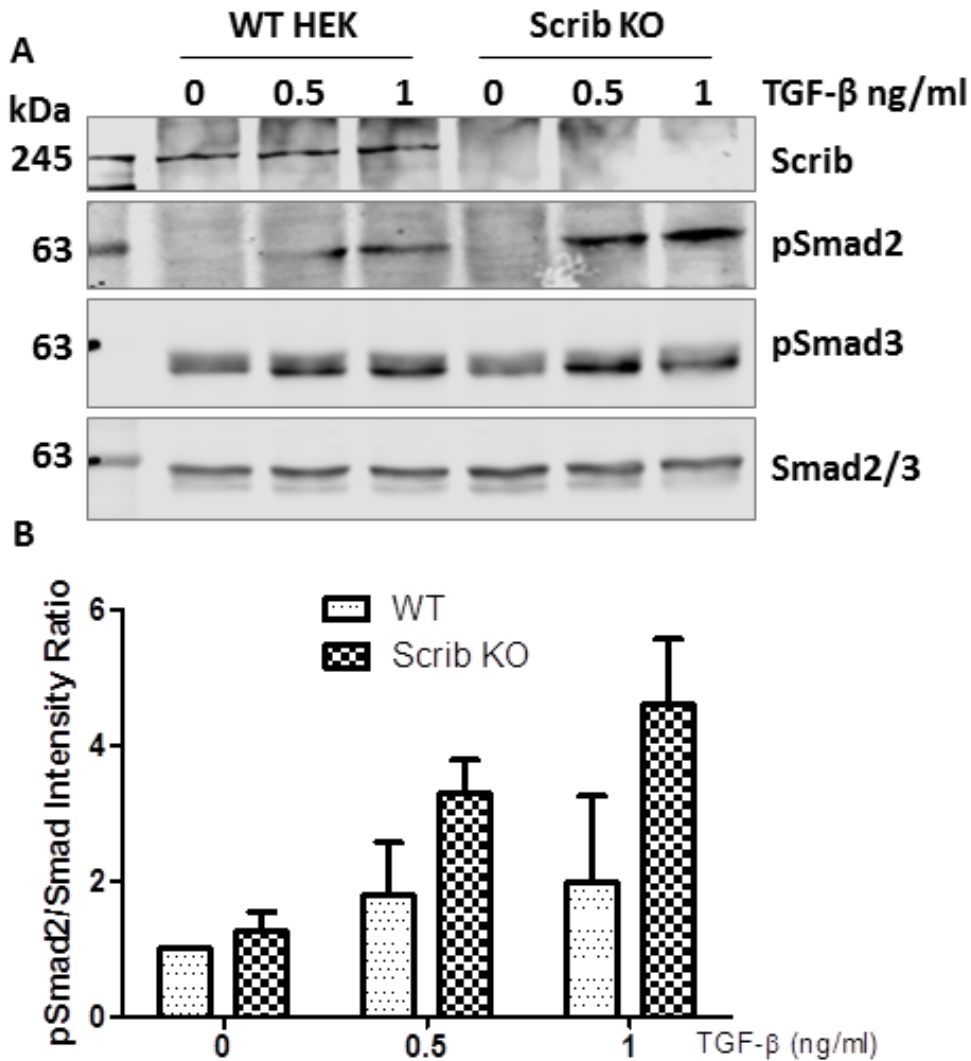


**Figure 6.9. Scrib KO increases Smad2 phosphorylation.** (A) HEK-293T WT and Scrib KO28 were seeded into 6-well plates at a density of  $6 \times 10^5$  cells per well in DMEM supplemented with 10% FBS. After 24 h, the medium was replaced by starvation medium (DMEM without FBS) for 18 h before stimulated with TGF-β at 0, 0.5 or 1 ng/ml in fresh starvation medium for 30 min. Cells were then washed in PBS and cell lysates were analysed by immunoblotting. (B) Levels of pSmad2 relative to Smad2/3 as quantified by densitometry. Data shown are representative of 2 independent experiments carried out in 2 Scrib KO cell lines.

Deletion of A55 or C2 prevents VACV-induced degradation of Scrib, so it was examined if loss of A55 or C2 abolishes Smad-activation by VACV. An infection time course of VACV and  $\Delta$ A55 was carried out in HaCaT cells after transfection with CAGA-Luc and Renilla-Luc control (Figure 6.10A, B), however no difference in reporter activity was observed between VACV and  $\Delta$ A55. Recently, VACV was shown to induce phosphorylation of Smad2 and Smad3 (Gowripalan et al., 2020)

and loss of Scrib increases Smad2 phosphorylation after TGF- $\beta$  stimulation (Figure 6.9). Therefore the phosphorylation of Smad2 or Smad3 was examined following infection by WT VACV or v $\Delta$ A55 (Figure 6.10C). HEK-293Ts were seeded and starved before infection. Compared to mock, VACV increased Smad2 phosphorylation 14 h p.i. and Smad3 phosphorylation 8 h p.i., but this was not altered by loss of A55. Although the infection loadings were not exactly equal between two viruses, the phenotype observed here did not change in repeat experiments.

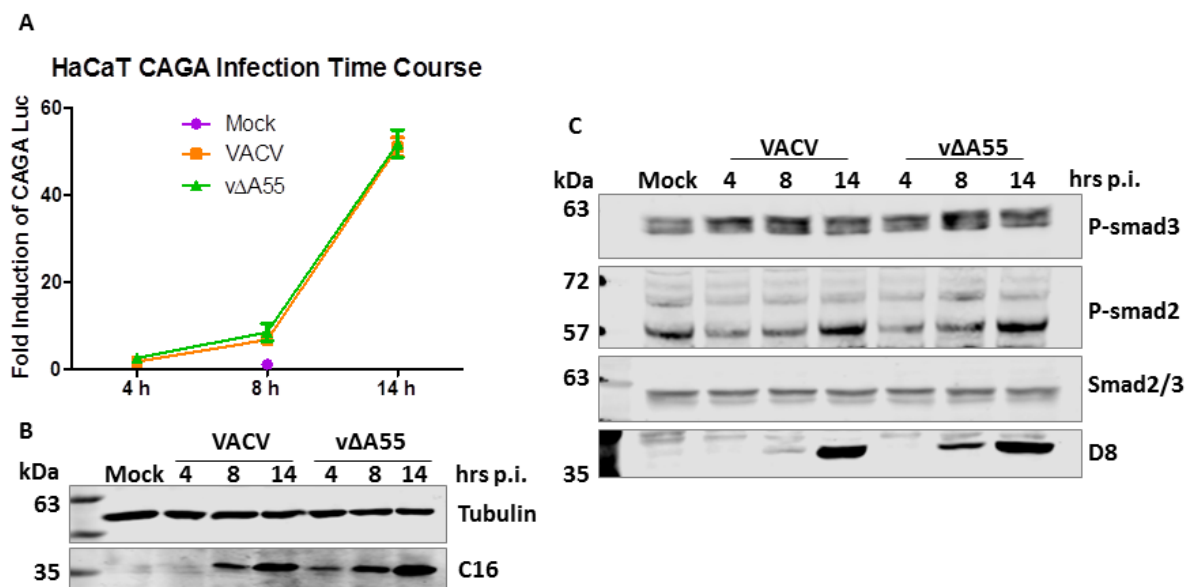


**Figure 6.10. Loss of A55 does not change the effect of VACV on CAGA-Luc or phosphorylation of Smad2 and Smad3.** (A) HaCaT cells were transfected with the CAGA reporter and SV40-Renilla luciferase for 18 h before being mock treated or infected with WT VACV or v $\Delta$ A55 at 5 p.f.u./cell for indicated time. Data shown (mean  $\pm$  SD) are representative of 3 experiments carried out in quadruplicate and were analysed by an unpaired Student's t-test (\*\* P<0.01, \*\*\* P<0.001, \*\*\*\* P<0.0001) in comparison to mock control. (B) Immunoblotting of C16 and tubulin for whole cell lysates treated in (A). (C) HEK-293Ts were seeded into 6-well plates at a density of  $6 \times 10^5$  cells per well in DMEM supplemented with 10% FBS. After 24 h, the medium was replaced by starvation medium (DMEM with 1% FBS) for 18 h before cells were infected WT VACV or v $\Delta$ A55 at 5 p.f.u./cell for indicated time. Phosphorylated Smad2 and Smad3 were probed by SDS-PAGE and immunoblotting. Data shown are representative of 2 experiments.

As CAGA-Luc is a common Smad responder, and Smad2 and Smad3 are TGF- $\beta$  activated R-Smads, it was tested if loss of A55 or C2 changed the activation of BRE-Luc, which contains BMP-responsive elements that are activated by Smad1/5 specifically (Daly et al., 2008; Korchynskyi and ten Dijke, 2002). HaCaT cells were transfected with the BRE reporter and SV40-Renilla Luc for 18 h before infection with WT VACV /  $\Delta$ A55 /  $\Delta$ C2 at 5 p.f.u./cell for 4, 8, or 14 h. At 8 h p.i.,  $\Delta$ A55 and  $\Delta$ C2 infected cells showed a lower activation level of BRE-Luc compared to WT VACV, whilst at 14 h p.i.,  $\Delta$ A55 infected cells caught up with VACV, but  $\Delta$ C2-infected cells still showed a lower level of BRE-Luc, i.e. Smad1/5 reporter activity (Figure 6.11). The difference between  $\Delta$ A55 and  $\Delta$ C2 could be that in the absence of A55, Scrib still associates with C2, which might affect Smad1/5 signalling. Notably the infection loading for both 8 and 14 h infection was not perfectly equal among 3 viruses, especially for  $\Delta$ C2. However, VACV and  $\Delta$ A55 had a similar infection level, but showed a difference at 8 h p.i. It is difficult to draw conclusions based on these data due to the difficulty of getting the equal infection loading in these assays. However, the same difference was not seen in other Smad reporter assays such as CAGA, which was carried out at the same time using the same virus stock. In summary, although these assays provide possibilities that losing A55 or C2 might regulate Smad1 or Smad5, more repeats should be carried out to optimise the infection loading to draw any conclusion.

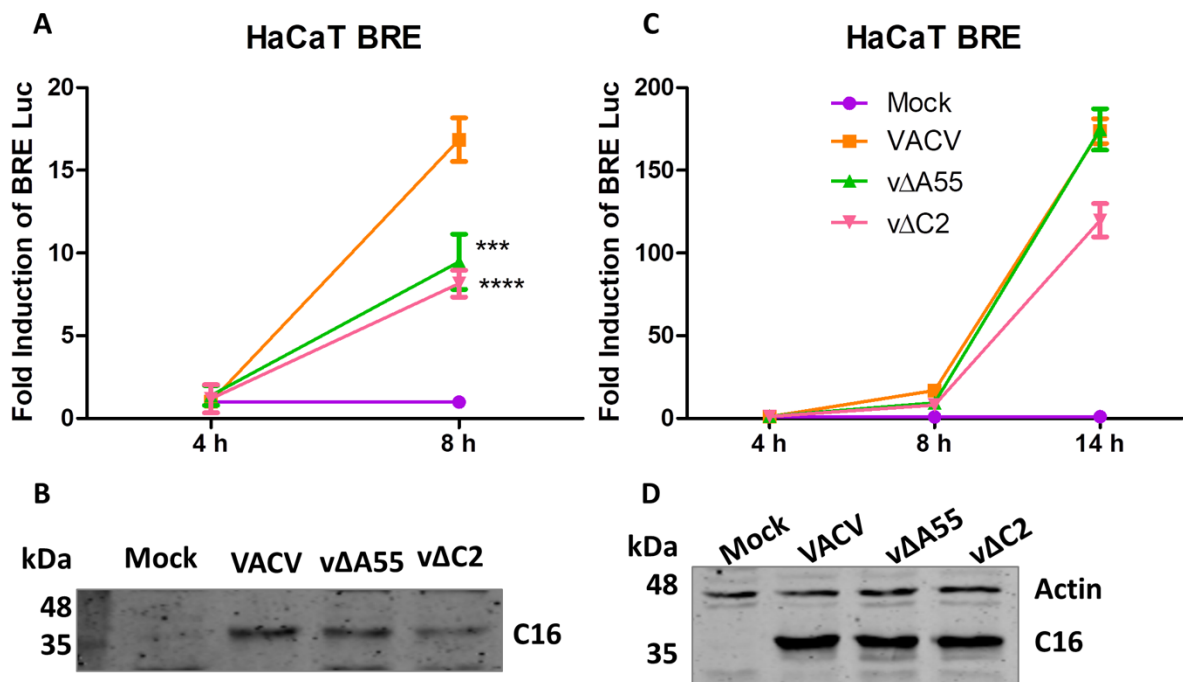


**Figure 6.11. Loss of A55 or C2 may change Smad1/5 activation by VACV.** (A, C) HaCaT cells were transfected with the BRE-luciferase and SV40-renilla luciferase for 18 h before cells were mock treated or infected with WT VACV, vΔA55 or vΔC2 at 5 p.f.u./cell for indicated time. Data shown (mean ± SD) are representative of 2 experiments carried out in quadruplicate and were analysed by an unpaired Student's t-test (\*\*\*)  $P < 0.001$ , \*\*\*\*  $P < 0.0001$ ) in comparison to mock control. (B) Immunoblotting of C16 and tubulin for whole cell lysates treated in (A). (D) Immunoblotting of C16 and tubulin for whole cell lysates of 14 h p.i. group in (C).

Taken together, these data suggest that VACV activates Smad signalling and loss of Scrib enhances the activation of TGF- $\beta$  stimulated Smad signalling by unknown mechanisms. As VACV degrades Scrib, it is possible that VACV activates the pathway by targeting Scrib or at least loss of Scrib would contribute to this. Interestingly, the kinetics of VACV-induced activation of Smad signalling matches the kinetics of VACV-induced Scrib degradation. VACV showed a sharp increase in Smad signal after 8 h p.i., and Scrib was mostly degraded after 8-9 h p.i. (Figure 5.1 and Figure 5.3). Loss of Smad4 was shown to attenuate VACV spread and VACV-induced cell motility (Gowripalan et al., 2020). Therefore, VACV might target Scrib to

enhance the activation of Smad signalling, and the latter promotes VACV spread by increasing VACV-induced cell motility. Although  $v\Delta A55$  or  $v\Delta C2$  did not abolish the activation of common Smad responder CAGA-Luc induced by VACV and Scrib KO cells, other viral proteins might play a role in the regulation of Smad signalling, or this might be due to the KO cells having no Scrib at all, whilst infected cells only lose Scrib over a time course (8-12 h p.i.), and loss of A55 or C2 might regulate Smad1/5 activity specifically during infection.

Scrib has also been reported to positively regulate the Hippo pathway kinases. In mammals, Hippo signalling regulates cell contact inhibition, organ size, cell proliferation, apoptosis and cancer development (Angus et al., 2012). Upon upstream signals, MST1/2 is phosphorylated, and this causes phosphorylation of Lats1/2. Once activated, Lats1/2 phosphorylates YAP/TAZ and promotes their interaction with 14-3-3, which results in cytoplasmic retention or degradation following ubiquitylation by  $\beta$ -TrCP and proteosomal degradation (Zhao et al., 2010). When dephosphorylated, YAP/TAZ can enter the nucleus. Without intrinsic DNA-binding domains, YAP/TAZ binds to the promoter of target genes by interacting with DNA-binding transcription factors (Yu and Guan, 2013). These include TEAD1-4, which regulate genes involved in cell proliferation and cell death (Vassilev et al., 2001), and also other transcription factors such as Smad1 (Alarcón et al., 2009), Smad2/3 (Varelas et al., 2008) and Smad7 (Ferrigno et al., 2002).

Numerous upstream regulators have been identified for the Hippo pathway, and many of them are known components of tight junctions, adherence junctions or apical-basal polarity protein complexes, such as Scrib (Yu and Guan, 2013). Down-regulation of Scrib leads to YAP/TAZ activation (Chen et al., 2012; Cordenonsi et al., 2011). In epithelial cells, as the cell-polarity determinant, Scrib localises at the cell

membrane at cell contact areas and forms a complex with TAZ. Loss or delocalisation of Scrib, or induction of the EMT, disrupts the inhibitory association of TAZ with the core Hippo kinases MST and Lats (Cordenonsi et al., 2011).

Given those reported roles of Scrib in the Hippo signalling pathway, it was investigated if VACV infection or loss of Scrib showed an effect in the regulation of Hippo signalling. For this purpose, the localisation of YAP/TAZ, phosphorylation of YAP/TAZ and YAP/TAZ-responsive genes at transcriptional levels were investigated. Preliminary data showed that infection of cells at low cell density by vΔC2 caused a slight cytoplasmic retention of YAP compared to mock infection, which could be that when Scrib is present (vΔC2), YAP could form a complex with Scrib in the cytoplasm. In addition, Two well-characterised YAP responsive genes *CYR61* and *ATF3* (Choi et al., 2015; Plouffe et al., 2018) were found upregulated by VACV at transcriptional levels, and loss of A55 or C2 diminished the upregulation. These data show that VACV activates the transcription of *CYR61* and *ATF3* dependent on the presence of A55 or C2. However, these data do not establish a direct link between VACV infection and the activation of Hippo/YAP because these two genes are not only regulated by YAP/TAZ. *ATF3* has also been shown as a direct transcription target of TGF-β (Kang et al., 2003), and *CYR61* can be induced by growth factors, protein kinase C (PKC), cAMP and Ca<sup>2+</sup> (O'Brien et al., 1990). Interestingly, studies have shown that loss of Scrib induces *ATF3* expression (Donohoe et al., 2018), and ATF3 associates with Smad3 (Kang et al., 2003). Further studies should be carried out to investigate the direct links among VACV, Scrib and TGF-β/Hippo signalling.

## 7 Results 5 – C2 is a potential Cdc42 activator

### 7.1 C2 associates with Cdc42

Previously, it was shown that loss of C2 induces changes in plaque morphology and cellular projections during VACV infection (Pires de Miranda et al., 2003). To investigate the mechanism and cellular targets of C2, stable isotopic labelling in cell culture (SILAC) and mass spectrometry analysis was carried out in an inducible C2 cell line, and identified Cdc42 (cell division control protein 42) as a potential binding partner of C2 (unpublished data by Carlos Maluquer de Motes & Laura Gonzales, data analysed by Ed Emmot). Human Cdc42 is a plasma membrane-associated small GTPase of the Rho family, which cycles between an active GTP-bound and an inactive GDP-bound state (Qadir et al., 2015). Cdc42 is characterised to regulate cell signalling involved in cell morphology, migration, endocytosis and cell cycle progression. This is interesting as the association between Cdc42 and C2 might explain the morphology change in  $\Delta$ C2-infected plaques (Pires de Miranda et al., 2003). In addition, although not essential, Cdc42 enhances VACV-induced actin polymerisation by stabilising the essential N-WASP protein in stimulating Arp2/3-mediated actin polymerisation and hence promotes actin tail formation (Humphries et al., 2014).

To validate the association between C2 and Cdc42, HEK-293Ts were co-transfected with TAP-tagged C2, the BTB and Kelch domains of C2, A55, together with Myc-tagged Cdc42 or hASC (human apoptosis-associated speck-like protein containing a CARD) as the negative control. hASC was chosen as the negative control because it has a similar mass to Cdc42 and a plasmid encoding a Myc-tagged version was available in our lab. After Flag-IP, Flag-C2 was enriched at similar levels to Flag-A55,

and Myc-Cdc42 co-IPed with C2 but not with A55 (Figure 7.1). As a negative control hASC was not co-IPed by either C2 or A55. Interestingly, Cdc42 was co-IPed by the BTB domain of C2 but not the Kelch domain (Figure 7.1), despite the fact that the Kelch domain is usually recognised as the substrate adaptor of the BTB-Kelch protein. The C2-BTB domain therefore interacts with both the A55-BTB domain and Cdc42, whereas the C2-Kelch domain interacts with hScrib, although whether any of these interactions are direct, or via other proteins, is unknown. The association between C2 and Cdc42 via the C2-BTB domain is interesting because overexpression of C2 or C2-BTB, but not C2-Kelch, altered cell morphology and induced cell rounding (Figure 3.9A). This hints that there may be a functional link between this interaction and this morphology change.

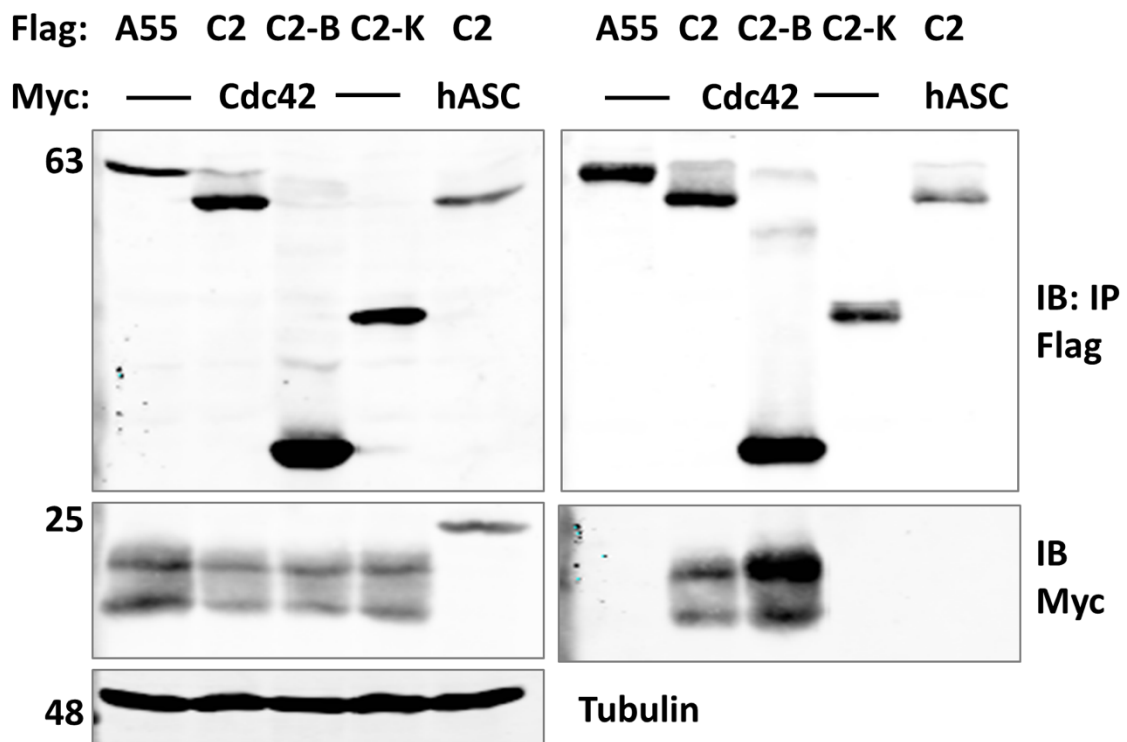


**Figure 7.1. Flag-C2 co-IPs Myc-Cdc42 via the C2-BTB domain.** HEK-293Ts were co-transfected with TAP-tagged A55, C2, C2-B or C2-K together with Myc-tagged Cdc42 or hASC for 16 h. Cells were then lysed in 0.5% NP-40/PBS followed by Flag-tagged IP of cleared lysates. Co-IP of Myc was probed with an anti-Myc antibody. Molecular masses (in kDa) are indicated on the left. Data shown are representative of 3 experiments.

## 7.2 C2 is a potential Cdc42 activator

Next it was investigated if C2 affects the activity of Cdc42. The Rac/Cdc42 (p21) binding domain (PBD) of human p21 activated kinase 1 protein (PAK) binds specifically the GTP-bound, but not GDP-bound Cdc42. Therefore, this domain can be used to specifically precipitate active, GTP-bound Cdc42 (Scott et al., 2002). The PBD protein was expressed as a GST-fusion protein in *E. coli*, and was purified by binding to a glutathione resin. This resin containing the PBD of PAK was then used to bind the active form of Cdc42 from the mammalian cell lysates (Etienne-Manneville and Hall, 2001; Osmani et al., 2006). To investigate the activity of Cdc42 during VACV infection and whether C2 affects this, HEK-293Ts were mock-treated or infected with VACV (vC2) or vΔC2 for 8 and 14 h. Cells were then lysed in RIPA buffer and cleared lysates were incubated with the GST-PBD beads for 45 min at 4 °C. Affinity-purified GTP-bound Cdc42 (IP lane, right) and total Cdc42 (INPUT lane, left) were eluted with SDS-sample buffer and analysed by immunoblotting. Eluted GST (IP) showed similar levels of GST-PBD protein across different groups. Active Cdc42 was enriched in WT VACV-infected cells (vC2) and loss of C2 (vΔC2) impaired the activation of Cdc42 (Figure 7.2A). Although in this figure Cdc42 was activated more at 8 h than 14 h p.i., this pattern was not observed consistently, and in a repeat experiment active Cdc42 was again increased following WT VACV infection, but not by vΔC2 and active cdc42 was observed at 14 h p.i. These data suggest Cdc42 is activated by VACV, and C2 contributes to this activation, because in its absence Cdc42 is less or not activated.

To investigate whether C2 regulates the activity of Cdc42 by preferably associating with the active or inactive form of Cdc42, the interaction of C2 with the dominant positive (D/P) or the dominant negative form (D/N) of Cdc42 was investigated. The

D/P form of Cdc42 (Cdc42<sup>Q61L</sup>) contains a glutamine to leucine substitution at residue 61, leading to decreased intrinsic GTPase activity of Cdc42, thereby shifting the mutant protein to an “activated” GTP-bound state (constitutively active) (Ziman et al., 1991). The D/N form of the Cdc42 protein (Cdc42<sup>T17N</sup>) contains a threonine to asparagine substitution at residue 17. The asparagine substitution abolishes the protein's affinity for GTP and reduces its affinity for GDP (constitutively inactive) (Luo et al., 1994). HEK-293Ts were co-transfected with TAP-tagged C2 and Myc-tagged Cdc42 (wild type and the two mutants). Cells were lysed in 0.5% NP-40/PBS followed by Flag-IP (Figure 7.2B). Consistently, although WT Myc-Cdc42 was co-IPed by Flag-C2, neither the D/P (constitutively active) nor D/N (constitutively inactive) form of Myc-Cdc42 was co-IPed by C2. The conclusion that C2 does not IP with these cdc42 mutants needs confirmation by further experiments, particularly as the level of C2 obtained by transfection, and immunoprecipitated, was quite variable. It would be useful to investigate if these mutant proteins interacted with C2 during viral infection, or when C2 was expressed in cell lines. Given that these mutant constructs were artificially made, they would provide limited insights of how C2 modulates the activity of Cdc42 under natural circumstances anyways. Taken together, these data show that C2 activates Cdc42 during infection, but as C2 may not associate with D/P or D/N Cdc42, it is unclear if C2 associates preferably with the active or inactive state of Cdc42. The mechanism of C2 activating Cdc42 remains to be investigated.

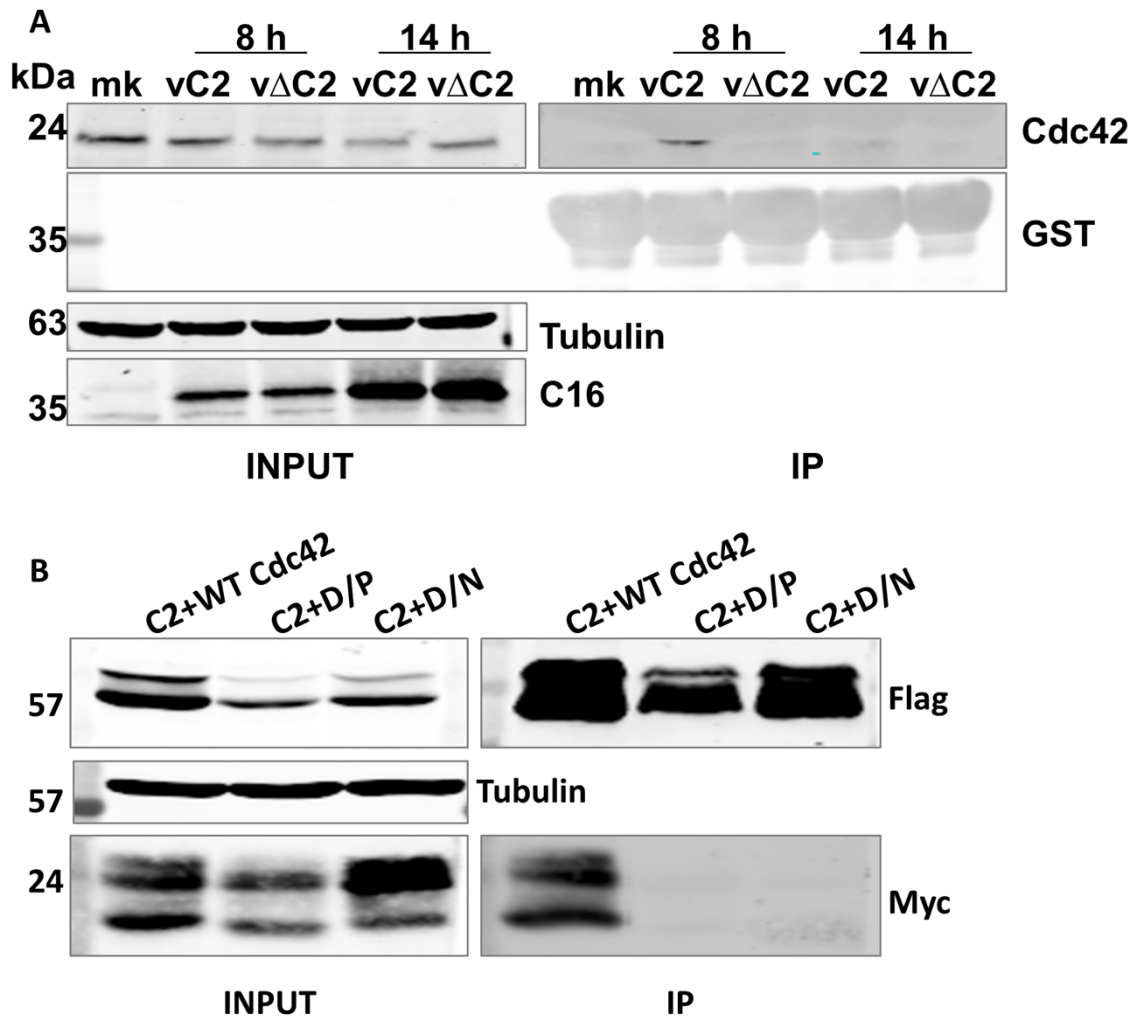


**Figure 7.2. C2 is a potential Cdc42 activator.** (A) HEK-293Ts were mock-treated (mk) or infected by vC2 or vΔC2 at 5 p.f.u./cell for indicated time. Cells were then lysed in RIPA buffer and cleared lysates were incubated with the GST-PBD beads for 45 min at 4 °C. Affinity-purified GTP-bound Cdc42 (IP lane, right) and total Cdc42 (INPUT lane, left) were analysed by immunoblotting. Cdc42 was probed with an endogenous anti-Cdc42 antibody. (B) HEK-293Ts were co-transfected with TAP-tagged C2 and Myc-tagged WT Cdc42 or dominant positive Cdc42 (D/P) or dominant negative (D/N) mutants of Cdc42 (D/N). Cells were lysed in 0.5% NP-40/PBS followed by Flag-IP of cleared lysates. Co-IP of Cdc42 was probed with an anti-Myc antibody. Molecular masses (in kDa) are indicated on the left. Data shown are representative of 2 independent experiments.

### 7.3 Loss of Cdc42 does not affect Scrib degradation by VACV

Scrib has been shown to regulate the activity and the effectors of Cdc42. For example, Scrib interacts with βPIX, which bridges Scrib to Cdc42 effector PAK, and Scrib is required for the correct localisation of βPIX and PAK at the leading edge of motile epithelial cells (Nola et al., 2008). Therefore, it was possible that Cdc42 might

be required for VACV to degrade Scrib and this was investigated in Cdc42 KO cells. Hap WT and Hap Cdc42 KO cells were mock-treated or infected with vC2, and cleared lysates were analysed by immunoblotting (Figure 7.3). Scrib was degraded after infection of both WT Hap cells and Cdc42 KO cells compared to uninfected cells, and therefore Cdc42 is not required for the degradation of Scrib by VACV proteins A55 and C2. It remains to be investigated if Cdc42 localises differently in Scrib KO cells.

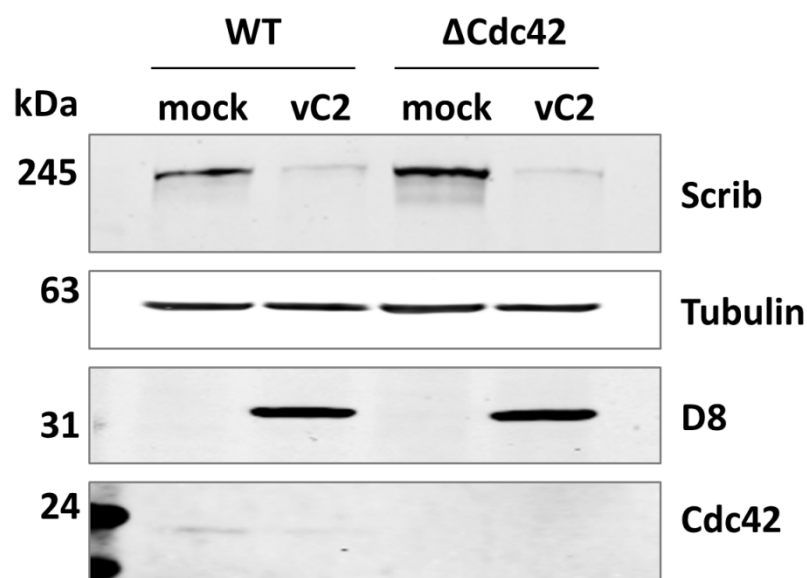


**Figure 7.3. Loss of Cdc42 does not affect Scrib degradation by VACV.** Hap WT or Hap Cdc42 KO cells were mock-treated or infected with vC2 at 5 p.f.u./cell for 14 h. Cleared lysates were harvested and analysed by immunoblotting. Molecular masses (in kDa) are indicated on the left. Data shown are representative of 2 independent experiments.

In summary, C2 associates with Cdc42 via the C2-BTB domain, and it activates Cdc42 during infection by an unknown mechanism. Although there is a link between Scrib and Cdc42 in cells, and they are both co-precipitated by VACV protein C2, Cdc42 is not required for A55 and C2 to degrade Scrib. The effect of Scrib on the localisation of Cdc42 remains to be studied. It should also be further investigated

whether Cdc42 and/or Scrib are needed for the plaque morphology effect caused by C2 by using Cdc42 / Scrib KO cell lines.

## 8 Discussion

VACV has been a valuable tool to study the host immune response to virus infection, the host-virus interaction and how the virus manipulates the host's immune system to aid virus survival and transmission. A better understanding of the virulence and immunomodulatory function of VACV also helps to develop safer and more effective vaccines against both infectious diseases and tumours. VACV has been found to encode a plethora of immunomodulatory proteins (Smith et al., 2013), among which only three proteins with a BTB-Kelch structure were found, which are A55, C2 and F3. Proteins containing BTB and Kelch domains function as adapters for the Cul3-based ubiquitylation system. In theory, a BTB-Kelch protein interacts with Cul3 via its BTB domain and substrates via its Kelch domain, leading to the ubiquitylation, modification or degradation of substrates. Although non-essential for viral replication, these three BTB/BACK-Kelch (BBK) proteins of VACV A55, C2 and F3 do affect lesion sizes in intradermal murine models, either resulting in larger lesion size when infected with viruses lacking A55 or C2, or smaller lesion size when lacking F3 compared to WT VACV infection. Viruses lacking any one of these three BBK proteins also increased inflammatory cells infiltration in lesions, suggesting an anti-inflammatory effect of these proteins during VACV infection. Moreover, deleting *A55R* or *C2L* also causes different plaque morphology and cytopathic effect in cultured cells (Beard et al., 2006; Froggatt et al., 2007; Pires de Miranda et al., 2003). The objectives of this study were to investigate the mechanisms by which VACV BBK proteins inhibit the host's inflammatory response to VACV infection, whether these BBK proteins associate with Cul3 and how the interaction with Cul3 fits the phenotypes caused by these proteins, and to identify the cellular substrates of A55, C2 and/or F3 and the outcomes of targeting these substrates.

## 8.1 A55, C2 and F3 are inhibitors of NF- $\kappa$ B pathway

Virus PAMPs are recognised by PRRs that then activate innate immune signalling pathways leading to the activation of transcription factors such as NF- $\kappa$ B, AP-1, IRF3 and IRF7. These translocate into the nucleus and promote expression of pro-inflammatory molecules including cytokines, chemokines and type I IFNs that activate and recruit immune cells to the infection sites (section 1.2.1). VACV inhibits the IFN response at multiple stages, including inhibiting IFN production, preventing the engagement of IFN receptors by IFNs, blocking the signal transduction induced by IFN-receptor engagement, and inhibiting the antiviral effect of IFN-induced proteins. The induction of IFN expression requires activation of intracellular signalling pathways that lead to IRF3 or NF- $\kappa$ B activation, and VACV expresses numerous proteins to inhibit these pathways. For instance, there are several VACV proteins that influence IRF-3 activation (section 1.2.1.2) and 16 VACV proteins have been identified to inhibit NF- $\kappa$ B signalling pathway at different levels (section 1.2.1.1). Furthermore, the ECTV orthologue of A55, ECTV EVM150, was reported to inhibit NF- $\kappa$ B signalling (Wang et al., 2014). Therefore, this study first investigated whether VACV BBK proteins A55, C2 and F3 affect activation of the NF- $\kappa$ B signalling pathway.

Reporter gene assays measuring the activity of a NF- $\kappa$ B-luciferase reporter showed that all three VACV BBK proteins inhibit NF- $\kappa$ B signalling pathway (Figure 3.3). Each of these proteins inhibited the pathway induced by IL-1 $\beta$ , TNF $\alpha$ , TRAF2 or TRAF6, suggesting each protein inhibits at a position at or downstream of where the IL-1 $\beta$  and TNF $\alpha$  pathways converge. This inhibitory effect of A55, C2 or F3 was further validated by alternative assays including RT-qPCR and ELISA to measure the expression of endogenous NF- $\kappa$ B-responsive genes at the transcriptional and

secreted protein levels. In these assays, all three BBK proteins inhibited the transcription of *IL-8* and the secretion of IL-8 (Figure 3.5). Together these data showed A55, C2 and F3 inhibit NF- $\kappa$ B signalling pathway at or downstream of where IL-1 $\beta$  and TNF $\alpha$ -induced signalling pathways converge.

Typically the BTB domain and the Kelch domain have different biological functions, with the BTB domain interacting with Cul3 whilst the Kelch domain binds different substrates. An understanding of which domain is responsible for the inhibition of NF- $\kappa$ B signalling may therefore shed a light on the mechanism by which these proteins inhibit the pathway. Reporter gene assays, RT-qPCR and ELISA showed that both the BTB-BACK and the Kelch domains of C2 inhibited the pathway activity independently, although neither domain alone was as potent as the full length protein. In contrast, for A55 and F3, it is the Kelch domain that inhibits the pathway but not the BTB domain (Figure 3.6) (Pallett et al., 2019). Notably, the ECTV orthologue of A55, EVM150, was reported to inhibit NF- $\kappa$ B via its BTB domain. whereas EVM150-Kelch did not show inhibitory activity (Wang et al., 2014). VACV A55 and EVM150 share 93 % amino acid identity. Nonetheless, the observed difference might be due to the slightly different sequences of these BBK proteins, or alternatively different expression levels of the BTB and the Kelch domains when expressed separately. Another difference was the precise domains of A55 and EVM150 that were expressed. A55 and C2 were divided into BTB/BACK and Kelch domains, so that A55-B and C2-B contain both the BTB and the BACK domains. In contrast, neither EVM150-B nor EVM150-K included the BACK domain. In addition, A55-B or C2-B expressed at higher levels than A55-K or C2-K, when the same amount of DNA was transfected for both domains, and this was adjusted to give equivalent expression levels for reporter gene assays by decreasing the amount of BTB plasmids

transfected. Another explanation for the difference between A55 and EVM150 discussed by (Pallett et al., 2019) is that the inhibitory activity of A55-B may be due to the toxic effects on the cell caused by overexpression of the BTB domain. EVM150 inhibits NF- $\kappa$ B activation independent of its interaction with Cul3 (Wang et al., 2014). The fact that the Kelch domains of A55, C2 and F3 inhibit the pathway suggests that VACV BBKs inhibit NF- $\kappa$ B activation independent of their interaction with Cul3 as well.

To narrow down where the BBK proteins inhibit the pathway, the NF- $\kappa$ B-luciferase activity was measured when the pathway was activated by over-expression of TAB1/TAK1, IKK $\beta$  or p65. BBKs inhibited the pathway when it was activated by TAK1/TAB1, IKK $\beta$ , or p65 in a dose-dependent manner (Figure 3.7), suggesting these proteins inhibit the pathway at or downstream of p65. This was consistent with the observation that the BBKs did not prevent the degradation of I $\kappa$ B $\alpha$  (Figure 3.8). Further, immunofluorescence showed that BBKs inhibited p65 nuclear translocation (Figure 3.9). This was a partial inhibitory effect (~50% inhibition by A55 and C2, 80% for F3), but was consistent with the inhibition observed in other assays. Notably C2 and C2-B induced cell rounding, making the data collection less certain. However, cells expressing C2-K were not affected and still showed inhibition of p65 nuclear translocation. Alternative assays that are less affected by the cell morphology such as cytoplasmic-nuclear fractionation assay could be carried out in the future to obtain independent data on the effect of C2 and C2-B on p65 nuclear translocation.

It was also shown that ectopic C2 does not associate with Cul3 (Figure 3.10A). Notably full length C2 as well as the BTB or Kelch domains of C2 inhibit the NF- $\kappa$ B signalling pathway. Together these data show that C2 inhibits the NF- $\kappa$ B signalling pathway independent of Cul3 binding, consistent with the observations for A55

(Pallett et al., 2019) and EVM150 (Wang et al., 2014) that A55 and EVM150 inhibit NF- $\kappa$ B activation independent of their interaction with Cul3. A55 impairs p65 translocation into the nucleus by associating with importin  $\alpha$ -1 (KPNA2) and thereby diminishing its interaction with p65 (Pallett et al., 2019). C2 however, did not co-IP endogenous KPNA2 (Figure 3.10B).

In summary, VACV BBKs A55, C2 and F3 inhibit NF- $\kappa$ B signalling pathway by diminishing p65 nuclear translocation, among which A55 competitively associates with KPNA2 and impairs the interaction between KPNA2 and p65, hence negatively affects p65 import into the nucleus. These data are consistent to the EVM150 work, where EVM150 was shown to inhibit the NF- $\kappa$ B luciferase activity in response to IL- $1\beta$  and TNF $\alpha$  by preventing p65 nuclear translocation without affecting I $\kappa$ B $\alpha$  levels (Wang et al., 2014). All three BBKs are very likely to inhibit the pathway independent of Cul3 binding, because: 1) both BTB and Kelch domains of C2, and the Kelch domain of A55 and F3 inhibit the pathway, and 2) C2, A55-K or F3-K does not interact with Cul3. However, all these assays were performed with BBKs overexpressed outside of the context of infection, and an association with Cul3 might still affect NF- $\kappa$ B signalling during infection. Pharmacological inhibitors of Cul3 or knocking down Cul3 could help provide further evidence.

The mechanisms by which C2 or F3 inhibit the pathway are still unknown. In a steady-state condition, I $\kappa$ B $\alpha$  masks entirely the nuclear translocation signal of p65. Once the pathway is activated and I $\kappa$ B $\alpha$  is degraded, p65 shuttles between the nucleus and cytoplasm, in a manner that is tightly controlled by importins (Karyopherin) and exportins (Giridharan and Srinivasan, 2018). Importin  $\alpha$ 1 (KPNA2), importin  $\alpha$ 3-5 (KPNA4, 3, 1), importin  $\beta$ 1 (KPNB1), importin 8 (IPO8), exportin CRM1 (XPO1) and XPO7 are all involved in the nuclear import of p65, among which KPNA2

binds to p65 and plays a major role (Liang et al., 2013b). Unlike A55, C2 was found not to associate with KPNA2 under the conditions tested. Further IPs could be attempted by overexpressing KPNA2 in case the interaction between C2 and KPNA2 is too weak to detect at an endogenous level. It could also be investigated whether C2 or F3 associates with other importins or exportins that regulate p65 nuclear translocation.

In addition to NF- $\kappa$ B signalling pathway, other innate immune signalling pathways in response to VACV infection including AP-1, JAK/STAT and IRF3 signalling should also be investigated about whether VACV BBKs regulate these pathways, both in or out of the context of infection. Preliminary data suggest that C2, but not A55 or F3, may upregulate AP-1 activation.

## **8.2 C2 associates with Cul3 when A55 is present**

A key question to answer when working with BTB proteins is whether the target protein interacts with Cul3 and the consequences of this interaction. The ECTV homologues of C2 and F3, EVM018 and EVM027, associate with Cul3 during infection but do not when expressed ectopically (Couturier, 2009a; Wilton et al., 2008a). In contrast, A55 interacts with Cul3 directly. The co-crystal structure of the A55-BTB-BACK domain (A55BB) and Cul3 N-terminal domain was determined, revealing a 2:2 complex in solution. Surprisingly, A55BB binds to Cul3 much more tightly than do cellular BTB proteins such as KLHL3, suggesting A55 could be an effective competitor for the interaction of Cul3 and its cellular binding partners (Gao et al., 2019). VACV BBKs share high amino acid identity with their orthopoxvirus BBK orthologues (> 90%, Table 3.2) but share low sequence identity with each other (~ 20%, Table 3.1) and most of the Cul3-binding residues of A55, including the

residues in the  $\phi X(D/E)$  motif and the adjacent Ile-48 residue, are not conserved in C2 or F3, suggesting that C2 and F3 are unlikely to interact with Cul3 (Gao et al., 2019). This observation is consistent with the data in this study that ectopically expressed C2 does not associate with Cul3 (Figure 3.10A).

When investigating the interaction between C2 and Cul3, it was difficult to detect C2 by immunoblotting. The technical problem of visualising C2 using immunoblotting was first solved by not boiling the proteins samples before loading onto the polyacrylamide gel (Figure 4.1). The reason that not boiling improves C2 visualisation by immunoblotting is unknown, possibly due to protein aggregation by overheating. Consistent with EVM018, C2 co-IPs Cul3 during infection (Figure 4.2) but C2 expressed ectopically does not (Figure 3.10A). Although C2 co-IPed with Cul3 during infection, this interaction was lost when cells were infected with VACV strains lacking A55 (Figure 4.3), indicating that C2 requires the presence of A55 to associate with Cul3. In addition, other viral factors are not needed for C2-Cul3 association, because co-expression of A55 with C2, but not other viral protein controls such as C6 or B14, enabled C2 to co-IP Cul3 outside the context of infection. The same experiments also showed that A55 and C2 associate with each other (Figure 4.4). Data also suggest that A55 and C2 associate with each other both via their BTB domains to form heterodimers (Figure 4.5). This is interesting because the N-terminal dimerisation helix of the BTB domain seems to be missing in C2, suggesting that C2 may not be able to form homo- or heterodimers via the same mechanism as most BTB-Kelch proteins, such as A55 (Gao et al., 2019). C2 may interact with A55 via non-conventional binding sites, or indirectly via additional cellular binding partners. Experiments were attempted to determine whether C2 interacts with A55 directly, however unfortunately sufficient purified C2 protein could

not be obtained for *in vitro* binding experiments. Notably F3, F3-B and F3-K did not co-IP with Cul3 or A55 (Figure 4.5A), which is consistent with the findings by (Gao et al., 2019) that the Cul3-binding residues are absent in F3.

Taken together, this study shows that C2 associates with Cul3 via A55, which interacts with Cul3 directly and with high affinity. A hypothesis is that in this complex formed by A55, Cul3 and C2, A55 binds Cul3 via its BTB domain, whilst C2 brings in substrates potentially via its Kelch domain, leading to the ubiquitylation of substrates followed by protein degradation or modification. A55 as a BBK protein should still have its ability to bring in substrates as well. The next step would be to test the hypothesis of this working model and to identify novel viral BBKs substrates, hence an unbiased TMT-Mass spec was carried out.

### **8.3 A55 and C2 collaborate to target cellular proteins for degradation**

An unbiased quantitative temporal viromic analysis of VACV infection was performed by others (Soday et al., 2019). HFFFs were infected by WT VACV or by viruses lacking individual viral genes for 12 h (Soday et al., 2019). The aim of this study was to identify the cellular proteins targeted by VACV and to identify the VACV gene(s) that are responsible for the alteration in abundance of each cellular protein, by comparing protein levels when cells were infected by WT VACV or virus strains lacking specific VACV genes. About 9000 cellular proteins and ~80% of the viral proteins were quantified at seven time points during VACV infection. Notably 265 cellular proteins are downregulated more than 2-fold compared to mock-infected cells, and 70% of these viral targets were downregulated by proteasomal degradation. With several VACV mutants lacking an individual gene, there was a specific alteration in the abundance of one or more cellular protein. For example,

HDAC4 and HDAC5 were shown to be degraded in a proteasome-dependent way that was dependent upon VACV protein C6 (Lu et al., 2019; Soday et al., 2019).

The same study identified three cellular proteins Fer, Scrib and RASA2 that are targeted by A55 and C2 collaboratively (Figure 5.1). The levels of Fer, Scrib and RASA2 in WT VACV-infected cells dropped to less than half of those in mock infected cells. The presence of cytosine arabinoside (AraC), a drug that interferes with DNA synthesis, does not alter the downregulation of these three proteins by VACV, suggesting that early genes are sufficient and intermediate or late viral gene products are not needed. To identify the specific viral genes that downregulate these proteins, cells were infected with WT VACV or viruses lacking individual genes including A55, C2, F3, C16, C4, A40 and A56. Interestingly, the protein levels of Fer, Scrib or RASA2 were rescued when infecting cells with  $\Delta$ C2 or  $\Delta$ A55 compared to WT VACV, and other mutant viruses showed a consistent flat line the same as WT. This indicated that both A55 and C2, but not other tested VACV proteins, are needed for VACV to downregulate these three proteins. This also shows that F3 is not necessary for A55 and C2 to collaboratively target cellular proteins. Notably cellular proteins targeted by a single VACV BBK protein were also identified in this study. For example, FRMD6 is solely targeted by A55 but not C2. This initial screen suggested a few hits targeted by C2 or F3, however there is no obvious difference when carefully comparing the protein abundance in the  $\Delta$ C2 or  $\Delta$ F3 group with WT or other mutant viruses. It could be that C2 or F3 do not interact with Cul3 directly, hence it is unlikely for them to degrade cellular proteins without the aid of A55, which supports the model above.

The viromic data was validated by immunoblotting. Consistent with the viromic data, the level of Scrib in HEK-293T cells was decreased after infection with WT VACV.

Adding MG132, a proteasome inhibitor, prevented VACV-induced Scrib downregulation, suggesting that this downregulation is proteasome dependent (Figure 5.3). Viruses lacking C2 or A55 did not induce Scrib degradation (Figure 5.4A), indicating both A55 and C2 are needed for Scrib degradation. A virus lacking both C2 and A55 resulted in similar levels of Scrib to infection with viruses lacking either A55 or C2 (Figure 5.4B), which showed that loss of either has the same outcome as loss of both. Immunoblotting also validated that FRMD6 is downregulated by WT VACV but not by  $\Delta$ A55 (Figure 5.4C), indicating that FRMD6 is targeted by A55 but not C2. Together these immunoblotting data validated the viromic data : 1) Scrib and FRMD6 are targeted by VACV; 2) Scrib degradation by VACV is proteasome dependent; 3) VACV needs both A55 and C2 to degrade Scrib; 4) FRMD6 is targeted by A55 but not C2, proving that A55 and/or C2 target cellular proteins collaboratively or independently.

It was then investigated whether A55 and C2 are the only viral factors responsible for Scrib degradation. HEK-293T cell lines that inducibly expresses A55, C2 or both A55 and C2 were constructed. The cell lysates of these inducible cell lines were analysed by immunoblotting. Scrib was clearly visible in cell lines expressing only A55 or C2, but was not detected in the cell line expressing both A55 and C2 (Figure 5.5). These assays show that A55 and C2 are sufficient to degrade Scrib in the absence of other viral factors, yet it cannot be ruled out at this stage whether other cellular factors are contributing to Scrib degradation induced by A55 and C2.

The working model of A55 and C2 target cellular proteins collaboratively is based on the fact that A55 binds Cul3 directly leading to the degradation of substrate proteins that are recruited to the complex by C2 (Figure 4.7). To test this, whether the degradation of Scrib requires the interaction between A55 and Cul3 needs to be

determined. Both ITC (Gao et al., 2019) and immunoblotting (Figure 5.6) show that the A55 I48E mutation greatly reduces the binding of A55 to Cul3, therefore a mutant VACV containing the same mutation named vI48E was constructed by inserting A55R containing I48E mutation into v $\Delta$ A55 (Figure 5.7). When HEK-293Ts were infected with this mutant virus, Scrib or FRMD6 were no longer degraded compared to WT, indicating that the degradation of Scrib and FRMD6 requires the interaction between A55 and Cul3. It was then found that ectopic Myc-tagged Scrib was co-IPed by TAP-tagged C2 but not A55, F3 or C6 (Figure 5.9), showing that Scrib is indeed recruited by C2 as the substrate, although it is unknown whether directly or indirectly.

Collectively, A55 and/or C2 target cellular proteins collaboratively (Fer, Scrib and RASA2) or independently (FRMD6 by A55). The unbiased quantitative temporal viromic analysis identified the targets, and the degradation of Scrib and downregulation of FRMD6 by VACV was validated by immunoblotting. The degradation of Scrib requires the interaction between A55 and Cul3 whilst C2 associates with Scrib (Figure 5.10). It would be interesting to know whether C2 interacts with Scrib directly and if not, what the other binding partners are in this complex, and whether the existence of those binding partners is necessary for Scrib degradation by VACV. It is also unclear whether Scrib associates with the BTB or the Kelch domain of C2. Hypothetically, the Kelch domain of C2 might associate with Scrib because the Kelch domain is usually the substrate-binding domain in a BTB-Kelch protein. Further experiments should investigate: 1) FRMD6 degradation by VACV and whether it is proteasome dependent; 2) whether FRMD6 interacts with A55; 3) Fer and RASA2 degradation by VACV and rescue by losing A55 or C2; 4) how Fer and RASA2 interact with A55 or C2; 5) the biological outcome of targeting these cellular proteins by VACV; 6) whether there is a link among these identified

proteins such as functioning on the same pathway and/or forming a complex. One other interesting direction is vI48E. The phenotypes should be compared among VACV, vI48E and vΔA55 both *in vitro* and *in vivo*, such as the virulence in animal models and the modulatory effect on innate immune signalling. It is interesting to know whether vI48E and vΔA55 share a similar phenotype, which would indicate whether A55 loses its function completely or not when losing its ability to bind Cul3, although it is already known that A55 inhibits NF-κB independent of its interaction with Cul3. Preliminary data of plaque assays show that the plaques formed on confluent BSC-1 cells by vI48E were different from those formed by WT VACV and exhibited an indistinct border similar to that described for viruses lacking A55 or C2 (Beard et al., 2006; Pires de Miranda et al., 2003), although the average size of the plaques was not significantly different compared to WT VACV.

#### **8.4 Scrib in VACV infection**

Scrib is downregulated or re-localised by multiple viruses to disrupt its function in cell polarity, cell migration, cell apoptosis and innate and adaptive immunity (section 5.1.4). This study shows Scrib is also degraded by VACV. Chapter 5 demonstrated that VACV degrades Scrib via the proteasome, and the degradation requires the interaction between A55 and Cul3 as well as the association between C2 and Scrib.

Next it was investigated whether and how Scrib affects VACV replication or spread. Scrib KO cell lines were constructed for this purpose (Figure 6.3). Two Scrib KO cell lines were infected at high or low MOI to observe the yield of virus and the size of virus plaques. At low MOI, both KO cell lines showed increased virus yield after infection compared to WT, but at high MOI the differences were marginal (Figure 6.4), indicating that loss of Scrib affects virus spread and has limited effect on viral

replication. The sizes of virus plaques were measured too after infecting Scrib KO cell lines. The average plaque area formed on both KO cell lines was larger than WT (Figure 6.5). Taken together, these data suggest Scrib restricts VACV spread.

Scrib is a critical regulator for cell polarity. Scrib interacts with Discs large homolog 1-4 (DLG1-4) and Lethal giant larvae (LGL1/2) to form the Scribble complex, which resides along the basolateral membrane of epithelial cells and is concentrated at tight junctions (Assémat et al., 2008; Humbert et al., 2008). Disruption of cell-cell adhesion and cell polarity leads to the loss of epithelial identity through the EMT (epithelial to mesenchymal transition) process, a crucial step in epithelial cancer progression (Pearson et al., 2015). VACV CPE has been linked to EMT due to their shared characteristics (McKenzie, 2016). Among the three major EMT signalling pathways, namely TGF- $\beta$ , Wnt and Notch signalling, Scrib has been shown to prevent EMT by inhibiting the activation of TGF- $\beta$  signalling (Yamben et al., 2013). Therefore, it was investigated first whether VACV and loss of Scrib regulate TGF- $\beta$  signalling.

Consistent with other published work, VACV activates TGF- $\beta$  signalling in a CAGA-Luciferase (derived from the promoter of the Smad3/4-responsive genes) reporter assay in HaCaT cells (Figure 6.6) (Gowripalan et al., 2020). The same assay was carried out using Scrib KO cell lines and loss of Scrib enhanced the activation of CAGA-Luc upon TGF- $\beta$  stimulation (Figure 6.7A), and complementing Scrib reverts the enhancement of TGF- $\beta$ /Smad signalling caused by Scrib KO (Figure 6.7C). Further, it was shown that Scrib KO increases Smad2 but not Smad3 phosphorylation upon TGF- $\beta$  stimulation (Figure 6.9). Collectively these data show VACV enhances TGF- $\beta$ /Smad activation, to which loss of Scrib is contributing. However, there was no difference between VACV and v $\Delta$ A55 (Scrib is not degraded)

infection in the CAGA-Luc reporter activity (Figure 6.10A). Although VACV increases the phosphorylation of Smad2 and Smad3,  $v\Delta A55$  did not make an obvious difference compared to VACV (Figure 6.10C). There may be a difference between VACV and  $v\Delta A55$  in the activity of a more specific Smad reporter, BRE-Luc, which indicates Smad1/5 activity specifically (Figure 6.11), however the assay needs to be further optimised to draw a conclusion. In summary, there is evidence that VACV enhances the activation of TGF- $\beta$ -stimulated Smad signalling, and Scrib contributes to the counteractive effect. VACV can still activate Smad3/4 with or without Scrib, suggesting there might be other viral factors regulating the pathway. A recent study shows that loss of Smad4 attenuates VACV spread and VACV-induced cell motility (Gowripalan et al., 2020). This could be a mechanism by which Scrib restricts VACV spread. In the future, it would be useful to test the activation of TGF- $\beta$  during VACV infection or in Scrib KO cell lines at transcriptional levels, by measuring the mRNA levels of TGF- $\beta$ -responsive genes, to further validate the effect of VACV or loss of Scrib on TGF- $\beta$  signalling. It should also be investigated whether Scrib KO cell lines benefit VACV spread by enhancing the activation of TGF- $\beta$  signalling. This could be attempted with a Smad4 KO cell line.

Additional evidence has shown that besides its critical role in maintaining cell polarity and cell-cell contact in epithelial cells, Scrib is involved in fundamental functions of T cells (Ludford-Menting et al., 2005) and human APCs including DCs, macrophages and monocytes (Barreda et al., 2020; Barreda et al., 2018; Zheng et al., 2016). Scrib is indispensable for the uropod formation, migration and antigen presentation of T cells (Ludford-Menting et al., 2005). DCs and macrophages express Scrib too, and the NS1 protein of influenza A virus targets Scrib in DCs by colocalisation (Barreda et al., 2018). Within macrophages, Scrib is required for the reactive oxygen species

(ROS) generation and bacterial clearance (Zheng et al., 2016). M1 macrophages are key regulators of host defence to pathogen infection and inflammation (Benoit et al., 2008). However, loss of Scrib enhances M1 polarisation and decreases M2 polarisation (Zheng et al., 2016). Scrib is also necessary for adequate CD86 upregulation during DC maturation, and DC dysfunctions due to loss of Scrib result in inefficient T-cell stimulation (Barreda et al., 2020). Given these, A55/C2 may contribute to viral infection in a different way in T cells or APCs. Notably VACV would need to infect these cells to alter levels of Scrib, and these are not the natural cells VACV infects.

Scrib also has pro-apoptotic functions. Both downregulation and mislocalisation of Scrib from cell-cell junctions leads to inhibition of apoptosis (Zhan et al., 2008). The influenza A virus non-structural protein NS1 interacts with Scrib and relocalises Scrib from the plasma membrane to cytoplasmic puncta, and thereby protects infected cells from Scrib's pro-apoptotic functions (Liu et al., 2010). It would be interesting to investigate whether VACV degrades Scrib to inhibit host apoptosis.

## **8.5 C2 is a potential Cdc42 activator**

Unpublished SILAC data (Carlos Maluquer de Motes & Laura Gonzales, 2013) identified Cdc42 as a potential binding partner of C2, and this has possible relevance to the plaque morphology and cellular projections during WT VACV or v $\Delta$ C2 virus infection was investigated (Pires de Miranda et al., 2003). The association between Cdc42 and C2 was validated by IP (Figure 7.1). Interestingly, C2 associates with Cdc42 via the C2-BTB domain, but not C2-Kelch, the usual domain in a BBK protein that specifically interacts with substrates. However, this links to the observation that C2 and C2-B both caused cells to round up (Figure 3.9). It should be investigated

whether Cdc42 is required for this phenotype, for example IF can be performed in Cdc42 KO cells over-expressing C2, C2-B and C2-K, or overexpressing constitutively inactive Cdc42. Importantly, according to the viromic data, the Cdc42 level is stable during VACV infection, which means C2 does not degrade Cdc42 via A55/Cul3.

Cdc42 cycles between active and inactive states. The PAK-PBD pulldown assay shows Cdc42 is activated by VACV, and this activation is reduced in the absence of C2 (Figure 7.2A), however C2 does not co-IP either the constitutively active or the constitutively inactive form of Cdc42 (Figure 7.2B). Notably these constructs have been mutated, and therefore they may not bind due to the mutation preventing binding directly or indirectly to C2, so these domains may be important for the interaction. It should be further investigated whether C2 activates Cdc42 on its own without the context of infection, or whether C2 needs A55 or other viral factors to activate Cdc42 collaboratively, using cell lines expressing C2, A55 or both.

Scrib interacts with  $\beta$ PIX and regulates the activity of Cdc42 (Nola et al., 2008), therefore it was investigated whether Cdc42 is required for VACV to degrade Scrib. WT and Cdc42 KO cell lines were mock-treated or infected with VACV, and the detection of Scrib in cell lysates was analysed by immunoblotting. In WT Hap cells, Scrib was degraded when cells were infected with VACV compared to mock and similar results were observed in the Cdc42 KO cells (Figure 7.3). This shows Cdc42 is not required for the degradation of Scrib by A55 and C2. It remains unknown whether Scrib has a function in the filopodia formation by C2, and whether Scrib degradation changes Cdc42 localisation.

## 8.6 Summary

In summary, the VACV BBK proteins A55, C2 and F3 inhibit the NF- $\kappa$ B signalling pathway. A55 inhibits NF- $\kappa$ B signalling by associating with KPNA2 and diminishing its binding to p65, thereby blocking p65 nuclear translocation. C2 and F3 both inhibit NF- $\kappa$ B signalling at or downstream of p65 nuclear translocation by unknown mechanisms, and C2 inhibits NF- $\kappa$ B independent of Cul3.

A55 interacts with Cul3 directly. C2 does not interact with Cul3, but associates with Cul3 via A55. A55, C2 and Cul3 form a complex to target cellular proteins such as Scrib. Scrib is degraded by VACV and is a novel cellular target by poxviruses. A55 and C2 are sufficient to degrade Scrib in the absence of other viral factors. In two cell lines lacking Scrib, VACV formed larger plaques compared to controls. In addition, after low, but not high, MOI infection there was an increased virus yield. Collectively, these data suggest that loss of Scrib is affecting virus spread by an unknown mechanism. Furthermore, VACV upregulates TGF- $\beta$ /Smad signalling and Scrib has roles in the regulation of the pathway.

In addition, C2 associates with Cdc42 via its BTB domain. C2 activates Cdc42, and Cdc42 is not essential for Scrib degradation by VACV.

This study shows that VACV expresses the family of BBK proteins to inhibit the activation of host innate immune signalling (NF- $\kappa$ B), which could contribute to the mechanism by which loss of A55 and C2 increase immune cell recruitment *in vivo*. Furthermore, this study provides additional evidence that VACV hijacks host Cul3-ubiquitin system to target cellular proteins, or deploys host cell migration mechanisms in order to benefit viral replication/spread.

## 9 Bibliography

- (WHO), W.H.O. (2020). Naming the coronavirus disease (COVID-19) and the virus that causes it.
- Adams, J., Kelso, R., and Cooley, L. (2000). The kelch repeat superfamily of proteins: propellers of cell function. *Trends in Cell Biology* *10*, 17-24.
- Ahmad, K.F., Engel, C.K., and Privé, G.G. (1998). Crystal structure of the BTB domain from PLZF. *Proc Natl Acad Sci U S A* *95*, 12123-12128.
- Ahn, J., Truesdell, P., Meens, J., Kadish, C., Yang, X., Boag, A.H., and Craig, A.W.B. (2013). Fer Protein-Tyrosine Kinase Promotes Lung Adenocarcinoma Cell Invasion and Tumor Metastasis. *Molecular Cancer Research* *11*, 952.
- Alarcón, C., Zaromytidou, A.-I., Xi, Q., Gao, S., Yu, J., Fujisawa, S., Barlas, A., Miller, A.N., Manova-Todorova, K., Macias, M.J., *et al.* (2009). Nuclear CDKs drive Smad transcriptional activation and turnover in BMP and TGF-beta pathways. *Cell* *139*, 757-769.
- Alcami, A., Khanna, A., Paul, N.L., and Smith, G.L. (1999). Vaccinia virus strains Lister, USSR and Evans express soluble and cell-surface tumour necrosis factor receptors. *Journal of General Virology* *80*, 949-959.
- Alcami, A., and Smith, G.L. (1992). A soluble receptor for interleukin-1 $\beta$  encoded by vaccinia virus: A novel mechanism of virus modulation of the host response to infection. *Cell* *71*, 153-167.
- Allen, M., Chu, S., Brill, S., Stotler, C., and Buckler, A. (1998). Restricted tissue expression pattern of a novel human rasGAP-related gene and its murine ortholog. *Gene* *218*, 17-25.
- Amanat, F., and Krammer, F. (2020). SARS-CoV-2 Vaccines: Status Report. *Immunity* *52*, 583-589.
- Amara, A., and Mercer, J. (2015). Viral apoptotic mimicry. *Nat Rev Microbiol* *13*, 461-469.
- Amarante-Mendes, G.P., Adjemian, S., Branco, L.M., Zanetti, L.C., Weinlich, R., and Bortoluci, K.R. (2018). Pattern Recognition Receptors and the Host Cell Death Molecular Machinery. *Front Immunol* *9*.
- Angel, P., and Karin, M. (1991). The role of Jun, Fos and the AP-1 complex in cell-proliferation and transformation. *Biochimica et Biophysica Acta (BBA)-Reviews on Cancer* *1072*, 129-157.
- Angus, L., Moleirinho, S., Herron, L., Sinha, A., Zhang, X., Nestrata, M., Dholakia, K., Prystowsky, M.B., Harvey, K.F., Reynolds, P.A., and Gunn-Moore, F.J. (2012). Willin/FRMD6 expression activates the Hippo signaling pathway kinases in mammals and antagonizes oncogenic YAP. *Oncogene* *31*, 238-250.
- Arafah, R., Qutob, N., Emmanuel, R., Keren-Paz, A., Madore, J., Elkahlon, A., Wilmott, J.S., Gartner, J.J., Di Pizio, A., Winograd-Katz, S., *et al.* (2015). Recurrent inactivating RASA2 mutations in melanoma. *Nat Genet* *47*, 1408-1410.
- Assémat, E., Bazellières, E., Pallesi-Pocachard, E., Le Bivic, A., and Massey-Harroche, D. (2008). Polarity complex proteins. *Biochimica et Biophysica Acta (BBA) - Biomembranes* *1778*, 614-630.
- Audebert, S., Navarro, C., Nourry, C., Chasserot-Golaz, S., Lécine, P., Bellaiche, Y., Dupont, J.-L., Premont, R.T., Sempéré, C., Strub, J.-M., *et al.* (2004). Mammalian Scribble Forms a Tight Complex with the  $\beta$ PIX Exchange Factor. *Current Biology* *14*, 987-995.
- Awad, A., Sar, S., Barré, R., Cariven, C., Marin, M., Salles, J.P., Erneux, C., Samuel, D., and Gassama-Diagne, A. (2013). SHIP2 regulates epithelial cell polarity through its lipid product, which binds to Dlg1, a pathway subverted by hepatitis C virus core protein. *Mol Biol Cell* *24*, 2171-2185.
- Bablanian, R. (1968). The Prevention of Early Vaccinia-virus-induced Cytopathic Effects by Inhibition of Protein Synthesis. *Journal of General Virology* *3*, 51-61.
- Bardwell, V.J., and Treisman, R. (1994). The POZ domain: a conserved protein-protein interaction motif. *Genes & Development* *8*, 1664-1677.
- Barreda, D., Ramón-Luing, L.A., Duran-Luis, O., Bobadilla, K., Chacón-Salinas, R., and Santos-Mendoza, T. (2020). Scrib and Dlg1 polarity proteins regulate Ag presentation in human dendritic cells. *Journal of leukocyte biology n/a*.

Barreda, D., Sánchez - Galindo, M., López - Flores, J., Nava - Castro, K.E., Bobadilla, K., Salgado - Aguayo, A., and Santos - Mendoza, T. (2018). PDZ proteins are expressed and regulated in antigen - presenting cells and are targets of influenza A virus. *Journal of leukocyte biology* *103*, 731-738.

Barry, M., Van Buuren, N., Burles, K., Mottet, K., Wang, Q., and Teale, A. (2010). Poxvirus exploitation of the ubiquitin-proteasome system. *Viruses* *2*, 2356-2380.

Baxby, D. (1981). Jenner's smallpox vaccine: the riddle of vaccinia virus and its origin (Heinemann Educational Publishers).

Beard, P.M., Froggatt, G.C., and Smith, G.L. (2006). Vaccinia virus kelch protein A55 is a 64 kDa intracellular factor that affects virus-induced cytopathic effect and the outcome of infection in a murine intradermal model. *Journal of General Virology* *87*, 1521-1529.

Beerli, C., Yakimovich, A., Kilcher, S., Reynoso, G.V., Fläschner, G., Müller, D.J., Hickman, H.D., and Mercer, J. (2019). Vaccinia virus hijacks EGFR signalling to enhance virus spread through rapid and directed infected cell motility. *Nat Microbiol* *4*, 216-225.

Bennink, J.R., Yewdell, J.W., Smith, G.L., Moller, C., and Moss, B. (1984). Recombinant vaccinia virus primes and stimulates influenza haemagglutinin-specific cytotoxic T cells. *Nature* *311*, 578-579.

Benoit, M., Desnues, B., and Mege, J.-L. (2008). Macrophage polarization in bacterial infections. *The Journal of Immunology* *181*, 3733-3739.

Bidgood, S.R. (2019). Continued poxvirus research: From foe to friend. *PLOS Biology* *17*, e3000124.

Bilder, D., and Perrimon, N. (2000). Localization of apical epithelial determinants by the basolateral PDZ protein Scribble. *Nature* *403*, 676-680.

Blasco, R., and Moss, B. (1992). Role of cell-associated enveloped vaccinia virus in cell-to-cell spread. *J Virol* *66*, 4170-4179.

Bonchuk, A., Denisov, S., Georgiev, P., and Maksimenko, O. (2011). Drosophila BTB/POZ Domains of "ttk Group" Can Form Multimers and Selectively Interact with Each Other. *Journal of Molecular Biology* *412*, 423-436.

Bonilla, F.A., and Oettgen, H.C. (2010). Adaptive immunity. *Journal of Allergy and Clinical Immunology* *125*, S33-S40.

Bork, P., and Doolittle, R.F. (1994). Drosophila kelch motif is derived from a common enzyme fold. *Journal of Molecular Biology* *236*, 1277-1282.

Bosu, D.R., and Kipreos, E.T. (2008). Cullin-RING ubiquitin ligases: global regulation and activation cycles. *Cell Division* *3*, 7.

Bravo Cruz, A.G., and Shisler, J.L. (2016). Vaccinia virus K1 ankyrin repeat protein inhibits NF- $\kappa$ B activation by preventing RelA acetylation. *Journal of General Virology* *97*, 2691-2702.

Bretscher, A., Edwards, K., and Fehon, R.G. (2002). ERM proteins and merlin: integrators at the cell cortex. *Nature Reviews Molecular Cell Biology* *3*, 586-599.

Bryant, P.J. (1997). Junction genetics. *Developmental Genetics* *20*, 75-90.

Bulgin, R.R., Arbeloa, A., Chung, J.C.S., and Frankel, G. (2009). EspT triggers formation of lamellipodia and membrane ruffles through activation of Rac-1 and Cdc42. *Cellular Microbiology* *11*, 217-229.

Burles, K., van Buuren, N., and Barry, M. (2014). Ectromelia virus encodes a family of Ankyrin/F-box proteins that regulate NF $\kappa$ B. *Virology* *468-470*, 351-362.

Cargnello, M., and Roux, P.P. (2011). Activation and function of the MAPKs and their substrates, the MAPK-activated protein kinases. *Microbiol Mol Biol Rev* *75*, 50-83.

Carter, G.C., Law, M., Hollinshead, M., and Smith, G.L. (2005). Entry of the vaccinia virus intracellular mature virion and its interactions with glycosaminoglycans. *Journal of General Virology* *86*, 1279-1290.

Carter, G.C., Rodger, G., Murphy, B.J., Law, M., Krauss, O., Hollinshead, M., and Smith, G.L. (2003). Vaccinia virus cores are transported on microtubules. *Journal of General Virology* *84*, 2443-2458.

Chaharbakhshi, E., and Jemc, J.C. (2016a). Broad-complex, tramtrack, and bric-a-brac (BTB) proteins: Critical regulators of development. *Genesis* *54*, 505-518.

Chaharbakhshi, E., and Jemc, J.C. (2016b). Broad-complex, tramtrack, and bric-à-brac (BTB) proteins: Critical regulators of development. *genesis* *54*, 505-518.

Chen, D., Sun, Y., Wei, Y., Zhang, P., Rezaeian, A.H., Teruya-Feldstein, J., Gupta, S., Liang, H., Lin, H.-K., Hung, M.-C., and Ma, L. (2012). LIFR is a breast cancer metastasis suppressor upstream of the Hippo-YAP pathway and a prognostic marker. *Nat Med* 18, 1511-1517.

Chen, J., and Archer, T.K. (2005). Regulating SWI/SNF subunit levels via protein-protein interactions and proteasomal degradation: BAF155 and BAF170 limit expression of BAF57. *Mol Cell Biol* 25, 9016-9027.

Chen, Q., Su, Y., Wesslowski, J., Hagemann, A.I., Ramialison, M., Wittbrodt, J., Scholpp, S., and Davidson, G. (2014). Tyrosine phosphorylation of LRP6 by Src and Fer inhibits Wnt/ $\beta$ -catenin signalling. *EMBO Rep* 15, 1254-1267.

Chen, R.A.J., Ryzhakov, G., Cooray, S., Randow, F., and Smith, G.L. (2008). Inhibition of I $\kappa$ B kinase by vaccinia virus virulence factor B14. *PLoS Pathog* 4, e22-e22.

Chen, X., and Prywes, R. (1999). Serum-induced expression of the *cdc25A* gene by relief of E2F-mediated repression. *Mol Cell Biol* 19, 4695-4702.

Choi, H.-J., Zhang, H., Park, H., Choi, K.-S., Lee, H.-W., Agrawal, V., Kim, Y.-M., and Kwon, Y.-G. (2015). Yes-associated protein regulates endothelial cell contact-mediated expression of angiopoietin-2. *Nature Communications* 6, 6943.

Chung, C.-S., Chen, C.-H., Ho, M.-Y., Huang, C.-Y., Liao, C.-L., and Chang, W. (2006). Vaccinia virus proteome: identification of proteins in vaccinia virus intracellular mature virion particles. *J Virol* 80, 2127-2140.

Condit, R.C., Moussatche, N., and Traktman, P. (2006). In a nutshell: structure and assembly of the vaccinia virion. *Advances in virus research* 66, 31-124.

Cooray, S., Bahar, M.W., Abrescia, N.G.A., McVey, C.E., Bartlett, N.W., Chen, R.A.J., Stuart, D.I., Grimes, J.M., and Smith, G.L. (2007). Functional and structural studies of the vaccinia virus virulence factor N1 reveal a Bcl-2-like anti-apoptotic protein. *J Gen Virol* 88, 1656-1666.

Cordeiro, J.V., Guerra, S., Arakawa, Y., Dodding, M.P., Esteban, M., and Way, M. (2009). F11-mediated inhibition of RhoA signalling enhances the spread of vaccinia virus in vitro and in vivo in an intranasal mouse model of infection. *PLoS One* 4, e8506-e8506.

Cordenonsi, M., Zanconato, F., Azzolin, L., Forcato, M., Rosato, A., Frasson, C., Inui, M., Montagner, M., Parenti, Anna R., Poletti, A., *et al.* (2011). The Hippo Transducer TAZ Confers Cancer Stem Cell-Related Traits on Breast Cancer Cells. *Cell* 147, 759-772.

Couturier, B. (2009a). Characterization of Ectromelia BTB/kelch proteins and their potential role as substrate adaptors for cullin-3 ubiquitin ligases. In Department of Medical Microbiology and Immunology (Edmonton, Alberta, University of Alberta).

Couturier, B.A. (2009b). Characterization of Ectromelia BTB/kelch proteins and their potential role as substrate adaptors for cullin-3 ubiquitin ligases. In Department of Medical Microbiology and Immunology (Edmonton, Alberta, University of Alberta).

Cullen, P.J., Hsuan, J.J., Truong, O., Letcher, A.J., Jackson, T.R., Dawson, A.P., and Irvine, R.F. (1995). Identification of a specific Ins(1,3,4,5)P<sub>4</sub>-binding protein as a member of the GAP1 family. *Nature* 376, 527-530.

Daly, A.C., Randall, R.A., and Hill, C.S. (2008). Transforming growth factor beta-induced Smad1/5 phosphorylation in epithelial cells is mediated by novel receptor complexes and is essential for anchorage-independent growth. *Mol Cell Biol* 28, 6889-6902.

de Magalhães, J.C., Andrade, A.A., Silva, P.N., Sousa, L.P., Ropert, C., Ferreira, P.C., Kroon, E.G., Gazzinelli, R.T., and Bonjardim, C.A. (2001). A Mitogenic Signal Triggered at an Early Stage of Vaccinia Virus Infection IMPLICATION OF MEK/ERK AND PROTEIN KINASE A IN VIRUS MULTIPLICATION. *Journal of Biological Chemistry* 276, 38353-38360.

De Silva, F.S., Lewis, W., Berglund, P., Koonin, E.V., and Moss, B. (2007). Poxvirus DNA primase. *Proceedings of the National Academy of Sciences* 104, 18724-18729.

Dennler, S., Itoh, S., Vivien, D., ten Dijke, P., Huet, S., and Gauthier, J.-M. (1998a). Direct binding of Smad3 and Smad4 to critical TGF $\beta$ -inducible elements in the promoter of human plasminogen activator inhibitor-type 1 gene. *The EMBO journal* 17, 3091-3100.

Dennler, S., Itoh, S., Vivien, D., ten Dijke, P., Huet, S., and Gauthier, J.M. (1998b). Direct binding of Smad3 and Smad4 to critical TGF beta-inducible elements in the promoter of human plasminogen activator inhibitor-type 1 gene. *The EMBO Journal* *17*, 3091-3100.

Deshaies, R.J., and Joazeiro, C.A. (2009). RING domain E3 ubiquitin ligases. *Annual review of biochemistry* *78*.

DiPerna, G., Stack, J., Bowie, A.G., Boyd, A., Kotwal, G., Zhang, Z., Arvikar, S., Latz, E., Fitzgerald, K.A., and Marshall, W.L. (2004). Poxvirus Protein N1L Targets the I- $\kappa$ B Kinase Complex, Inhibits Signaling to NF- $\kappa$ B by the Tumor Necrosis Factor Superfamily of Receptors, and Inhibits NF- $\kappa$ B and IRF3 Signaling by Toll-like Receptors. *Journal of Biological Chemistry* *279*, 36570-36578.

Dobbelstein, M., and Shenk, T. (1996). Protection against apoptosis by the vaccinia virus SPI-2 (B13R) gene product. *J Virol* *70*, 6479-6485.

Dolgachev, V., Panicker, S., Balijepalli, S., McCandless, L.K., Yin, Y., Swamy, S., Suresh, M.V., Delano, M.J., Hemmila, M.R., Raghavendran, K., and Machado-Aranda, D. (2018). Electroporation-mediated delivery of FER gene enhances innate immune response and improves survival in a murine model of pneumonia. *Gene Ther* *25*, 359-375.

Dong, E., Du, H., and Gardner, L. (2020). An interactive web-based dashboard to track COVID-19 in real time. *The Lancet Infectious Diseases* *20*, 533-534.

Donohoe, C.D., Csordás, G., Correia, A., Jindra, M., Klein, C., Habermann, B., and Uhlirova, M. (2018). Atf3 links loss of epithelial polarity to defects in cell differentiation and cytoarchitecture. *PLOS Genetics* *14*, e1007241.

Dow, L.E., Brumby, A.M., Muratore, R., Coombe, M.L., Sedelies, K.A., Trapani, J.A., Russell, S.M., Richardson, H.E., and Humbert, P.O. (2003). hScribble is a functional homologue of the Drosophila tumour suppressor Scribble. *Oncogene* *22*, 9225-9230.

Edelmann, K.H., and Wilson, C.B. (2001). Role of CD28/CD80-86 and CD40/CD154 costimulatory interactions in host defense to primary herpes simplex virus infection. *J Virol* *75*, 612-621.

Elsam, I.A., Martin, C., and Humbert, P.O. (2013). Scribble regulates an EMT polarity pathway through modulation of MAPK-ERK signaling to mediate junction formation. *Journal of Cell Science* *126*, 3990-3999.

Etienne-Manneville, S., and Hall, A. (2001). Integrin-Mediated Activation of Cdc42 Controls Cell Polarity in Migrating Astrocytes through PKC $\zeta$ . *Cell* *106*, 489-498.

Fagerlund, R., Kinnunen, L., Köhler, M., Julkunen, I., and Melén, K. (2005). NF- $\kappa$ B Is Transported into the Nucleus by Importin  $\alpha$ 3 and Importin  $\alpha$ 4. *Journal of Biological Chemistry* *280*, 15942-15951.

Fahy, A.S., Clark, R.H., Glyde, E.F., and Smith, G.L. (2008). Vaccinia virus protein C16 acts intracellularly to modulate the host response and promote virulence. *Journal of General Virology* *89*, 2377-2387.

Falkner, F.G., and Moss, B. (1988). Escherichia coli gpt gene provides dominant selection for vaccinia virus open reading frame expression vectors. *J Virol* *62*, 1849-1854.

Fenner, F., Henderson, D.A., Arita, I., Jezek, Z., Ladnyi, I.D., and World Health, O. (1988). Smallpox and its eradication / F. Fenner ... [et al.]. (Geneva, World Health Organization).

Ferguson, B.J., Benfield, C.T.O., Ren, H., Lee, V.H., Frazer, G.L., Strnadova, P., Sumner, R.P., and Smith, G.L. (2013). Vaccinia virus protein N2 is a nuclear IRF3 inhibitor that promotes virulence. *J Gen Virol* *94*, 2070-2081.

Ferrigno, O., Lallemand, F., Verrecchia, F., L'Hoste, S., Camonis, J., Atfi, A., and Mauviel, A. (2002). Yes-associated protein (YAP65) interacts with Smad7 and potentiates its inhibitory activity against TGF- $\beta$ /Smad signaling. *Oncogene* *21*, 4879-4884.

Froggatt, G.C., Smith, G.L., and Beard, P.M. (2007). Vaccinia virus gene F3L encodes an intracellular protein that affects the innate immune response. *J Gen Virol* *88*, 1917-1921.

Furukawa, M., He, Y.J., Borchers, C., and Xiong, Y. (2003). Targeting of protein ubiquitination by BTB-Cullin 3-Roc1 ubiquitin ligases. *Nat Cell Biol* *5*, 1001-1007.

Gack, M.U., Shin, Y.C., Joo, C.-H., Urano, T., Liang, C., Sun, L., Takeuchi, O., Akira, S., Chen, Z., Inoue, S., and Jung, J.U. (2007). TRIM25 RING-finger E3 ubiquitin ligase is essential for RIG-I-mediated antiviral activity. *Nature* *446*, 916-920.

Gao, C., Pallett, M.A., Croll, T.I., Smith, G.L., and Graham, S.C. (2019). Molecular basis of cullin-3 (Cul3) ubiquitin ligase subversion by vaccinia virus protein A55. *The Journal of biological chemistry* *294*, 6416-6429.

Garneau, J.E., Dupuis, M.-È., Villion, M., Romero, D.A., Barrangou, R., Boyaval, P., Fremaux, C., Horvath, P., Magadán, A.H., and Moineau, S. (2010). The CRISPR/Cas bacterial immune system cleaves bacteriophage and plasmid DNA. *Nature* *468*, 67-71.

Gasiunas, G., Barrangou, R., Horvath, P., and Siksnys, V. (2012). Cas9-crRNA ribonucleoprotein complex mediates specific DNA cleavage for adaptive immunity in bacteria. *Proc Natl Acad Sci U S A* *109*, E2579-E2586.

Gazon, H., Barbeau, B., Mesnard, J.-M., and Peloponese, J.-M. (2018). Hijacking of the AP-1 Signaling Pathway during Development of ATL. *Frontiers in Microbiology* *8*.

Geshelin, P., and Berns, K.I. (1974). Characterization and localization of the naturally occurring cross-links in vaccinia virus DNA. *Journal of Molecular Biology* *88*, 785-796.

Ghosh, S., and Karin, M. (2002). Missing pieces in the NF- $\kappa$ B puzzle. *Cell* *109*, S81-S96.

Giridharan, S., and Srinivasan, M. (2018). Mechanisms of NF- $\kappa$ B p65 and strategies for therapeutic manipulation. *J Inflamm Res* *11*, 407-419.

Görlich, D., and Kutay, U. (1999). Transport Between the Cell Nucleus and the Cytoplasm. *Annual Review of Cell and Developmental Biology* *15*, 607-660.

Gowripalan, A. (2018). The role of Smad signalling during vaccinia virus infection (PhD thesis). In Faculty of Science (Sydney, University of Sydney), p. 257.

Gowripalan, A., Abbott, C.R., McKenzie, C., Chan, W.S., Karupiah, G., Levy, L., and Newsome, T.P. (2019). Cell-to-cell spread of vaccinia virus is promoted by TGF- $\beta$ -independent Smad4 signalling. *Cellular Microbiology* *n/a*, e13206.

Gowripalan, A., Abbott, C.R., McKenzie, C., Chan, W.S., Karupiah, G., Levy, L., and Newsome, T.P. (2020). Cell-to-cell spread of vaccinia virus is promoted by TGF- $\beta$ -independent Smad4 signalling. *Cellular Microbiology* *22*, e13206.

Gray, C.H., McGarry, L.C., Spence, H.J., Riboldi-Tunncliffe, A., and Ozanne, B.W. (2009). Novel  $\beta$ -Propeller of the BTB-Kelch Protein Krp1 Provides a Binding Site for Lasp-1 That Is Necessary for Pseudopodial Extension. *The Journal of Biological Chemistry* *284*, 30498-30507.

Greer, P. (2002). Closing in on the biological functions of fps/fes and fer. *Nature Reviews Molecular Cell Biology* *3*, 278-289.

Griffith, T.S., and Ferguson, T.A. (2011). Cell death in the maintenance and abrogation of tolerance: the five Ws of dying cells. *Immunity* *35*, 456-466.

Grossegeisse, M., Doellinger, J., Fritsch, A., Laue, M., Piesker, J., Schaade, L., and Nitsche, A. (2018). Global ubiquitination analysis reveals extensive modification and proteasomal degradation of cowpox virus proteins, but preservation of viral cores. *Scientific reports* *8*, 1807.

Gubser, C., Bergamaschi, D., Hollinshead, M., Lu, X., van Kuppeveld, F.J.M., and Smith, G.L. (2007). A New Inhibitor of Apoptosis from Vaccinia Virus and Eukaryotes. *PLoS Pathog* *3*, e17.

Gubser, C., Hué, S., Kellam, P., and Smith, G.L. (2004). Poxvirus genomes: a phylogenetic analysis. *Journal of General Virology* *85*, 105-117.

Gunn-Moore, F.J., Welsh, G.I., Herron, L.R., Brannigan, F., Venkateswarlu, K., Gillespie, S., Brandwein-Gensler, M., Madan, R., Tavaré, J.M., Brophy, P.J., *et al.* (2005). A novel 4.1 ezrin radixin moesin (FERM)-containing protein, 'Willin'. *FEBS Letters* *579*, 5089-5094.

Guo, C., and Stark, G.R. (2011). FER tyrosine kinase (FER) overexpression mediates resistance to quinacrine through EGF-dependent activation of NF- $\kappa$ B. *Proc Natl Acad Sci U S A* *108*, 7968-7973.

Ha, H., Han, D., and Choi, Y. (2009). TRAF - mediated TNFR - family signaling. *Current protocols in immunology* *87*, 11.19 D. 11-11.19 D. 19.

Hao, Q.L., Heisterkamp, N., and Groffen, J. (1989). Isolation and sequence analysis of a novel human tyrosine kinase gene. *Mol Cell Biol* 9, 1587.

Harte, M.T., Haga, I.R., Maloney, G., Gray, P., Reading, P.C., Bartlett, N.W., Smith, G.L., Bowie, A., and O'Neill, L.A. (2003). The poxvirus protein A52R targets Toll-like receptor signaling complexes to suppress host defense. *The Journal of experimental medicine* 197, 343-351.

Hayden, M.S., and Ghosh, S. (2008). Shared principles in NF- $\kappa$ B signaling. *Cell* 132, 344-362.

Henkel, T., Machleidt, T., Alkalay, I., Krönke, M., Ben-Neriah, Y., and Baeuerle, P.A. (1993). Rapid proteolysis of I $\kappa$ B- $\alpha$  is necessary for activation of transcription factor NF- $\kappa$ B. *Nature* 365, 182-185.

Huang, B., Yang, X.-D., Lamb, A., and Chen, L.-F. (2010). Posttranslational modifications of NF-kappaB: another layer of regulation for NF-kappaB signaling pathway. *Cell Signal* 22, 1282-1290.

Huang, W., Cui, X., Chen, Y., Shao, M., Shao, X., Shen, Y., Liu, Q., Wu, M., Liu, J., and Ni, W. (2016). High VRK1 expression contributes to cell proliferation and survival in hepatocellular carcinoma. *Pathology-Research and Practice* 212, 171-178.

Humbert, P., Grzeschik, N., Brumby, A., Galea, R., Elsum, I., and Richardson, H. (2008). Control of tumourigenesis by the Scribble/Dlg/Lgl polarity module. *Oncogene* 27, 6888-6907.

Humbert, P., Russell, S., and Richardson, H. (2003). Dlg, Scribble and Lgl in cell polarity, cell proliferation and cancer. *BioEssays* 25, 542-553.

Humphries, A.C., Donnelly, S.K., and Way, M. (2014). Cdc42 and the Rho GEF intersectin-1 collaborate with Nck to promote N-WASP-dependent actin polymerisation. *Journal of Cell Science* 127, 673-685.

Ichihashi, Y., and Oie, M. (1983). The activation of vaccinia virus infectivity by the transfer of phosphatidylserine from the plasma membrane. *Virology* 130, 306-317.

Israël, A. (2010). The IKK complex, a central regulator of NF- $\kappa$ B activation. *Cold Spring Harb Perspect Biol* 2, a000158.

Ito, N., Phillips, S.E.V., Yadav, K.D.S., and Knowles, P.F. (1994). Crystal Structure of a Free Radical Enzyme, Galactose Oxidase. *Journal of Molecular Biology* 238, 704-814.

Itoh, K., Wakabayashi, N., Katoh, Y., Ishii, T., Igarashi, K., Engel, J.D., and Yamamoto, M. (1999). Keap1 represses nuclear activation of antioxidant responsive elements by Nrf2 through binding to the amino-terminal Neh2 domain. *Genes & Development* 13, 76-86.

Ivanova, I.A., Vermeulen, J.F., Ercan, C., Houthuijzen, J.M., Saig, F.A., Vlug, E.J., van der Wall, E., van Diest, P.J., Vooijs, M., and Derksen, P.W.B. (2013). FER kinase promotes breast cancer metastasis by regulating  $\alpha$ 6- and  $\beta$ 1-integrin-dependent cell adhesion and anoikis resistance. *Oncogene* 32, 5582-5592.

Janeway, C.A.J., and Medzhitov, R. (2002). Innate Immune Recognition. *Annual Review of Immunology* 20, 197-216.

Javelaud, D., and Mauviel, A. (2004). Mammalian transforming growth factor- $\beta$ s: Smad signaling and physio-pathological roles. *The International Journal of Biochemistry & Cell Biology* 36, 1161-1165.

Jinek, M., Chylinski, K., Fonfara, I., Hauer, M., Doudna, J.A., and Charpentier, E. (2012). A programmable dual-RNA-guided DNA endonuclease in adaptive bacterial immunity. *Science* 337, 816-821.

Kalluri, R., and Weinberg, R.A. (2009). The basics of epithelial-mesenchymal transition. *J Clin Invest* 119, 1420-1428.

Kanayama, A., Seth, R.B., Sun, L., Ea, C.-K., Hong, M., Shaito, A., Chiu, Y.-H., Deng, L., and Chen, Z.J. (2004). TAB2 and TAB3 activate the NF- $\kappa$ B pathway through binding to polyubiquitin chains. *Molecular cell* 15, 535-548.

Kang, Y., Chen, C.-R., and Massagué, J. (2003). A Self-Enabling TGF $\beta$  Response Coupled to Stress Signaling: Smad Engages Stress Response Factor ATF3 for Id1 Repression in Epithelial Cells. *Molecular cell* 11, 915-926.

Karin, M., and Ben-Neriah, Y. (2000). Phosphorylation Meets Ubiquitination: The Control of NF- $\kappa$ B Activity. *Annual Review of Immunology* 18, 621-663.

Karin, M., and Delhase, M. (2000). The I $\kappa$ B kinase (IKK) and NF- $\kappa$ B: key elements of proinflammatory signalling. In *Seminars in immunology* (Elsevier), pp. 85-98.

Kettle, S., Alcam  $\checkmark$   $\neq$ , A., Khanna, A., Ehret, R., Jassoy, C., and Smith, G.L. (1997). Vaccinia virus serpin B13R (SPI-2) inhibits interleukin-1 $\beta$ -converting enzyme and protects virus-infected cells from TNF- and Fas-mediated apoptosis, but does not prevent IL-1 $\beta$ -induced fever. *Journal of General Virology* 78, 677-685.

Kibler, K.V., Shors, T., Perkins, K.B., Zeman, C.C., Banaszak, M.P., Biesterfeldt, J., Langland, J.O., and Jacobs, B.L. (1997). Double-stranded RNA is a trigger for apoptosis in vaccinia virus- infected cells. *J Virol* 71, 1992-2003.

Kim, J.-E., You, D.-J., Lee, C., Ahn, C., Seong, J.Y., and Hwang, J.-I. (2010). Suppression of NF- $\kappa$ B signaling by KEAP1 regulation of IKK $\beta$  activity through autophagic degradation and inhibition of phosphorylation. *Cell Signal* 22, 1645-1654.

Kim, S.-H., Ryu, H.G., Lee, J., Shin, J., Harikishore, A., Jung, H.-Y., Kim, Y.S., Lyu, H.-N., Oh, E., and Baek, N.-I. (2015). Ursolic acid exerts anti-cancer activity by suppressing vaccinia-related kinase 1-mediated damage repair in lung cancer cells. *Scientific reports* 5, 1-13.

Koch, T., Dahlke, C., Fathi, A., Kupke, A., Krähling, V., Okba, N.M.A., Halwe, S., Rohde, C., Eickmann, M., Volz, A., *et al.* (2020). Safety and immunogenicity of a modified vaccinia virus Ankara vector vaccine candidate for Middle East respiratory syndrome: an open-label, phase 1 trial. *The Lancet Infectious Diseases*.

Kochneva, G., Kolosova, I., Lupan, T., Sivolobova, G., Yudin, P., Grazhdantseva, A., Ryabchikova, E., Kandrina, N.Y., and Shchelkunov, S. (2009a). Orthopoxvirus genes for kelch-like proteins: III. Construction of mousepox (ectromelia) virus variants with targeted gene deletions. *Molecular biology* 43, 567-572.

Kochneva, G., Kolosova, I., Maksyutova, T., Ryabchikova, E., and Shchelkunov, S. (2005). Effects of deletions of kelch-like genes on cowpox virus biological properties. *Archives of virology* 150, 1857-1870.

Kochneva, G., Taranov, O., Lupan, T., Iudin, P., Rubtsov, N., Baïborodin, S., Kolosova, I., Shchelkunov, S., Drozdov, I., and Riabchikova, E. (2009b). Investigation of the impact of cowpox virus BTB/kelch gene deletion on some characteristics of infection in vitro. *Voprosy virusologii* 54, 28.

Komander, D., and Rape, M. (2012). The ubiquitin code. *Annual review of biochemistry* 81, 203-229.

Korchynskiy, O., and ten Dijke, P. (2002). Identification and Functional Characterization of Distinct Critically Important Bone Morphogenetic Protein-specific Response Elements in the Id1 Promoter. *Journal of Biological Chemistry* 277, 4883-4891.

Kvansakul, M. (2017). Viral Infection and Apoptosis. *Viruses* 9, 356.

Lamothe, B., Besse, A., Campos, A.D., Webster, W.K., Wu, H., and Darnay, B.G. (2007). Site-specific Lys-63-linked tumor necrosis factor receptor-associated factor 6 auto-ubiquitination is a critical determinant of I $\kappa$ B kinase activation. *Journal of Biological Chemistry* 282, 4102-4112.

Lamouille, S., Xu, J., and Derynck, R. (2014). Molecular mechanisms of epithelial-mesenchymal transition. *Nat Rev Mol Cell Biol* 15, 178-196.

Lauer, U.M., Schell, M., Beil, J., Berchtold, S., Koppenhöfer, U., Glatzle, J., Königsrainer, A., Möhle, R., Nann, D., and Fend, F. (2018). Phase I study of oncolytic vaccinia virus GL-ONC1 in patients with peritoneal carcinomatosis. *Clinical Cancer Research* 24, 4388-4398.

Lauffenburger, D.A., and Horwitz, A.F. (1996). Cell Migration: A Physically Integrated Molecular Process. *Cell* 84, 359-369.

Law, M., Carter, G.C., Roberts, K.L., Hollinshead, M., and Smith, G.L. (2006). Ligand-induced and nonfusogenic dissolution of a viral membrane. *Proceedings of the National Academy of Sciences* 103, 5989-5994.

Lee, D.-F., Kuo, H.-P., Liu, M., Chou, C.-K., Xia, W., Du, Y., Shen, J., Chen, C.-T., Huo, L., Hsu, M.-C., *et al.* (2009). KEAP1 E3 ligase-mediated downregulation of NF- $\kappa$ B signaling by targeting IKK $\beta$ . *Molecular cell* 36, 131-140.

Lee, D.H., and Goldberg, A.L. (1998). Proteasome inhibitors: valuable new tools for cell biologists. *Trends in Cell Biology* 8, 397-403.

Letwin, K., Yee, S.-P., and Pawson, T. (1989). Novel protein-tyrosine kinase cDNAs related to Fps/Fes and Eph cloned using anti-phosphotyrosine antibody. *Oncogene* 3, 621-627.

Leventis, P.A., and Grinstein, S. (2010). The Distribution and Function of Phosphatidylserine in Cellular Membranes. *Annual Review of Biophysics* 39, 407-427.

Li, X., Peng, H., Schultz, D.C., Lopez-Guisa, J.M., Rauscher, F.J., and Marmorstein, R. (1999). Structure-Function Studies of the BTB/POZ Transcriptional Repression Domain from the Promyelocytic Leukemia Zinc Finger Oncoprotein. *Cancer Research* 59, 5275-5282.

Liang, P., Zhang, H., Wang, G., Li, S., Cong, S., Luo, Y., and Zhang, B. (2013a). KPNB1, XPO7 and IPO8 Mediate the Translocation of NF- $\kappa$ B/p65 into the Nucleus. *Traffic* 14, 1132-1143.

Liang, P., Zhang, H., Wang, G., Li, S., Cong, S., Luo, Y., and Zhang, B. (2013b). KPNB1, XPO7 and IPO8 Mediate the Translocation of NF- $\kappa$ B/p65 into the Nucleus. *Traffic* 14, 1132-1143.

Liu, F., Du, F., and Chen, X. (2014). Multiple tumor marker protein chip detection system in diagnosis of pancreatic cancer. *World J Surg Oncol* 12, 333-333.

Liu, H., Golebiewski, L., Dow, E.C., Krug, R.M., Javier, R.T., and Rice, A.P. (2010). The ESEV PDZ-binding motif of the avian influenza A virus NS1 protein protects infected cells from apoptosis by directly targeting Scribble. *J Virol* 84, 11164-11174.

Liu, S., Cai, X., Wu, J., Cong, Q., Chen, X., Li, T., Du, F., Ren, J., Wu, Y.-T., Grishin, N.V., and Chen, Z.J. (2015). Phosphorylation of innate immune adaptor proteins MAVS, STING, and TRIF induces IRF3 activation. *Science* 347, aaa2630.

Liu, S., Chen, J., Cai, X., Wu, J., Chen, X., Wu, Y.-T., Sun, L., and Chen, Z.J. (2013). MAVS recruits multiple ubiquitin E3 ligases to activate antiviral signaling cascades. *eLife* 2, e00785.

Liu, S., and Chen, Z.J. (2011). Expanding role of ubiquitination in NF- $\kappa$ B signaling. *Cell research* 21, 6-21.

Liu, T., Zhang, L., Joo, D., and Sun, S.-C. (2017). NF- $\kappa$ B signaling in inflammation. *Signal Transduction and Targeted Therapy* 2, 17023.

Lockyer, P.J., Kupzig, S., and Cullen, P.J. (2001). CAPRI regulates Ca<sup>2+</sup>-dependent inactivation of the Ras-MAPK pathway. *Current Biology* 11, 981-986.

Lu, Y., Stuart, J.H., Talbot-Cooper, C., Agrawal-Singh, S., Huntly, B., Smid, A.I., Snowden, J.S., Dupont, L., and Smith, G.L. (2019). Histone deacetylase 4 promotes type I interferon signaling, restricts DNA viruses, and is degraded via vaccinia virus protein C6. *Proceedings of the National Academy of Sciences* 116, 11997-12006.

Ludford-Menting, M.J., Oliaro, J., Sacirbegovic, F., Cheah, E.T.-Y., Pedersen, N., Thomas, S.J., Pasam, A., Iazzolino, R., Dow, L.E., and Waterhouse, N.J. (2005). A network of PDZ-containing proteins regulates T cell polarity and morphology during migration and immunological synapse formation. *Immunity* 22, 737-748.

Luo, L., Liao, Y.J., Jan, L.Y., and Jan, Y.N. (1994). Distinct morphogenetic functions of similar small GTPases: *Drosophila* Drac1 is involved in axonal outgrowth and myoblast fusion. *Genes & Development* 8, 1787-1802.

Macara, I.G. (2001). Transport into and out of the Nucleus. *Microbiology and Molecular Biology Reviews* 65, 570-594.

Maekawa, M., Li, S., Iwamatsu, A., Morishita, T., Yokota, K., Imai, Y., Kohsaka, S., Nakamura, S., and Hattori, S. (1994). A novel mammalian Ras GTPase-activating protein which has phospholipid-binding and Btk homology regions. *Mol Cell Biol* 14, 6879-6885.

Maluquer de Motes, C., Schiffner, T., Sumner, R.P., and Smith, G.L. (2014). Vaccinia virus virulence factor N1 can be ubiquitinated on multiple lysine residues. *J Gen Virol* 95, 2038-2049.

Maluquer de Motes, C., and Smith, G.L. (2017). Vaccinia virus protein A49 activates Wnt signalling by targeting the E3 ligase  $\beta$ -TrCP. *J Gen Virol* 98, 3086-3092.

Mansur, D.S., Maluquer de Motes, C., Unterholzner, L., Sumner, R.P., Ferguson, B.J., Ren, H., Strnadova, P., Bowie, A.G., and Smith, G.L. (2013). Poxvirus Targeting of E3 Ligase  $\beta$ -TrCP by

Molecular Mimicry: A Mechanism to Inhibit NF- $\kappa$ B Activation and Promote Immune Evasion and Virulence. *PLoS Pathog* 9, e1003183.

Massagué, J., Seoane, J., and Wotton, D. (2005). Smad transcription factors. *Genes & Development* 19, 2783-2810.

Mauviel, A., Nallet-Staub, F., and Varelas, X. (2012). Integrating developmental signals: a Hippo in the (path)way. *Oncogene* 31, 1743-1756.

McKenzie, C.D. (2016). Activation of oncogenic signalling pathways by vaccinia virus. . In School of life and environmental sciences. (Sydney, University of Sydney).

Medzhitov, R. (2007). Recognition of microorganisms and activation of the immune response. *Nature* 449, 819-826.

Medzhitov, R., and Janeway Jr, C.A. (1997). Innate immunity: impact on the adaptive immune response. *Current opinion in immunology* 9, 4-9.

Mei, Z.-Z., Chen, X.-Y., Hu, S.-W., Wang, N., Ou, X.-L., Wang, J., Luo, H.-H., Liu, J., and Jiang, Y. (2016). Kelch-like Protein 21 (KLHL21) Targets I $\kappa$ B Kinase- $\beta$  to Regulate NF- $\kappa$ B Signaling Negatively. *Journal of Biological Chemistry*.

Mell, L.K., Brumund, K.T., Daniels, G.A., Advani, S.J., Zakeri, K., Wright, M.E., Onyeama, S.-J., Weisman, R.A., Sanghvi, P.R., and Martin, P.J. (2017). Phase I trial of intravenous oncolytic vaccinia virus (GL-ONC1) with cisplatin and radiotherapy in patients with locoregionally advanced head and neck carcinoma. *Clinical Cancer Research* 23, 5696-5702.

Mercer, J., and Helenius, A. (2008). Vaccinia Virus Uses Macropinocytosis and Apoptotic Mimicry to Enter Host Cells. *Science* 320, 531-535.

Merlet, J., Burger, J., Gomes, J.E., and Pintard, L. (2009). Regulation of cullin-RING E3 ubiquitin-ligases by neddylation and dimerization. *Cellular and Molecular Life Sciences* 66, 1924-1938.

Minev, B.R., Lander, E., Feller, J.F., Berman, M., Greenwood, B.M., Minev, I., Santidrian, A.F., Nguyen, D., Draganov, D., Killinc, M.O., *et al.* (2019). First-in-human study of TK-positive oncolytic vaccinia virus delivered by adipose stromal vascular fraction cells. *Journal of Translational Medicine* 17, 271.

Moreno-Bueno, G., Portillo, F., and Cano, A. (2008). Transcriptional regulation of cell polarity in EMT and cancer. *Oncogene* 27, 6958-6969.

Morreale, F.E., and Walden, H. (2016). Types of Ubiquitin Ligases. *Cell* 165, 248-248.e241.

Morrison, D.K. (2012). MAP kinase pathways. *Cold Spring Harb Perspect Biol* 4, a011254.

Moss, B. (1991). Vaccinia virus: a tool for research and vaccine development. *Science* 252, 1662-1667.

Moss, B. (1996). Genetically engineered poxviruses for recombinant gene expression, vaccination, and safety. *Proc Natl Acad Sci U S A* 93, 11341-11348.

Moss, B. (2006). Poxvirus entry and membrane fusion. *Virology* 344, 48-54.

Moss, B. (2013). Poxvirus DNA replication. *Cold Spring Harb Perspect Biol* 5, a010199.

Mulhern, O., and Bowie, A.G. (2010). Unexpected roles for DEAD-box protein 3 in viral RNA sensing pathways. *European Journal of Immunology* 40, 933-935.

Nagasaka, K., Nakagawa, S., Yano, T., Takizawa, S., Matsumoto, Y., Tsuruga, T., Nakagawa, K., Minaguchi, T., Oda, K., Hiraike-Wada, O., *et al.* (2006). Human homolog of *Drosophila* tumor suppressor Scribble negatively regulates cell-cycle progression from G1 to S phase by localizing at the basolateral membrane in epithelial cells. *Cancer Science* 97, 1217-1225.

Nakagawa, S., and Huijbregtse, J.M. (2000). Human scribble (Vartul) is targeted for ubiquitin-mediated degradation by the high-risk papillomavirus E6 proteins and the E6AP ubiquitin-protein ligase. *Mol Cell Biol* 20, 8244-8253.

Nezu, J.-i., Oku, A., Jones, M.H., and Shimane, M. (1997). Identification of two novel human putative serine/threonine kinases, VRK1 and VRK2, with structural similarity to vaccinia virus B1R kinase. *Genomics* 45, 327-331.

Nola, S., Sebbagh, M., Marchetto, S., Osmani, N., Nourry, C., Audebert, S., Navarro, C., Rachel, R., Montcouquiol, M., Sans, N., *et al.* (2008). Scrib regulates PAK activity during the cell migration process. *Human Molecular Genetics* 17, 3552-3565.

O'Brien, T.P., Yang, G.P., Sanders, L., and Lau, L.F. (1990). Expression of *cyr61*, a growth factor-inducible immediate-early gene. *Mol Cell Biol* *10*, 3569-3577.

Oeckinghaus, A., and Ghosh, S. (2009). The NF- $\kappa$ B family of transcription factors and its regulation. *Cold Spring Harb Perspect Biol* *1*, a000034.

Olson, A.T., Rico, A.B., Wang, Z., Delhon, G., and Wiebe, M.S. (2017). Deletion of the Vaccinia Virus B1 Kinase Reveals Essential Functions of This Enzyme Complemented Partly by the Homologous Cellular Kinase VRK2. *J Virol* *91*, e00635-00617.

Osmani, N., Vitale, N., Borg, J.-P., and Etienne-Manneville, S. (2006). Scrib Controls Cdc42 Localization and Activity to Promote Cell Polarization during Astrocyte Migration. *Current Biology* *16*, 2395-2405.

Pallett, M.A., Ren, H., Zhang, R.-Y., Scutts, S.R., Gonzalez, L., Zhu, Z., Maluquer de Motes, C., and Smith, G.L. (2019). Vaccinia Virus BBK E3 Ligase Adaptor A55 Targets Importin-Dependent NF- $\kappa$ B Activation and Inhibits CD8(+) T-Cell Memory. *J Virol* *93*, e00051-00019.

Parkinson, J.E., and Smith, G.L. (1994). Vaccinia Virus Gene A36R Encodes a Mr 43-50 K Protein on the Surface of Extracellular Enveloped Virus. *Virology* *204*, 376-390.

Pearson, H.B., McGlenn, E., Phesse, T.J., Schlüter, H., Srikumar, A., Gödde, N.J., Woelwer, C.B., Ryan, A., Phillips, W.A., Ernst, M., *et al.* (2015). The polarity protein Scrib mediates epidermal development and exerts a tumor suppressive function during skin carcinogenesis. *Molecular Cancer* *14*, 169.

Perez, E.E., Wang, J., Miller, J.C., Jouvenot, Y., Kim, K.A., Liu, O., Wang, N., Lee, G., Bartsevich, V.V., Lee, Y.-L., *et al.* (2008). Establishment of HIV-1 resistance in CD4+ T cells by genome editing using zinc-finger nucleases. *Nat Biotechnol* *26*, 808-816.

Philips, J., and Herskowitz, I. (1998). Identification of Kel1p, a Kelch Domain-containing Protein Involved in Cell Fusion and Morphology in *Saccharomyces cerevisiae*. *The Journal of Cell Biology* *143*, 375-389.

Pickart, C.M., and Fushman, D. (2004). Polyubiquitin chains: polymeric protein signals. *Current Opinion in Chemical Biology* *8*, 610-616.

Pintard, L., Willems, A., and Peter, M. (2004a). Cullin-based ubiquitin ligases: Cul3-BTB complexes join the family. *The EMBO journal* *23*, 1681-1687.

Pintard, L., Willems, A., and Peter, M. (2004b). Cullin-based ubiquitin ligases: Cul3-BTB complexes join the family. *The EMBO Journal* *23*, 1681-1687.

Pires de Miranda, M., Reading, P.C., Tschärke, D.C., Murphy, B.J., and Smith, G.L. (2003). The vaccinia virus kelch-like protein C2L affects calcium-independent adhesion to the extracellular matrix and inflammation in a murine intradermal model. *Journal of General Virology* *84*, 2459-2471.

Plouffe, S.W., Lin, K.C., Moore, J.L., 3rd, Tan, F.E., Ma, S., Ye, Z., Qiu, Y., Ren, B., and Guan, K.-L. (2018). The Hippo pathway effector proteins YAP and TAZ have both distinct and overlapping functions in the cell. *The Journal of biological chemistry* *293*, 11230-11240.

Postigo, A., Martin, M.C., Dodding, M.P., and Way, M. (2009). Vaccinia-induced epidermal growth factor receptor-MEK signalling and the anti-apoptotic protein F1L synergize to suppress cell death during infection. *Cellular Microbiology* *11*, 1208-1218.

Qadir, M.I., Parveen, A., and Ali, M. (2015). Cdc42: Role in Cancer Management. *Chemical Biology & Drug Design* *86*, 432-439.

Ran, F.A., Hsu, P.D., Wright, J., Agarwala, V., Scott, D.A., and Zhang, F. (2013). Genome engineering using the CRISPR-Cas9 system. *Nat Protoc* *8*, 2281-2308.

Randall, R.E., and Goodbourn, S. (2008). Interferons and viruses: an interplay between induction, signalling, antiviral responses and virus countermeasures. *Journal of General Virology* *89*, 1-47.

Rempel, R.E., Anderson, M., Evans, E., and Traktman, P. (1990). Temperature-sensitive vaccinia virus mutants identify a gene with an essential role in viral replication. *J Virol* *64*, 574-583.

Ridley, A.J. (2015). Rho GTPase signalling in cell migration. *Curr Opin Cell Biol* *36*, 103-112.

Roberts, K.L., and Smith, G.L. (2008). Vaccinia virus morphogenesis and dissemination. *Trends in Microbiology* *16*, 472-479.

Rosato, R., Veltmaat, J.M., Groffen, J., and Heisterkamp, N. (1998). Involvement of the tyrosine kinase fer in cell adhesion. *Mol Cell Biol* 18, 5762-5770.

Ryerson, M.R., Richards, M.M., Kvensakul, M., Hawkins, C.J., and Shisler, J.L. (2017). Vaccinia Virus Encodes a Novel Inhibitor of Apoptosis That Associates with the Apoptosome. *J Virol* 91, e01385-01317.

Salzano, M., Vázquez-Cedeira, M., Sanz-García, M., Valbuena, A., Blanco, S., Fernández, I.F., and Lazo, P.A. (2014). Vaccinia-related kinase 1 (VRK1) confers resistance to DNA-damaging agents in human breast cancer by affecting DNA damage response. *Oncotarget* 5, 1770.

Sanderson, C.M., Frischknecht, F., Way, M., Hollinshead, M., and Smith, G.L. (1998a). Roles of vaccinia virus EEV-specific proteins in intracellular actin tail formation and low pH-induced cell-cell fusion. *Journal of General Virology* 79, 1415-1425.

Sanderson, C.M., and Smith, G.L. (1998). Vaccinia Virus Induces Ca<sup>2+</sup>-Independent Cell-Matrix Adhesion during the Motile Phase of Infection. *J Virol* 72, 9924-9933.

Sanderson, C.M., Way, M., and Smith, G.L. (1998b). Virus-induced cell motility. *J Virol* 72, 1235-1243.

Santoni, M.-J., Pontarotti, P., Birnbaum, D., and Borg, J.-P. (2002). The LAP family: a phylogenetic point of view. *Trends in Genetics* 18, 494-497.

Satheshkumar, P.S., Anton, L.C., Sanz, P., and Moss, B. (2009). Inhibition of the ubiquitin-proteasome system prevents vaccinia virus DNA replication and expression of intermediate and late genes. *J Virol* 83, 2469-2479.

Sato, S., Sanjo, H., Takeda, K., Ninomiya-Tsuji, J., Yamamoto, M., Kawai, T., Matsumoto, K., Takeuchi, O., and Akira, S. (2005). Essential function for the kinase TAK1 in innate and adaptive immune responses. *Nature immunology* 6, 1087-1095.

Schmelz, M., Sodeik, B., Ericsson, M., Wolffe, E.J., Shida, H., Hiller, G., and Griffiths, G. (1994). Assembly of vaccinia virus: the second wrapping cisterna is derived from the trans Golgi network. *J Virol* 68, 130-147.

Schröder, M., Baran, M., and Bowie, A.G. (2008a). Viral targeting of DEAD box protein 3 reveals its role in TBK1/IKKε-mediated IRF activation. *The EMBO Journal* 27, 2147-2157.

Schröder, M., Baran, M., and Bowie, A.G. (2008b). Viral targeting of DEAD box protein 3 reveals its role in TBK1/IKKε-mediated IRF activation. *The EMBO Journal* 27, 2147-2157.

Schulman, B.A., Carrano, A.C., Jeffrey, P.D., Bowen, Z., Kinnucan, E.R.E., Finnin, M.S., Elledge, S.J., Harper, J.W., Pagano, M., and Pavletich, N.P. (2000). Insights into SCF ubiquitin ligases from the structure of the Skp1-Skp2 complex. *Nature* 408, 381-386.

Schupbach, T., and Wieschaus, E. (1991). Female Sterile Mutations on the Second Chromosome of *Drosophila Melanogaster*. II. Mutations Blocking Oogenesis or Altering Egg Morphology. *Genetics* 129, 1119-1136.

Scott, G., Leopardi, S., Printup, S., and Madden, B.C. (2002). Filopodia are conduits for melanosome transfer to keratinocytes. *Journal of Cell Science* 115, 1441-1451.

Scutts, S.R. (2017). Investigations into the vaccinia virus immunomodulatory proteins C4 and C16. In Department of Pathology (Cambridge, University of Cambridge).

Sebastian, S., and Gilbert, S.C. (2016). Recombinant modified vaccinia virus Ankara-based malaria vaccines. *Expert Rev Vaccines* 15, 91-103.

Sharma, P., Yan, F., Doronina, V.A., Escuin-Ordinas, H., Ryan, M.D., and Brown, J.D. (2012). 2A peptides provide distinct solutions to driving stop-carry on translational recoding. *Nucleic Acids Res* 40, 3143-3151.

Shchelkunov, S., Totmenin, A., and Kolosova, I. (2002). Species-Specific Differences in Organization of Orthopoxvirus Kelch-Like Proteins. *Virus Genes* 24, 157-162.

Shchelkunov, S.N. (2010). Interaction of orthopoxviruses with the cellular ubiquitin-ligase system. *Virus Genes* 41, 309-318.

Shi, J.-H., and Sun, S.-C. (2018). Tumor Necrosis Factor Receptor-Associated Factor Regulation of Nuclear Factor κB and Mitogen-Activated Protein Kinase Pathways. *Front Immunol* 9.

Sietske, R.H., van Beek, J., de Jonge, J., Luytjes, W., and van Baarle, D. (2014). T cell responses to viral infections - opportunities for Peptide vaccination. *Front Immunol* 5, 171-171.

Sievers, F., Wilm, A., Dineen, D., Gibson, T.J., Karplus, K., Li, W., Lopez, R., McWilliam, H., Remmert, M., Söding, J., *et al.* (2011). Fast, scalable generation of high-quality protein multiple sequence alignments using Clustal Omega. In *Mol Syst Biol*, p. 539.

Siveen, K.S., Prabhu, K.S., Achkar, I.W., Kuttikrishnan, S., Shyam, S., Khan, A.Q., Merhi, M., Dermime, S., and Uddin, S. (2018). Role of Non Receptor Tyrosine Kinases in Hematological Malignances and its Targeting by Natural Products. *Molecular Cancer* 17, 31.

Smith, G.L. (2008). Vaccinia Virus. In *Encyclopedia of Virology (Third Edition)*, B.W.J. Mahy, and M.H.V. Van Regenmortel, eds. (Oxford: Academic Press), pp. 243-250.

Smith, G.L., Benfield, C.T.O., Maluquer de Motes, C., Mazzon, M., Ember, S.W.J., Ferguson, B.J., and Sumner, R.P. (2013). Vaccinia virus immune evasion: mechanisms, virulence and immunogenicity. *Journal of General Virology* 94, 2367-2392.

Smith, G.L., Mackett, M., and Moss, B. (1983). Infectious vaccinia virus recombinants that express hepatitis B virus surface antigen. *Nature* 302, 490-495.

Soday, L., Lu, Y., Albarnaz, J.D., Davies, C.T.R., Antrobus, R., Smith, G.L., and Weekes, M.P. (2019). Quantitative Temporal Proteomic Analysis of Vaccinia Virus Infection Reveals Regulation of Histone Deacetylases by an Interferon Antagonist. *Cell Reports* 27, 1920-1933.e1927.

Soltysik-Espanola, M., Rogers, R.A., Jiang, S., Kim, T.-A., Gaedigk, R., White, R.A., Avraham, H., and Avraham, S. (1999). Characterization of Mayven, a Novel Actin-binding Protein Predominantly Expressed in Brain. *Mol Biol Cell* 10, 2361-2375.

Soulat, D., Bürckstümmer, T., Westermayer, S., Goncalves, A., Bauch, A., Stefanovic, A., Hantschel, O., Bennett, K.L., Decker, T., and Superti-Furga, G. (2008). The DEAD-box helicase DDX3X is a critical component of the TANK-binding kinase 1-dependent innate immune response. *The EMBO Journal* 27, 2135-2146.

Stickl, H., Hochstein-Mintzel, V., Mayr, A., Huber, H.C., Schäfer, H., and Holzner, A. (1974). MVA-Stufenimpfung gegen Pocken. *Dtsch Med Wochenschr* 99, 2386-2392.

Stogios, P.J., Downs, G.S., Jauhal, J.J.S., Nandra, S.K., and Privé, G.G. (2005). Sequence and structural analysis of BTB domain proteins. *Genome Biol* 6, R82-R82.

Stogios, P.J., and Privé, G.G. (2004). The BACK domain in BTB-kelch proteins. *Trends in Biochemical Sciences* 29, 634-637.

Stuart, J.H., Sumner, R.P., Lu, Y., Snowden, J.S., and Smith, G.L. (2016). Vaccinia Virus Protein C6 Inhibits Type I IFN Signalling in the Nucleus and Binds to the Transactivation Domain of STAT2. *PLoS Pathog* 12, e1005955.

Sun, S.-C., Chang, J.-H., and Jin, J. (2013). Regulation of nuclear factor- $\kappa$ B in autoimmunity. *Trends in immunology* 34, 282-289.

Swain, S.L., McKinstry, K.K., and Strutt, T.M. (2012). Expanding roles for CD4<sup>+</sup> T cells in immunity to viruses. *Nat Rev Immunol* 12, 136-148.

Tait, S.W.G., and Green, D.R. (2008). Caspase-independent cell death: leaving the set without the final cut. *Oncogene* 27, 6452-6461.

Tait, S.W.G., and Green, D.R. (2010). Mitochondria and cell death: outer membrane permeabilization and beyond. *Nature Reviews Molecular Cell Biology* 11, 621-632.

Takeuchi, O., and Akira, S. (2010). Pattern Recognition Receptors and Inflammation. *Cell* 140, 805-820.

Tang, Q., Chakraborty, S., and Xu, G. (2018). Mechanism of vaccinia viral protein B14 mediated inhibition of I $\kappa$ B kinase  $\beta$  activation. *Journal of Biological Chemistry*.

Teale, A., Campbell, S., Van Buuren, N., Magee, W.C., Watmough, K., Couturier, B., Shipclark, R., and Barry, M. (2009). Orthopoxviruses Require a Functional Ubiquitin-Proteasome System for Productive Replication. *J Virol* 83, 2099-2108.

Thiery, J.P., Acloque, H., Huang, R.Y.J., and Nieto, M.A. (2009). Epithelial-Mesenchymal Transitions in Development and Disease. *Cell* 139, 871-890.

Thomas, M., and Banks, L. (2018). Upsetting the Balance: When Viruses Manipulate Cell Polarity Control. *Journal of Molecular Biology* 430, 3481-3503.

Tooze, J., Hollinshead, M., Reis, B., Radsak, K., and Kern, H. (1993). Progeny vaccinia and human cytomegalovirus particles utilize early endosomal cisternae for their envelopes. *European journal of cell biology* 60, 163-178.

Torres, A.A., Albarnaz, J.D., Bonjardim, C.A., and Smith, G.L. (2016). Multiple Bcl-2 family immunomodulators from vaccinia virus regulate MAPK/AP-1 activation. *J Gen Virol* 97, 2346-2351.

Townsley, A.C., Weisberg, A.S., Wagenaar, T.R., and Moss, B. (2006). Vaccinia virus entry into cells via a low-pH-dependent endosomal pathway. *J Virol* 80, 8899-8908.

Trahey, M., and McCormick, F. (1987). A cytoplasmic protein stimulates normal N-ras p21 GTPase, but does not affect oncogenic mutants. *Science* 238, 542.

Tsung, K., Yim, J.H., Marti, W., Buller, R.M., and Norton, J.A. (1996). Gene expression and cytopathic effect of vaccinia virus inactivated by psoralen and long-wave UV light. *J Virol* 70, 165-171.

Twardzik, D.R., Brown, J.P., Ranchalis, J.E., Todaro, G.J., and Moss, B. (1985). Vaccinia virus-infected cells release a novel polypeptide functionally related to transforming and epidermal growth factors. *Proceedings of the National Academy of Sciences* 82, 5300-5304.

Unterholzner, L., Sumner, R.P., Baran, M., Ren, H., Mansur, D.S., Bourke, N.M., Randow, F., Smith, G.L., and Bowie, A.G. (2011a). Vaccinia virus protein C6 is a virulence factor that binds TBK-1 adaptor proteins and inhibits activation of IRF3 and IRF7. *PLoS Pathog* 7, e1002247-e1002247.

Unterholzner, L., Sumner, R.P., Baran, M., Ren, H., Mansur, D.S., Bourke, N.M., Randow, F., Smith, G.L., and Bowie, A.G. (2011b). Vaccinia Virus Protein C6 Is a Virulence Factor that Binds TBK-1 Adaptor Proteins and Inhibits Activation of IRF3 and IRF7. *PLoS Pathog* 7, e1002247.

Upton, C., Slack, S., Hunter, A.L., Ehlers, A., and Roper, R.L. (2003). Poxvirus orthologous clusters: toward defining the minimum essential poxvirus genome. *J Virol* 77, 7590-7600.

Valderrama, F., Cordeiro, J.V., Schleich, S., Frischknecht, F., and Way, M. (2006). Vaccinia Virus-Induced Cell Motility Requires F11L-Mediated Inhibition of RhoA Signaling. *Science* 311, 377-381.

Varelas, X., Sakuma, R., Samavarchi-Tehrani, P., Peerani, R., Rao, B.M., Dembowy, J., Yaffe, M.B., Zandstra, P.W., and Wrana, J.L. (2008). TAZ controls Smad nucleocytoplasmic shuttling and regulates human embryonic stem-cell self-renewal. *Nature Cell Biology* 10, 837-848.

Vassilev, A., Kaneko, K.J., Shu, H., Zhao, Y., and DePamphilis, M.L. (2001). TEAD/TEF transcription factors utilize the activation domain of YAP65, a Src/Yes-associated protein localized in the cytoplasm. *Genes & Development* 15, 1229-1241.

Veyer, D.L., Carrara, G., Maluquer de Motes, C., and Smith, G.L. (2017). Vaccinia virus evasion of regulated cell death. *Immunology Letters* 186, 68-80.

Veyer, D.L., Maluquer de Motes, C., Sumner, R.P., Ludwig, L., Johnson, B.F., and Smith, G.L. (2014). Analysis of the anti-apoptotic activity of four vaccinia virus proteins demonstrates that B13 is the most potent inhibitor in isolation and during viral infection. *J Gen Virol* 95, 2757-2768.

Volz, A., Kupke, A., Song, F., Jany, S., Fux, R., Shams-Eldin, H., Schmidt, J., Becker, C., Eickmann, M., Becker, S., and Sutter, G. (2015). Protective Efficacy of Recombinant Modified Vaccinia Virus Ankara Delivering Middle East Respiratory Syndrome Coronavirus Spike Glycoprotein. *J Virol* 89, 8651-8656.

Volz, A., and Sutter, G. (2017). Modified vaccinia virus Ankara: history, value in basic research, and current perspectives for vaccine development. In *Advances in virus research* (Elsevier), pp. 187-243.

Walsh, D., McCarthy, J., O'Driscoll, C., and Melgar, S. (2013). Pattern recognition receptors—molecular orchestrators of inflammation in inflammatory bowel disease. *Cytokine & growth factor reviews* 24, 91-104.

Walsh, S.R., and Dolin, R. (2011). Vaccinia viruses: vaccines against smallpox and vectors against infectious diseases and tumors. *Expert Rev Vaccines* 10, 1221-1240.

Wang, G., Yu, Y., Sun, C., Liu, T., Liang, T., Zhan, L., Lin, X., and Feng, X.H. (2016). STAT3 selectively interacts with Smad3 to antagonize TGF- $\beta$  signalling. *Oncogene* 35, 4388-4398.

Wang, Q., Burles, K., Couturier, B., Randall, C.M.H., Shisler, J., and Barry, M. (2014). Ectromelia virus encodes a BTB/kelch protein, EVM150, that inhibits NF- $\kappa$ B signaling. *J Virol* 88, 4853-4865.

Wasilenko, S.T., Stewart, T.L., Meyers, A.F.A., and Barry, M. (2003). Vaccinia virus encodes a previously uncharacterized mitochondrial-associated inhibitor of apoptosis. *Proc Natl Acad Sci U S A* *100*, 14345-14350.

Watson, J.R., Owen, D., and Mott, H.R. (2017). Cdc42 in actin dynamics: An ordered pathway governed by complex equilibria and directional effector handover. *Small GTPases* *8*, 237-244.

Weissman, A.M. (2001). Themes and variations on ubiquitylation. *Nature Reviews Molecular Cell Biology* *2*, 169-178.

WHO (2020). Draft landscape of COVID-19 candidate vaccines.

Williams, B.R. (1999). PKR; a sentinel kinase for cellular stress. *Oncogene* *18*, 6112-6120.

Wilton, B.A., Campbell, S., Van Buuren, N., Garneau, R., Furukawa, M., Xiong, Y., and Barry, M. (2008a). Ectromelia virus BTB/kelch proteins, EVM150 and EVM167, interact with cullin-3-based ubiquitin ligases. *Virology* *374*, 82-99.

Wilton, B.A., Campbell, S., Van Buuren, N., Garneau, R., Furukawa, M., Xiong, Y., and Barry, M. (2008b). Ectromelia Virus BTB/kelch Proteins, EVM150 and EVM167, Interact with Cullin-3 Based Ubiquitin Ligases. *Virology* *374*, 82-99.

Witteck, R., and Moss, B. (1980). Tandem repeats within the inverted terminal repetition of vaccinia virus DNA. *Cell* *21*, 277-284.

Xue, F., and Cooley, L. (1993). Kelch encodes a component of intercellular bridges in Drosophila egg chambers. *Cell* *72*, 681-693.

Yamben, I.F., Rachel, R.A., Shatadal, S., Copeland, N.G., Jenkins, N.A., Warming, S., and Griep, A.E. (2013). Scrib is required for epithelial cell identity and prevents epithelial to mesenchymal transition in the mouse. *Dev Biol* *384*, 41-52.

Yang, Z., Bruno, D.P., Martens, C.A., Porcella, S.F., and Moss, B. (2010a). Simultaneous high-resolution analysis of vaccinia virus and host cell transcriptomes by deep RNA sequencing. *Proceedings of the National Academy of Sciences* *107*, 11513-11518.

Yang, Z., Bruno, D.P., Martens, C.A., Porcella, S.F., and Moss, B. (2010b). Simultaneous high-resolution analysis of vaccinia virus and host cell transcriptomes by deep RNA sequencing. *Proc Natl Acad Sci U S A* *107*, 11513-11518.

Yoneyama, T., Angata, K., Bao, X., Courtneidge, S., Chanda, S.K., and Fukuda, M. (2012). Fer kinase regulates cell migration through  $\alpha$ -dystroglycan glycosylation. *Mol Biol Cell* *23*, 771-780.

Yu, F.-X., and Guan, K.-L. (2013). The Hippo pathway: regulators and regulations. *Genes & Development* *27*, 355-371.

Zhan, L., Rosenberg, A., Bergami, K.C., Yu, M., Xuan, Z., Jaffe, A.B., Allred, C., and Muthuswamy, S.K. (2008). Deregulation of Scribble Promotes Mammary Tumorigenesis and Reveals a Role for Cell Polarity in Carcinoma. *Cell* *135*, 865-878.

Zhang, H., and Sun, S.-C. (2015). NF- $\kappa$ B in inflammation and renal diseases. *Cell & bioscience* *5*, 63.

Zhang, L., Blackwell, K., Altaeva, A., Shi, Z., and Habelhah, H. (2011). TRAF2 phosphorylation promotes NF- $\kappa$ B-dependent gene expression and inhibits oxidative stress-induced cell death. *Mol Biol Cell* *22*, 128-140.

Zhang, L., Villa, N.Y., and McFadden, G. (2009). Interplay between poxviruses and the cellular ubiquitin/ubiquitin-like pathways. *FEBS Letters* *583*, 607-614.

Zhao, B., Li, L., Tumaneng, K., Wang, C.-Y., and Guan, K.-L. (2010). A coordinated phosphorylation by Lats and CK1 regulates YAP stability through SCF $\beta$ -TRCP. *Genes & Development* *24*, 72-85.

Zheng, W., Umitsu, M., Jagan, I., Tran, C.W., Ishiyama, N., BeGora, M., Araki, K., Ohashi, P.S., Ikura, M., and Muthuswamy, S.K. (2016). An interaction between Scribble and the NADPH oxidase complex controls M1 macrophage polarization and function. *Nature Cell Biology* *18*, 1244-1252.

Ziman, M., O'Brien, J.M., Ouellette, L.A., Church, W.R., and Johnson, D.I. (1991). Mutational analysis of CDC42Sc, a *Saccharomyces cerevisiae* gene that encodes a putative GTP-binding protein involved in the control of cell polarity. *Mol Cell Biol* *11*, 3537-3544.

Zollman, S., Godt, D., Privé, G.G., Couderc, J.L., and Laski, F.A. (1994). The BTB domain, found primarily in zinc finger proteins, defines an evolutionarily conserved family that includes several developmentally regulated genes in *Drosophila*. *Proc Natl Acad Sci U S A* *91*, 10717-10721.

Zwilling, J., Sliva, K., Schwantes, A., Schnierle, B., and Sutter, G. (2010). Functional F11L and K1L genes in modified vaccinia virus Ankara restore virus-induced cell motility but not growth in human and murine cells. *Virology* *404*, 231-239.